UNIVERSIDAD DE MURCIA

ESCUELA INTERNACIONAL DE DOCTORADO

Impact of Melon EIF4E Editing on Virus Resistance and Melon Fertility

Impacto de la Edición de EIF4E sobre la Resistencia a Virus y la Fertilidad en Plantas de Melón

D. Giuliano Sting Pechar

2022

“Impact of melon *EIF4E* editing on virus resistance and melon fertility”. “Impacto de la edición de *EIF4E* sobre la resistencia a virus y la fertilidad en plantas de melón”

Memoria presentada para optar al grado de doctor por la Universidad de Murcia

D. Giuliano Sting Pechar

Directores:

Dr. Miguel Ángel Aranda Regules

Dra. Livia Donaire Segarra

Dr. Roque Carlos García-Almodóvar

A mio padre

Este trabajo ha sido posible gracias al Ministerio Economia y Competitividad, que ha financiado mi contrato predoctoral FPI (BES-2016-077826) vinculado al proyecto del Plan Nacional AGL2015-65838, y gracias a la Consejería de Empleo, Universidades y Empresa de la Región de Murcia, dentro del Programa RIS3Mur (ref. 2I16SA000057). Una vez finalizado mi contrato predoctoral, he disfrutado de un contrato con cargo al proyecto PLEC2021-007715, financiado por el Ministerio de Ciencia e Innovación.

Table of contents

List of figures

List of tables

Resumen

En este trabajo se ha estudiado el impacto de la edición del gen que codifica el factor de iniciación de la traducción en eucariotas (*eukariotic translation initiation factor*, eIF) 4E sobre la susceptibilidad a virus y la fertilidad de la flor masculina en melón (*Cucumis melo* L.). eIF4E es una proteína de unión a la caperuza 5' (5'-cap) de los ARNs mensajeros (ARNm) que a través de su interacción con eIF4G, constituye el núcleo del complejo eIF4F, el cual desempeña un papel clave en la circularización de los ARNm y su posterior traducción cap-dependiente. Además de su papel fundamental en la traducción de ARNm en eucariotas, eIF4E ha sido ampliamente descrito como factor de susceptibilidad a virus de plantas, ya que puede ser reclutado por numerosos virus y permitir el establecimiento de la infección, participando en procesos fundamentales para el virus, como es la traducción de los ARNm virales. Más allá de su papel en la traducción canónica de los ARNm celulares, se han sugerido otras funciones para eIF4E en la biología de los organismos eucariotas, incluido el desarrollo sexual.

El silenciamiento de *EIF4E* mediante ARN de interferencia en plantas transgénicas se ha utilizado con éxito como un enfoque alternativo para generar resistencia a uno o varios virus en infecciones mixtas (Rodríguez-Hernández et al., 2012; Wang et al., 2013). La proteína VPg de los potyvirus puede interactuar específicamente con eIF4E o con eIF(iso)4E y esta especificidad está determinada por las combinaciones huésped-virus y puede variar de una cepa a otra (Nicaise et al., 2007; Schaad et al., 2000; Sato et al., 2005). Por lo tanto, a menudo, las mutaciones inducidas en una isoforma de eIF4E pueden proporcionar resistencia a un potyvirus determinado. Se han descrito varios aislados virulentos de potyvirus que superan la resistencia recesiva conferida por mutaciones en los alelos de *EIF4E/EIF(iso)4E*. En la mayoría de los casos, la superación de la resistencia se debe a mutaciones que resultan en la substitución de amino ácidos en la proteína VPg (Ayme et al., 2007; Moury et al., 2004). Aunque las substituciones en la VPg se han relacionado a veces con una mayor afinidad por la proteína eIF4E/(iso)4E

de resistencia (Charron et al., 2008), en otros casos no se ha observado esta mayor afinidad (Gao et al., 2004; Kang et al., 2005; Gallois et al., 2010).

Numerosos estudios sugieren que las isoformas de eIF4E y eIF4G son selectivas en la traducción de ARNm. Estudios en animales y plantas muestran que el destino final de las células germinales y embrionarias se ve muy afectado por los complejos de factores eIF4 exclusivos de esos tipos de células (Dinkova et al., 2005; Friday & Keiper, 2015; Cao & Richter, 2002; Minshall et al., 2007; Hernández et al., 2013; Henderson et al., 2009; Baker & Fuller, 2007; Ruffel et al., 2006). El uso conjunto de la genética y la bioquímica ha identificado funciones únicas para las isoformas eIF4E y eIF4G en reproducción. Además, las proteínas eIF4E de plantas, moscas y ranas tienen funciones únicas en el desarrollo sexual, a juzgar por los fenotipos reproductivos resultantes de sus deficiencias (Ghosh & Lasko, 2015; Rodríguez et al., 1998; Hernández et al., 2005; Patrick et al., 2014). Los virus podrían aprovechar estas funciones biológicas adicionales para controlar la estabilidad de sus proteínas, regular su replicación y facilitar su movimiento intra e intercelular.

Desde que se describió el sistema CRISPR/Cas9 como herramienta de edición del genoma, éste ha sido utilizado para crear mutantes resistentes a diversas enfermedades víricas en especies modelo y de cultivo, incluidas las cucurbitáceas. Para generar resistencia a virus de plantas, varios trabajos han elegido *EIF4E* o *EIF(iso)4E* como diana. En 2016, Pyott y sus colaboradores emplearon la tecnología CRISPR/Cas9 para editar el gen *EIF(iso)4E* en Arabidopsis. Los mutantes *knock-out* resultantes de la eliminación de *EIF(iso)4E* eran resistentes a la infección por el virus del mosaico del nabo (TuMV) sin afectar otros rasgos, incluyendo la biomasa y el tiempo de floración (Pyott et al., 2016). Chandrasekaran y sus colaboradores (2016) demostraron que plantas de pepino *knock-out* para *EIF4E* eran resistentes a una amplia gama de virus, incluyendo el virus de las venas amarillas del pepino (CVYV), el virus del mosaico amarillo del calabacín (ZYMV) y el virus de la mancha anular de la papaya (PRSV-W) (Chandrasekaran et al., 2016), todos ellos de la familia *Potyviridae*. Por último, Gómez y sus colaboradores (2019) demostraron que la edición simultánea mediada por CRISPR/Cas9 de las isoformas nCBP-1 y nCBP-2 de eIF4E en yuca redujo la gravedad y la incidencia de los síntomas de

la enfermedad de la estría marrón de la yuca causada por el ipomovirus del mismo nombre (Gómez et al., 2019).

Con estos antecedentes, los objetivos de esta tesis han sido los siguientes: (I) Generar, mediante la tecnología CRISPR/Cas9, líneas de melón no transgénicas mutadas en el gen que codifica eIF4E y, una vez obtenidas, comprobar la asociación de la mutación de *EIF4E* con el fenotipo de susceptibilidad al virus marroquí del mosaico de la sandía (*Moroccan watermelon mosaic virus*, MWMV), y el fenotipo de esterilidad masculina en melón. (II) Caracterizar el desarrollo floral y los procesos de diferenciación y determinación sexual a través de análisis morfológicos y transcriptómicos de flores de melón en diferentes estadios de desarrollo en una línea andromonoica. Y (III) evaluar el posible papel de eIF4E en el desarrollo de los gametos masculinos del melón mediante un análisis comparativo del desarrollo floral masculino en las plantas de tipo silvestre comparadas con las plantas mutantes *knock-out* de *EIF4E* obtenidas en el primer objetivo.

Específicamente, los resultados de esta tesis se dividen en tres secciones distintas. En la primera sección de los resultados, se describe la generación de un mutante *knock-out* de *EIF4E* mediante la edición del genoma mediada por CRISPR/Cas9. Las líneas mutantes T0 mostraron una deleción de un solo nucleótido en homocigosis que debe dar lugar a una putativa proteína eIF4E truncada; de manera significativa para esta tesis, la supresión de *EIF4E* originó un fenotipo de androesterilidad en melón. El cruce entre plantas transgénicas homocigotas para la mutación con plantas de tipo silvestre (WT) del mismo genotipo dio lugar a una generación F1 que incluía individuos no transgénicos que presentaban la misma deleción que en la T0, pero en heterocigosis. A continuación, se fecundaron individuos F1 fértiles no transgénicos para obtener una generación F2 totalmente libre de transgen. Las plantas de la generación F2 segregante fueron inoculadas con MWMV; las plantas homocigotas para la mutación de *EIF4E* mostraron resistencia al virus, mientras que las plantas heterocigotas y las no mutantes mostraron síntomas de la enfermedad. Tras cuatro meses desde la inoculación, se observaron síntomas de infección por MWMV en dos de las plantas resistentes. Estas plantas sintomáticas fueron positivas para MWMV por RT-qPCR, por lo que se realizó un ensayo de retroinoculación que confirmó la presencia de un aislado que superaba la

resistencia (*resistance-breaking*, RB). A continuación, se amplificó por RT-PCR el gen de la VPg de MWMV, se secuenció y se identificó una única sustitución de un nucleótido que daba lugar al cambio de aminoácido N163Y en el aislado RB. Dados los antecedentes publicados sobre la superación de la resistencia mediada por eIF4E en potyvirus, es muy probable que la mutación N163Y en la VPg de MWMV sea la responsable de la superación de la resistencia de las plantas editadas de melón. En cuanto a la fertilidad, todas las plantas homocigotas, y sólo ellas, mostraron el fenotipo de esterilidad masculina observado en T0, mostrando una perfecta correlación entre la segregación del fenotipo de esterilidad masculina y la segregación de la mutación en *EIF4E*.

Dado el interés, tanto en términos de investigación básica como en sus aplicaciones biotecnológicas y de mejora, del fenotipo de androesterilidad, y considerando la falta de información detallada sobre el posible papel de eIF4E en la determinación de la fertilidad en plantas, se decidió caracterizar este fenotipo mediante un estudio comparativo del desarrollo floral de las plantas mutantes con respecto al tipo silvestre del mismo fondo genético. Para abordar este objetivo, y dada la falta de estudios específicos sobre el desarrollo floral en melón, se realizó un estudio de desarrollo floral para conocer los mecanismos que subyacen al desarrollo floral en esta especie. Hasta donde sabemos, este es el único trabajo que describe la edición del genoma de melón con la tecnología CRISPR/Cas9 para lograr una resistencia de amplio espectro a virus, y el primer trabajo que describe la asociación entre la edición de *EIF4E* y el desarrollo de la esterilidad masculina en melón.

En el segundo apartado de los resultados de este trabajo, se realizó el análisis morfológico y transcriptómico de las flores de melón en diferentes etapas de desarrollo. En primer lugar, se analizó la morfogénesis de las flores masculinas y hermafroditas de melón, identificando mediante microscopía óptica y de barrido 12 estadios de formación floral, que van desde la aparición de los meristemos florales hasta la antesis. Las primeras diferencias estructurales entre las flores masculinas y hermafroditas aparecieron entre los estadios 6 y 7, por lo que se llevó a cabo una descripción detallada de las etapas que conducen a la formación de los órganos y estructuras en ambos tipos de flores. Por último, mediante el procesamiento de los datos transcriptómicos, y estableciendo una correlación entre los estadios de desarrollo y los episodios que

agrupan algunos de ellos, se identificaron los patrones de expresión de los genes expresados de forma diferencial que son específicos de un episodio determinado, identificando aquellos que definen el paso de un episodio al siguiente según el modelo ABCDE de desarrollo floral. Este trabajo integra un análisis morfológico por microscopía muy detallado, con un análisis transcriptómico exhaustivo para la caracterización de los mecanismos estructurales y moleculares que determinan la formación floral de un genotipo andromonoico en melón. En conjunto, nuestros resultados proporcionan una primera visión de las redes de regulación génica en el desarrollo floral de melón que pueden ser críticas para la floración y la formación de polen, destacando potenciales dianas para la manipulación genética con el fin de mejorar el rendimiento del cultivo de melón en el futuro. En este sentido, la tecnología CRISPR/Cas constituye una valiosa herramienta para la identificación de las funciones de los genes y el estudio de los mecanismos que subyacen al desarrollo floral en las cucurbitáceas para la investigación fundamental (Zhang et al., 2021), o, una vez identificados, para aprovechar las potenciales aplicaciones biotecnológicas a través de la edición del genoma, como en el caso de la generación de pepino ginóico no transgénico con CRISPR/Cas9 para la producción de híbridos (Hu et al., 2017).

En la tercera parte de este trabajo, se llevó a cabo un análisis comparativo del desarrollo floral masculino de melón entre las plantas de tipo silvestre y las mutantes *knock-out* de *EIF4E*, con el fin de investigar el papel de *EIF4E* en la formación de los gametos masculinos de melón. El análisis comparativo de las estructuras de las anteras realizado mediante microscopía mostró que el fenotipo de esterilidad es post-meiótico y esporofítico, ya que la inusual secreción de material proteico en los primeros estadios, y las diferencias en el momento de la degradación del tapetum en los últimos estadios entre el mutante y el WT, son característicos de este tipo de esterilidad. En consonancia con esto, los datos transcriptómicos identificaron una regulación general a la baja de los genes implicados en el desarrollo del tapetum y en la germinación del polen en las flores masculinas del mutante de *EIF4E* frente al WT. Por último, *EIF4G* mostró un patrón de regulación a la baja en tres de los cuatro episodios del desarrollo floral masculino en el mutante con respecto al WT. Dada la evidencia que apoya un papel diferencial de las isoformas de eIF4F en la traducción de los mRNAs en las células germinales, se ha

propuesto un modelo en el que la interacción entre eIF4E y eIF4G es un requisito previo para iniciar específicamente la traducción de los ARNm que codifican proteínas que limitan la formación de los gametos masculinos.

Este trabajo combina un detallado análisis morfológico comparativo por microscopía con un exhaustivo análisis transcriptómico para caracterizar la asociación entre la mutación en *EIF4E* y la generación de un fenotipo de androesterilidad. En conjunto, los resultados de esta tesis proporcionan una primera visión de las redes de regulación génica en el desarrollo de los gametos masculinos del melón que pueden ser críticas para la correcta formación y maduración del polen. Además, sugieren por primera vez un papel específico de *EIF4E* en la regulación de los procesos que determinan la fertilidad en melón.

Abbreviations

Virus abbreviations (alphabetical order)

BPYV	beet pseudo-yellows virus
CABYV	cucurbit aphid-borne yellows virus
CaMV	cauliflower mosaic virus
CGMMV	cucumber green mottle mosaic virus
CMV	cucumber mosaic virus
CuLCrV	cucurbit leaf crumple virus
CVYV	cucumber vein yellowing virus
CYSDV	cucurbit yellow stunting disorder virus
KGMMV	kyuri green mottle mosaic virus
LIYV	lettuce infectious yellows virus
LMV	lettuce mosaic virus
MNSV	melon necrotic spot virus
MWMV	Moroccan watermelon mosaic virus
PPV	plum pox virus
PRSV	papaya ringspot virus
PVY	potato virus Y
RYMV	rice yellow mottle virus
TEV	tobacco etch virus
ToLCNDV	tomato leaf curl New Delhi virus
TuMV	turnip mosaic virus
WmCSV	watermelon chlorotic stunt virus
WMV	watermelon mosaic virus
ZYMV	zucchini yellow mosaic virus

Other abbreviations and acronyms (alphabetical order)

eIF4E	eukaryotic translation initiation factor 4E
eIF4G	eukaryotic translation initiation factor 4G
3’ UTR	3´ untranslated region
3'-poly(A)	3’ polyadenylated tail
5’-cap	5’cap
5’ m7G cap	5’7-methylguanylate cap
ACS	1-aminocyclopropane-l-carboxylic acid synthase
AN	anthesis
BA	6-benzylaminopurine
bp	base pair
BP	bicellular pollen
C	canonical
CD	cap-dependent

cDNA	complementary DNA
CDS	coding sequence
CI	cap-independent
CITE	cap-independent translation enhancer
CMS	cytoplasmic male sterility
CP	capsid protein
CRISPR/Cas	clustered regularly interspaced short palindromic repeats nuclease
crRNA	CRISPR RNA sequence
DEG	differentially expressed genes
dMsp	degraded microspores
DNA	deoxyribonucleic acid
Ds	dyads
DSB	double strand break
DsRed	red fluorescent protein
E	epidermis
eIF3	eukaryotic translation initiation factor 3
eIFs	eukaryotic translation initiation factors
En	endothecium
ERM	elongation-rooting medium
ESTs	expressed sequence tags
FPKM	fragments per kilobase per million mapped reads
FS	floral structures
GI	gamete initiation
GM	gamete maturation
GMS	genic male sterility
GO	gene ontology
gRNA	Cas9 nuclease guide RNA
HDR	homology directed repair
IAA	indole-3-acetic acid
LB	Luria-Bertani
MAS	marked-assisted selection
MCM	minichromosome maintenance
MES	2-(N-morpholino) ethanesulfonic acid
miRNA	microRNA
ML	middle layer
MP	mature pollen
mRNA	messenger ribonucleic acid
MRs	morphogenic regulators
Ms	microsporocyte
MS	Murashige and Skoog
Msp	microspores
MTm	million metric tonnes
NAA	1-naphthaleneacetic acid
NC	non-canonical
NCBp	novel cap-binding protein
NHEJ	non-homologous end joining
nptII	*neomycin phosphotransferase II*

PABP	poly(A)-binding protein
PAM	protospacer adjacent motif
PCA	principal component analysis
PCD	programmed cell death
PCR	polymerase chain reaction
PMCs	pollen mother cells
RB	resistance breaking
R-Genes	resistance genes
RM	regeneration medium
RNA	ribonucleic acid
RNAi	RNA interference
RNA-Seq	RNA sequencing
rRNA	ribosomal RNA
RT-qPCR	reverse transcription quantitative polymerase chain reaction
SDGs	sex determination genes
SNP	single nucleotide polymorphisms
T	tapetum
TALEN	transcription activator-like effector-based nucleases
T-DNA	transfer DNA
Tds	tetrads
tracrRNA	crRNA transactivator sequence
VPg	viral protein genome-linked
WT	wild type
ZFNs	zinc finger nucleases

1 INTRODUCTION

1.1 Importance of melon

1.1.1 Statistics of melon cultivation

The family *Cucurbitaceae* consists mostly of low temperature sensitive, tendril-bearing vine plants that are distributed throughout the tropical and subtropical areas of the globe. Nonetheless, there are xerophytic species that can be adapted to harsher climatic conditions. This family consists of two subfamilies, eight tribes, about 120 genera and 800 species. They are mostly cultivated as crops, being fruits the most commonly eaten part of the plant, but seeds, flowers, tendrils, very young shoots, and roots are also used for food production (Nuñez-Palenius et al., 2008). Cucurbit fruits can have other destinations, as is the case *of Luffa* spp., which fully developed fruits are the source of scrubbing sponges used in bathrooms and kitchens. The most relevant cultivated cucurbits, based on total global production in 2020, are watermelon *(Citrullus lanatus* Thunb.), cucumber (*Cucumis sativus* L.), cantaloupe and other melons (*Cucumis melo* L.), pumpkin (*Cucurbita* spp.), and squash (*Cucurbita* spp.) (FAOstat). Among the major cucurbit vegetables, *C. melo* probably has the highest polymorphism in terms of fruit types and botanical varieties due to the genetic diversity in this species (Mliki et al., 2001). The world melon production was estimated at more than 27 million tons (MTm) in 2020, with the main producing countries being China (13.4 MTm), Turkey (1.8 MTm), India (1.3 MTm), Kazakhstan (1 MTm), Iran (0.85 MTm), Egypt and the United States (0.7 MTm), along with Spain, which is the eighth producer (FAOstat). In our country, the cultivation of melon has a relevant economic importance. National production is estimated at just over 610,978 tons, of which Murcia represents 29 %. Regarding the destination of production, almost 3/4 of the national melon (74 %) is destined for export, which places Spain as the main exporting country; in recent years, about 20 % of world exports came from of Spain (FAOstat), being Murcia the region that allocates most of its melon production for this purpose.

1.1.2 Botany and Origin of Cucumis melo

Most melon plants can develop into indeterminate vines up to 15 m long; however, modern cultivars have been bred to obtain shortened internodes, bushy appearance and concentrated production. The stem is round in shape, the leaves are simple, either three- or five-lobed, and borne singly at the nodes, and they may have a great variation in size, colour, and shape. Tendrils are borne in the leaf axis and are simple (unbranched) (Nuñez-Palenius et al., 2008). Melon fruits are generally classified as an indehiscent "pepo", which is a modified berry, characterised by three ovary sections termed locules. The edible fruit flesh is derived from the mesocarpic tissue or placenta. *Cucumis melo* L. includes all of the dessert melons often referred to as muskmelons. *Cucumis melo* is a species characterised by great polymorphism and has been further classified into groups. One of the most complete and widely used classifications is the early one proposed by the French botanist Charles Naudin (1859). Naudin ascribed domesticated melons to the group *C. melo* var. melo, while wild melons were assigned to a single variable taxon named *C. melo* var. agrestis, which includes melons of smaller-sized fruits, leaves, and flowers and often bitter or unpleasant taste of the fruit pulp (Naudin, 1859). Several classifications of cultivated melons have been proposed along the years, mainly attending to fruit traits such as shape, size, skin, pulp colour and aromas, maturation, and also to sex determination (Robinson and Decker-Walters 1999; Guis et al., 1998). The geographic origin of melon and its domestication history has been studied by Endl et al. (2018) among others. These authors sequenced seven DNA regions of a large collection of melon and wild relative accessions to infer their evolutionary origins. They found that modern melon cultivars belong to two lineages which may have diverged around 2 million years ago, one lineage restricted to Asia (*C. melo* subsp. melo) and the second to Africa (*C. melo* subsp. meloides); the Asian lineage has given rise to current commercial cultivars and market types, whereas the African lineage gave rise to cultivars grown regionally in Sudan (Endl et al., 2018). More recent genomic analyses using different accessions have confirmed Endl et al. (2018) results (Zhang et al., 2019; Liu et al., 2020; Demirci et al., 2021).

1.1.3 Flower development and sexual determination

The family *Cucurbitaceae* is characterised by intraspecific sexual systems that rely on conserved molecular pathways to give rise to different phenotypic outputs depending on the species. The flowers of many species are bisexual, developing both male (stamen) and female (carpel) reproductive organs (Figure 1.1). Melon may have different combinations of male, female or hermaphrodite flowers, depending on the genotype and environmental conditions (Figure 1.2). In important members of this family, such as cucumber and melon, sex determination has been demonstrated to depend on the developmental arrest of sex-specific organs during early stages of flower development. Previous studies on cucumber have identified 12 stages of development, from the floral meristem initiation (stage 1) to subsequent broadening and initiation of sepal, petal, stamen and carpel primordia (stages 2 to 5 respectively). From stages 6 onwards, flower ontogenesis can take two different paths depending on the developmental fate of the flower (Table 1.1). While in unisexual flowers sexual determination depends on the specific repression of one of the male or female organ primordia by the activation or inactivation of specific genes (Hao et al., 2003; Bai et al., 2004) thereby promoting the exclusive formation of male or female (imperfect) flowers, bisexual flowers depend on the simultaneous differentiation of both stamen and pistil, giving rise to a hermaphrodite (perfect) flower. At least three sex-determining loci, *A* (*andromonoecious*), *G* (*gynoecious*) and *M* (*monoecious*), are involved in sex determination in melon, and the development of male or female reproductive structures is thought to occur as a result of a developmental selective arrest driven by genes involved in ethylene biosynthesis, transcription factors and epigenetics, whose allele interactions can lead to a variety of sexual phenotypes (Table 1.1) (Boualem et al., 2008, 2009, 2015; Martin et al., 2009).

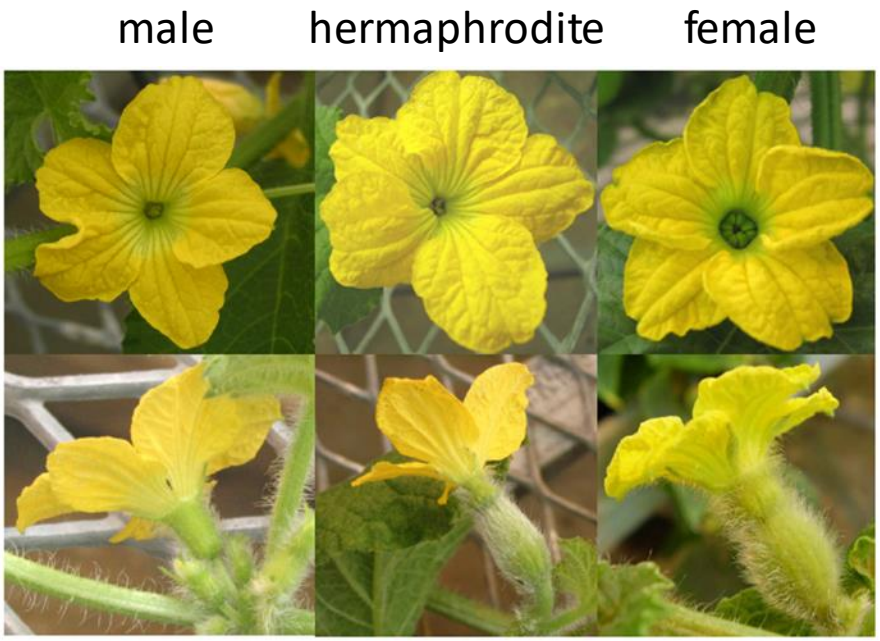

Figure 1.1. Top and side view of male (cv. 'Hale's Best Jumbo'), bisexual (cv. 'Hale's Best Jumbo') and female (cv. 'Wisconsin 998') melon flowers at anthesis. Bisexual and female flowers have a pronounced inferior ovary. Pistils in the bisexual flower are largely hidden by stamens. Figure modified from Grumet et al. (2007).

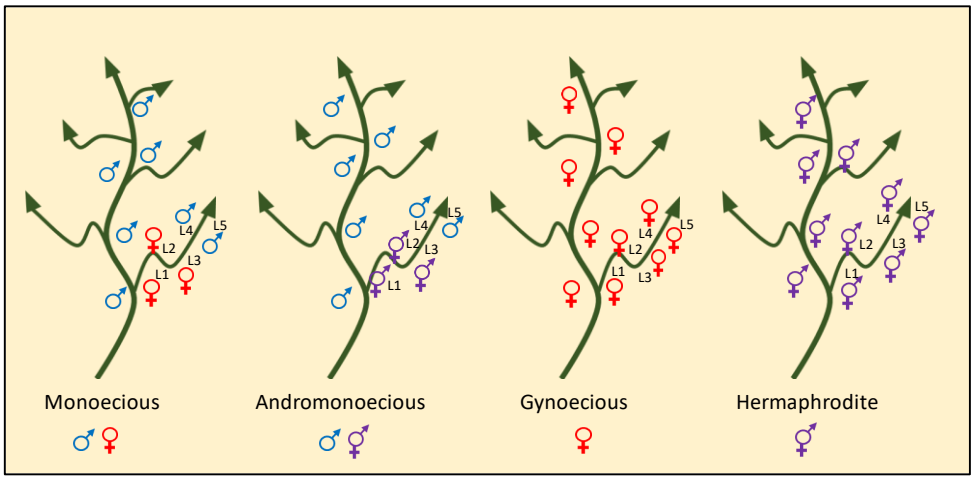

Figure 1.2. Schematic representation of sexual morphologies and genotypes present in melon. Monoecious melon lines develop male flowers in the main stem. In the lateral branches, female flowers are located in the first three nodes, followed by male flowers in the subsequent nodes. Andromonoecious lines present the same distribution but instead of female, hermaphrodite flowers develop. Gynoecious and hermaphrodite lines develop only female and hermaphrodite flowers, respectively. Figure modified from Boualem et al. (2015).

Table 1.1. Genotype and sex loci combination of melons sexual systems

Genotype			Phenotype	Developmental progression
G locus	M locus	A locus		
wip1/wip1	*acs7/acs7*	*-/-*	Hermaphrodite	Bisexual
WIP1/-	*acs7/acs7*	*ACS11/-*	Andromonoeciuos	Male, bisexual and male
wip1/wip1	*ACS7/-*	*-/-*	Gynoecious	Female
WIP1/-	*ACS7/-*	*ACS11/-*	Monoecious	Male, female and male

(-) stands for the existence of any allelic variant at the corresponding locus

Environmental conditions and exogenous hormone applications can cause a conversion between sexual types of developing buds or cause them to appear at earlier or later nodes (*e.g*., female to male or bisexual; bisexual to male or female). In general, the supply of gibberellins promotes masculinity, while brassinosteroids, auxins and ethylene promote feminisation (Pawełkowicz, 2019). In cucumber, ethylene production by shoot apices has been related to sexual type, so that gynoecious lines can produce up to 2-3 times more ethylene than monoecious or andromonoecious lines (Yamasaki et al., 2003). Consistent with the role of ethylene as a feminizing agent, *CmACS11* and *CmACS7*, that have been previously described to be determinant in the development of sex specific floral organs, are members of the *1-aminocyclopropane-l-carboxylic acid synthase* (*ACS*) gene family, which is involved in many steps of the ethylene biosynthetic pathway. In monoecious melon and cucumber, sex is determined by the differential expression of sex determination genes (SDGs) and adoption of sex-specific transcriptional programs; *CmACS11* and *CmWIP1* are master SDGs, whereas histone modifications such as H3K27me3 seem to be a hallmark associated to unisexual flower development (Boualem et al., 2008, 2015; Rodriguez-Granados et al., 2021).

In melon, a model has been proposed integrating both genetic and epigenetic aspects of sex determination (Figure 1.3). According to this model, flower sexuality depends on the differential expression of functional and non-functional (allelic variants) proteins encoded by the *A*, *M* and *G* genes. Hermaphrodite lines result from the simultaneous inactivation of stamen *CmACS7*, and carpel *CmWIP1*, inhibitors (Figure 1.3B). Male flower in monoecious and andromonoecious lines results from the lack of

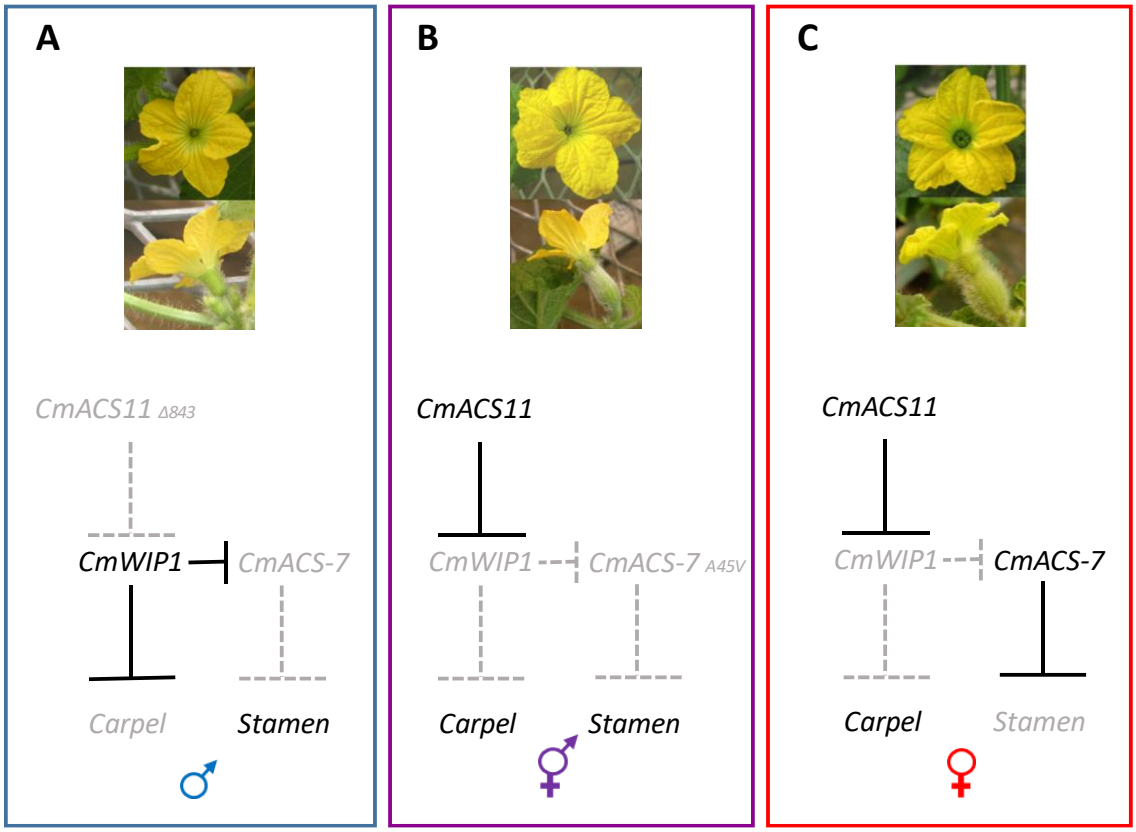

Figure 1.3. Sex determination pathway in melon. Genetic pathway leading to the development of male (A), hermaphrodite (B) and female flowers (C). Figure modified from Boualem et al. (2015).

expression of *CmACS11*, thus *CmWIP1* is expressed and it can repress carpel development and *CmACS7* expression (Figure 1.3A). By contrast, female flower development in monoecious plants is promoted by the expression of *CmACS11*, which represses *CmWIP1* and allows the expression of *CmACS7* (Figure 1.3C). The andromonoecious phenotype emerges from the expression of a non-functional *CmACS7* allele giving rise to hermaphrodite flowers instead of female (Figure 1.3B). More recently, other studies have linked increased differential expression of ethylene biosynthetic genes *1-aminocyclopropane carboxylate synthase and oxidase* (*ACS*, *ACO*) to the development of sexual organs in cucumber (Chen et al., 2016; Zhang et al., 2021). MADS-box genes also play a central role in plant development processes, especially in floral organ development. The ABC model, later expanded to include D- and E-class genes, of floral development was established through several studies on model plants, such as Arabidopsis and *Antirrhinum majus* (Coen & Meyerowitz, 1991, Ditta et al. 2004). The development of sex-specific organs relies on the combinatorial and differential

expression of homeotic genes over time and space (Guo et al., 2015). In this model, A- and -E function genes (APETALA1 (AP1)-SEPALLATA (SEP)) are involved in the determination of sepal development; A-, B-, and E-class proteins (AP1-SEP-AP3-PISTILLATA (PI)) determines petals; the B-, C-, and E-class complex (AGAMOUS (AG)-SEP-AP3-PI) specifies stamens; the C- and E-class complex (AG-SEP) specifies carpels and the D- and E-class complex (SEEDSTICK (STK)-SEP) specifies ovules (Bowman et al., 2012; Guo et al. 2015). Despite the extensive research on MADS-box genes in Arabidopsis (Pařenicová et al., 2003), and cucumber (Hu & Liu, 2012), in depth research on melon MADS-box genes has not been performed apart from the genome-wide identification of the MADS-box gene family in melon performed by Hao et al. (2016). A recent study showed that melon homologs to Arabidopsis LIKE HETEROCHROMATIN PROTEIN1 (HP1), *CmLHP1* A and B, redundantly control several aspects of plant development, including sex expression. The *Cmlhp1ab* double mutants obtained in that study, in fact, displayed pleiotropic phenotypes together with a general increase of the male:female ratio associated with a general deregulation of some hormonal response genes and a local activation of male-promoting SDGs and MADS-box transcription factors (Rodriguez-Granados et al., 2021).

1.1.4 The melon genome and transcriptome

The availability of genome sequences from higher plants is an important resource for understanding plant evolution and the genetic variability existing within cultivated species. Genome sequences are also becoming a strategic tool for the development of methods to improve plant breeding. Due to the great economic and scientific interest in melon plants, numerous genetic and molecular tools have been developed over the years. One of the most important milestones in melon genetics was the *de novo* sequencing of the genome of the DHL92 line (Garcia-Mas et al., 2012). A whole-genome shotgun strategy was used which resulted in 14.8 million single-shotgun and 7.7 million paired-ends reads. After filtering the mitochondria and chloroplast genome, 13.52x coverage of the melon genome (450 Mb in size) was obtained (Garcia-Mas et al., 2012). Annotation of the assembled genome resulted in the prediction of

27,427 genes with 38,848 predicted transcripts encoding 32,487 predicted polypeptides. The average gene size was 2,776 bp with 5.85 exons per gene (similar to Arabidopsis) and a density of 7.3 genes per kb. A total of 18,948 genes (69.1 %) supported by a transcript and/or protein alignment were detected. For each protein sequence, protein signatures and orthologous groups were identified and orthology-derived information was used to annotate metabolic pathways (Garcia-Mas et al., 2012). Further improvements of the assembly of the melon DHL92 pseudochromosomes were introduced by using targeted single nucleotide polymorphisms (SNP) selection and long reads provided by single-molecule sequencing (Argyris et al., 2015; Castanera et al., 2020). Refinement of the DHL92 genome annotation has resulted in a succession of versions for which the more recent one is v4, as included in the Melonomics database (https://www.melonomics.net/melonomics.html#/) (Ruggieri et al., 2018). Melonomics, which has been extensively used in this work, contains a JBrowser and other powerful tools to explore the melon genome and transcriptome (see below). Together with Melonomics, I have also used the IcuGI database, which contains the melon DHL92 genome v3.6.1 (http://cucurbitgenomics.org).

After García-Mas et al. (2012) pioneering work, other melon genomics initiatives have been developed. The Japanese melon cultivar 'Harukei-3' is known for its excellent sweetness and rich aroma. Yano and co-workers (2020) used 'Harukei-3' melon as standard material for genetic and molecular biological studies, developing the 'Melonet-DB' database (https://melonet-db.dna.affrc.go.jp/ap/top) to enable efficient searching of genomic and gene function information in the Harukei-3 reference genome (Yano et al., 2020).

In addition to whole genome sequencing, another fundamental tool for gene discovery, large-scale expression analysis and genome annotation is the description of whole transcriptomes. Early work by Gonzalez-Ibeas et al. (2007) and Blanca et al. (2011) resulted in the sequencing of large collections of melon expressed sequence tags (ESTs) from cDNA libraries from different melon cultivars and conditions (Gonzalez-Ibeas et al., 2007; Blanca et al., 2011). These works were instrumental for the annotation of the DHL92 genome assembly (García-Mas et al., 2012), and also for the design of a melon microarray (Mascarell-Creus et al., 2009) which has been used in numerous functional

analyses (*e.g.*, Gonzalez-Ibeas et al., 2012; Gómez-Aix et al., 2016). The sharp decrease in the costs associated to high-throughput sequencing has allowed massive RNA sequencing to be generally adopted for melon transcriptomes description. RNA-Seq and all variants of massive RNA sequencing, including small and long non coding RNA sequencing, have been used to describe and compare melon transcriptomes for a large variety of genotypes, tissues and conditions (*e.g.*, Sáez et al., 2022; Villalba-Bermell et al., 2021; Chen et al., 2021). The 'Melonet-DB' database (https://melonet-db.dna.affrc.go.jp/ap/top) includes an interesting gene expression atlas with a graphical display which I have used extensively along my thesis.

1.1.5 Viruses affecting melon crops

About 30 plant viruses are currently cited affecting cucurbits production in the Mediterranean basin (Lecoq et al., 2003; Lecoq & Desbiez, 2012). The occurrence of new viral diseases is becoming more and more common due to the evolution of the pathogens, the increased seed and fruits trade, the intensification of cultural practices, and to climate change (Navas-Castillo et al., 2014; Pozzi et al., 2020). The emergence of viruses affecting cucurbit species, leading to economic losses and endangering food security, has been observed and studied for decades. Common symptoms caused by viruses in cucurbits comprise leaf mosaic and curling, plant size reduction, severe wilting, deformation, decolouration, mottling, yellowing and necrosis which affect the aesthetic value, the yields and the quality of produced fruit (Blancard et al., 1994). Effective disease prevention and management strategies depend on knowledge of the viruses and their vectors (including biological properties and epidemiology), the application of prophylactic measures, and recourse to biological and chemical control methods (Radouane et al., 2021). Cucurbits in general, and melon in particular, are infected by a variety of viruses belonging to different families. The family *Geminiviridae* (especially begomoviruses like tomato leaf curl New Delhi virus (ToLCNDV)) includes the largest number of viruses reported to cause significant economic losses to cucurbit production (Lecoq & Desbiez, 2012). Other economically important viruses belong to families *Potyviridae*, *Bromoviridae*, *Vergaviridae* and *Luteoviridae*. These include

cucurbit aphid-borne yellows virus (CABYV), watermelon mosaic virus (WMV), Moroccan watermelon mosaic virus (MWMV), zucchini yellow mosaic virus (ZYMV), papaya ringspot virus (PRSV), cucumber mosaic virus (CMV), which are transmitted by aphids; whereas cucurbit yellow stunting disorder virus (CYSDV), beet pseudoyellows virus (BPYV) and cucumber vein yellowing virus (CVYV) are transmitted by whiteflies. Finally, it is worth mentioning cucumber green mottle mosaic virus (CGMMV) which is a tobamovirus mainly seed-borne and mechanically-transmitted. Most of these viruses are associated with important economic production losses at a global scale and in most Mediterranean countries (Adams et al., 2011; Lecoq & Desbiez, 2012), including Spain (Luis-Arteaga et al., 1998; Kassem et al., 2007; 2013; Juarez et al., 2013; Juárez et al., 2019) (Figure 1.4).

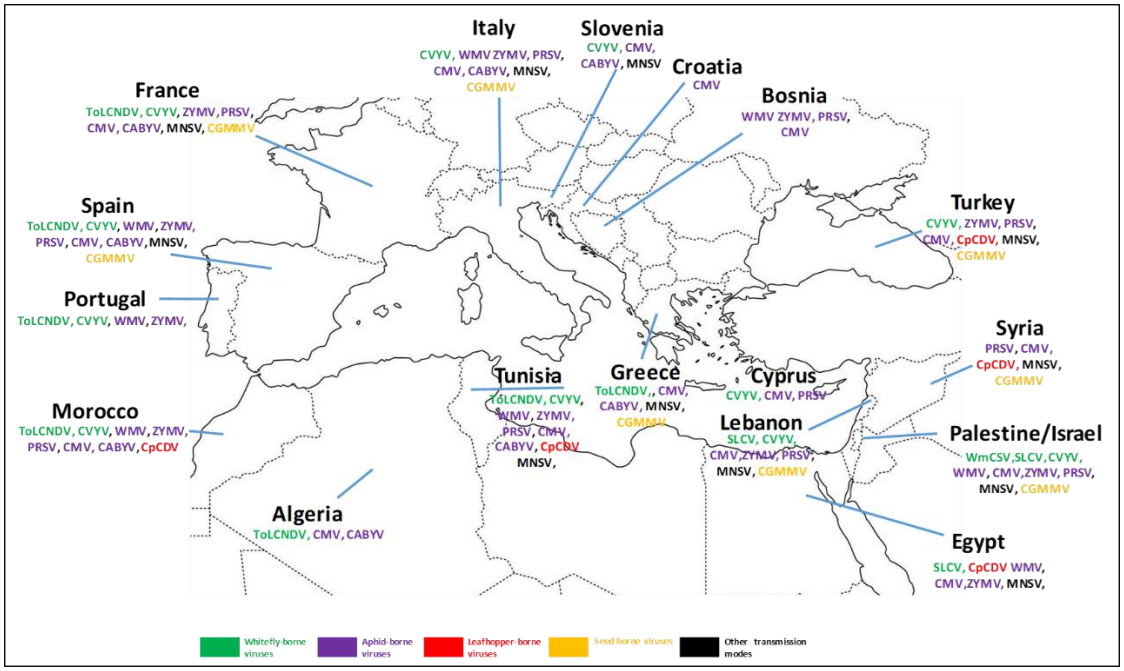

Figure 1.4. Geographic distribution of viruses affecting melon crops in the Mediterranean region. Figure modified from Radouane et al. (2021).

1.2 Genetic resistance as a strategy for the control of plant diseases caused by viruses

1.2.1 Plant pathogenic viruses

Viruses constitute the second group of plant pathogens, after fungi, in terms of number and importance of diseases they provoke (Pérez & Garcia-Arenal., 2005). As discussed in the previous section, diseases caused by viruses affect food quality and reduce cucurbit yields, and are very difficult to control due to the lack of effective control measures. Plant viruses are obligate parasites that exploit the host cellular machinery to complete their life cycle. Viral particles, usually composed of one or multiple strands of nucleic acids protected by a protein-like envelope called capsid, penetrate the cell and release the viral genome, initiating the infectious cycle. This cycle includes the expression and replication of the viral genome, the assembly of new virions and the cell-to-cell and long-distance movement of newly formed nucleoprotein complexes (Hull et al., 2016). As parasitic organisms, the survival of viruses depends on their ability to be transmitted to new hosts. This process is central to the study of the ecology and epidemiology of plant viruses and can be of two types: vertical, if it is transmitted to the offspring of the host, or horizontal, if the virus is transmitted to other plants (Cooper & Jones, 2006; Jones, 2009, Jones, 2014; Jones & Naidu, 2019; Malmstrom et al., 2011). As partly commented in previous sections, there are numerous modes of viral transmission, ranging from transmission by infected seed or pollen, the vegetative spread of infected plants, contact with contaminated soil and water, to the more common routes of transmission by vectors such as insects, acarids, zoosporic fungi or root-knot nematodes. Another common route of transmission is through wounds caused by pruning and other cultural practices (Hull, 2016; Jones, 2018). Due to the lack of antiviral compounds in agriculture, it is necessary to use combined strategies to control viruses in order to mitigate losses caused by them.

The use of resistant varieties, where possible, is one of the fundamental tools in integrated virus control programmes. The use of genetic resistance to viruses, either

natural or engineered, has often proved to be the only viable control strategy against a number of viral diseases (Fraser, 1990). This method of control has proved to be the most efficient in the long term, as it appears not to affect native fauna in the affected areas, minimize the use of polluting pesticides and can be easily coupled with other complementary control measures. Therefore, the search for sources of resistance to virus diseases and their application is considered one of the most desirable strategies to reduce losses caused by viruses (Revers & Nicaise, 2014).

1.2.2 Breeding for resistance

The development of resistant cultivars that are not compromised in their high productivity and excellent quality remains a challenge for breeders (Koornneef & Stam, 2001; Strange & Scott, 2005). Breeders and plant pathologists traditionally approach breeding for resistance in the following ways: (i) screening germplasm collections to identify sources of resistance and characterise their phenotypes; (ii) studying genetic inheritance mechanisms and identifying markers to be used in marked-assisted selection (MAS) (Collard & Mackill, 2008); and (iii) introducing resistance traits into elite cultivars and testing their performance under pathogen challenge in the field (Harrison, 2002; Gómez et al., 2009).

Among cucurbits, an important part of the available information refers to resistance to melon viruses. The majority of resistances have been identified in accessions of the subspecies agrestis, mainly in the Asian groups conomon, momordica, and acidulus. Some particularly important accessions show resistance to several viruses, as in the case of the Indian accessions PI 414723 and PI 124112 that are resistant to many potyviruses (Anagnostou et al., 2000). Others bear resistances to viruses of different families, like the Korean accession PI 161375, resistant to CMV, melon necrotic spot virus (MNSV), Kyuri green mottle mosaic virus (KGMMV), and BPYV; the Indian PI 313970, resistant to CYSDV, CABYV, watermelon chlorotic stunt virus (WmCSV), lettuce infectious yellows virus (LIYV), and Cucurbit leaf crumple virus (CuLCrV); and the African TGR-1551, resistant to WMV, CYSDV, and CABYV (Pitrat, 2016). These accessions are

very powerful genetic resources for pyramiding diverse resistances in elite cultivars (Martín-Hernández & Picó, 2021).

1.2.3 Mechanisms of virus resistance in plants

Once a virus is transmitted to a plant, it must be able to replicate in infected primary cells, move to adjacent cells via plasmodesmata, colonise the whole plant from primary foci through vasculature, and then be acquired by vectors to reinitiate the infection cycle. Due to the small size of their genomes, viruses need to recruit host factors to complete their infective cycle. A compatible interaction between host factors and viral products can result in susceptibility. Otherwise, an incompatible interaction, due to a modification or absence of the correct version of one or more of these factors, determines the suppression or a drastic reduction of viral accumulation, leading to resistance (Fraser, 1990; Gómez et al., 2009). Host factors that determine the compatibility of the virus-plant interaction are called susceptibility factors (Truniger & Aranda, 2009) or proviral factors (Garcia-Ruiz, 2018; Garcia-Ruiz, 2019) (Figure 1.5A).

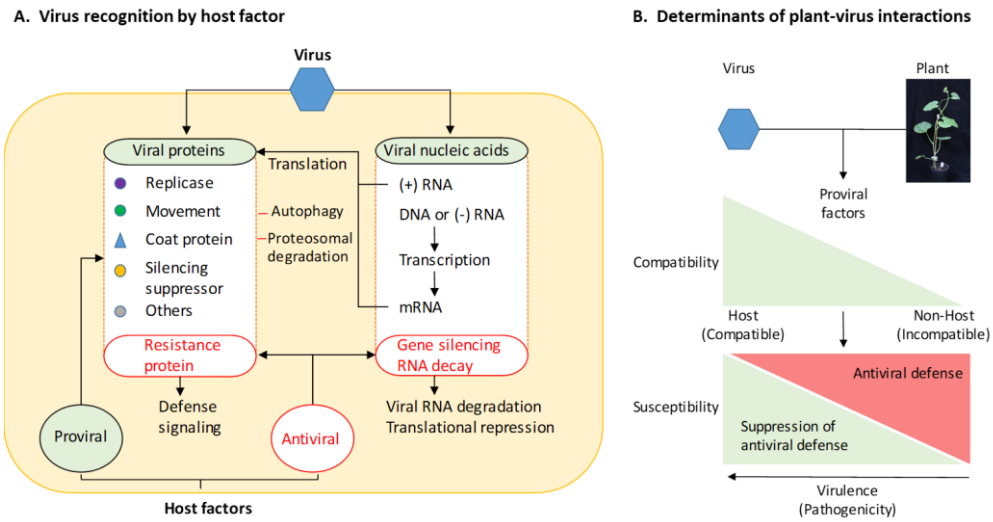

Figure 1.5. Genetic determinants of plant–virus interactions. (A) Viruses encode proteins to execute parts of the infection cycle. Their expression is dependent on the host RNA translation machinery. Their activity requires host factors (pro-viral) and resources. Antiviral immunity consists of host factors that target viral proteins or nucleic acids to restrict virus infection. (B) A two-step model in plant–virus interactions. Compatibility is determined by the availability of pro-viral host factors. Susceptibility is determined by the balance between antiviral defence and suppression of antiviral defence. Figure modified from Garcia-Ruiz (2019).

They enable the establishment of infection by participating in fundamental processes for the virus, such as viral RNA translation, the formation of replication complexes, viral accumulation and replication, local or systemic virus movement, virion assembly and transmission (Garcia & Pallás, 2015). The absence or elimination of one or more susceptibility factors will result in an unsuccessful plant-virus interaction, which will impact on virus infectivity, replication and movement (Hofius et al., 2007; Lellis et al., 2002; Wang & Nagy, 2008) (Figure 1.5B).

Plants, on the other hand, have virus defence mechanisms in the form of so-called antiviral factors. These are innate immunity, gene silencing or repression of protein translation and degradation mediated by autophagy or ubiquitination (Garcia-Ruiz, 2018; Wu et al., 2019) (Figure 1.5A). The establishment of an infection is then genetically determined both by the presence of susceptibility factors and by the balance between host defence mechanisms and the suppression of defence responses by the virus (Garcia-Ruiz, 2019) (Figure 1.5B).

1.2.4 Resistance mediated by proviral or susceptibility factors

Susceptibility factor-mediated resistance is more correctly defined as loss of susceptibility or passive resistance. This type of resistance is usually recessive, as a single copy of the allele is sufficient for the virus to complete its life cycle (Fraser, 1990; Nicaise, 2014; Diaz-Pendon et al., 2004; Truniger & Aranda, 2009; Hashimoto et al., 2016; Garcia-Ruiz, 2018). Recessive resistances have been described more frequently against plant viruses than against other pathogens, in which dominant R genes predominate. In fact, it is known that approximately 50 % of the alleles responsible for virus resistance are recessive (Kang et al., 2005; Truniger & Aranda, 2009). Moreover, this type of resistance is more frequent against potyviruses than against other types of viruses (Diaz-Pendon et al., 2004). At present, the most frequent and best characterised passive resistance mechanisms are those based on the eukaryotic translation initiation factors (eIF) 4E and 4G and their isoforms (Julio et al., 2015; Revers and Nicaise, 2014; Sanfaçon, 2015; Truniger & Aranda, 2009; Wang & Krishnaswamy, 2012), which will be discussed in

detail below. In recent years, an increasing number of recessive resistance genes that do not encode translation initiation factors have been described. Examples are the *ra* gene, which prevents vascular transport of potato virus A (PVA) (Hämäläinen et al., 2000), or the *rlm1* and *rpv1* genes that confer resistance to lettuce mosaic virus (LMV) and plum pox virus (PPV) respectively, and are located in a genomic region that does not contain genes encoding translation factors (Decroocq et al., 2006; Revers et al., 2003). Other genes that do not co-segregate with *EIF4E* or *EIF4G* are the *dstm1* gene, which confers resistance to TMV (Serrano et al., 2008) or *sha3*, that confers systemic resistance to PPV (Pagny et al., 2012). Mutations in *TOM1* and *TOM2* confer resistance to TMV as these genes encode transmembrane proteins located in the tonoplast necessary for virus replication (Ishibashi et al., 2012; Ishibashi & Ishikawa, 2013). The study of plant-virus interactions and the identification of new susceptibility factors are important activities for the identification of new sources of resistance and, therefore, for the breeding of new resistant varieties.

1.2.5 The role of eIF4E as a virus susceptibility factor

Screening of a collection of *A. thaliana* mutants identified *lsp1*, in which replication and/or expression of the potyviruses tobacco etch virus (TEV) and turnip mosaic virus (TuMV) genomes was suppressed. *Lsp1* codes for eIF(iso)4E (Lellis et al., 2002). Since then, other studies have demonstrated the involvement of eIF4E and its isoforms in resistance mechanisms against other potyviruses and viruses of other groups, such are bymoviruses (Kanyuka et al., 2005; Stein et al., 2005), cucumoviruses (Yoshii et al., 2004), ipomoviruses (Chandrasekaran et al., 2016), sobemoviruses (Albar et al., 2006), gammacarmoviruses (Nieto et al., 2006) and waikiviruses (Wang & Krishnaswamy, 2012). The genomes of potyviruses possess a 3'-poly(A) tail and a covalently linked virus-encoded protein (VPg) at the 5'-end. The VPg cistron encodes an avirulence determinant in many potyvirus/host combinations (Ayme et al., 2006; Borgstrøm & Johansen, 2001; Moury et al., 2004; Robaglia & Caranta, 2006), and eIF4E/VPg interactions appear to correlate with virus infectivity (Léonard et al., 2000; Charron et al., 2008). However, the exact molecular mechanisms underlying eIF4E-

mediated potyvirus resistance remain unravelled. As the main function of eIF4E in cellular mRNA translation consists of binding the cap structure to the 5' mRNA end and promoting recruitment of the translation machinery, it has been suggested that VPg may act as a cap surrogate, such that the specific eIF4E/VPg interaction may be required for translation initiation of viral genomic mRNAs (Léonard et al., 2000; Charron et al., 2008). However, other studies have suggested that the role of eIF4E in the potyvirus viral cycle may be distinct from its physiological function of cellular mRNA translation (Gallois et al., 2018). Natural recessive resistance to potyviruses is generally associated with mutations of *EIF4E* or *EIF(iso)4E* that disrupt their interaction with the VPg protein. Most of these mutations are localised in two surface-exposed regions of eIF4E near the cap-binding pocket (Charron et al., 2008; Moury et al., 2014). However, mutations in the pepper *EIF4E pvr1* allele that conferred resistance to TEV presented no correlation with reduced cap-binding activity (Kang et al., 2005). Trans-complementation studies of naturally occurring mutated *EIF4E* alleles (pea *sbm1* and lettuce *mo1* resistance genes) with overexpressed wild-type or mutated forms of eIF4E have also demonstrated that mutants of eIF4E isoforms with weak interactions with potyviruses are not affected in their ability to bind to the cap structure or to other translation factors (Charron et al., 2008; Ashby et al., 2011; German-Retana et al., 2008). Consequently, sometimes, mutated eIF4E isoforms implicated in virus resistance are fully functional in cellular mRNA translation.

Resistance conferred by eIF4E variants is not limited to members of the family *Potyviridae*, but can also target other (+) strand RNA viruses. For instance, a well-studied case of natural recessive resistance is that of the melon *nsv1 EIF4E* allele against MNSV (genus *Gammacarmovirus*, family *Tombusviridae*) (Nieto et al., 2006). The MNSV RNA genome is neither capped nor polyadenylated and also not bound to a VPg. Virulence in the MNSV-264 strain is dependent on mutations in the 3’ UTR, more specifically in a cap-independent translation enhancer (CITE) sequence (Truniger et al., 2008; Díaz et al., 2004). The 3’ CITE from the avirulent MNSV strain is only capable of promoting translation in resistant melon cells if the *EIF4E* allele from susceptible melon is provided *in trans*. By contrast, the 3’ CITE from the MNSV-264 strain directs effective translation in both susceptible and resistant melon (Truniger et al., 2008).

EIF4E forms the eIF4F complex, which also includes the scaffolding eIF4G protein. eIF4F controls cap-dependent translation initiation. Perhaps not surprisingly, mutations in eIF4G have also been shown to associate to recessive resistance to plant viruses. For instance, eIF(iso)4G corresponding to several alleles of *rymv1* naturally found in *Oryza sativa* (rymv1-2) or *O. glaberrima* (*rymv1-3, rymv1-4, rymv1-5*) have been described to be correlated with resistance to rice yellow mottle virus (RYMV) in rice (Albar et al., 2006; Thiémélé et al., 2010).

1.2.6 eIF4E biotechnology and virus resistance

Silencing *EIF4E* by RNA interference in transgenic plants has been successfully used as an alternative approach to engineer resistance to one or several viruses (Rodríguez-Hernández et al., 2012; Wang et al., 2013). Additionally, overexpression of mutated *EIF4E* (or *EIF(iso)4E*) alleles has been used to transfer resistance from one plant species to another (Kang et al., 2007; Kim et al., 2014). The potyvirus VPg protein can interact specifically with either eIF4E or eIF(iso)4E and this specificity is determined by host-virus combinations and can vary from one strain to another (Nicaise et al., 2007; Schaad et al., 2000; Sato et al., 2005). Hence, mutations induced in a single eIF4E isoform can often provide resistance to a target potyvirus. Yeast two-hybrid screens, *in vivo* bimolecular fluorescence complementation assays or *in-vitro* co-immunoprecipitation can be useful preliminary steps to identify the specific plant eIF4E isoform-VPg interaction for the virus prior to engineering potyvirus resistance based on manipulation of eIF4E isoforms. Nevertheless, some potyviruses have been shown to recruit either eIF4E or eIF(iso)4E indistinctly and down-regulation or mutation of both isoforms may be necessary to induce durable resistance (Rubio et al., 2009; Hwang et al., 2009; Jenner et al., 2010). In addition, some plant species present multiple functional copies of *EIF4E* (or *EIF(iso)4E*) genes that may be used specifically or interchangeably by potyviruses. It is the case of some *Brassica rapa* lines that present three copies of *EIF(iso)4E* and TuMV was shown to use at least two of these genes (Jenner et al., 2010). Similarly, distinct potyviruses interact with tomato *EIF4E1* and/or *EIF4E2* genes and simultaneous silencing of both genes was required to provide broad-spectrum virus resistance (Mazier

et al., 2011). Furthermore, due to the essential role of eIFs for plant viability, silencing of *EIF4E*, *EIF4G* or *EIF4A* and their corresponding isoforms can lead to imbalances in normal plant development and even to a lethal phenotype (Nicaise et al., 2007; Patrick et al., 2014).

1.2.7 eIF4E resistance durability

Several virulent potyvirus isolates have been described to overcome recessive resistance conferred by mutations in *EIF4E/(iso)4E* alleles. In most cases, the overcoming of resistance has been due to mutations in the VPg protein (Ayme et al., 2007; Moury et al., 2004). Although mutations in the VPg have sometimes been linked to an increased affinity for the resistance eIF4E/iso4E protein (Charron et al., 2008), in other cases this increased affinity has not been observed (Gao et al., 2004; Kang et al., 2005; Gallois et al., 2010). In at least one case, mutation of VPg does not increase its affinity for other eIF4E isoforms either, excluding the possibility that other isoforms of eIF4E are used by the virulent virus (Gallois et al., 2010). So, it was proposed that the mutated VPg may bind to other viral or host factors associated with the VPg-eIF4E complex. It is the case of the lettuce *mo1* resistance gene, that was shown to be overcome by mutations in the CI protein in virulent LMV isolates (Abdul-Razzak et al., 2009; (Sorel, Svanella-Dumas, et al., 2014). The CI protein is a multifunctional protein that interacts with both VPg and eIF4E (Tavert-Roudet et al., 2012). The CI-VPg-eIF4E complex may be necessary for viral replication and/or movement, possibly in association with eIF4G and microtubules (Wang & Krishnaswamy, 2012; Sorel, Garcia, et al., 2014). Viruses can evolve towards resistance breaking through the acquisition of mutations that either restore compatible interactions with the mutated host susceptibility factor, as seen in pepper (*Capsicum annuum*) with the *pvr2*/eIF4E1 resistance breakdown (Charron et al., 2008), or that possibly allow potato virus Y (PVY) to switch from eIF4E to the isoform eIF(iso)4E, as recently suggested in tobacco (*Nicotiana tabacum*) (Takakura et al., 2018) (Figure 1.6).

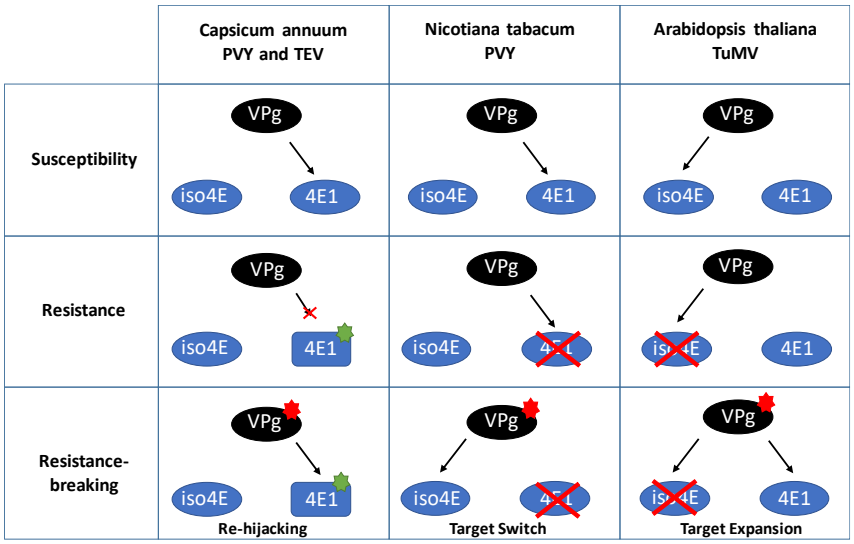

Figure 1.6. Different resistance-breaking pathways for potyviruses in plants. Potyviruses are represented by their VPg (main virulent determinant for *eIF4E*-mediated resistance). Two plant translation initiation factors are represented: eIF4E1 (4E1) and its isoform eIF(iso)4E (iso4E). Mutations affecting eIF4E1 or the viral VPg are represented by green and red stars, respectively. Knock-out mutants for *eIF4E* or *eIF(iso)4E* are crossed out. The figure is a schematic representation of resistance-breaking strategies in *Capsicum annuum, Nicotiana tabacum* and *Arabidopsis thaliana* as mentioned in the text, respectively. Briefly, in *Capsicum annuum*, mutation in the viral VPg allows the virus to hijack the resistant eIF4E1 protein; in *Nicotiana benthamiana*, it allows the virus to recruit eIF(iso)4E while losing its initial ability to recruit eIF4E1; finally, in *Arabidopsis thaliana*, it allows the virus to recruit both eIF4E1 and eIF(iso)4E. Figure modified from Gallois et al. (2010).

Lastly, Bastet et al., (2018) showed how mutation within the TuMV-VPg, associated with loss-of-function (knock-out) of *EIF(iso)4E* resistance-breaking (Gallois et al., 2010), expanded the virus ability to recruit both isoforms, eIF(iso)4E and eIF4E1. These results indicate that the interaction potyviruses/eIF4E isoforms is complex and the resistance can be overcome by mutations in various regions of the viral genome. Studies on the co-evolution between PVY and *EIF4E* recessive resistance alleles in *Capsicum* species did not reveal clear trends, possibly because of pleiotropic effects of mutations in the VPg protein, making difficult the prediction of virulence emergence (Moury et al., 2014). However, it has been suggested that *EIF4E* mutations conferring broad-spectrum resistance to PVY isolates may be better candidates for durable resistance. Recently, a series of eIF(iso)4E variants were designed based on amino acids implicated in other potyvirus-eIF4E/(iso)4E interactions. Overexpression of these variants in transgenic *B. rapa* seemed to provide broad-spectrum and durable resistance to TuMV isolates (Kim et al., 2014).

Aside potyviruses, another well-studied case of resistance breaking corresponds to MNSV overcoming the *nsv* resistance in melon. For MNSV, a mechanism different than that proposed for potyviruses is operating, as the resistance breaking factor in the virus is a non-coding RNA sequence that acts as 3´CITE (see above). For MNSV, it seems that recombination rather than punctual mutation is playing a pivotal role in acquiring the right 3´CITE for the *EIF4E* allele present in the host (Diaz-Pendon et al., 2004; Truniger et al., 2008; Miras et al., 2014).

1.2.8 Biological functions of eIF4E in plants: Translation of cellular mRNAs

Translation initiation is a key stage of protein synthesis that involves several eIFs (Figure 1.7). Translation of eukaryotic mRNAs relies on the binding of eIF4E to their 5' m7G cap structure and is enhanced by interaction of the poly(A)-binding protein (PABP) with their 3' poly(A) tail. The eIF4G scaffold protein binds to eIF4E and PABP promoting circularization of the mRNA. The interaction between eIF4E and eIF4G constitute the central core of the eIF4F complex. eIF4G also interacts with eIF4A, a DEAD-box ATPase and ATP-dependent RNA helicase that unwinds the mRNA to facilitate ribosome scanning. The eIF4G-eIF4A interaction is weaker than that between eIF4G and eIF4E so that eIF4A is easily lost during eIF4F purification. eIF4E, eIF4G, eIF4A and other DEAD-box RNA helicases are key translation factors frequently recruited by viruses and are good targets for antiviral strategies (Figure 1.7). The eIF3 protein complex interacts with both eIF4G and the 40S ribosome subunit to bind the 43S pre-initiation complex (which includes the 40S subunit and the eIF2-GTP-$tRNA^{Met}$ ternary complex) to the mRNA (Sanfaçon, 2015).

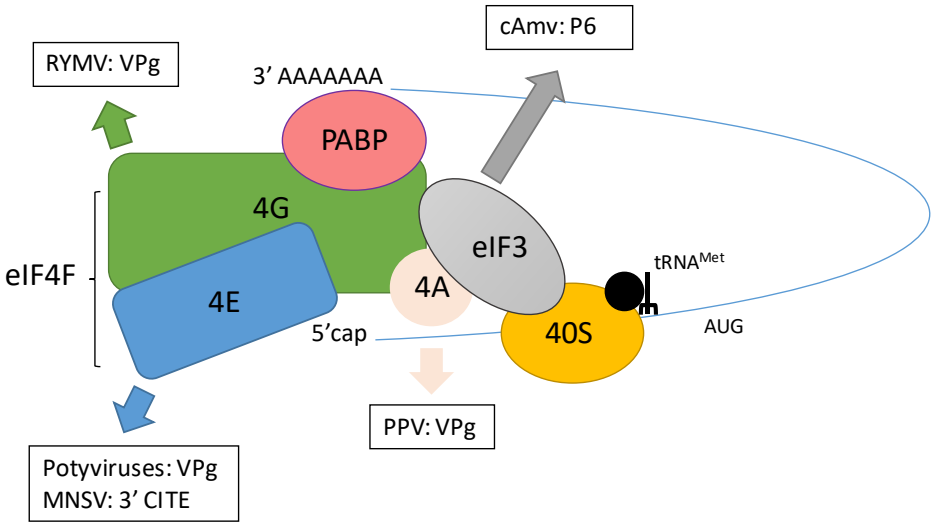

Figure 1.7. Role of translation factors in canonical eukaryotic translation and interactions with viral RNAs or proteins. Simplified diagram of translation initiation. Key initiation factors are shown as well as the best characterized interactions with viral components. Figure modified from Sanfaçon (2015).

In plants, two isoforms of eIF4F are described: eIF4F, consisting of eIF4E and eIF4G, and eIF(iso)4F, including eIF(iso)4E and eIF(iso)4G (Browning, 2004; Roy & Arnim, 2013). These isoforms are often encoded by multi-gene families so that there are 1–4 genes coding for eIF(iso)4G depending on the plant species (two for *A. thaliana*) (Patrick & Browning, 2012). eIF4E and eIF(iso)4E share approximately 50 % amino acid sequence identity. eIF4G (~180 kDa) and eIF(iso)4G (~86 kDa) share common binding motifs for eIF4E, eIF4A and eIF3, and in their C-terminal domains are pretty different in size due to a large truncation of the N-terminal region of eIFiso4G. Knock-out of *EIF(iso)4G* in *A. thaliana* causes major imbalances in plant development. By contrast, down-regulation or knock-out of *EIF4E* or *EIF(iso)4E* is well tolerated and plants show little signs of damage (Duprat et al., 2002; Combe et al., 2005). Interestingly, knock-out of *EIF(iso)4E* is balanced by an increased expression of eIF4E, evoking functional redundancy between the two isoforms (Duprat et al., 2002). However, eIF4F and eIF(iso)4F exhibit distinct specificity for mRNAs *in vitro* (Mayberry et al., 2009). Of interest for this thesis is that the 3D structure of melon eIF4E in complex with a eIF4G peptide has been determined, supporting a universal bipartite binding mode for protein translation (Miras et al., 2017).

1.2.9 Additional biological functions of eIF4E

Beyond their involvement in the canonical translation of cellular mRNAs, other biological functions have been demonstrated for translation factors for both viruses and plant development. In mammalian cells, a sub-population of eIF4E accumulates in nuclear bodies and has been linked to the regulated nuclear export of mRNAs that contain a specific structure called 4E-sensitivity element (Wang & Krishnaswamy, 2012; Goodfellow & Roberts, 2008; Culjkovic et al., 2007). In *A. thaliana* cultured cells, eIF4E has a predominantly cytoplasmic localisation although its partition to the nucleus is regulated by the cell growth cycle (Bush et al., 2009). eIF(iso)4E is equally distributed in the nucleus and cytoplasm. Thus, a role for the plant eIF4E and/or eIF(iso)4E in nuclear export is expected. Another interesting aspect is the association of the plant eIF(iso)4F complex with microtubules, facilitating their end-to-end annealing and suggesting a role in the regulation of microtubule dynamics (Hugdahl et al., 1995). The microtubule localization of eIF(iso)4F relies on a direct interaction between eIF(iso)4G and microtubules (Bokros et al., 1995). Finally, multiple studies suggest that eIF4E and eIF4G isoforms are highly selective in translating mRNAs, and there may be a gradation of cap-dependent to cap-independent requirements to the selection. Animal and plant studies show that germ cell and embryonic fates are greatly affected by the eIF4 factor complexes unique to those cell types (Dinkova et al., 2005; Friday & Keiper, 2015; Cao & Richter, 2002; Minshall et al., 2007; Hernández et al., 2013; Henderson et al., 2009; Baker & Fuller, 2007; Ruffel et al., 2006). The coupled use of genetics and biochemistry identified unique roles for eIF4E and eIF4G isoforms in reproduction. Furthermore, eIF4Es in plants, flies and frogs have shown unique roles in sexual development, judging by the reproductive phenotypes resulting from their deficiencies (Ghosh & Lasko, 2015; Rodriguez et al., 1998; Hernández et al., 2005; Patrick et al., 2014). Viruses could take advantage of these additional biological functions to control protein stability, regulate their replication and facilitate their intra and inter cellular movements.

1.3 Melon biotechnology

Melon breeding has originally been carried out through conventional hybridization techniques, as strong interspecific and intergeneric sexual incompatibility barriers reduce the chances of playing with its genetic potential to obtain new cultivars with high levels of disease resistance, flavour and sweetness (Chovelon et al., 2011). Biotechnological strategies can increase the genetic diversity by somatic hybridization or gene transfer and to optimize conventional breeding programmes by the implementation of genetic maps (see above). The application of plant biotechnology methods to melon breeding can be considered as a fundamental tool to overcome the limitations of natural genetic incompatibilities and obtain new varieties with desirable horticultural traits (Vasil, 2003).

1.3.1 Improvement through genetic engineering

During the 1970s, both molecular biology and genetic engineering research set the basis for the development, in 1983, of transgenic transformation technology in plants, through the use of the Ti plasmid from the soil bacterium *Agrobacterium tumefaciens* (Herrera-Estrella et al., 1983). This bacterium is capable of integrating a given fragment of the Ti plasmid (T- DNA), which is engineered to bring a selectable marker and/or genes of interest, into the plant nuclear genome under *in-vitro* conditions. Once inserted, it is possible to select non-transformed plants in culture by the use of the toxic substance to which the marker gene codes resistance. Subsequently, using *in vitro* culture techniques, transformed plant cells regenerate whole transformed plants on a plant regeneration culture medium. Within the plant biotechnology discipline, plant tissue culture methods have had a central role, allowing the obtention of transgenic plants with a number of desirable agronomic, pest resistance, and food traits. The term “plant tissue culture” is widely accepted to refer to *in vitro* cultivation on nutrient media of any plant part including single cells, tissues, or organs, under a sterile environment, leading to a whole *de novo* regenerated plant (Nuñez-Palenius et

al., 2008). After the achievement by Herrera-Estrella et al. (1983), several technological difficulties were overcome, allowing the cloning and insertion of many genes to engineer transgenic plants with different characteristics: Tolerance to biotic and abiotic stress, improved nutritional and agronomical quality of fruits and vegetables, novel production of pharmaceutical proteins and reduced production of allergens and phytoremediation activity (James & Krattiger, 1996; Vasil, 2003; Nuñez-Palenius et al., 2008; Abiri et al., 2016). Nowadays, more than 60 genetically modified crops have been approved for commercial planting, and at least 110 more are under field trials and/or regulatory review (Vasil, 2003; Lobato-Gómez et al., 2021). The use of CRISPR/Cas9 and associated genome editing technologies for the development or enhancement of fruit crops may open the door to new commercial opportunities, potentially circumventing restrictions on genetically modified crops in many parts of the world (Menz et al., 2020).

1.3.2 Melon regeneration

The use of a competent *de novo* regeneration system from *in vitro* cultures is crucial to achieve a successful commercial application from biotechnology in melon (Guis et al., 1998). Melon plant regeneration can be achieved through adventitious buds, somatic embryos, shoot primordia, protoplasts, and axillary buds. There are many physical and biological factors influencing *in-vitro* regeneration capacity that have to be taken into account in order to develop an efficient melon regeneration protocol. The first and most important factor determining regeneration potential is genotype, and this is due to the great genetic variability in melon (see above). Melon varieties and commercial cultivars present a great variability in their regeneration capacity under the same *in-vitro* protocol and environmental conditions (Kintzios & Taravira, 1997). Both organogenesis and somatic embryogenesis responses in melon *in-vitro* cultures are genotype dependent. In general, it has been reported that *reticulatus* varieties are more prone to produce *in vitro* somatic embryos than *inodorus* ones. Plant regeneration through organogenesis is also under the control of the genetic backgound (Ficcadenti & Rotino, 1995; Kintzios & Taravira, 1997; Galperin et al., 2003b). These authors generally

describe small shoot regeneration rates in *inodorus* types, whereas wide differences were noted among the *reticulatus* types.

Together with the genotype, the explant source or type has a main role on melon *in-vitro* regeneration (Adelberg et al., 1994; Ficcadenti & Rotino, 1995; Curuk et al., 2002; García-Almodóvar et al., 2017). Shoots, roots, and whole melon plants have been *de novo* regenerated through organogenesis starting from diverse explant origins, among them cotyledons from immature and quiescent seeds and/or seedlings, hypocotyls, roots, leaves, protoplasts, and shoot meristems. This *in-vitro* organogenetic pathway may produce plants by direct regeneration, involving a noncallus formation between explant culture and *de novo* shoot induction, or indirect regeneration involving callus growth before de novo shoot induction. Explants produced from true leaves or cotyledons commonly show a higher regeneration frequency (> 80 %) of *de novo* shoots using direct organogenesis compared to other melon explants (Yadav et al., 1996; Nuñez-Palenius et al., 2002). In addition to explant type, environmental factors and media composition may have some influence on the efficiency of melon regeneration through organogenesis. In general, for direct regeneration, a cytokinin/auxin ratio >1 is used to induce *de novo* bud formation; nevertheless, auxins are not always indispensable to obtain this result being cytokinins alone able to induce bud formation. The most frequently used cytokinin is BA in high levels (1 mg/L or higher) to induce bud formation. BA concentration is in some cases lowered to 0.5 mg/L to allow shoot elongation. Elongated shoots are then transferred to a plant growth regulator-free medium or with low-auxin level [1-naphthaleneacetic acid (NAA) or indole-3-acetic acid (IAA)] to induce the rooting process (García-Almodóvar et al., 2017).

1.3.3 Genetic Transformation

Two main genetic transformation processes have been used to produce melon transgenic plants; *A. tumefaciens* mediated transformation and particle gun bombardment. Transformation efficiencies via *Agrobacterium* or particle gun bombardment is genotype-, explant source-, and *in-vitro* culture conditions dependent

(Fang & Grumet, 1990; Yoshioka et al., 1992; Gonsalves et al., 1994; Gray et al., 1995; Clendennen et al., 1999; Ezura et al., 2000; Nuñez-Palenius et al., 2002; Akasaka-Kennedy et al., 2004). The *Agrobacterium* strain, vector structure, and co-cultivation with acetosyringone also have an influence on melon transformation capacity (Yoshioka et al., 1992; Vallés & Lasa, 1994; Bordas et al., 1998). Different bacterial and plant genes, which provide resistance or tolerance to several selectable chemical agents, have been employed to inhibit non-transformed bud growth during the selection process. Among them, the most used is neomycin phosphotransferase (*nptII*), which provides tolerance to aminoglycoside antibiotics (Fang & Grumet, 1990; Yoshioka et al., 1992; Vallés and Lasa, 1994; Gonsalves et al., 1994; Gray et al., 1995; Bordas et al., 1998; Kennedy et al., 2004). Genetic transformation efficiency rate in melon is normally lower than that in other plant species (Fang and Grumet, 1990; Gonsalves et al., 1994; Bordas et al., 1998; Akasaka- Kennedy et al., 2004). Several transformation rate and efficiency values have been reported with different transformation protocols and melon cultivar used and average efficiencies generally range from 3-7 % have been described (Fang and Grumet, 1990; Gonsalves et al., 1994; Bordas et al., 1998; Guis et al., 2000; Akasaka-Kennedy et al., 2004). Unfortunately, in many cases, and especially for the higher reported efficiency rates, most of the recovered transgenic plants have somaclonal variation like ploidy changes, (octaploids, mixoploids) or had morphogenetic altered characteristics, which were expressed in the T0 and T1 generation (Gonsalves et al., 1994).

1.3.4 Improvement of disease resistance by genetic transformation

The first virus-resistant transgenic melon plants were obtained by Yoshioka et al. (1992). These authors transferred and overexpressed the gene coding for the CMV coat protein via *A. tumefaciens* using “Prince”, “EG360” and “Sunday Aki” melon cotyledons. These transgenic melon plants, which overexpressed the CMV-CP gene, were found to be resistant to infection after inoculation with a low dose of CMV grown under greenhouse conditions (Yoshioka et al., 1993). In addition, transgenic plants overexpressing either CMV-CP for specific viral strains (Gonsalves et al., 1994) or multivirus resistance (CMV, WMV, and ZYMV) have been described (Clough and Hamm,

1995; Fuchs et al., 1997). High-level resistance to ZYMV, as measured by lack of symptom development and virus accumulation for a 30-day period in the greenhouse, was also achieved with the ZYMV-CP gene (Fang and Grumet, 1993).

1.3.5 CRISPR/Cas9 as a tool for development of disease resistance and crop improvement

In recent years, genetic engineering has greatly progressed in developing several applications in agriculture that have led to the improvement of important agronomic traits including pathogen resistance, abiotic tolerance, plant development and morphology and also secondary metabolism and fiber production (Wang et al., 2019; Zhang et al., 2021). Although great progress has been achieved and many transgenic plants have been widely adopted around the world, the majority of transgenic crops that can be found in the field are insect- and/or herbicide-resistant crops due to the scarcity of desirable foreign genes (Bennett et al., 2013). Moreover, inserting these genes into the plant genome is always random and it may affect genetic stability leading to gene silencing or altered expression (Gelvin, 2003). Thus, more precision is needed to edit the genes for both gene function studies and crop improvement. Recently, eukaryotic genome editing has been incorporated into the field of crop breeding, allowing precise modifications in organism's DNA through the addition, deletion or alteration of genetic material. The high impact and rapid evolution of genome editing has allowed the corresponding technologies to be rapidly adapted for plants (Van Eck, 2020).

Genome editing technology works on a specific sequence within the genome. To achieve this, genome editing tools require specific restriction nucleases that can recognize the sequences; these nucleases locate the genome position and serve as molecule scissors to cut the specific sequences. Up to now, there are four major families of nucleases used for genome editing: meganucleases, zinc finger nucleases (ZFNs), transcription activator-like effector-based nucleases (TALEN), and the clustered regularly interspaced short palindromic repeats associated nucleases (CRISPR/Cas) (Gaj et al., 2013). Although all of them have been successfully applied in plant genome

editing, ZFNs and TALENs are limited by their high complexity and limited efficiency, while CRISPR/Cas is characterised by being a simpler, more efficient, economical and versatile technology, being by far the most widely used technique in plants (Pennisi, 2013; Karkute et al., 2017). I will focus on CRISPR/Cas technology for this reason and because it was used during the experimental work in this thesis.

1.3.5.1. CRISPR/Cas9 as a plant genome editing system

The CRISPR/Cas system is based on the adaptive immune defence mechanism that bacteria exhibit in response to viruses and plasmids (Doudna & Charpentier, 2014). This bacterial defence mechanism was first identified in the *E. coli* genome in 1987 (Ishino et al., 1987), and officially reported by Jansen et al. in 2002). However, it was not until 2005 that CRISPR spacer sequences were shown to be homologous to virus and plasmid sequences, suggesting a correlation between CRISPR and acquired immunity (Bolotin et al., 2005; Mojica et al., 2005; Pourcel et al., 2005). The transition of the CRISPR/Cas system from a bacterial defence mechanism to a genome editing system is based on the possibility of reprogramming the DNA target by rearranging the 20 nucleotides of the RNA sequence encoded by the CRISPR genes (crRNA). The combination of this crRNA with the RNA sequence that interacts with the crRNA and is recognised by the Cas protein (tracrRNA), forms a chimeric RNA guide (gRNA) that recognises the target DNA (Jinek et al., 2012) (Figure 1.8). In the few years since its discovery, the CRISPR/Cas technology has been efficiently used for genomic editing in different organisms and with different applications (Kaboli & Babazada, 2018; Wang et al., 2019; Zhang et al., 2021).

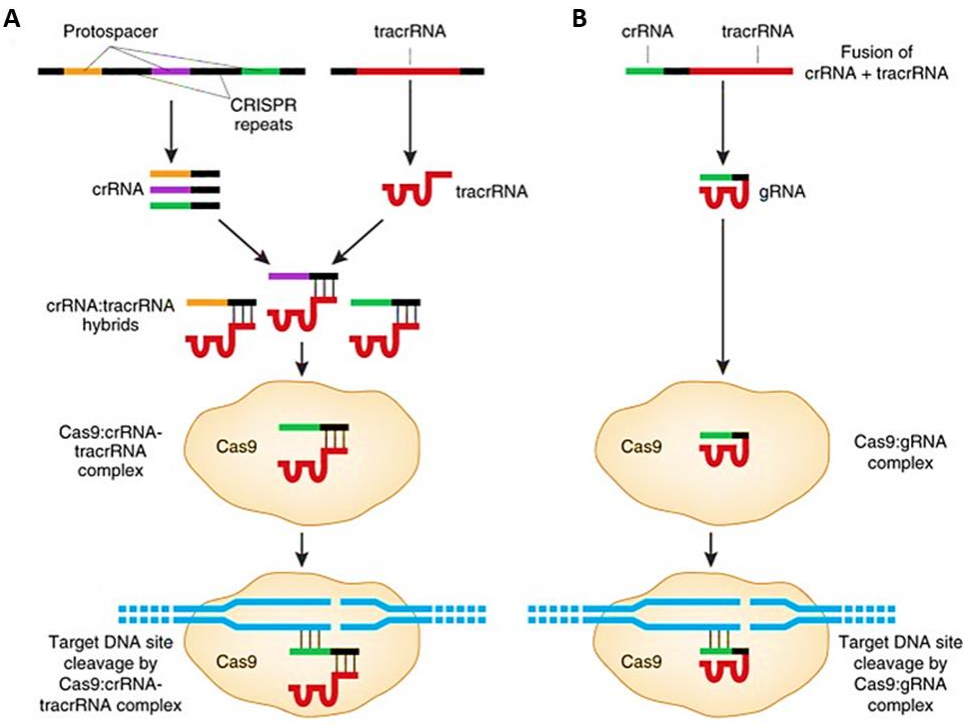

Figure 1.8. Schematic representation of the mechanism of action of the CRISPR/Cas9 system in bacteria and as a genome editing system. (A) CRISPR systems of bacterial origin incorporate exogenous DNA sequences into CRISPR arrays. These sequences that separate the CRISPR repeats are called proto-spacers, which together with the former form crRNAs complementary to the exogenous DNA sequences. The crRNAs hybridise to the tracrRNAs, allowing the association of the crRNA:tracrRNA pair with Cas9. The Cas9:crRNA-tracrRNA complexes recognise and cleave exogenous DNA complementary to that of the protospacer sequence. (B) The CRISPR/Cas9 system used for genome editing uses the fusion between the crRNA and a synthetic tracrRNA as a single transcript, forming the gRNA. The gRNA is recognised by Cas9 to form the Cas9:gRNA complex, producing a cut in the target DNA sequence. Figure modified from Sander and Joung, 2014.

CRISPR/Cas systems are divided into two classes: Class I, which includes CRISPR type I and III systems, commonly found in Archaea; and Class II, comprising CRISPR type II, IV, V and VI systems (Kooning et al., 2017). The most widely used CRISPR/Cas system is CRISPR/Cas9 belonging to type II, which requires only a single protein, CRISPR-associated protein 9 (Cas9) from *Streptococcus pyogenes*, *Lachnospiraceae bacterium* or *Francisella novicida*, for RNA-guided DNA double-strand recognition and cutting via its RuvC and HNH domains (Bortesi & Fischer, 2015; Doudna & Charpentier, 2014) (Figure 1.9A).

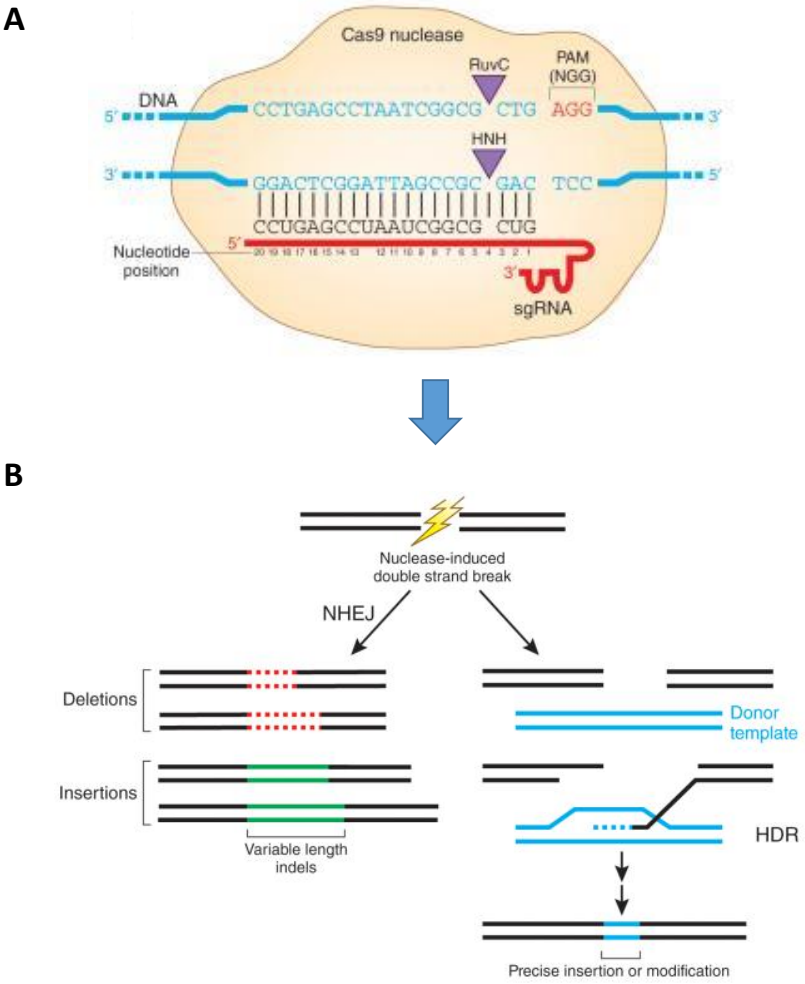

Figure 1.9. Constituent elements of the CRISPR/Cas9 system as a genome editing tool and possible DNA repair pathways following Cas9-induced double-strand breaks. (A) Hybridisation of the gRNA of the Cas9: gRNA complex to its target sequence directs Cas9 to the specific site of action, where recognition of the PAM sequence by the endonuclease is required for the DNA double-strand break to occur via the RuvC and HNH cleavage domains. (B) DNA double-strand breaks trigger cellular DNA repair mechanisms. In the absence of template DNA, non-homologous end joining (NHEJ) repair occurs, leading to insertions or deletions in the target sequence. In the presence of artificially supplied template DNA, direct homology repair (HDR) occurs, based on homologous recombination of the supplied template DNA and the target sequence, resulting in precise repair or modification. Figure modified from Sander and Joung (2014).

1.3.5.2. Gene knock-out for silencing an individual gene

Gene knock-out is the main application of CRISPR/Cas-based genome editing. The most commonly used CRISPR/Cas9 and other CRSIPR/Cas systems usually cut the

double-stranded DNA and generate a double strand break (DSB) with sequence specificity. This specificity is due to the gRNA sequence designed to be complementary to the target DNA sequence that will later be cut by the Cas9 endonuclease. The Cas9 cleavage domain recognises DNA, setting the cleavage site three nucleotides upstream of a three-nucleotide sequence, typically 5'-NGG-3' (Anders et al., 2014), termed the protospacer adjacent motif (PAM) (Bortesi & Fischer, 2015) (Figure 1.9A). In most cases, a DSB will be repaired by the non-homologous end joining (NHEJ) repair pathway, randomly producing insertions, deletions and/or substitutions at the cleavage site (Puchta, 2017) (Figure 1.9B). Due to that fact that one or more nucleotides are deleted or added, this will interrupt the expression of the targeted gene usually resulting in gene silencing or gene knock-out. Compared to T-DNA mutagenesis, CRISPR/Cas has the advantage to specifically target individual genes without other side effects. This is particularly useful for studying a given gene function or to eliminate undesirable traits controlled by a specific gene. On the other hand, the presence of a template DNA sequence activates the homology directed repair (HDR) pathway (Figure 1.9B), based on homologous recombination of genomic DNA and template DNA, which allows precise and controlled genome editing. However, HDR is less common in plants, as it is much less efficient compared to NHEJ (Yin et al., 2017). One of the concerns related to CRISPR/Cas9 is the possibility that off-targets can be produced by the binding of the gRNA to more than one site in the genome, thereby compromising the specificity of the system. However, numerous informatics platforms are now available, such as CRISPR-P 2.0 (Liu et al., 2017), CRISPR-Plant v2 (Minkenberg et al., 2019) or BreakingCas (Oliveros et al., 2016), which assist in the process of designing and evaluating gRNAs in terms of specificity, reducing the likelihood of the gRNA binding to more than one target. One of the main advantages offered by the CRISPR/Cas9 system in plants is the possibility of segregating the transgene in subsequent generations, so that it is possible to obtain progeny with the desired mutation without the Cas9-containing transgene and without foreign DNA elements integrated into the host genome (van Eck, 2020).

1.3.5.3. Application of CRISPR/Cas on crop improvement

Since CRISPR/Cas9 was described as a genome editing tool, it has been promptly used to create genome editing mutants with resistance to various viral diseases in model and crop species, including cucurbits. For resistance to plant viruses, a number of works chose eIF4E or eIF(iso)4E as target. In 2016, Pyott and colleagues employed CRISPR/ Cas9 technology and successfully eliminate *EIF(iso)4E* gene out in Arabidopsis. The resulting *EIF(iso)4E* knock-out mutants were resistant to the infection of TuMV without affecting other traits, including biomass and flowering time (Pyott et al., 2016). Chandrasekaran and colleagues (2016) also demonstrated that knock-out of *EIF4E* resulted in cucumber resistance to a broad range of viral disease, including the ipomovirus CVYV, and the potyviruses ZYMVand PRSV-W (Chandrasekaran et al., 2016). Finally, Gomez and colleagues (2019) showed that simultaneous CRISPR/Cas9-mediated editing of cassava eIF4E isoforms *nCBP-1* and *nCBP-2* reduced cassava brown streak disease symptom severity and incidence (Gomez et al., 2019).

1.3.6 Limitations in genome editing of recalcitrant species

No matter what purpose, CRISPR/Cas-based genome editing begins with a single cell editing occurrence, and it requires the single cell to become an entire plant for later study and application at an organism level. Currently, plant transformation and regeneration systems still are the bottlenecks for genome editing in plants and this is mainly due to the existence of plant species that have low regeneration capacity and/or that are recalcitrant to genetic transformation. Thus, the development of efficient delivery and plant regeneration systems is crucial. Agrobacterium-mediated genetic transformation is one of the most widely used delivery methods, allowing T-DNA cassettes including CRISPR/Cas machinery to be transferred into plant cells or explants. T-DNA can be also delivered to plant cells by biolistic bombardment, or into protoplasts by PEG-mediated transfection, but these technologies are strongly limited by low transformation efficiencies and could cause chromosome damage and a range of DNA rearrangement processes (Liu et al., 2019). Alternatively, magnetofection and

electroporation transformation methods transferring the T-DNA cassette to microspore and pollen have been used for cotton and wheat genome editing, although the transformation efficiency is extremely low (Zhao et al., 2017; Bhowmik et al., 2018; Vejlupkova et al., 2020), the technology is time consuming, and its applicability to different types of plant species is highly doubtful. For all these reasons, simple and high-throughput T-DNA binary vector cloning systems, which can express CRISPR/Cas reagents, including Cas9 and a sgRNA or multiplexed gRNAs under the control of the cauliflower mosaic virus (CaMV) 35S and U6/U3 promoters, have been widely used for plant genome editing (Kim et al., 2016; Oh et al., 2020). However, regeneration of transformants remains a limiting factor for most recalcitrant species, such as melon. One of the most recent, and possibly most promising, techniques to overcome the limitations in terms of regeneration and transformation of recalcitrant species is *de novo* induction of meristems; this technique has been achieved by using morphogenic regulators (MRs) in plants, and it possesses the potential to produce transgenic plants without the need for a tissue culture procedure. In general, by harnessing the plant cells totipotency, the ectopic expression of MRs in somatic cells can led to the induction of newly formed meristems (Maher, Nasti, Vollbrecht, Starker, Clark, & Voytas, 2020). Theoretically, this delivery system could be applied to various plant species, but still requires a deep study of plant-specific MR genes, together with a classical tissue culture system to generate Cas9 overexpressing transgenic plants.

1.3.7 Natural and induced male sterility: implications in plant breeding

Androsterility refers to the failure in the development of dehiscent anthers, functional pollen, or viable male gametes. When the potential of hybrid vigour as a breeding tool was recognised (Birchler et al., 2016), male sterility was incorporated in crop species and started to represent an important tool in genetic improvement programs. A 'hybrid' can be defined as any offspring of a cross between two genetically different individuals. The creation of hybrid crops is not an easy procedure from a technical point of view since producing hybrid seeds avoiding self-pollination often requires emasculation (*i.e.*, removing functional pollen grains to prevent self-

pollination). Until the twentieth century, this technique involved tiding manual work or chemical treatments, making it costly, inefficient, and harmful to the environment. The use of male sterility introduced the possibility to reduce the cost of hybrid seed production (Chen & Liu, 2014). Natural male sterility includes both genic (GMS) and cytoplasmic (CMS) male sterility; while the first one is caused only by genes encoded in the nuclear genome (Chen & Liu, 2014), the second one is caused by mitochondrial genes that directly or indirectly affect nuclear gene functions. In GMS, a Mendelian inheritance can be observed, in which the offspring of a male sterile genotype (female line) could be entirely male fertile or segregate 50 % male sterile: 50 % male fertile depending on whether the parental line (male fertile) is homozygous or heterozygous, respectively. In CMS, the production of sterile pollen is maternally inherited and conditioned by cytoplasmic (mitochondrial) genes associated with nuclear genes. In general, the exploitation of both natural genetic (GMS) and cytoplasmic (CSM) male sterility for hybrid production is limited by the complicated and time consuming techniques necessary for the identification and perpetuation of the male sterile lines. In this sense, the CRISPR/Cas technology constitutes a valuable tool for the identification of genes and the study of the mechanisms underlying male sterility in plants, and, once identified, to generate male sterile lines through gene editing. In this regard, Hexokinase *hxk5* rice mutants originated by CRISPR/Cas9 resulted in male sterility (Lee et al., 2020). Gene knock-out of *COPII* components sarib and saric also altered pollen development and caused male sterility in Arabidopsis (X. Liang et al., 2020).

2 OBJECTIVES

The main objective of the work described in this thesis manuscript was to edit the melon *EIF4E* gene using the CRISPR/Cas9 technology to achieve broad-spectrum virus resistance. During this work, the unexpected appearance of a male sterility phenotype apparently associated to *EIF4E* editing raised a number of questions, given both the fundamental and applied interests of this observation. This, together with the scarcity of detailed information on floral development and gametogenesis in andromonoecious melon, made that two new objectives emerged.

Therefore, the specific objectives of this work were as follows:

1. To generate through the CRISPR/Cas9 technology non-transgenic melon lines mutated in the gene encoding eIF4E and, once obtained, to check the association of the *eIF4E* mutation with the phenotypes of susceptibility to Moroccan watermelon mosaic virus, a virus that depends on it for its replication, and male sterility.

2. To characterize floral development and sexual differentiation and determination processes through morphological and transcriptomic analyses of melon flowers at different stages of development in an andromonoecious line.

3. To assess the possible role of eIF4E in the development of male melon gametes through a comparative analysis of melon male floral development between wild type and *eif4e* knock-out mutant plants obtained in objective 1.

3 MATERIALS AND METHODS

3.1 Bacteria cultures

The multiplication of the different plasmids generated was performed in the electro competent Top10 and HST08 StellarTM Competent Cells (Takara) *Escherichia coli* strains listed in Table 3.1.

Table 3.1. *E. coli* strains used in this thesis

Strain	Genotype	Reference
Top10	*Δ(araA-leu)7697, [araD139]B/r, Δ(codB-lacI)3, φ80dlacZ58(M15), galK0, mcrA0, galU-, recA1, endA1, nupG-, rpsL-(strR), Δ(mcrC-mrr)715*	(Edwards et al., 2011)
HST08 StellarTM	*F–, endA1, supE44, thi-1, recA1, relA1, gyrA96, phoA, Φ80d lacZΔ M15, Δ(lacZYA-argF) U169, Δ(mrr-hsdRMS-mcrBC), ΔmcrA, λ–*	Takara (www.takarabio.com/)

In this thesis, *Agrobaterium tumefaciens* strains GV3101 (RifR) and EHA105 (RifR) have been used for stable transformation of melon. Both strains contain the virulence factors in the pMP90 vector (Konczl & Schell, 1986).

3.2 DNA constructs

The design of the RNA guides (gRNA) directed to the different genetic targets was carried out using the online tool CRISPR-P (http://crispr.hzau.edu.cn/CRISPR2/) (Lei

et al., 2014). The following parameters were set up: "protospacer adjacent motif (PAM) NGG (Streptococcus pyogenes 5'-NGG-3' SpCas9), U6 snoRNA promoter, guide length 20 nucleotides, *Cucumis melo* reference genome. The coding sequence of each target to be edited was introduced. The choice of RNA guides among the options offered by the program was made based on: i) position, as close as possible to the translation start site; ii) minimum number of possible non-specific targets, choosing those that did not present any non-specific target with less than 3 nt unpaired; iii) secondary structure of the gRNA, which had to meet the parameters described by Liang et al., (2016), according to the structural prediction of the mfold tool (http://unafold.rna.albany.edu/?q=mfold) (Zuker, 2003), not only for the most likely structural prediction but also for the one with an immediately lower Gibbs free energy.

Once the guide sequence was chosen, a pair of complementary primers was designed for each gene to be edited (Table 3.2) by adding the cutting sequence of the *BbsI* enzyme at the 5' ends of each of them, leaving cohesive ends. Each primer pair was incubated for 5 min at 95 °C and allowed to cool at room temperature, favouring DNA duplexes to form. The gene-specific duplex DNAs were cloned into the plasmid pBS_KS_gRNA_BbsI (hereafter pA58; unpublished, property of Abiopep S.L.), previously digested with *BbsI*, in which the duplex DNAs are fused between the Arabidopsis ubiquitin promoter U6-26 and the scaffold sequence (which after *in planta* transcription will form the so-called gRNA). The resulting plasmids were digested with the restriction enzymes *SpeI* and *KpnI*. The products of the digestion were fractionated by agarose gel electrophoresis, the band of interest was cut out and purified on column (GeneClean Turbo Kit, MP Biomedicals). The purified DNA fragments (AtU6-26-gRNA) were cloned by ligation into the binary vector pK7_CAS9-TPC_MCS (hereafter pA60; unpublished, property of Abiopep S.L.), which includes the sequence of the Cas9 protein CDS and the Neomycin phosphotransferase II (*nptII*) gene that confers resistance to kanamycin in plants, and sequenced to check the correct insertion of the fragment. Finally, the pA60-gRNA plasmids were transformed into electrocompetent *A. tumefaciens* cells strain GV3101 and used for transformation of melon explants.

Table 3.2. Oligonucleotides used as primers in this thesis

ID	5'-3' sequence	Description
AB338	ATTGCAAAACCCTAGAGGACGTGG	gRNA used for editing the gene encoding eIF4E
AB339	AAACCCACGTCCTCTAGGGTTTTG	
AB385	GGGCGGTGCCATTCTTCTTC	Genotyping of *EIF4E* mutant lines with Phire polymerase
AB386	GAGTCGAGGTCGTCGTCGCC	
CE1601	GAGGCTATTCGGCTATGACTG	Amplification of the *nptII* Kanamycin resistance gene
CE1602	ATCGGGAGCGGCGATACCGTA	
CE2176	CGCTAACAGAAACTTCATGCA	Primers to amplify *Cas9* from A60 constructs
CE2177	AGCGTTAAGGTAAGCATCGTGAG	
CE2881	GGGACTTTCAGGGTTCCAA	Absolute quantification of MWMV accumulation by RT-qPCR
CE2882	TGCCCTAGTGTTGGACAGG	
CE3116	CCTTTGTCAAGACGCATTGG	Primers to amplify the complete sequence of VPg from MWMV
CE3117	CCTGACGTGTTTGTGAGATG	

3.3 Plant materials and tissue collection

The M2 genotype from the 'Piel de Sapo' melon type, the melon accession BGV-130 and three other genotypes (C-46, M9 and M5) of melon corresponding to the types 'Cantalupensis', 'Piel de Sapo' and 'Amarillo' were used in this study. For the regeneration and transformation experiments, seeds were peeled off with the help of tweezers to remove the seed coat and then surface-disinfected in a solution of 1 % hypochlorite for 20 min and rinsed six times with sterile distilled water. The disinfected seeds were placed on 5 ml distilled sterile water in a Petri dish and stored in the dark overnight at 26 °C before being used for the production of explants. For the determination of ploidy status, cotyledon explants (2 or 3 days old after imbibition) and young leaves of different leaf tiers from mutant and wild type plants were sampled from melon seedlings growth on germination medium containing MS salt medium (Murashige and Skoog 1962), 3 % (w/v) sucrose and 0.8 % (w/v) agar (Conda Laboratories) with the pH adjusted to 5.7 before autoclaving (120 °C, 20 min).

For germination of F1 and F2 mutant plants, pre-germinated M2 and BGV-130 seeds were sown in a substrate composed of peat, coconut fiber and perlite in a 6:3:1 ratio and covered with vermiculite, and kept in a greenhouse or growth chamber with a

temperature adjusted to 25 °C day and 18 °C night in a long cycle photoperiod (16 h light / 8 h dark) and a relative humidity of 50 - 60 %.

For the microscopy analysis of flower development, floral buds from at least 20 wild type and *eif4e* mutant melon plants were collected by cutting the shoot tip containing young floral buds at various stages of development. Flower buds were separated into male and hermaphrodite and buds of the same sex were pooled together according to the length of each individual bud. Four floral episodes were sampled: floral structure formation episode (FS) (buds < 2mm in length), gamete initiation episode (GI) (floral buds of 3 to 5 mm), gamete maturation episode (GM) (buds of 8 to 10 mm), and finally anthesis episode (AN) (buds >2cm in length). For each episode, up to 100 buds were pooled for each of three biological replicates, at a time interval of 15-20 days, allowing the formation of new flower buds between samplings. The samples were separated into two equal halves for processing: samples from one half were fixed in paraffin for light microscopy observations, whereas the samples from the other half were processed for scanning electron microscopy analysis. In both cases, flower buds were immersed in 70 % alcohol and stored at 4 °C for 24 h prior to fixation. For the collection of samples for RNA-seq analysis, flower buds at different stages of development were sampled according to the procedure previously described for the microscopy analysis. Buds were hand-dissected and collected in the morning, immediately frozen in liquid nitrogen and stored at -80°C until RNA extraction.

3.4 Plant regeneration

Half of the proximal parts of the cotyledons from 3-day-old seeds after imbibition were cut and used as explants for shoot regeneration. The explants were placed on regeneration medium (RM) consisting of MS salt medium (Murashige, 1962) plus B5 Vitamins (Gamborg et al. 1968), 3 % (w/v) sucrose, 3 µM 2-(N-morpholino) ethanesulfonic acid (MES), 4 µM $CuSO4{\cdot}5H2O$, 4.4 µM 6-benzylaminopurine (BAP) and 0.8 % (w/v) agar (Conda Laboratories). After four weeks, regenerated shoots were excised and transferred to elongation-rooting medium (ERM) with a composition similar

to RM but free of plant growth regulators. In all media, the pH was adjusted to 5.7 before autoclaving. Plant regeneration and development were done in a growth chamber at 26–28 °C with a light intensity of 55 µmol m^{-2} s^{-1} during a 16-h day photoperiod.

3.5 *Agrobacterium tumefaciens*-mediated stable transformation of melon

The transformation was carried out using 3-day-postgermination hypocotyl explants from the different melon accessions described above; 0.5-1 mm of the proximal parts of hypocotyls were cut longitudinally and included the proximal part of the cotyledon. In the experiments of regeneration and transformation efficiency of the different melon genotypes, *A. tumefaciens* strains were transformed with the binary vector pMOG800 harbouring the dsRed reporter gene under the control of the CaMV 35S promoter. In the case of the CRISPR/Cas editing experiments, strain GV3101 was transformed with the binary vector A60 carrying (or not for controls) the gRNA-expressing sequences.

The methodology used for the stable transformation of melon was that described in García-Almodóvar et al., 2017. *A. tumefaciens* clones cryopreserved in glycerol were refreshed and transformed with p35SdsRed or pA60-gRNA constructs for each gene to be edited. A single colony was inoculated into 50 ml of Luria-Bertani (LB) medium (pH 7.0) containing the antibiotics required for the selection. This culture was incubated overnight at 28 °C on a rotary shaker at 140 rpm. After centrifugation (15 min at 4000 rpm at 20 °C), the *A. tumefaciens* suspension was adjusted at OD600 0.4 with inoculation medium (SIM, 2 % sucrose and 0.6 % trisodium citrate, pH 5.5) containing 100 µM acetosyringone. The explants were immersed in the *A. tumefaciens* suspension for 20 min with orbital shaking (50 rpm) at 22 °C. Later, the bacterial suspension was removed and the explants were directly transferred to RM (without CuSO4·5H2O) containing 100 µM acetosyringone for a 72 h co-cultivation period at 26 °C in the dark. The explants were then washed with liquid RM supplemented with 200 mg/l of vancomycin and 300 mg/l of cefotaxime to control *A. tumefaciens* growth, and they

were subsequently placed onto selective RM with 150 mg/l kanamycin and the same antibiotics. After four weeks, regenerated buds were excised and sub-cultured to fresh selective RM for 2 weeks. In order to exclusively count independent transformation events, only buds physically separated within the explant were computed for regeneration percentages. The buds that regenerated from the primary explants were excised and were transferred to selective elongation RM (ERM) (150 mg/l kanamycin, 200 mg/l vancomycin and 300 mg/l cefotaxime) for rooting. Additionally, rooted plants were further checked by PCR for the marker gene *nptII* with specific primers. Once the elongated shoots produced roots, they were subcultured in ERM to select out the transformed shoots that were stably expressing the transgene. Once the root systems were well developed, the plants were transferred to soil and acclimatised in a growth chamber.

3.6 Ploidy estimation

The ploidy level of both, the wild type and transgenic regenerated plants was determined by flow cytometry. Crude samples of nuclei were prepared from the chopped leaves of *in-vitro* regenerated plants in 1 ml of DAPI and filtered according to the method of Galbraith et al. (1991). The DNA content of the isolated nuclei was analysed with a flow cytometer (Partec) calibrated from the nuclei of young leaves of diploid plants obtained from seeds. The noise signal derived from subcellular debris were eliminated by gating. The isolated populations of plant nuclei gave characteristic peaks of fluorescence emission, with the lowest peak corresponding to 2N nuclei and the other peaks representing 4C nuclei (Figure 4.4). Additionally, the ploidy level of transgenic plants was confirmed by phenotypic observations of plants cultivated in a confined greenhouse. According to Ezura et al. (1992), the phenotype of tetraploid melon plants is characterised by having large male and hermaphrodite flowers, protruding stigmas, low fertility, thickened leaves, short internodes and round seeds.

3.7 Detection of *dsRed* expression by fluorescence stereomicroscopy

Transformed explants were examined with a Leica MZ10F stereomicroscope equipped with different filter sets. The dsRed module contains a 545/30-nm excitation filter and a 620/60-nm emission filter. A metal-halide lamp containing mercury provided illumination. The red auto-fluorescence from chlorophyll was not blocked with any interference filter. Photos were taken by a Leica DFC7000 T colour camera.

3.8 PCR-genotyping of transgenic edited lines

As an additional verification of the stable genetic transformation by rooting in kanamycin selective medium, a fragment of the coding sequence of Cas9 was PCR-amplified. For this, a direct PCR of tissue from melon T0 plants was performed using the Phire Tissue direct PCR kit (Thermo Scientific) according to the manufacturer's specifications, and the primer pair CE2176 and CE2177 (Table 3.2). Then, the target region of *Cm-EIF4E* was amplified by direct tissue PCR using the primer pair AB385 and AB386 (Table 3.2). DNA from wild type plants of the same genotype was used as a negative control. For validation, the PCR products were purified by column with the GeneClean Turbo Kit (MP Biomedicals) and sequenced using an external service (STABVIDA, Caparica, Portugal). Analysis of the sequences obtained was performed using SnapGene software (GSL Biotech) and/or the bioinformatics tool CRISP-ID V1.1 (Dehairs et al., 2016).

3.9 Melon pollinations

The crossing of the homozygous male-sterile T0 lines, edited in *EIF4E*, by the WT lines of the same genotype (*eif4e*/*eif4e* x *EIF4E*/*EIF4E*) to obtain the F1 was performed

manually. For this purpose, male flowers were first selected from wild-type plants, from which the pollen was obtained and collected by gently tapping them on a Petri dish. Subsequently, the hermaphrodite flowers of the T0 plants to be pollinated (flowers close to anthesis) were selected. The flowers were emasculated and petals and sepals were removed. The stigmas were then impregnated with pollen, bagged with paper bags to avoid unwanted crosses and labelled. To obtain the F2 generation, the fertile heterozygous individuals were manually self-fertilised, each individual with pollen from its own plant, in a similar way as described for the obtention of the F1 generation. Once they had set about three fruits per plant, they were unbagged and the rest of the flowers were removed from the branch. The pollination process was repeated until about six fruits per plant were obtained.

3.10 Virus inoculations

Moroccan watermelon mosaic virus (MWMV) inoculation was performed by rubbing recently expanded cotyledons and young fully expanded leaves with fresh extracts (in 0.03 M potassium phosphate buffer, pH 8.0) from MWMV-infected squash plants (MWMV-SQ10_1.1) and re-inoculated 3 days later, following standard procedures (Hull, 2016). After the inoculation, plants were monitored daily for the appearance of symptoms. A pool of systemically infected leaves was harvested from each individual plant at 21 dpi.

3.11 RNA isolation

For the analysis of viral accumulation, leaf samples belonging to five individual plants within each group were grinded and cold-homogenised in a mortar using liquid N_2 and adding TNA buffer (2 % SDS, 100mM Tris HCl pH8, 10mM EDTA pH 8) at a ratio of 4 ml per gram of plant material, recovering 500 µl of each extract. Total RNA was extracted using Tri-reagent, purified by phenol-chloroform extraction, and treated with

DNaseI (Sigma-Aldrich, St. Louis, USA). The integrity of the RNA was checked on a 1 % agarose gel and RNA preparations were quantified using NanoDrop One (Thermo Scientific), normalised to 25 ng/µl and used as a template to quantify the absolute accumulation of MWMV.

For RNA sequencing analysis, the flower tissue from each sample was ground with a mortar and pestle in the presence of liquid N_2. Total RNA was extracted using Tri-reagent (MRC), purified by phenol-chloroform extraction, and treated with DNaseI (Sigma-Aldrich, St. Louis, USA) following the manufacturer recommendations. RNA preparations were quantified using NanoDrop One (Thermo Scientific) and normalized to equal amounts for each replicate. The RNA quality of the samples was analysed by agarose gel electrophoresis and with an Agilent 2100 Bioanalyser (Agilent Technologies, USA). The RNA integrity number (RIN) of all samples was above 7.

3.12 Viral load quantification by RT-qPCR

The MWMV accumulation was estimated by measuring the viral RNA accumulation by absolute real-time quantitative PCR (RT-qPCR) with a StepOnePlus System thermal cycler (Applied Biosystems, Foster City, CA) using One-step NZYSpeedy RT-qPCR Green kit, ROX plus (NZYTech, Lisboa, Portugal) and the primers CE2881 and CE2882 (Table3.2). For absolute quantification, a standard curve constructed from serial dilutions of MWMV CP viral RNA *in-vitro* transcript was used.

3.13 Paraffin sections and light microscopy

Shoot tips and floral buds at various stages were fixed in FAA (formaldehyde: acetic acid: ethanol: H_2O, 10:5:50:35, vol:vol) and then dehydrated through an ethanol series following the protocol described in Table 3.3. Dehydrated plant material was embedded in paraffin and longitudinal and transverse semi thin sections (1 µm) were cut using an ultra-microtome (Leica RM2155) and placed on Poly-L-L-Lysine cover slides

prior to staining. Samples were incubated for 2 hours at 40 °C in an oven for dewaxing and three steps (5 minutes each) were carried out in "Neo-Clear® (xylene substitute). Thin sections were then hydrated by three consecutive steps in ethanol at decreasing concentrations (100 %, 96 %, 70 %, 3 minutes each) and finally left in distilled water for 5 minutes. At this point, staining with Mayer's haematoxylin was carried out, leaving the sections in the stain for 10 minutes, followed by several washes with distilled water. Finally, a second staining was carried out with alcoholic Eosin, followed by three steps of dehydration in ethanol at increasing concentrations (70 %, 96 %, 100 %, 1-2 minutes each). The procedure ended with a two-step, three-minute rinsing phase (dealcoholisation) in Neo-Clear. Then, a drop of Neo-Mount was applied to the preparations and covered with a coverslip. The sections were observed, measured and photographed under a light microscope (Leica DMRB).

3.14 Scanning electron microscopy

Floral buds at various stages of development were fixed overnight in FAA and subsequently subjected to several washes. After that, buds were fixed in 3 % (v/v) glutaraldehyde diluted in 0.1 M cacodylate buffer during 3-5 hours and then washed in cacodylate buffer plus sucrose overnight. Subsequently, a postfixation procedure in 1 % tetroxide was followed by a second wash in cacodylate buffer plus sucrose overnight. At this point, a serial dehydration was performed in acetone solution at increasing concentrations (30 %, 50 %, 70 %, 90 %, 100 %, 10 minutes each). Materials were critical-point-dried using 100 % acetone and liquid CO_2, mounted on aluminium stubs with double-sided tape, 5 nm layer Platinum-coated with a Leica EM ACE600 sputter coater, and then examined through a field emission scanning electron microscope (ApreoS LoVac, Thermo Fisher), 5 kV and 3.2nA with a work distance of 15 mm and secondary electrons.

Table 3.3. Fixation and embedding steps for light microscopy

Solution	Incub. temperature	Incub. time	Notes
Fixative solution	on ice	20-30s	under vacuum, several times
Fixative solution	on ice	O/N	gentle shaking
1x saline	on ice	30min	Degass under vacuum before usage
30 % EtOH/saline	on ice	1-3h	Degass under vacuum before usage
40 % EtOH/saline	on ice	1-3h	Degass under vacuum before usage
50 % EtOH/saline	on ice	1-3h	Degass under vacuum before usage
60 % EtOH/saline	on ice	1-3h	Degass under vacuum before usage
70 % EtOH/saline	on ice	1-3h	Degas under vacuum before usage
85 % EtOH/saline	4˚C	1-3h	Degass under vacuum before usage
95 % EtOH/water	4˚C	1-4h	Degass under vacuum before usage
100 % EtOH	4˚C	1-4h	
100 % EtOH	4˚C	O/N	
100 % EtOH	RT	1-2h	
100 % EtOH, 0,1 % Eosin	RT	30min	
EtOH/Histoclear=3:1	RT	1-3h	
EtOH/Histoclear=1:1	RT	1-3h	
EtOH/Histoclear=1:3	RT	1-3h	
Histoclear	RT	1h	
Histoclear	RT	O/N	
Histoclear + WAX	RT	~1day	Add WAX chips several times
Histoclear + WAX	42˚C	2days	Add WAX chips several times
WAX	58˚C	2days	Change half volume of the wax 2-3 times a day
WAX	58˚C	2days	Change total volume of the wax 2-3 times a day
WAX	4˚C		After orientation store for unlimited time

3.15 RNA sequencing and data analysis

RNAseq Libraries were constructed according to the TrueSeq Stranded mRNA LT kit protocol (Illumina, USA) with ribosomal depletion using Ribo-Zero plant kit (Illumina, USA) and sequenced using the Illumina NovaSeq6000 platform (150 PE) (Macrogen Inc., South Korea). Approximately 66 to 85 million paired reads were generated for each sample. Quality of raw reads was analysed using FastQC (http://www.bioinformatics.babraham.ac.uk/projects/fastqc/). Poor quality reads (QC < 30 and length < 70 bp) and adapter sequences were filtered out, and the low quality

nucleotides at the 5' end of the reads were trimmed using Trimmomatic (Bolger et al., 2014). A second quality control of the filtered reads was performed again with FastQC, and reconstruction of paired-reads was performed with BBMap (www.sourceforege.net/projects/bbmap). Reads were then mapped against the melon genome (DHL92/v3.6.1) using the MEM algorithm of BWA software (Li & Durbin, 2009). Mapping quality was analysed with Qualimap bamqc (García-Alcalde et al., 2012).

The *FeatureCounts* function of the R package *Rsubread* was used to count the number of reads mapping to each mRNA (v4.0 of the gene models). For all comparisons, read counts were normalized to FPKM (fragments per kilobase per million mapped reads) using *DESeq2* R package to estimate the relative levels of expression. Genes were considered as expressed genes if the FPKM value was higher than 1 in the three biological replicates of at least one sample PCA and heatmaps were drawn using the R packages Factoextra and Pheatmap, respectively. Hierarchical clustering dendrograms of samples and genes were constructed using the R function *hClust* using Spearman and Pearson correlations, respectively. Kmer selection for clustering was performed using the R function *Cutree*. Plots of gene expression patterns were molten using *Reshape2* and drawn using *ggplot2* R packages. Venn diagrams were made using the *VennDiagram* R package. We used hierarchical clustering to group the genes by co-expression. For that, hClust was used to calculate the 'distance' between genes as 1 minus the Pearson correlation of one gene to another. This distance represents how differently one gene behaves compared to another. This distance was used to construct dendrograms of gene expression and from which, k=16 discrete gene clusters were extracted. Episode-specific genes were those genes for which the FPKM value in one episode was 2 fold the value in the remaining episodes for male and hermaphrodite flowers. Differential expression analyses among different developmental episodes or between WT and *eif4e* mutant episodes were performed using *DESeq2* R package. For each gene, an adjusted P value was computed by *DESeq2*, and those with an adjusted P value lower than 0.01 were considered differentially expressed. Gene Ontology (GO) analysis was done using the *Goseq* R Bioconductor package using the list of DEG or episode-specific genes created previously. GO terms with a corrected false discovery rate below 0.05 were considered to be significantly enriched.

3.16 Statistical analyses

Transformation experiments were repeated at least three times (approximately 100 explants per experiment) for the genotypes tested. Specific maximum likelihood contrasts were run to detect differences between genotypes. Differences were considered significant when $P < 0.05$. Markers segregation ratios of F2 progenies were contrasted by Chi square to expected values.

4 RESULTS

4.1 Editing *CmEIF4E* associates with virus resistance and male sterility

4.1.1 Regeneration and transformation efficiencies of four melon genotypes

Melon organogenesis is highly dependent on the genotype (Nuñez-Palenius et al., 2008). The regeneration ability of four melon genotypes was evaluated. Significant differences (P <0.05) were observed among genotypes on the number of regenerated buds, with M2 and M5 producing on average 1.7 and 2 buds per explant, respectively (Figure 4.1A). All the evaluated genotypes showed high capacity of regeneration, especially M2 and M5, which showed higher rates of explants with at least one regenerating bud than the rest of the genotypes (Figure 4.1B).

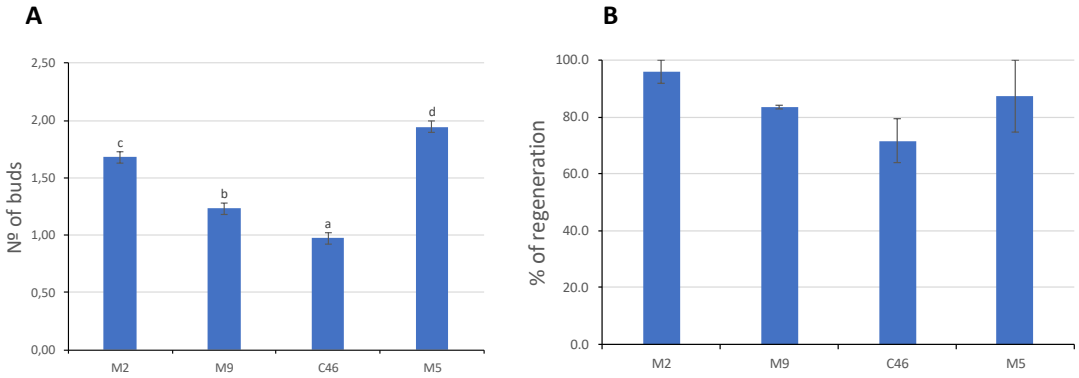

Figure 4.1. Number of buds (A) and percentage of regeneration (B) of the evaluated genotypes. Different letters (lowercase letters) indicate significant differences (P < 0.05) by maximum likelihood contrasts among explant types; error bars represent standard error of the mean.

We next used the fluorescent marker DsRed to evaluate the transformation efficiency of the four melon genotypes (Table 4.1).

Table 4.1. Transformation efficiency and rooted plants produced from different melon genotypes

Genotype (melon type)	Vector	Explants	Regeneration (%)[1]	dSRed + buds (%)[2]	Rooted lines	TE[3]
M2 (Piel de sapo)	p35S:dsRed	300	288 (96)	22 (7.3)	9	3,00
M9 (Piel de sapo)	p35S:dsRed	300	250 (83.4)	29 (9.7)	6	2,00
C-46 (Cantalupensis)	p35S:dsRed	300	215 (71.7)	32 (10.7)	2	0,67
M5 (Amarillo)	p35S:dsRed	300	262 (87.4)	45 (15)	4	1,33

[1]Regeneration: number of explants with, at least, one regenerating bud. Between brackets the regeneration rate: regeneration/total number of infected explants × 100
[2]Buds with DsRed expression/total number explants × 100
[3]Transformation efficiency (TE): number of rooted lines/total number explants × 100

After the infection of the explants, large foci of DsRed expression were detected in explants of all the genotypes examined, with more abundant foci observed for M5, C46 and M9. However, these three lines produced a lower number of rooted lines, which resulted in a lower transformation efficiency compared to M2 (Table 4.1). For this reason, we selected M2, which had the highest transformation efficiency (3 %), as the genotype to be used for the transformation experiments with the CRISPR/Cas9 constructs. Using M2, DsRed uniformly transformed buds were obtained (Figure 4.2).

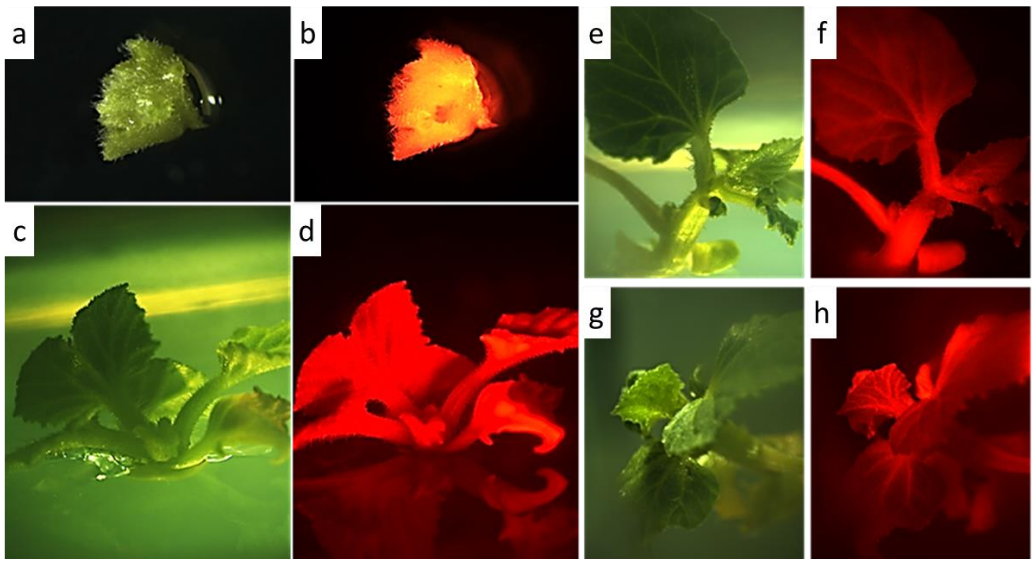

Figure 4.2. Uniformly expressing DsRed bud under white (a, c) and UV light (b, d). Micropropagated shoots under white (e, g) and UV light (f, h).

4.1.2 CRISPR/Cas9-mediated editing in T0 melon lines

In the melon genome, *EIF4E* (MELO3C002698.2) and *EIF(iso)4E* (MELO3C023037.2) encode eIF4E (235 amino acids) and eIF(iso)4E (203 amino acids), respectively, which share 61 % coding nucleotides and 52 % amino acid similarity. gRNA1 was designed to target the first exon of *EIF4E* gene and presented no sequence homology with *EIF(iso)4E*. Three independent transgenic T0 lines, initially named G1-1, G1-2 and G1-3, were generated by *Agrobacterium*-mediated transformation and rooted in kanamycin selective medium. To confirm the transgenic nature of the T0 lines and to determine the type of mutations possibly induced, we performed a PCR amplification in T0 plants of both the *Cas9* transgene and the target sequence using specific primers (Table 3.2). Sequencing of the PCR amplicons and alignments against the *EIF4E* reference sequence revealed a single nucleotide deletion, in homozygosis, three nucleotides upstream of the PAM sequence, that generated a premature stop codon downstream of the editing site. The third line alignment showed a WT sequence. All the lines tested positive for the *Cas9* transgene amplification (Figure 4.3).

Leaves from the T0 plants were used to evaluate their ploidy status by flow cytometry using leaves from a WT plant of the same genetic background as a control. We found that the ploidy levels of the two edited lines were similar to that of the control (Figure 4.4).

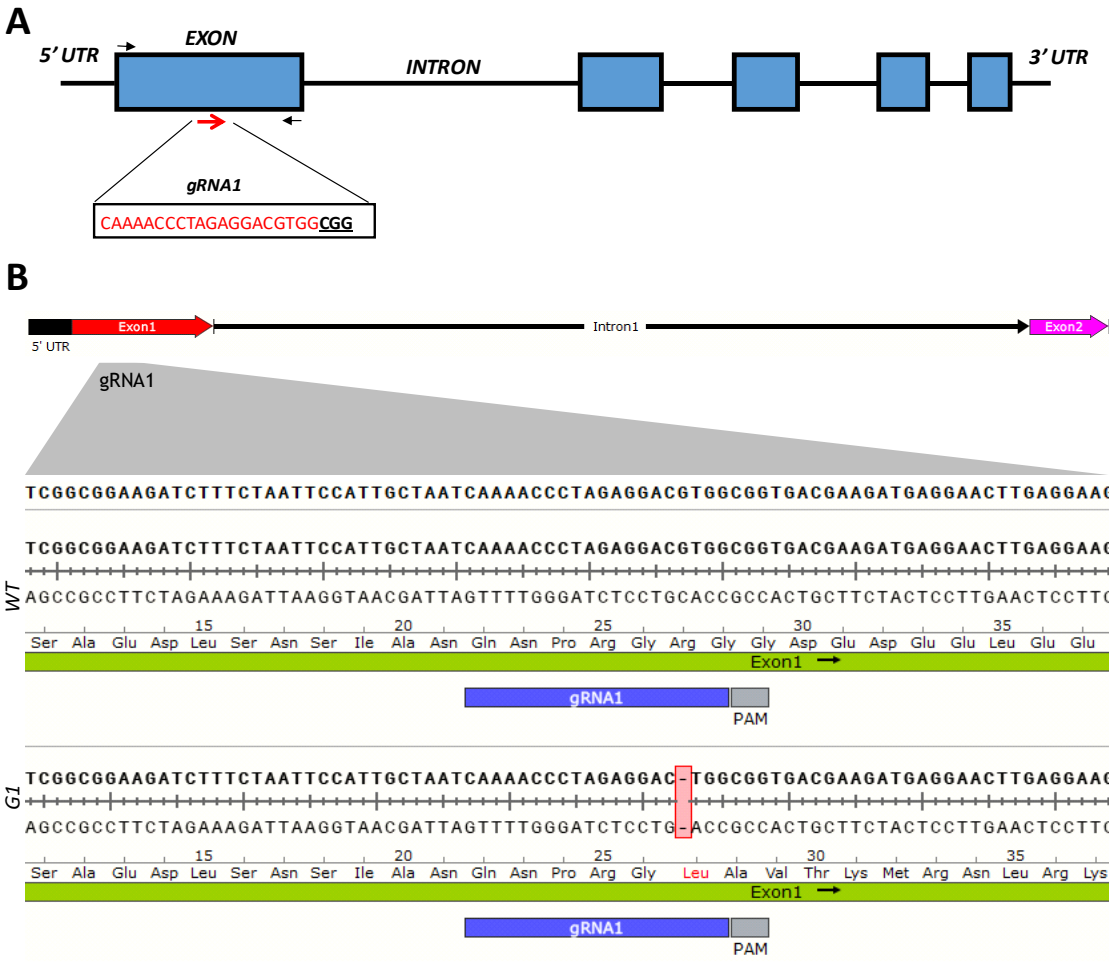

Figure 4.3. Gene editing of *EIF4E* mediated by CRISPR/Cas9 in transgenic melon T0 plants. (A) Schematic representation of the melon *EIF4E* genomic map and the gRNA1 target site (red arrows). The target sequence is shown in red letters, and the protospacer adjacent motif (PAM) is marked in bold underlined letters. The black arrows indicate the primers flanking the target sites used to detect the mutations. (B) *EIF4E* genomic DNA alignment between WT and mutated T0 lines of fragments corresponding to a DNA fragment containing the gRNA1 sequence representative of the G1-1 and G1-2 independent lines obtained. A DNA deletion is highlighted in a red box. (C) eIF4E protein sequence alignments between WT and mutated T0 lines. The protein sequence downstream of the deletion site is shown in green; the target region in red and the red asterisk represents a premature stop codon.

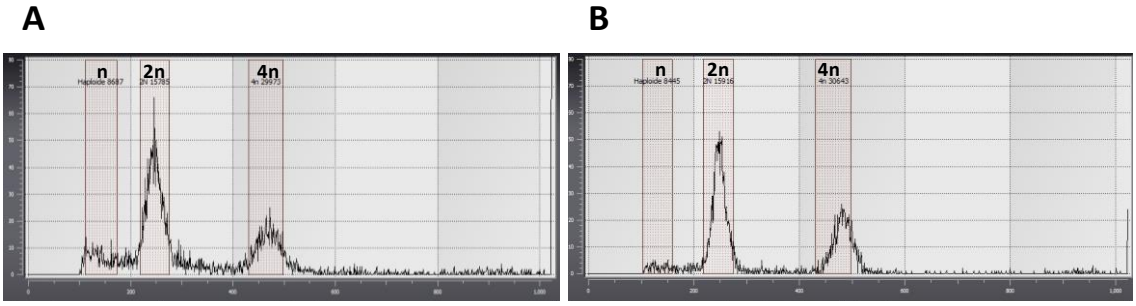

Figure 4.4. Histograms of ploidy determination by flow cytometry in (A) WT and (B) G1-1 mutated line, the letter "n" on the graphs refers to the number of haploid chromosomes.

4.1.3 Transmission of the EIF4E edition to F1 and F2 progenies

In order to confirm the heritability of the mutation and to perpetuate the edited lines, we acclimatized G1-1 y G1-2 T0 plants to *ex vitro* conditions and grew them to adults in a greenhouse. During the flowering phase, we detected the lack of pollen in G1-1 y G1-2 e*if4e* knock-out mutants, making selfing impossible. Nonetheless, female reproductive organs of hermaphrodite flowers appeared to be functional. We thus crossed G1-1 and G1-2 T0 (*eif4e*/*eif4e*) plants by WT (*EIF4E*/*EIF4E*) plants of the same genetic background to obtain the F1 generation (Figure 4.5). Since the two independent T0 lines displayed the same type of mutation, they will hereafter be referred to using the gRNA1-4E notation. Fourteen plants from the F1 progeny were used to determine the presence of the transgene by PCR. The segregation of transgenic *versus* non-transgenic plants in the F1 population was approximately 1:1, as expected for a single transgene insertion into the genome (Figure 4.6A). To evaluate the type of mutations in gRNA1-4E F1 plants, PCR amplicons including the target sequence of both transgenic and non-transgenic plants were sequenced. All non-transgenic evaluated lines (plants nº 1, 9, 10, 11, 12, 13, 14) presented the same single nucleotide deletion as in T0, but in heterozygosis, as expected for a *eif4e*/*eif4e* x *EIF4E*/*EIF4E* cross. These results demonstrated that induced mutations in melon can be stably transmitted through the germ line. In two of the transgenic lines (plants nº 3 and 7), the chromatogram revealed a single nucleotide deletion in both alleles, probably indicating that gRNA1 and Cas9 were still active and able to edit the WT allele after fecundation. All remaining transgenic

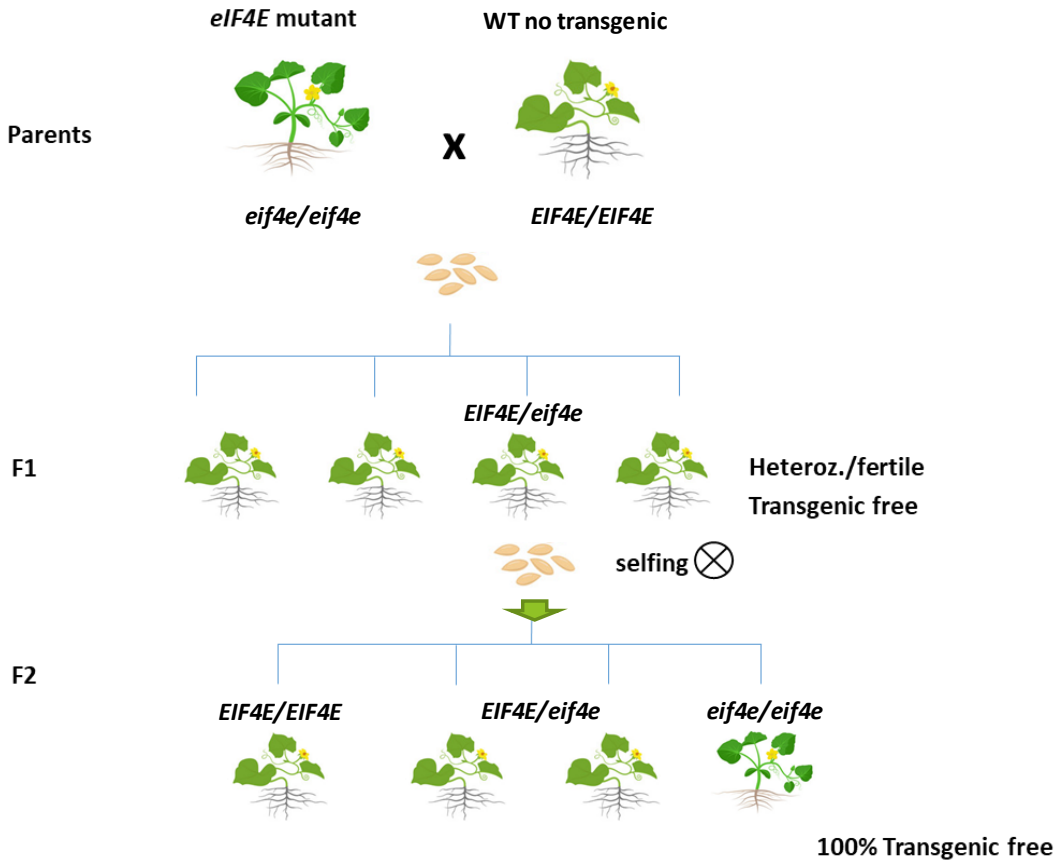

Figure 4.5. Schematic representation for obtaining of a segregating F2 population of *EIF4E* mutant. A transgenic plant, homozygous for the mutation in *EIF4E* (as female parent) was crossed by a non-transgenic WT plant of the same genotype (as male parent). From this first crossing, the F1 generation was obtained. The segregating F2 generation was obtained by self-pollination of heterozygous-fertile, non-transgenic individuals, selected in F1.

plants (plants nº 2, 4, 5, 6, 8) were heterozygous for the mutation in *EIF4E* (Figure 4.6B). Of note here is that amplicon direct Sanger sequencing revealed unambiguously the presence of the WT, the mutated or both mutated alleles in each F1 plant (Figure 4.7). Both transgenic and non-transgenic plants were transferred to the greenhouse and grown to adults for seed multiplication. During the flowering phase, we checked the phenotype of each individual: all heterozygous mutants (transgenic and non-transgenic) showed a fully fertile and normal growth phenotype. The two transgenic plants likely homozygous for the mutation showed a semi-infertile and reduced growth phenotype that lead, after attempting self-pollination, to a fail in fruit set or to reduced seed set and germination. We were able to normally self-pollinate and obtain fruits from all heterozygous mutants.

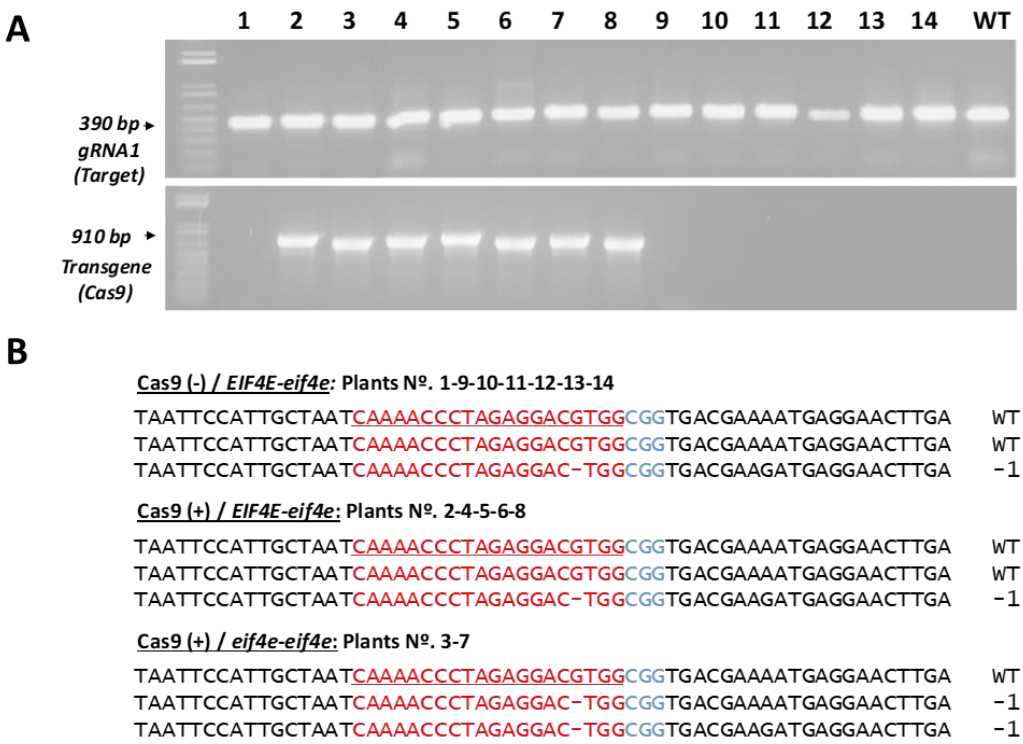

Figure 4.6. Genotyping of *EIF4E* mutants in 14 F1 progeny plants of the gRNA1-4E line. (A) Polymerase chain reaction (PCR) analysis amplifying a 390 bp genomic DNA sequence including the gRNA1 target site used to detect mutations (top panel) and amplifying a 910 bp DNA sequence corresponding to the *Cas9* transgene (bottom panel) in 14 F1 melon plants and non-mutant wild-type (WT). (B) Alignment of the genomic sequences of representative transgenic and non-transgenic *EIF4E/eif4e* heterozygous mutant plants with the WT sequence (top and middle panel) and alignment of the genomic sequence of a transgenic *eif4e/eif4e* mutant with the WT sequence (bottom panel). The sequences of each plant were obtained from the analysis of chromatograms resulting from the Sanger sequencing of purified PCR products. The first sequence of each panel represent the reference sequence, the underlying sequences represent the two alleles of the target gene. The target sequence is shown in red letters and the protospacer adjacent motif (PAM) is marked in blue letters. DNA deletions are marked with red dashes.

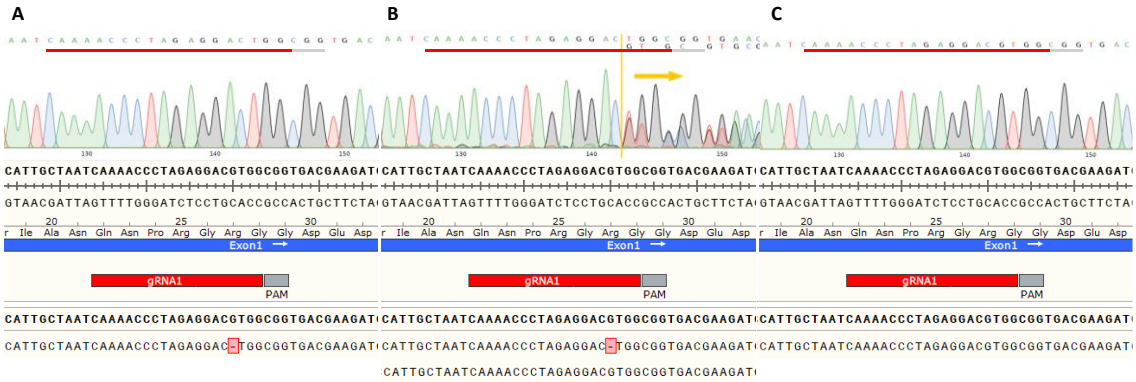

Figure 4.7. Chromatograms resulting from the Sanger sequencing of purified PCR products and corresponding genomic DNA sequence alignments with the wild-type sequence of (A) re-edited homozygous recessive (*eif4e/eif4e*) and (B) heterozygous (*EIF4E/eif4e*) representative gRNA1-4E individuals from F1 progeny compared to a (C) WT plant. The reference sequence is shown in bold letters, deletions in the mutant sequences are shown in red boxes.

In order to eliminate any possible disturbing effect of the transgene activity on the Mendelian segregation, we exclusively used seeds obtained from self-pollinations of non-transgenic F1 individuals to obtain the F2. We sowed 350 seeds but were able to obtain only 283 F2 plants. We genotyped each plant by Sanger sequencing of PCR fragments from individual plants as before. The F2 progeny segregated into three groups: homozygous mutant (*eif4e/eif4e*), heterozygous (*EIF4E/eif4e*) and homozygous WT (*EIF4E/EIF4E*) (Figure 4.8A). We then carried out a X^2 square test to analyse if the frequency of each group was consistent with that expected for a 1:2:1 segregation (homozygous mutant: heterozygous: homozygous WT). The statistical analysis rejected the null hypothesis, mainly due to a clear mismatch between the observed and the hypothesized frequencies for homozygous mutant plants (N = 283, ratio 1:2:1, degrees of freedom = 2, expected $X^2 = 13.82$, observed $X^2 = 57.6$, $P < 0.5$) (Figure 4.8B), suggesting an adverse effect of the mutation. If non-germinated seeds were arbitrarily assigned to the category homozygous mutant, a better fit with the frequencies of a 1:2:1 segregation could be deduced (N = 350, ratio 1:2:1, degrees of freedom =2, expected $X^2 = 4.61$, observed $X^2 = 4.3$, $P > 0.5$) (Figure 4.8C). The reduced growth phenotype observed in *eif4e* knock-out mutants would support the hypothesis of a negative effect of the *EIF4E* suppression resulting in poor seed germination.

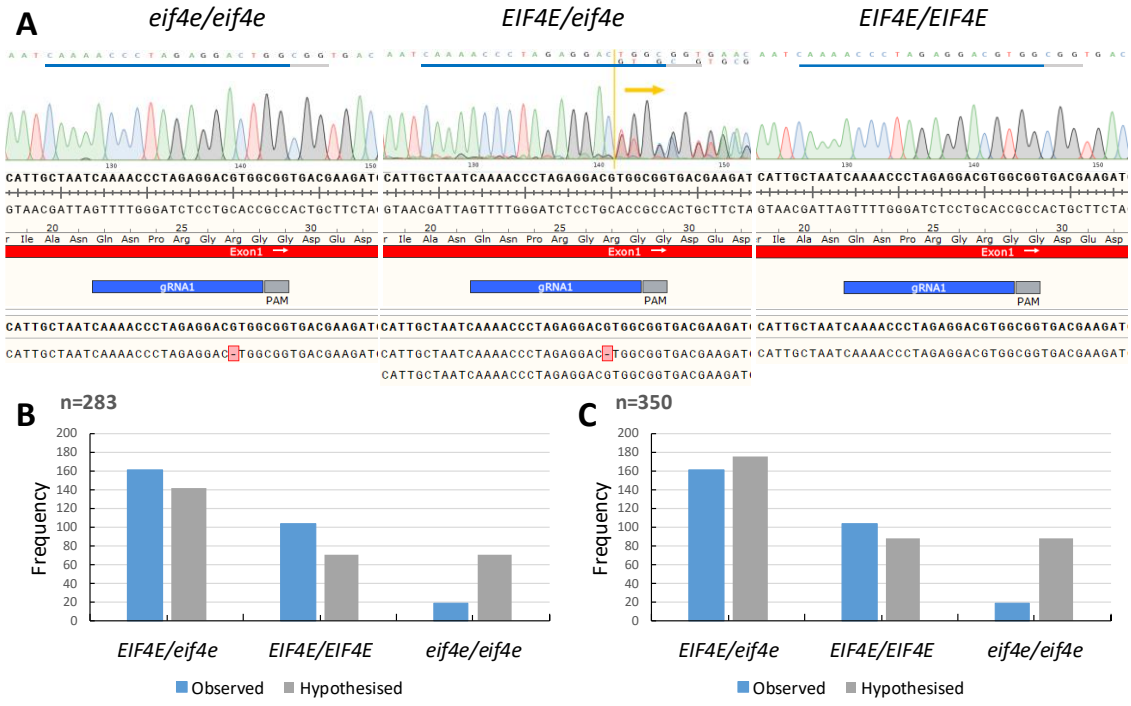

Figure 4.8. Genotyping of *eIF4E* mutants in F2 progeny plants of the gRNA1-4E line. (A) Chromatograms resulting from the Sanger sequencing of purified PCR products and corresponding genomic DNA sequence alignments with the wild-type sequence for 3 representative F2 plants showing the segregation into homozygous recessive (*eif4e*/*eif4e*), heterozygous (*EIF4E*/*eif4e*) and homozygous dominant (*EIF4E*/*EIF4E*) groups. The reference sequence is shown in bold letters, deletions in the mutant sequences are shown in red boxes. (B) Segregation and relative frequencies of the 283 F2 plants (excluding non-germinated seeds) (N = 283, Ratio 1:2:1, degrees of freedom = 2, expected X2 = 13.82, observed X2 = 57.6, P < 0.5) and (C) hypothesized segregation and relative frequencies of 350 F2 plants assigning non-germinated seeds to the homozygous recessive group (N = 350, Ratio 1:2:1, degrees of freedom =2, expected X2 = 4.61, observed X2 = 4.3, P > 0.5).

Next, gRNA1-4E potential off-targets were evaluated by using the CRISPR-P program (Liu et al., 2017) mapping the gRNA1 sequence against the melon genome. Five off-target candidates were identified (Table 4.2). PCR and sequencing of these candidate targets revealed no changes in the genome of non-transgenic F2 generation plants.

Table 4.2. Putative *EIF4E* CRISPR/Cas9 gRNA1 off-target sites

Sequence of the putative off-target site	Off-targetscore	MMs	Locus	Gene ID	Gene	Region
CAAAATCGTAGAAGACGTGGAGG	0.551	3MMs	scaffold00023:-5325134			Intergenic
CAAACTCCTAAAGGACGTGAAGG	0.435	4MMs	scaffold00006:+4019441	MELO3C006540	beta-galactosidase 7-like	CDS
CAAAACCGGAGAAGACGTGACGG	0.344	4MMs	scaffold00005:+401743	MELO3C005084	E3 ubiquitin-protein ligase	CDS
GAAAACGCGAGAGGACGAGGCGG	0.177	4MMs	scaffold00016:+4417626	MELO3C012320	sucrose-phosphatase 2	CDS
AAAAACCTTAGAAGAGGTGGAGG	0.124	4MMs	scaffold00038:-1390329	MELO3C019462	Membralin, putative	CDS
CAAACCCCTAGAAGACGTGGGAG	0.12	2MMs	scaffold00024:-2063176	MELO3C015061	Growth inhibition and differentiation	CDS
CAAAGACGTAGAGGACATGGCAG	0.104	4MMs	scaffold00004:+7609278			Intergenic
CAAAACCATTGAGGTCGTTGAGG	0.076	4MMs	scaffold00012:-3766001			Intergenic
CAAAACCTTGGAGGAGGAGGAGG	0.05	4MMs	scaffold00053:+1762859	MELO3C022610	Formin-like protein	CDS

4.1.4 Resistance to MWMV associates with EIF4E edition

We have demonstrated previously that transgenic RNAi *EIF4E* silenced melon plants show broad virus resistance, including resistance to the potyvirus Moroccan watermelon mosaic virus (MWMV) (Rodríguez-Hernández et al., 2012). To verify whether the knocking out of *EIF4E* confers virus resistance in melon, all seedlings of the F2 progeny described above were mechanically inoculated with MWMV. Seedlings started to develop mosaic symptoms at 10 dpi, turning to severe leaf deformation at around 14 dpi in heterozygous and WT non-mutant plants (Figure 4.9A). No symptoms were detected in any of the homozygous mutant plants at 20, 30 and 40 dpi. At 21 dpi, we sampled 15 plants from each group (homozygous mutant, heterozygous and

homozygous WT) and made pools of leaves above the inoculated ones from five individuals within each category and we performed RT-qPCR to determine the viral load. No MWMV RNA was detected in homozygous mutant plants, whereas variable but significant viral loads were detected for heterozygous and WT plants. In this experiment we introduced as a control plants of the RNAi *EIF4E* silenced melon line (Rodríguez-Hernández et al., 2012); no virus accumulation was observed in plants of this line (Figure 4.9B).

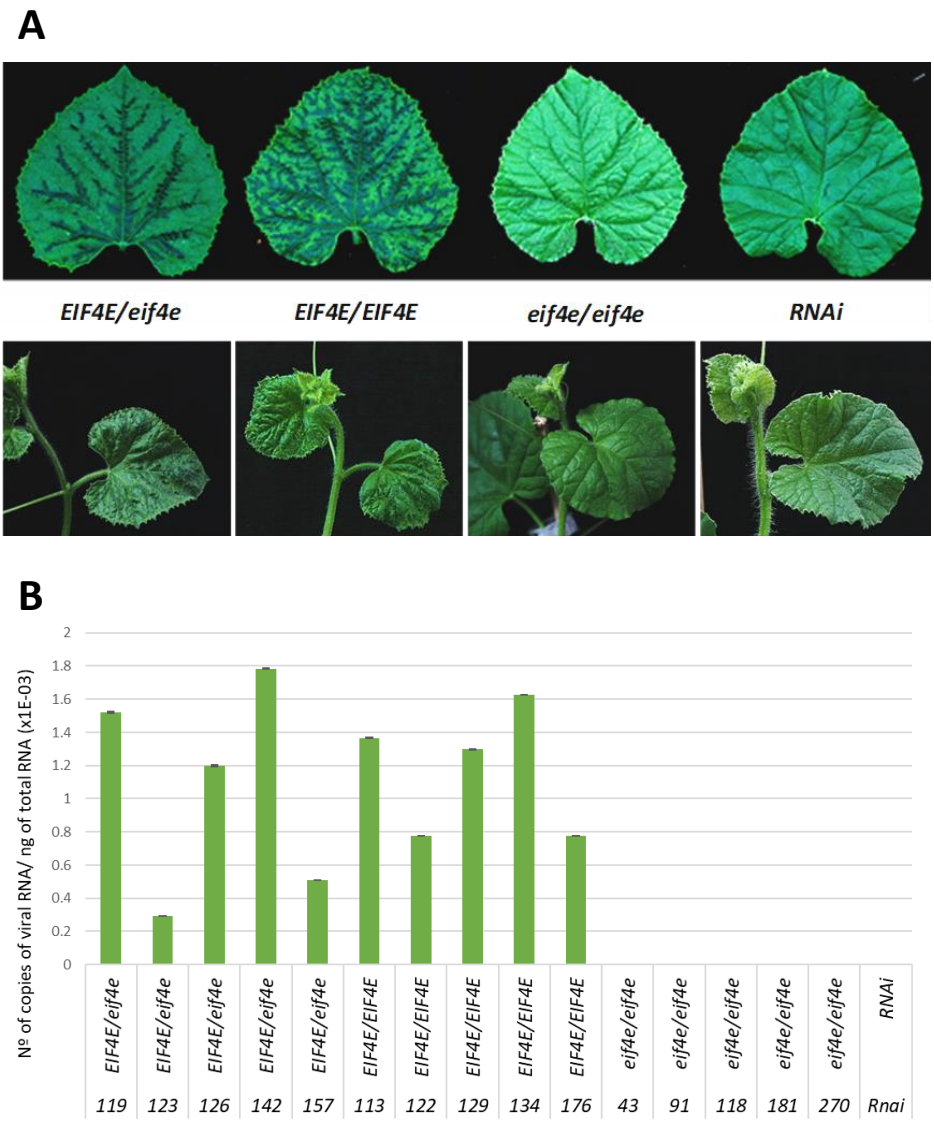

Figure 4.9. Homozygous *eif4e* mutant plants exhibited immunity to Moroccan watermelon mosaic virus (MWMV) infection. (A) Disease symptoms (leaves -upper panel- and plants -lower panel-) of heterozygous (*EIF4E/eif4e*), homozygous wild type (WT) (*EIF4E/EIF4E*), and recessive homozygous (*eif4e/eif4e*) of the F2 edited generation and RNAi (control) plants (Rodríguez-Hernández et al., 2012) at 14 days post inoculation (dpi). (B) Reverse transcription-quantitative polymerase chain reaction (RT-qPCR) analysis of MWMV RNA accumulation at 21 dpi in 5 individuals heterozygous (*EIF4E/eif4e*), homozygous WT (*EIF4E/EIF4E*), recessive homozygous (*eif4e/eif4e*) and RNAi (control) (Rodríguez-Hernández et al., 2012) plants.

Eighteen *eif4e/eif4e* plants from F2 were kept under observation for 6 months. Interestingly, after 4 months from inoculation, symptoms compatible with MWMV infection were observed in 2 of the 18 plants, suggesting a resistance-breaking event. To check whether the symptoms were caused by MWMV, young symptomatic leaves from the 2 plants affected were sampled and RT-qPCR was carried out to determine the presence of MWMV. Symptomatic plants tested positive for MWMV, therefore a back-inoculation assay (Figure 4.10A) was performed to confirm the presence of a resistance breaking (RB) MWMV isolate: We inoculated six WT and six RNAi plants with sap from the resistant plants that showed late symptoms, and another six WT and RNAi plants with the original inoculum. After 14 dpi, WT plants inoculated with both sources of inocula showed symptoms, but only the isolate in the inoculum prepared from the late-infected plants was able to infect the RNAi melon lines, overcoming resistance; from now on we will refer to this isolate as MWMV-resistance breaking (RB). An RT-qPCR analysis to determine viral load in individual plants using RNA extracted from systemically infected leaves from plants inoculated with both sources of inocula confirmed that MWMV-RB was able to overcome the resistance induced by silencing of *EIF4E*. MWMV-RB seemed to accumulate less in silenced plants (Figure 4.10B). It has been widely described that mutations in the viral VPg of potyviruses are frequently responsible for the overcoming of resistances associated with eIF4E (Gallois et al., 2018), we thus RT-PCR-amplified the entire *VPg* cistron and sequenced the DNA product. A sequence alignment showed a single nucleotide substitution leading to the single amino-acid change N163Y (Figure 4.10C) for the MWMV-RB isolate. In an attempt to further understand the interaction between eIF4E and viral VPg, we modelled the interaction between these two proteins, paying particular attention to residue 163, the replacement of which associated with the overcoming of resistance in plants deficient in *EIF4E*. Despite being involved in the interaction with the VPg of MWMV in all bioinformatics predictions of active residues (Haddock 2.2), residue 163 does not appear to be among those constituting the contact surface in the three-dimensional predictions of protein-protein interactions, neither in the models built for this thesis (Figure 4.10D) nor in the reference model for this two proteins based on the human eIF4E-PVY VPg interaction. Finally, we did a multiple sequence alignment of VPgs from different potyviruses and found that the amino-acid substitution N163Y is flanked by two very

conserved motifs within this virus family, suggesting possible structural and functional conservation across potyviruses (Figure 4.10E).

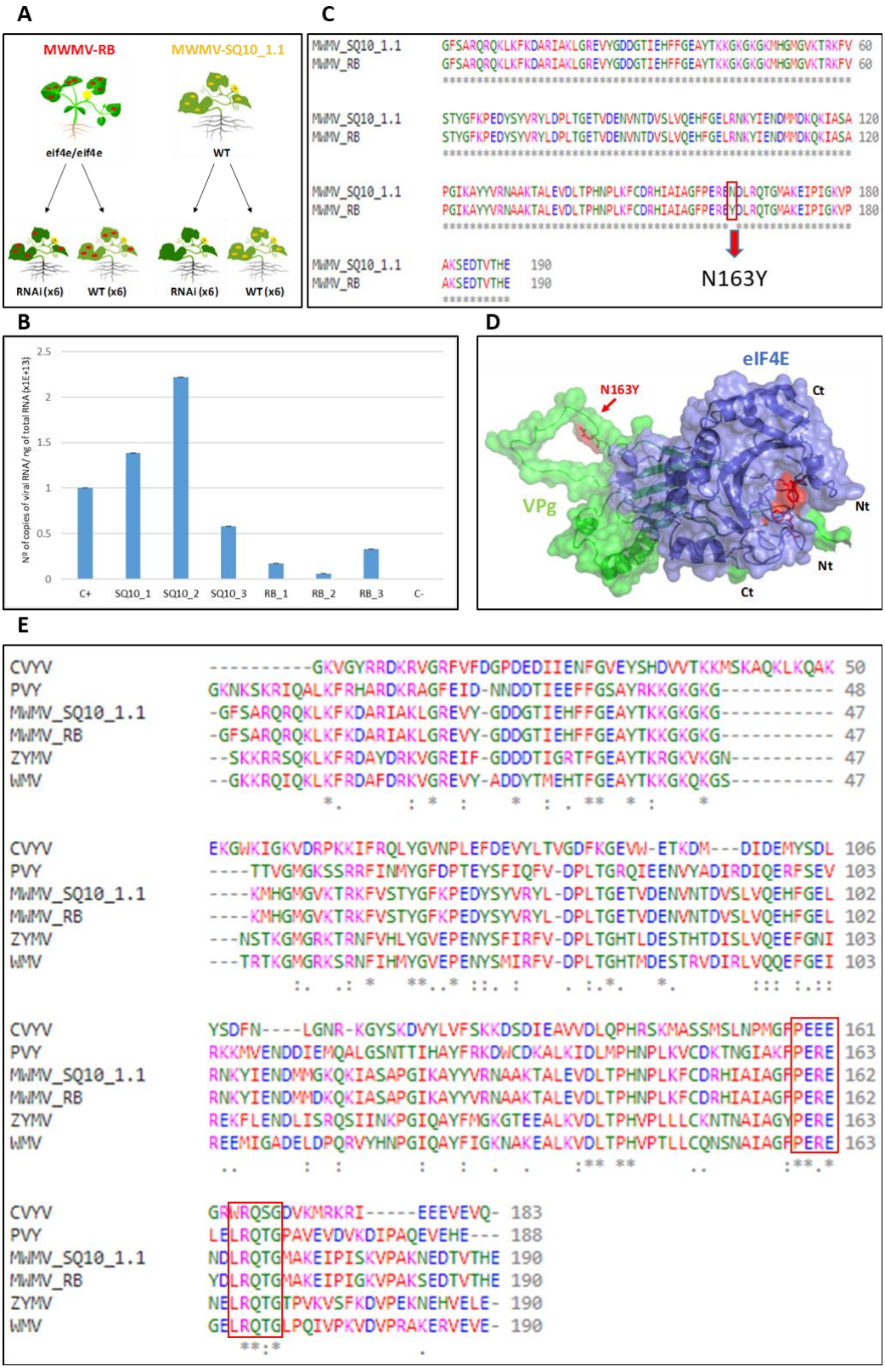

Figure 4.10. Analysis of a Moroccan watermelon mosaic virus (MWMV-SQ10_1.1) resistance breaking (RB) isolate. (A) back-inoculation assay: leaves from a *eif4e/eif4e* resistant plant that presented late MWMV symptoms were used as a source of inoculum (red spots). MWMV-SQ10_1.1 are WT plants infected with the original source of inoculum used to test for resistance the F2 mutants (yellow spots). (B) Reverse transcription-quantitative polymerase chain reaction (RT-qPCR) analysis of MWMV RNA accumulation at 14 dpi in individual plants. SQ10_1, SQ10_2 and SQ10_3 correspond to WT plants inoculated with SQ10_1.1. RB_1, RB_2 and RB_3 are RNAi lines infected with MWMV-RB. C+ is and F2 susceptible plant infected with MWMV. C- is a mock inoculated plant. (C) Multiple alignment of amino acid sequences of VPg from MWMV-RB and MWMV-SQ10_1.1. The unique amino-acid change between the two variants is underlined in red. (D) Simulated 3D surface model of the interaction between MWMV VPg (green) and eIF4E (blue) complex. Tryptophans W82 and W182 from eIF4E involved in the association with m7GTP Guanosine-5'-triphosphate cap analog are showed in sticks and coloured red. The N163Y substitution responsible for the overcoming of the resistance to MWMV is highlighted by a red arrow. (E) Multiple amino acid sequence alignment of VPg's from different potyviruses. Conserved motifs between the different viruses are highlighted with red boxes.

4.1.5 eif4e knock-out plants show male sterility

As described above, homozygous mutant T0 plants showed male sterility, and in a cross to the WT, we observed fertility restoration: When hermaphrodite T0 flowers were pollinated with WT pollen, all 18 representative F1 plants were fertile. The F2 showed a perfect correlation between the segregation of the male sterility phenotype and the segregation of the *EIF4E* mutation: Only homozygous mutant individuals, and all of them, showed the male sterility phenotype after examining a minimum of 10 flowers per plant along a time period of 60 days; all other plants, either homozygous WT or heterozygous produced staminate and perfect flowers with viable pollen. Vegetative growth seemed to show no significant differences from heterozygous or homozygous dominant plants in the first 40 days after germination. The most significant differences were observed from the flowering stage onwards in the adult plants: Homozygous recessive mutant plants bolted 1-5 days later, and their flowers had smaller, paler petals than those of heterozygous and WT plants. The mutant anthers were small and white, without mature pollen grains, and did not dehisce, resulting in complete male sterility (Figure 4.11).

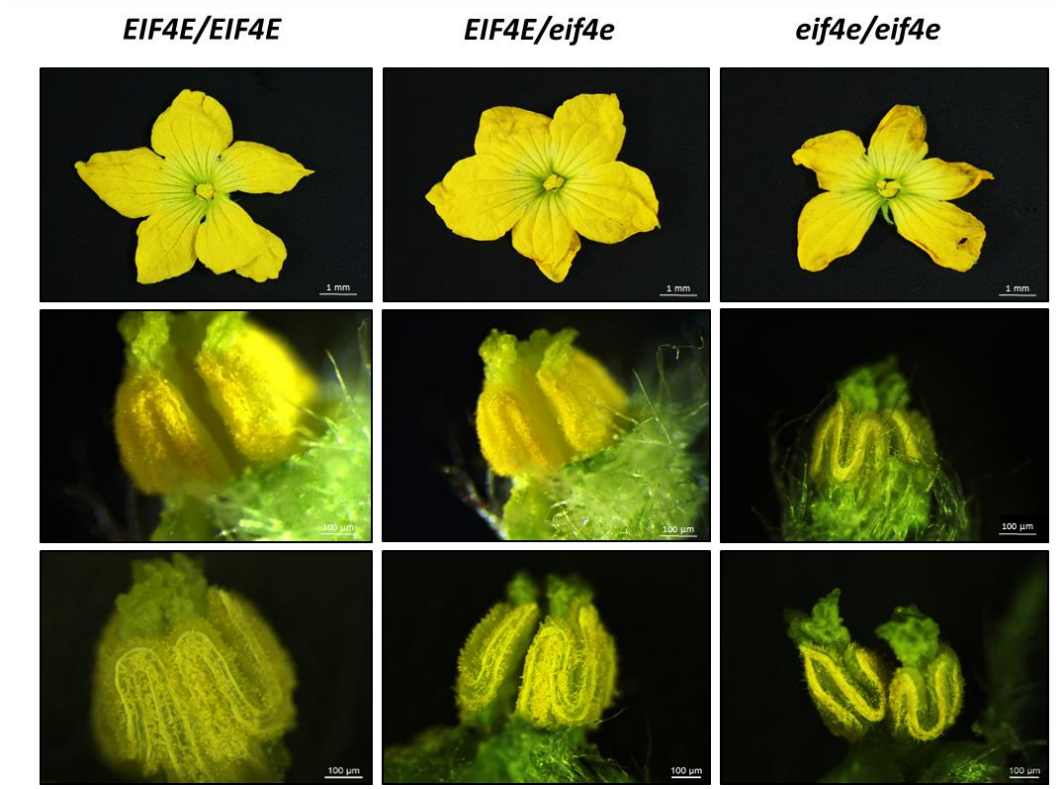

Figure 4.11. Genotype-phenotype association in F2 melon male flowers. Staminate and perfect flowers with viable pollen in the anthers of homozygous WT and heterozygous F2 plants, small and not dehiscent anthers, without mature pollen grains in homozygous recessive F2 plants at 40 days post germination.

4.2 Morphological and transcriptomic analysis of melon flowers at different stages of development

4.2.1 Morphogenesis of the melon flowers

4.2.1.1. Stages common to male and hermaphrodite flowers

To study the morphogenesis of the male and hermaphrodite flowers of melon, we analysed longitudinal sections of floral buds at different stages of development by light microscopy and scanning electron microscopy. In agreement with observations for other cucurbits (Hao et al., 2003, Bai et al., 2004) we identified 12 stages, ranging from meristem initiation to anthesis (Table 4.3 and Figure 4.12).

Table 4.3. Morphological indications and respective lengths of melon (*Cucumis melo*) floral buds at various stages of development

Stage	Morphological indications	Length of floral bud (mm)[a]	Sample figures
1	Floral meristem initiation and broadening	< 0.2	4.12A, 4.12B
2	Sepal primordia initiation	~ 0.2	4.12C
3	Petal primordia initiation	~ 0.3	4.12
4	Stamen primordia initiation	~ 0.4	4.12E
5	Carpel primordia initiation	~ 0.55	4.12F
6	Stamen differentiates anthers and filament	0.6-0.7	4.12G
7M	Anther expands	0.6-0.7	4.12H
7H	Carpel primordia differentiates stigmas and ovary, and the space in the potential placenta becomes parallel-sided	~ 0.9	4.13B
8M	Anther locules differentiate morphologically	~ 0.8	4.12I, 4.14A
8H	Stigma starts to grow beneath the stamens	1-1.5	4.13C, 4.14E, 4.14F
9M	Microsporocyte formation initiates	0.8-1	4.12J, 4.14B
9H	The placenta is clearly distinguishable, the differentiation between the stigma and the style is observed	2.5-3	4.13D, 4.14G
10M	Meiosis in anthers, nectary tissues initiate	2-5	4.12K, 4.14C
10H	Ovule primordia is initiated, the stigma further differentiates and nectary tissue forms a ring	4-5.5	4.13E, 4.14H
11M	Uninuclear pollen appears, nectary tissue forms a ring	6-10	4.12L, 4.14D
11H	Female meiosis occurs and embryo sacs are formed	8-10	4.13F, 4.15H
12M	Mature pollen is formed, anthesis occurs	>20	4.12M
12H	Nectary tissues vascularize before anthesis	>20	4.13G

[a] Floral length are given based on observations of at least 20 floral buds in the respective stages. M refers to male and H to hermaphrodite.

Stages 1 to 5 are shared by male and hermaphrodite flowers. Stage 1 was characterized by the formation of floral meristems in the axils of leaf primordia (arrowheads in Figure 4.12A). In stages 2 to 5, floral meristems underwent gradual broadening (Figure 4.12B) that led to the sequential initiation of sepals, petals, stamens

and carpels primordia (Figures 4.12C to 4.12F). Consistent with observations for the flower development of other cucurbits (Bai et al., 2004), we found no evidence of structural differences between male and hermaphrodite flowers prior to stage 5 (Figure 4.12F), which corresponds to the initiation of carpel primordia. Therefore, the morphogenetic process of male *versus* hermaphrodite flowers is described from stage 6 onwards (Table 4.3).

4.2.1.2. Stages specific for the male flowers

In stage 6 of the male flower development there was a consistent thickening of the stamen primordia, accompanied by a constriction at the base, indicating the gradual differentiation between the stamen and the filament; in contrast, the carpel primordia did not undergo changes in structure or size (Figure 4.12G). In stage 7 the anthers primordia begun to enlarge (Figure 4.12H), while in stage 8 we observed the initiation of locules differentiation together with the appearance of vascular bundles in the filaments (Figure 4.12I, K, M and Figure 4.14A). As there were no further distinguishable morphological changes in the anther, the following developmental stages were defined according to the differentiation of reproductive cells. Therefore, stage 9 was defined by microsporocyte formation (Figure 4.12J and Figure 4.14B), stage 10 by meiosis (Figure 4.12K and Figure 4.14C), stage 11 by uninuclear pollen appearance (Figure 4.12L, Figure 4.14D) and stage 12 coincided with mature pollen formation (Figure 4.12M).

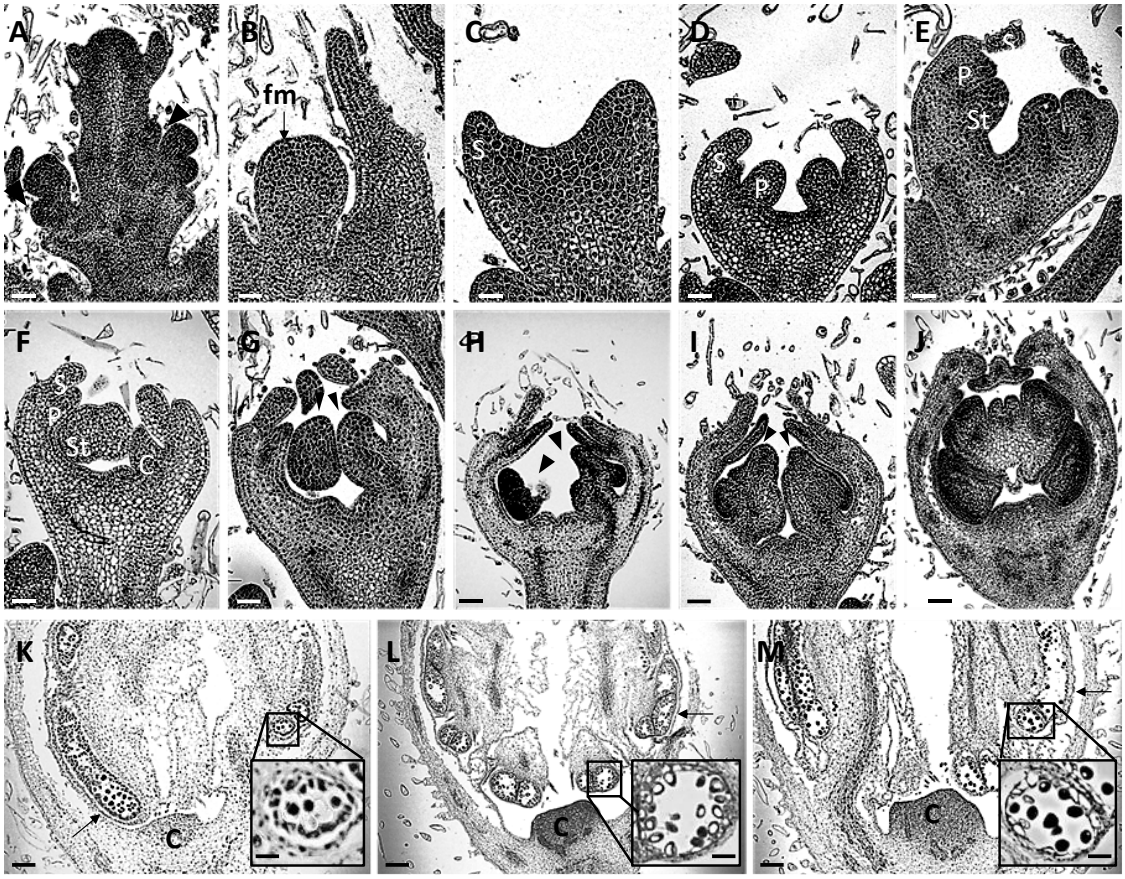

Figure 4.12. Development of male flowers of melon (*Cucumis melo*) as observed at the light microscope (A-M). (A) Shoot tip. The newly initiated floral buds (early stage 1) are indicated by arrowheads. (B) Floral meristem buds at stage 1. (C–F) A floral bud at stages 2 (C), 3 (D), 4 (E), and 5 (F). (G–J) Male floral buds at stages 6 (G), 7 (H), 8 (I), and 9 (J). The arrowheads indicate stamens. (K–M) Part of a male floral bud at stages 10 (K), 11 (L), and 12 (M). The arrows indicate locules containing microspore mother cells and tetrads, uninuclear pollen and mature pollen in K, L and M, respectively. Ca, carpel; Fm, floral meristem; P, petal; S, sepal; St, stamen. Bars = 15µm (A), 20 µm (B, C, D), 30 µm (E), 40 µm (F, G), 50 µm (H, I), 100 µm (J-L) or 200 µm (M). Scale bars in the magnifications of figures K, L, M = 30 µm.

4.2.1.3. Stages specific for the hermaphrodite flowers

In stage 6, the differences between male and hermaphrodite flowers were very subtle; in addition, unlike other varieties of melon that present separate sexes, for the variety studied the simultaneous development of the male and female structures made it difficult to clearly identify the initiation of the stigma at this stage. The first indication of differentiation was the elongation of carpel primordia which occurred simultaneously to the differentiation of the stamen between anther and filament (Figure 4.13A). In stage 7, the elongation of the carpel primordia was accentuated, creating a parallel-sided invagination into the space of the potential placenta, while the developing stigma almost reached the connection between the newly formed filament and the anther

(Figure 4.13B). From stage 8 onwards, the development of male and female reproductive structures occurred simultaneously: In stage 8 of hermaphrodite flowers, the primordial stigma reached a height approximately equal to that of the developing stamen (Figure 4.13C and Figure 4.14E and F). The male structures of the hermaphrodite flower at stage 8 were characterized by the enlargement of the carpel primordia (corresponding to stage 7 in the development of the male flower, Figure 4.12H). In stage 9 the placenta was clearly distinguishable, the differentiation between stigma and style was evident, and nectary cells started to initiate at the base of the style (arrowhead in Figure 4.13D and Figure 4.14G). In stage 10, the ovule primordia were initiated (white arrow in Figure 4.13E), the papillae cells were differentiated on the stigmas (Figure 4.14H) and the nectary cells arose clearly as a dome (Figure 4.13E). The male structures of the hermaphrodite flower at stage 10 were characterized by the microspore formation. During stage 11 (Figure 4.13F) the integuments were initiated (not shown), the stigma further differentiated (arrow in Figure 4.13F) and the nectary tissue formed a ring (arrowhead in Figure 4.13F). At stage 11 meiosis occurred and embryo sacs were formed (Figure 4.13H). Male structures at stage 11 were characterized by uninucleate pollen appearance after meiosis. Finally, in stage 12 nectary tissue vascularized before it broke for anthesis (Figure 4.13G). Mature pollen appeared in anthers at this stage (arrow in Figure 4.13G).

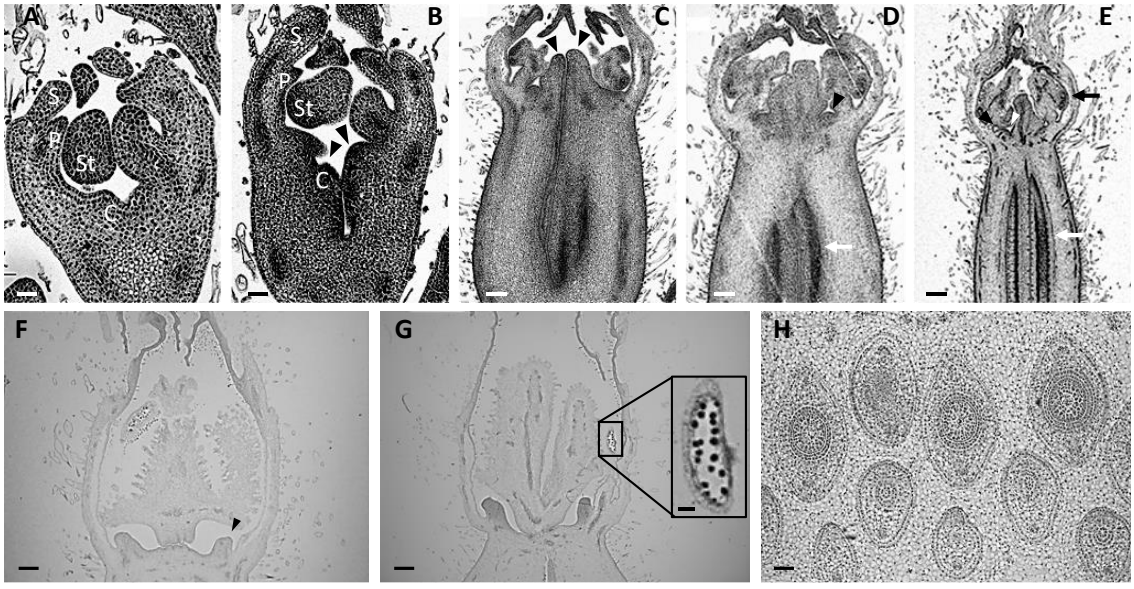

Figure 4.13. Development of female hermaphrodite flowers of melon (*Cucumis melo*) as observed by light microscopy (A-H). Floral buds at stages 6 (A), 7 (B), 8 (C), 9 (D), 10 (E). 11 (F and H) and 12 (G). The carpel primordia, the newly initiated stigmas and the nectary cells (stages 7, 8, 9 and 11, respectively) are

indicated by arrowheads (B, C, D, F, respectively). The placenta and the ovule primordia (stages 9 and 10, respectively) are indicated by white arrows (D, E). The microspore formation (stage 10) is indicated by a black arrow. Mature pollen in stage 12 is indicated in a black box and at higher magnification (G). Ca, carpel; P, petal; S, sepal; St, stamen. Bars = 40 µm (A), 50 µm (B), 400 µm (C), 500 µm (D), 1 mm (E), 500 µm (F, G) or 100 µm (H). Scale bar in the magnification of figure G = 60 µm.

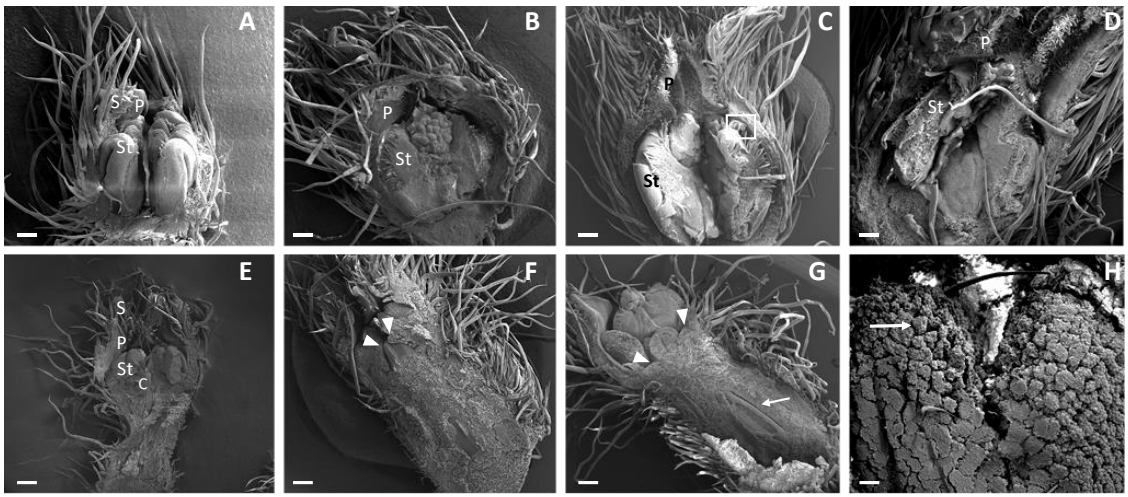

Figure 4.14. Development of male and hermaphrodite floral buds of melon (*Cucumis melo*) observed by scanning electron microscopy. (A–H) male floral buds at stages 8 (A), 9 (B), 10 (C), and 11 (D). (E-H) hermaphrodite floral buds at early stage 8 (E), stage 8 (F), stage 9 (G) and high magnification of the stigma at stage 10 (H). The newly initiated stigma and the nectary cells (stage 8 and 9, respectively) are indicated by white arrowheads. The placenta and the papillae cells (stages 9 and 10, respectively) are indicated by white arrows. Bars = 200 µm (A, E, F), 100 µm (B), 250 µm (C, G), 500 µm (D, H).

4.2.2 RNA-seq along flower developmental episodes

The stages defined above involve subtle morphological changes that cannot be observed without a proper microscopy study. Therefore, for the transcriptome analysis, flowers were collected pooling them according to their sizes (Table 4.3), with pools corresponding to four main episodes during floral development: For the floral structures formation (FS) episode, which is essentially shared between male and hermaphrodite flowers, the buds were of less than 2 mm in length likely grouping stages 1 to 8 together with stage 9M (Table 4.3). For the gamete initiation (GI) episode, the floral buds were of 2 to 5 mm in size and we likely collected flowers at stage 10 (Table 4.3). For the gamete maturation (GM) episode, buds were of 8 to 10 mm corresponding to stage 11 (Table 4.3). Finally, for the anthesis (AN) episode floral buds were larger than 2 cm. Logically, for the GI, GM and AN episodes, male and hermaphrodite buds were differentiated,

giving rise to pools GI-M/H, GM-M/H and AN-M/H. Fifty floral buds were pooled per biological replicate, and three replicates were prepared per each of the four floral episodes defined above. Total RNA was subjected to next-generation sequencing using an Illumina platform. RNA-seq reads were filtered by quality and then mapped to the melon reference genome (DHL92) (Annex 1, Table 8.1). For all comparisons, read counts were normalized to FPKMs to obtain the relative levels of expression. Genes were considered as expressed if there were mapping reads in all the replicates and if the average FPKM value between replicates was higher than 1 in at least one episode. Thus, ~15.500 genes were expressed in each stage (Figure 4.15A). A cluster dendrogram analysis of gene expression profiles, together with a PCA, showed that gene expression patterns among biological replicates were highly related except for two replicates, one for GM-H and the other for AN-H, respectively (Annex 2 Figure 8.1). When these two anomalous replicates were excluded from the analysis, both the PCA and the cluster dendrogram (Figure 4.15B and 4.15C) showed that replicates clustered together, providing confidence on the use of floral bud size as indicator of the flower developmental episode. Therefore, for the analyses described next, all treatments have three replicates except for GM-H and AN-H, which have two. In addition, the PCA showed a separation between the clusters of male and hermaphrodite samples (Figure 4.15C). Regarding expressed genes, 13,539 (80 %) were expressed in all four episodes in male flowers, whereas 14,581 (86 %) were expressed in hermaphrodite flowers during all episodes (Figure 4.15D). The number of genes expressed in only one episode in male flowers were 78, 284, 43 and 199 for FS, GI, GM and AN, respectively (Figure 4.15D), suggesting a more complex gene expression landscape during the gamete initiation and anthesis compared to the other episodes. The number of specific genes in the hermaphrodite flowers was 2, 425, 9 and 44 for FS, GI, GM and AN, respectively (Figure 4.15D), reflecting the same general trend observed for the male flowers.

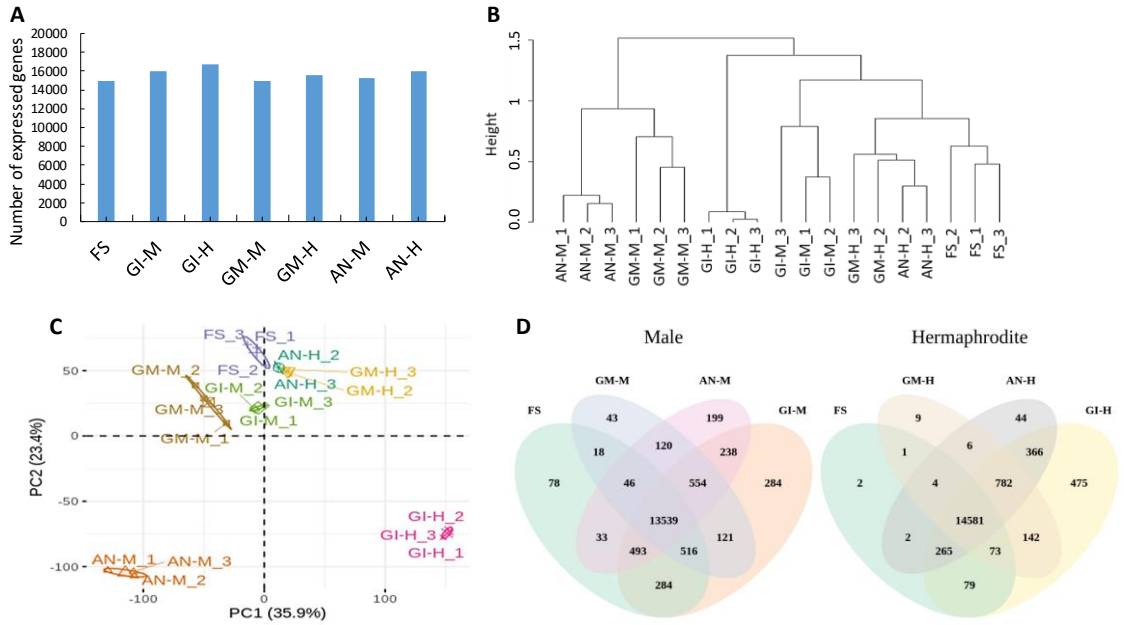

Figure 4.15. RNA-seq along flower developmental episodes. Four episodes during floral development were considered: Floral structures formation (FS), gamete initiation (GI), gamete maturation (GM) and anthesis (AN) episodes. (A) Number of expressed genes per episode. Expressed genes are considered those with an average value of FPKM (fragments per kilobase per million mapped reads) > 1 in at least one episode. (B) Cluster dendrogram of gene expression profiles between biological replicates and among different developmental episodes. The dendrogram shows the hierarchical clustering of the different replicates according to their gene expression profiles. (C) Principal Component Analysis (PCA) scores plotted for male and hermaphrodite floral development episodes. PCA was computed using expressed genes. PC1, principal component 1; PC2, principal component 2. The percentage of variance explained by PC1 and PC2 are 35.9 % and 23.4 %, respectively. Confidence ellipses were plotted around group mean points. (D) Venn diagrams showing the numbers of expressed genes specific or shared among flowers at different developmental episodes. Venn diagrams were drawn using expressed genes.

4.2.3 k-means analysis of differentially expressed genes in male and hermaphrodite flowers

To identify differentially expressed genes (DEGs), pairwise comparisons were conducted between all possible pair combinations of datasets across the four developmental episodes (Figure 4.16); only genes with an adjusted P value less than 0.05 were considered as differentially expressed. For male flowers, DEG numbers correlated with the developmental distance among pairs of episodes, *i.e*. the largest DEG number was found between FS and AN-M, whereas the contiguous episodes GM-M and AN-M had the smallest number of DEGs (Figure 4.16). In contrast, for hermaphrodite flowers this trend did not emerge with clarity; the largest number of DEGs occurred between FS

vs GI-H whereas FS vs AN-H had a moderate number of DEGs, smaller that FS vs GI-H, which had the largest DEG figure for hermaphrodite flowers (Figure 4.16). This is somehow counter-intuitive, but agrees well with previous results, where episodes FS, AN-H and GM-H appear close in the PCA and clustering analyses (Figure 4.15B and 4.15C). In total, the pairwise comparisons identified 12,469 and 11,574 DEGs in male and hermaphrodite flowers, respectively. These are the genes that were considered in the following analyses.

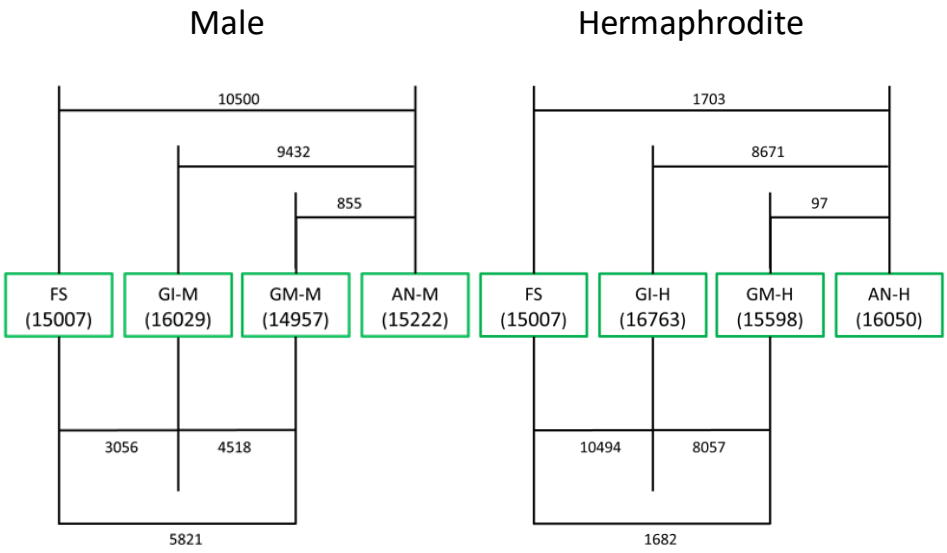

Figure 4.16. Numbers of differentially expressed genes (DEGs) between the specified melon male and hermaphrodite flower developmental stages. Numbers above lines indicate the number of DEGs between the compared episodes. Numbers in brackets indicate the number of genes expressed in each episode.

First, MADS-box genes were analysed along the floral developmental episodes. These genes have multiple functions during floral development, such as regulating the vegetative transition from the juvenile to the reproductive phases and are involved in the floral development of many plants. All DEGs as defined before which are annotated as MADS-box putative transcription factors in the gene model descriptions (version 3.6.1) were included in the analysis (Annex 3, Table 8.2). The results (Figures 4.17) showed that the Arabidopsis homolog MADS-box protein AGL42 (MADS83), which has been reported to play a role in promoting flowering at the shoot apical and axillary meristem, has elevated expression levels at the FS and GI stages for both male and

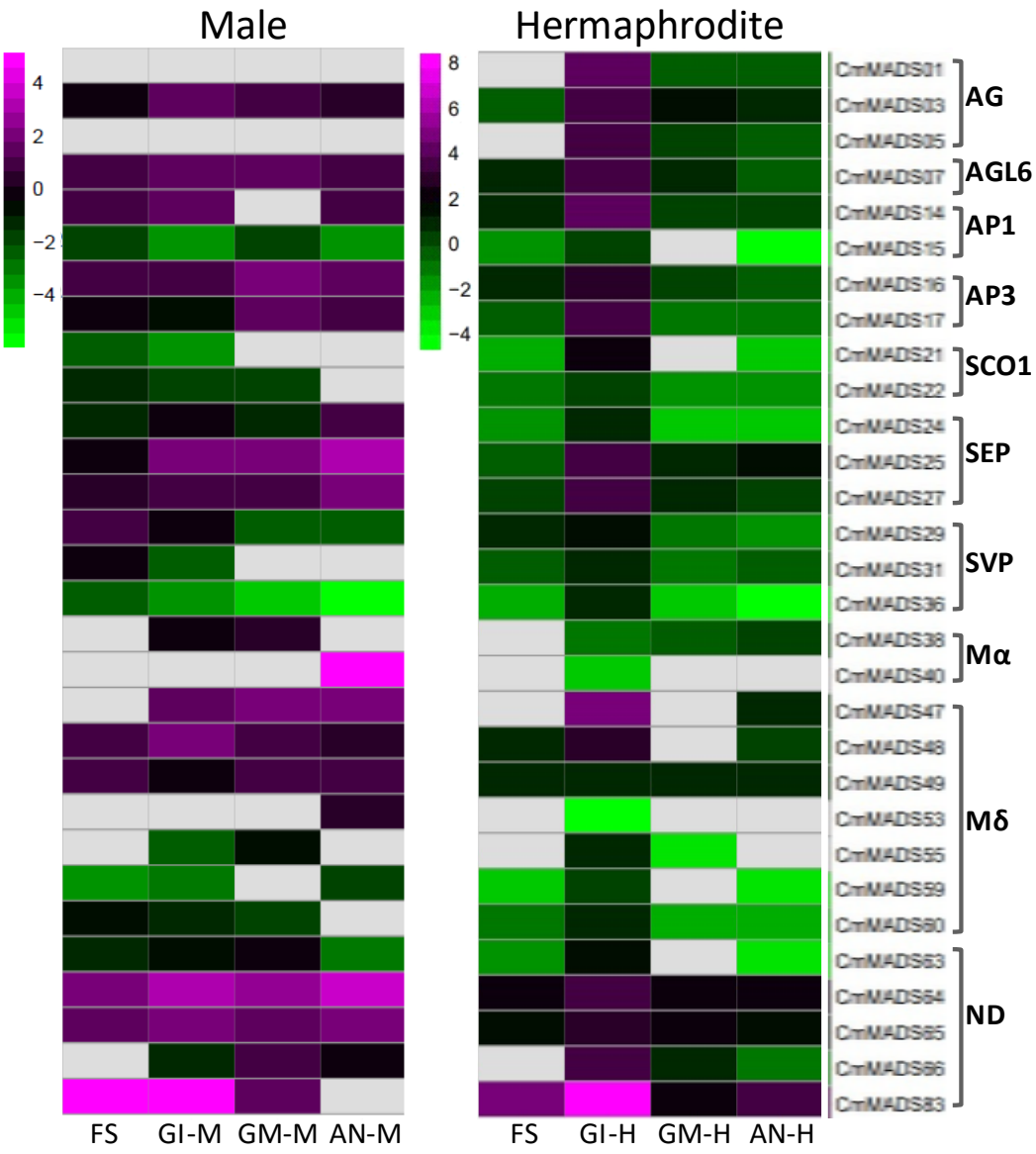

Figure 4.17. Differential expression of MADS-box transcription factors during male (left) and hermaphrodite (right) floral development in melon. Melon MADS-box genes are named and classified according to their distribution in subfamilies based on the phylogenetic relationships with their homologs in Arabidopsis and cucumber (Hao et al., 2016).

hermaphrodite flowers and its expression levels decline throughout the flowering process. Homologs of the MADS-box gene encoding protein SOC1 (MADS64 and MADS65), which are transcription activators active in flowering time control, had an almost male flower-specific expression, which was maintained, with slight fluctuations, throughout the whole process of flower development. The Arabidopsis homologs of AGAMOUS-LIKE proteins MADS25 and MADS27 showed an increasing expression pattern throughout male flower development, whereas in the hermaphrodite flower,

expression was concentrated in the GI stage. In contrast, MADS36 and MADS15, involved in the determination of floral meristem and sepal identity, were down-regulated throughout floral development for both sexual types.

A more general approach was followed next. A *k*-analysis was performed on the total number of DEGs for male and hermaphrodite flowers with k set to 16. The clusters showed distinct gene expression patterns that are likely to be associated with their functions throughout melon floral development. In the case of male flowers (Figure 4.18), 3,205 genes were found in clusters 2, 3 and 15 showing the highest expression values during FS, and these genes were down-regulated at later flower developmental episodes. The 749 genes in clusters 4 and 11 showed a GI-M specific pattern, while only cluster 5, with 745 genes, had the highest expression values at GM-M. The 244 genes of cluster 1 were mainly expressed in both GI-M and GM-M. Finally, the 1,777 genes of clusters 7 and 14 had expression patters showing a peak in AN-M, after different patterns of expression during early flower development (Figure 4.18). For hermaphrodite flowers, all 497 genes in clusters 5, 12 and 15 had a peak of expression at the FS stage, and these were down-regulated over the course of floral development. 5,865 genes in clusters 1, 8, 9, 10, and 11 had a specific GI-H pattern, while only 92 genes in cluster 14 had elevated GM-H expression. Finally, 1,002 genes in clusters 7 and 16 had an expression peak in AN-H, after an ascending pattern of expression throughout the developmental stages (Figure 4.19). As a general conclusion from this analysis, while clustering showed that genes can be de-regulated in more than one episode during floral development, some clusters showed specific up-regulation in just one episode, suggesting that the genes in these clusters can be the main drivers of floral transitions during development.

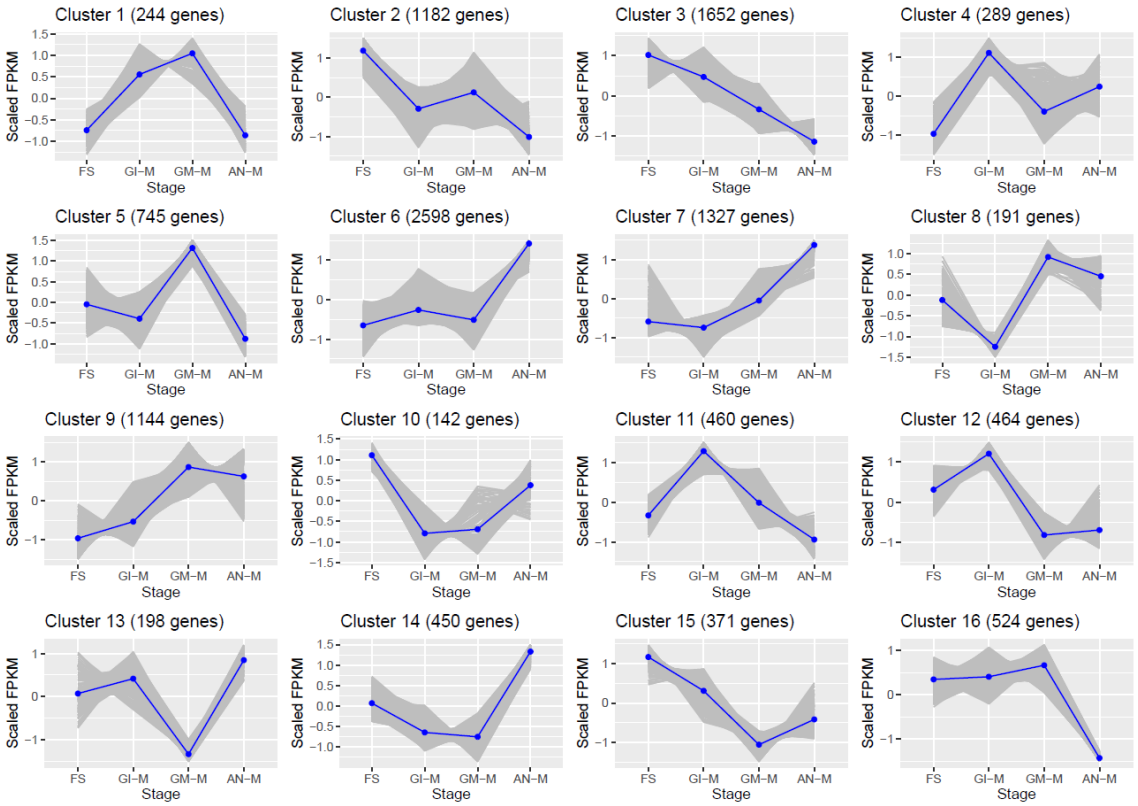

Figure 4.18. Expression patterns of genes expressed in male flower development episodes. The scaled FPKM value of differentially expressed genes (12,469) was subjected to hierarchical gene clustering by calculating the distances of the Pearson correlations of one gene to another. Discrete clusters were extracted setting k=16. Grey lines represent the scaled FPKM values of each gene inside a clusters in each episode. Blue lines represent the mean of scaled FPKM among the genes within a cluster in each episode.

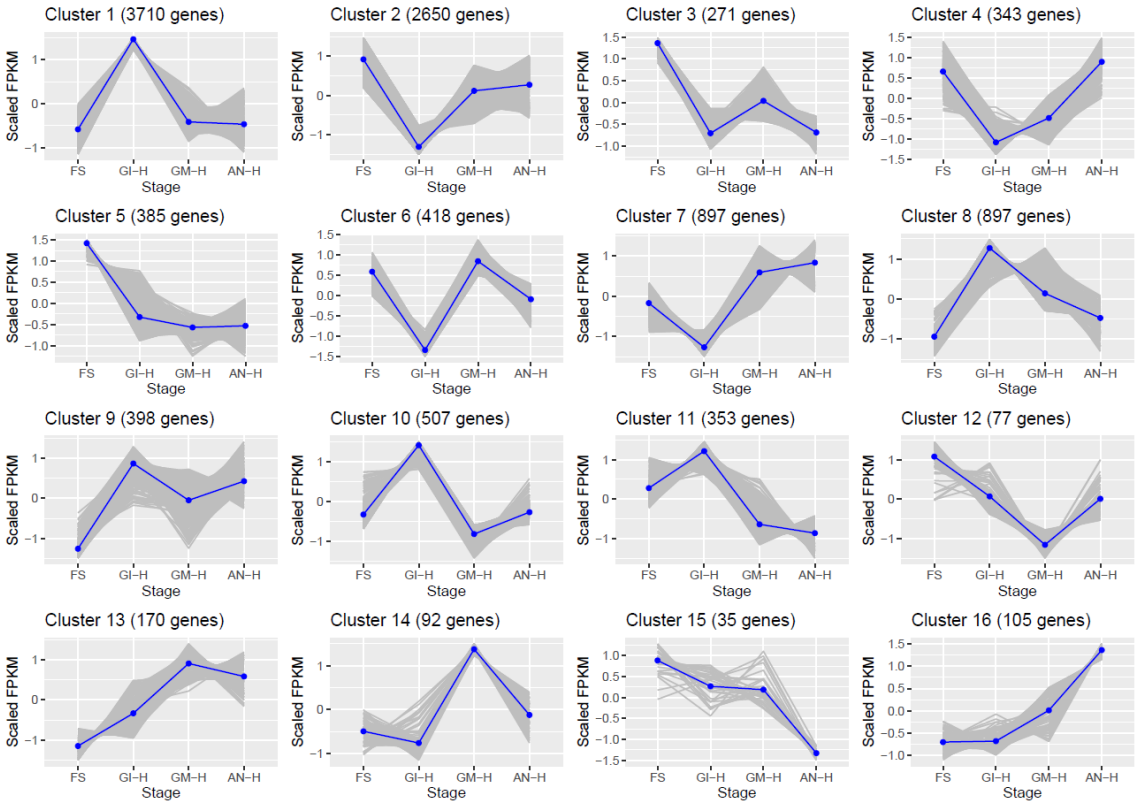

Figure 4.19. Expression patterns of genes expressed in hermaphrodite flower development episodes. The scaled FPKM value of differentially expressed genes (12.469) was subjected to hierarchical gene clustering by calculating the distances of the Pearson correlations of one gene to another. Discrete clusters were extracted setting k=16. Grey lines represent the scaled FPKM values of each gene inside a clusters in each episode. Blue lines represent the mean of scaled FPKM among the genes within a cluster in each episode

4.2.4 Genes specifically expressed during floral development

In order to identify genes that were differently expressed in just one of the flower developmental episodes, we compared the expression of DEGs. We considered as episode-specific genes those DEGs that had a level of expression 2-fold or more at one episode above those in the remaining episodes, for both flower types separately. Based on this, we identified 50 FS episode-specific genes (Figure 4.20A). The GO analysis did not detect any enriched category for this episode. These genes include, the cytochrome P450 78A5 and growth-regulating factor 4-like. Both melon genes, as well as their homologs in *Arabidopsis*, have been specifically linked to floral organ development. In addition, among the FS specific genes, we found homologues of Protein FANTASTIC FOUR 2, Protein LATERAL ROOT PRIMORDIUM 1, U4/U6 small nuclear ribonucleoprotein

PRP4-like protein and floricaula/leafy homolog, which are known in Arabidopsis to be involved in anther development. Characteristic hormone-related genes present at this stage were those involved in ethylene signalling (Annex 4, Table 8.3). A total of 128 genes potentially related to male gamete initiation were classified as GI-M specific (Figure 4.20B). GO enrichment analysis showed that this episode was enriched in “oxide-reduction” and “oxylipin biosynthetic process” genes (Figure 4.20E). Among the genes specifically expressed during this episode, we found those encoding SKP1-like protein 12, ECERIFERUM 1-like protein and WAT1-related protein. While the Arabidopsis homolog of the first one is involved in early flower reproductive development, for the other two a specific role in exine biosynthesis and pollen development has been described (Dezfulian et al., 2012; Bourdenx et al., 2011) (Annex 4, Table 8.3). We then examined the 200 genes that were specifically expressed at GM-M (Figure 4.20C). A GO analysis showed that the genes were enriched in the categories “metabolic processes”, “transferase activity”, “glycolytic processes” and “copper ion binding” (Figure 4.20E). Among the GM-M specific genes were those encoding expansin-B3-like, xyloglucan glycosyltransferase 4 and tubulin beta chain, among others. Arabidopsis homologs of the first two seem to be involved in gamete formation and pollen tube initiation, respectively, while for the latter a specific role in the mitotic cycle has been described (Annex 4, Table 8.3). In contrast to the first three developmental episodes, substantially more genes (1,731) were specifically expressed at AN-M (Figure 4.20D). These genes were enriched in numerous GO terms (Figure 4.20E), with "membrane", "integral component of membrane", "hydrolase activity", " transporter activity" and "transport" being the most represented, followed by "sulphate transport" and "peroxisome", among others. When checking the genes specifically expressed in AN-M, we found Arabidopsis homolog genes involved in sporopollenin biosynthesis of pollen such as protein ECERIFERUM 3; genes responsible for the programmed cell death process, such as those encoding accelerated cell death 11 and Eukaryotic initiation factor 4F subunit p150 isoform 1; genes related to germination and maturation of pollen such as pollen receptor-like kinase 1, somatic embryogenesis receptor kinase 2-like and genes controlling photoperiodism and flowering such as zinc finger protein CONSTANS-LIKE 2, protein GIGANTEA-like and Protein EARLY FLOWERING 3. Characteristic hormone-related genes expressed during this episode were those involved in ethylene signalling.

We also detected many homologs of the cytochrome p450 family, as well as several genes of the ABC transporter family (A, B, C, D, F and I) (Annex 4, Table 8.3).

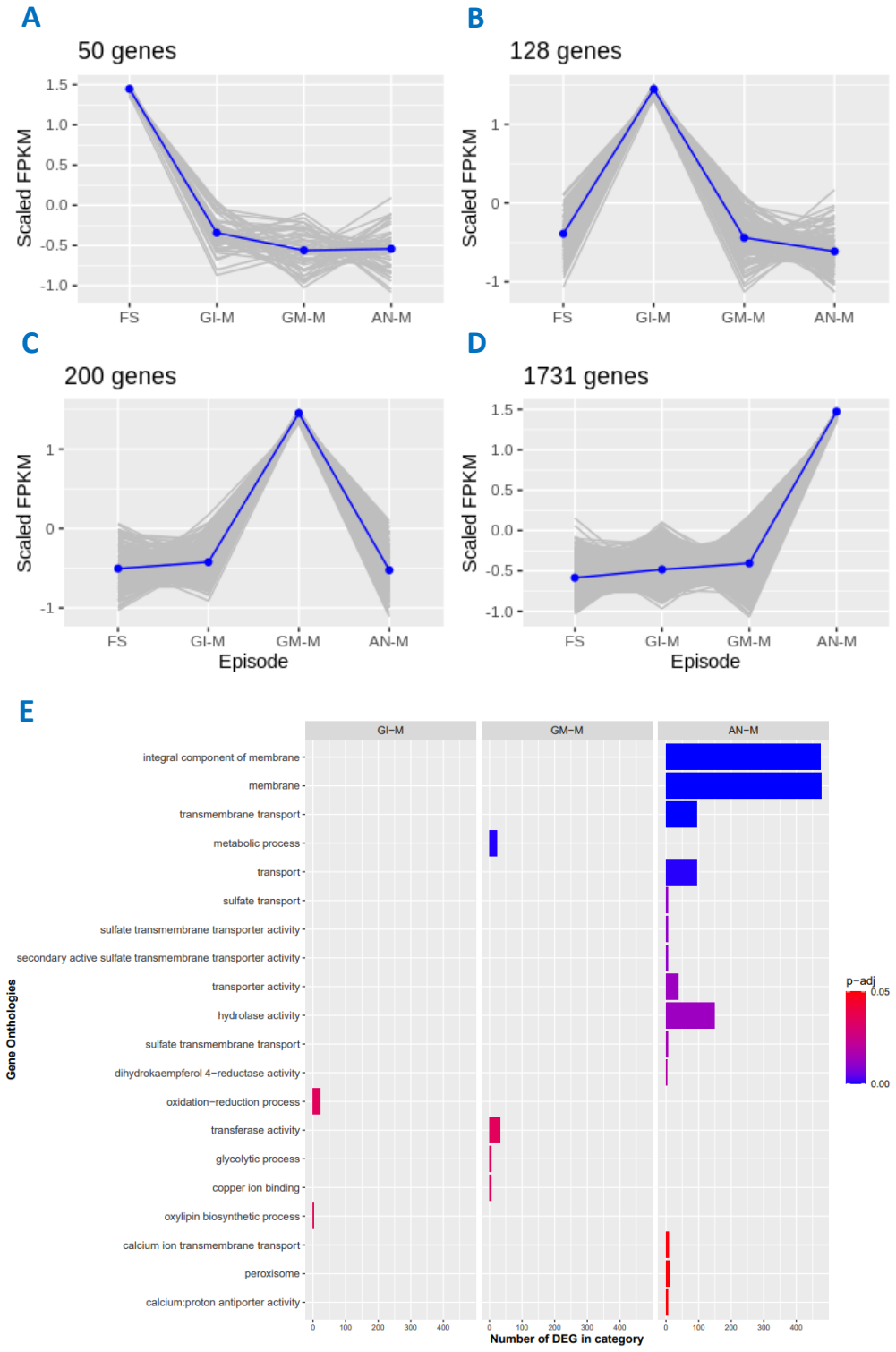

Figure 4.20. Up-regulated genes and Gene Ontology (GO) categories specific for each developmental episode during male floral development. (A-D) Expression patterns of stage-specific genes, with the average expression trend highlighted in blue. The Y-axis represents scaled FPKMs (fragments per kilobase per million mapped reads) of genes across the four developmental stages. (E) Enriched GO terms among male stage-specific genes. The Y-axis indicates the enriched categories, and the X-axis indicates the

differentially expressed gene numbers in each category. Enriched categories were considered those with a P-adjust lower than 0.05 which is represented here in a coloured scale from 0 (blues) to 0.05 (reds).

A total of 2,814 genes related to hermaphrodite gamete initiation were classified as GI-H specific (Figure 4.21B). A GO enrichment analysis showed that this episode was enriched in “DNA binding”, “RNA binding”, “nucleus”, “ribosome” and “translation”, among many others (Figure 4.21E). At this episode we found the largest number of genes, many of them were Arabidopsis homologs related to general floral development such as those encoding homeobox protein LUMINIDEPENDENS, Maternal effect embryo arrest 22, PHOTOPERIOD-INDEPENDENT EARLY FLOWERING 1 family protein, programmed cell death protein 5, protein FRIGIDA-ESSENTIAL 1 isoform X1, YABBY protein and Zinc finger protein CONSTANS. We also found genes directly related to the female gamete development, such as the genes encoding anaphase-promoting complex subunit 2 (mega gametogenesis), CHD3-type chromatin-remodeling factor PICKLE (carpel differentiation), chromatin structure-remodeling complex protein SYD isoform X1 (carpel and ovule development), DYAD protein (female meiosis), E3 ubiquitin-protein ligase Arkadia (embryonic development), germinal center kinase 1 isoform X1 (oogenesis) and protein YABBY 4-like (ovule development). Specific male gamete development genes were also identified in association to this episode, such as the genes encoding Apoptosis inhibitor 5-like protein API5 (involved in programmed cell death during anther development), callose synthase 7 (involved in callose synthesis at the forming cell plate during cytokinesis) and pollen Ole e 1 allergen and extensin family protein. A gene of particular relevance to hermaphrodite flowers was Kokopelli, whose function is double fertilization forming a zygote and endosperm. Typical hormone-related genes identified at this episode were those involved Ethylene signalling. We also detected many homologs of the cytochrome p450 family, ABC transporter family together with several member of MADS-Box transcription factors and Myb transcription factors (Annex 4, Table 8.4). The GM-H and AN-H episodes showed only 15 and 13 specific genes, respectively (Figure 4.21C and D). Although the enrichment analysis did

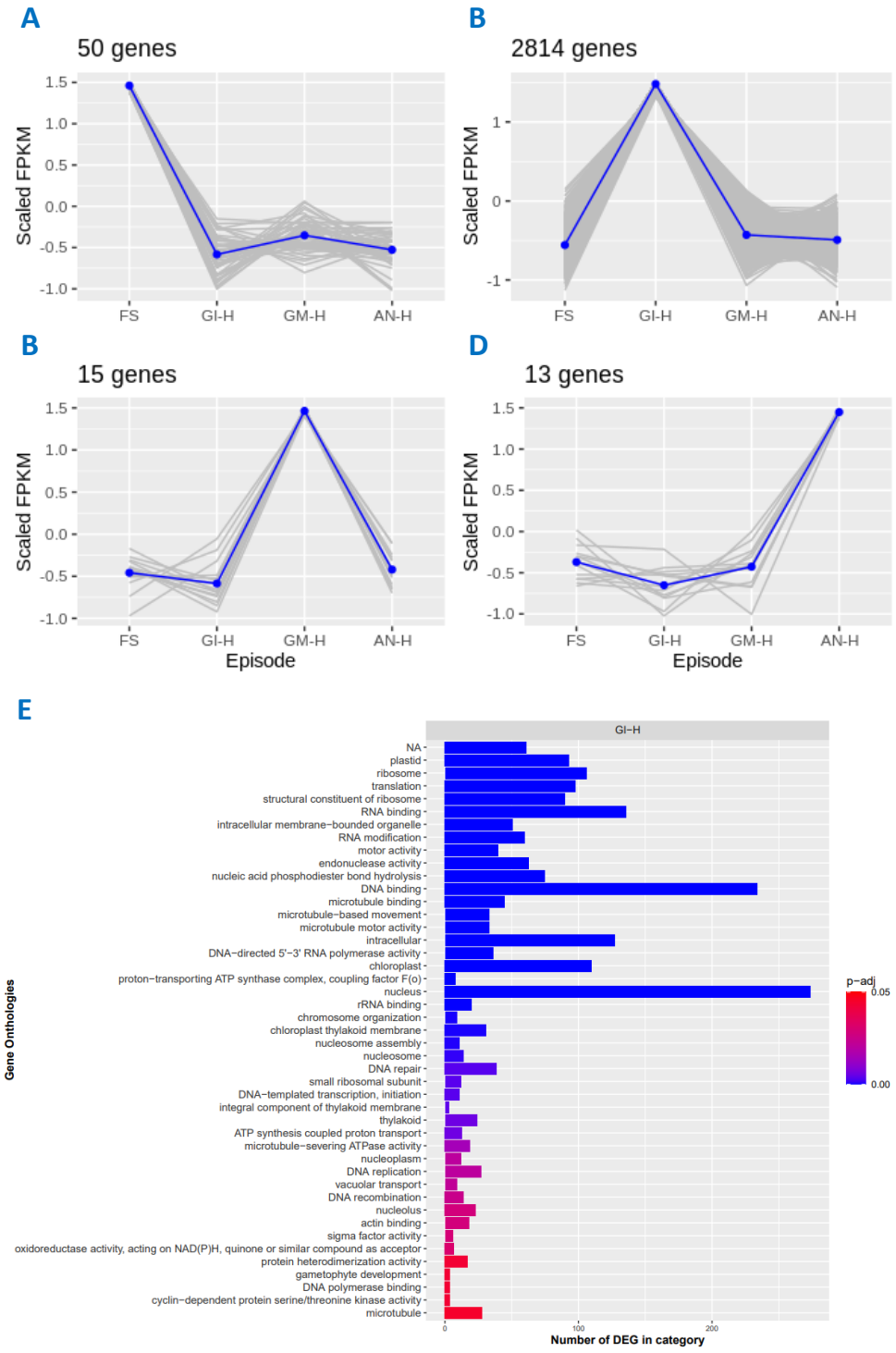

Figure 4.21. Up-regulated genes and Gene Onthology (GO) categories specific for each developmental episode during hermaphrodite floral development. (A-D) Expression patterns of genes specific to each developmental stage, with the average expression trend highlighted in blue. The Y-axis represents scaled FPKMs (fragments per kilobase per million mapped reads) of genes across the four developmental stages. (E) Enriched GO terms among hermaphrodite stage-specific genes. The Y-axis indicates the enriched categories, and the X-axis indicates the differentially expressed gene number in each category. Enriched categories were considered those with a P-adjust lower than 0.05 which is represented here in a coloured scale from 0 (blues) to 0.05 (reds).

not detect any GO category significantly overrepresented for them, among the GM-H specific genes we found Arabidopsis homologs that play key roles in floral development, such as the gene encoding PHD finger protein MALE STERILITY 1, which is a transcriptional activator required for anther and post-meiotic pollen development and maturation; it seems to regulate inflorescence branching and floral development and may control tapetal development by directly regulating tapetal programmed cell death (PCD) and breakdown. Implicated in pollen cytosolic components and wall development (*e.g*. exine and intine formation). Bidirectional sugar transporter SWEET and ABC transporter G family member 6 were also detected at this episode. Finally, among the AN-H specific genes, homologs of the genes encoding protein nuclear fusion defective 4 and WAT-1 related protein, which have been associated with the process of karyogamy during female gametophyte development and flower development, were found (Annex 4, Table 8.4).

4.2.5 Expression of sex-determining genes during floral development

Finally, we investigated the expression patterns of the genes *CmACS11*, *CmACS7* and *CmWIP1*, which have been reported to be critical for floral sex determination in melon (Figure 4.22). *ACS11* showed a pattern of expression specific to the GI episode, in the hermaphrodite flower, the same as ACS7, for which, however, a basal expression was detected in the FS, GI-M and AN-M episodes. *WIP1* was detected almost exclusively in the male flower, with the highest expression levels coinciding with the AN episode followed by FM and GM, although low levels of expression were detected in the GI-H episode.

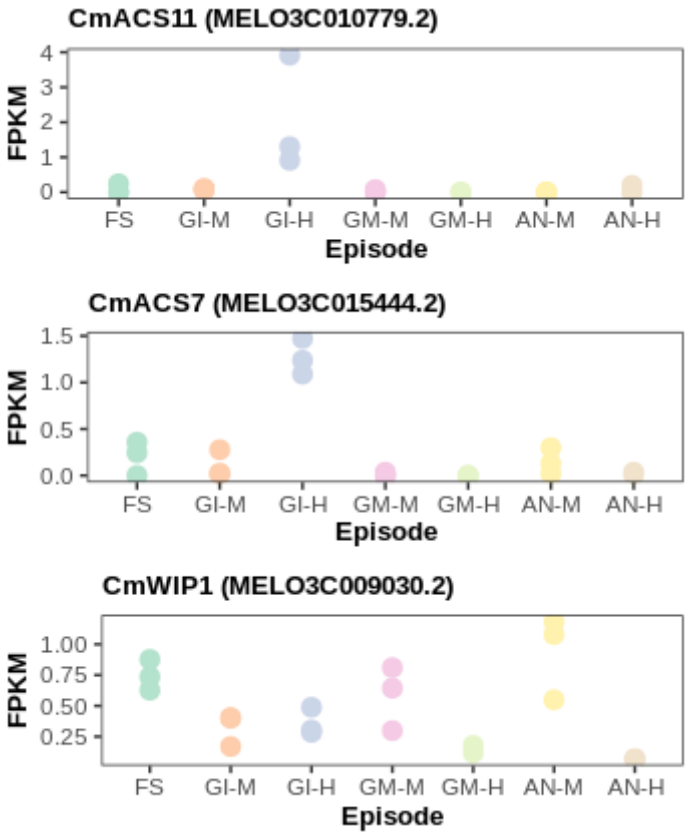

Figure 4.22. Expression patterns of *ACS11*, *ACS7* and *WIP1* genes across floral developmental episodes in male and hermaphrodite flowers. Gene expression is measured in FPKM (fragments per kilobase per million mapped reads).

4.3 Comparative analysis of melon male floral development between wild type and *eif4e* knock-out mutant plants

4.3.1 Comparative structural analysis of anther development between wild-type and eif4e mutant plants

To identify structural differences during pollen development of the *eif4e* mutant, longitudinal and transversal semithin sections of anthers at different stages of development from WT and *eif4e* mutant plants were examined. Based on microscopic analyses (see section 4.2.1.2), melon male flower development was divided into 12 stages, from the formation of the stamen primordium to the release of mature pollen

during anther dehiscence. No significant differences were detected in anther structures in the mutant plants compared to WT before stage 9 (data not shown), therefore the comparative analysis of anther development was carried out from stage 9 onwards. In stage 9, the WT anther primordia differentiated into a concentric structure, with pollen mother cells (PMCs) in the locule wrapped by a four-layered anther wall, from surface to interior of the epidermis, endothecium, middle layer, and tapetum (Figure 4.23A). The PMC subsequently underwent meiosis generating a tetrad by the end of stage 10. Meanwhile, tapetal cells initiated their programmed cell death (PCD) (Figure 4.23C) until their complete degradation (Figure 4.23E). By contrast, during the differentiation of the *eif4e* mutant male flowers, both the anther walls and microspores displayed a slightly abnormal development: The anthers and locules were generally smaller in size and hosted a smaller number of pollen mother cells (Figure 4.23B). The pollen mother cells in the WT were characterized by a polyhedral morphology, with highly condensed chromatin nuclei and surrounded by highly organized tapetum cells (Figure 4.23A). On the contrary, in the mutant, microsporocytes of a more rounded shape were observed, surrounded by a tapetum with more disorganized and smaller cells (Figure 4.23B). At the tetrad stage, structural differences in pollen development became more evident: in the WT, tetrads were clearly formed and at least three of the four cells of the tetrad could be observed in the sections (Figure 4.23C). In the mutant, microsporocytes seemed to have underwent incomplete meiosis and microspore individualization, as anthers in that stage appeared to contain most of the cells in the dyad stage (Figure 4.23D). Although some microspore cells could be observed after meiosis in the mutant, their structure was somehow collapsed in comparison with the rounded shape of the wild type (compare figures 4.23E and F). A remarkable distinction between WT and mutant anthers began to appear between stages 10 and 11: Normal vacuolated microspores were uniformly distributed along the tapetum side with round shapes with dark-stained pollen wall corresponding to the exine in the WT (Figure. 4.23G); in contrast, internal cavities of the mutant anthers became disorganized, instead of randomly distributed pollen grains inside the anther locules as in the WT, collapsed pollen grains in the mutant adhered to unstructured dark stained material that could

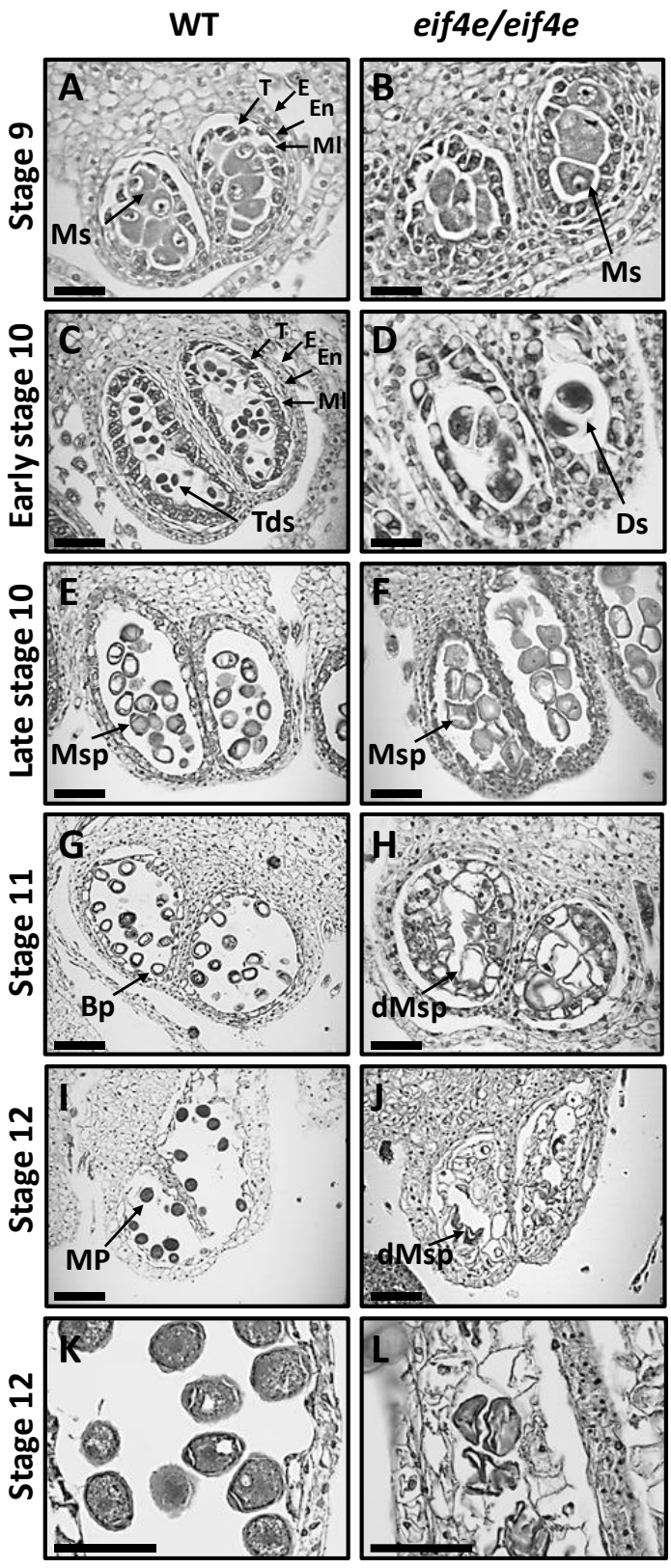

Figure 4.23. Transversal sections of anthers throughout development in wild-type (WT) and *eif4e* mutant observed by light microscopy. Locules from the WT (A, C, E, G, I, L) and *eif4e* mutant (B, D, F, H, J, L) anthers from stages 9 to 12 of development. BP, bicellular pollen; dMsp, degraded microspores; Ds, dyads; E, epidermis; En, endothecium; ML, middle layer; MP, mature pollen; Ms, microsporocyte; Msp, microspores; T, tapetum; Tds, tetrads. Scale bars = 50 µm (A, B, C, D, E, F), 100 µm (G, H, J, K), 30 µm (I, L)

correspond to incompletely degenerated tapetum inside the locule walls (Figure 4.23H). In this phase, the lumen of the anthers in the mutant was filled by large amounts of stained/dark material (Figure 4.24 A, B, C and D) that could originate from droplets of sporopollenin secreted by the tapetum as previously described in Arabidopsis and rice (Wang et al., 2013; Chang et al., 2016; Sun et al., 2018; Li et al., 2020). Between the pollen mitosis (stage 11) and the mature pollen stages (stage 12), WT grains were regularly covered by a double layer of exine and formed fertile pollen after two mitotic divisions, while the tapetum layer became thinner and degenerated until its almost complete disappearance at the end of stage 12. Mature pollen was dark-stained in the WT and the pollen grains appeared well structured as an indication of being full of nutrients, suggesting that the WT pollen grains had normal functions and are viable (Figure 4.23I and K and Figure 4.25A and C). Contrastingly, mutant anthers showed clumping of microspores unstructured as well as other stained/dark material of unknown origin in their anthers at stage 12 (Figure 4.23J and L, Figure 4.24C and F and Figure 4.25B and D).

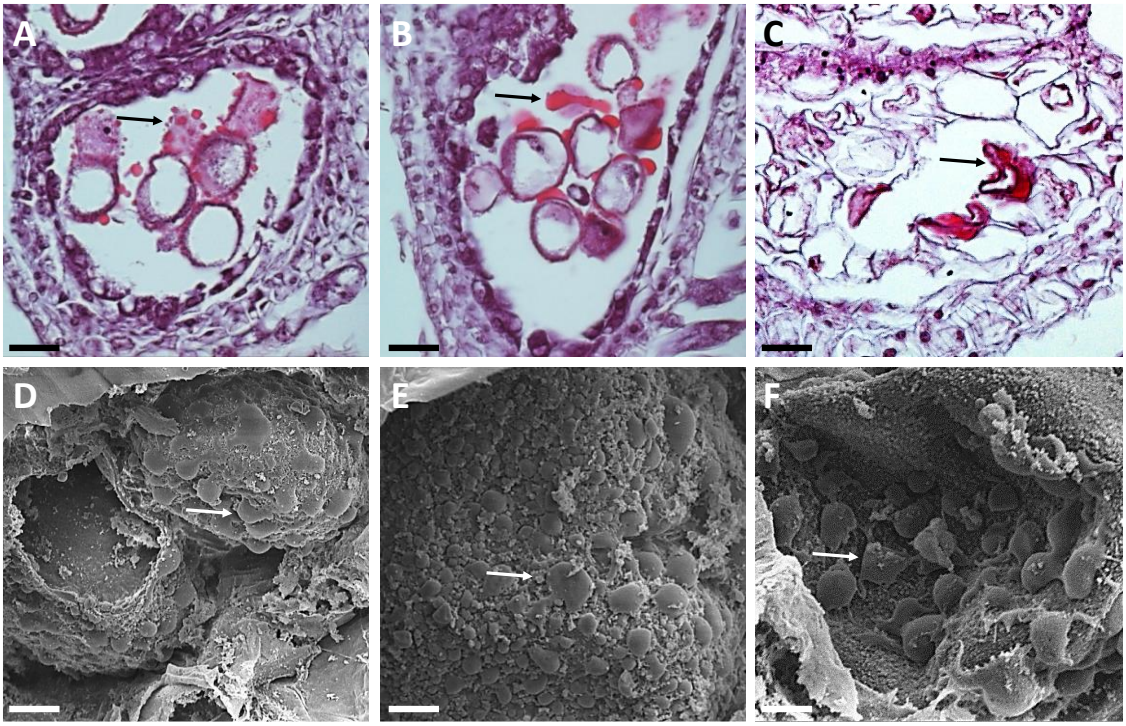

Figure 4.24. Light microscopy (A, B, C) and scanning electron microscopy (D, E, F) images of transversal sections throughout anther development in the *eif4e* mutant. (A, B, D, E) Locules are filled by large amounts of stained/dark material that could correspond to sporopollenin (arrows) in late stages 10 and

11. (C, F) Locules showing clumping of microspores unstructured as well as other stained/dark material of unknown origin (arrows) in late stage 11 and early stage 12. Scale bars = 25 µm, (A, B, C), 10 µm (D), 5 µm (E), 500 nm (F).

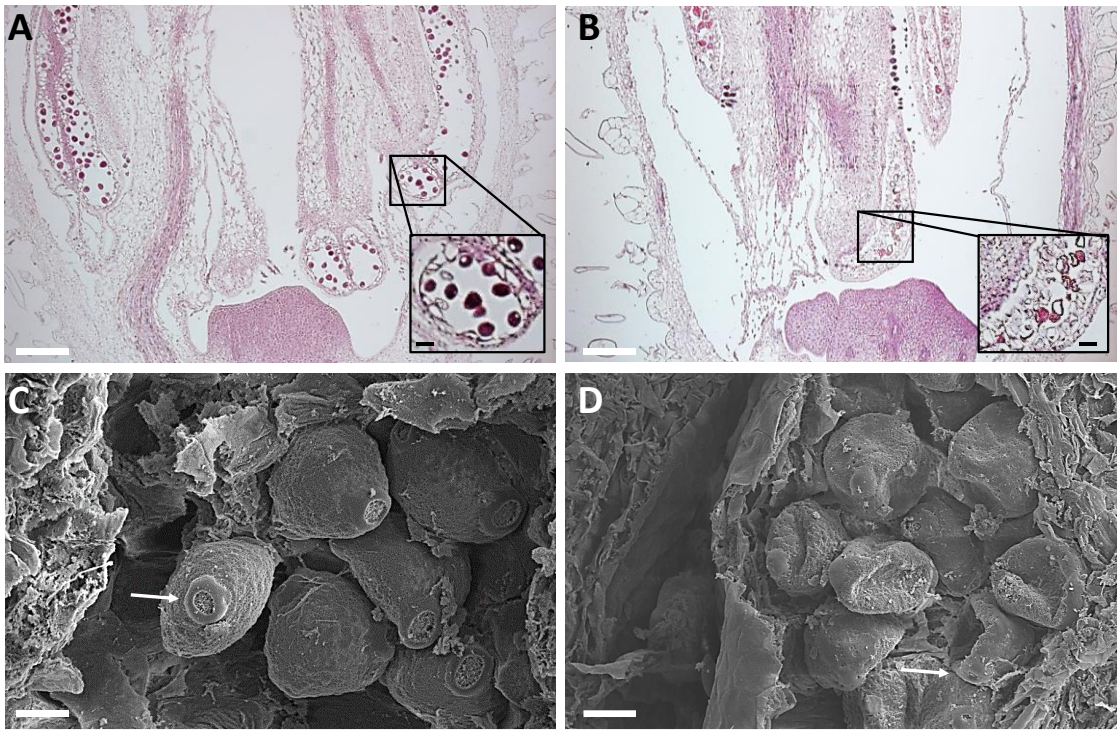

Figure 4.25. Light microscopy images from longitudinal sections of wild-type (A) and *eif4e* mutant anthers (B) in fully developed male flowers at low magnification. Scanning electron microscopy images of pollen grains at high magnification from wild-type (C) and *eif4e* mutant (D) between late stage 11 and stage 12. Scale bars = 100 µm, (A, B), 10 µm (C), 20 µm (D). Scale bars in the magnifications of figures A and B = 30 µm.

4.3.2 RNA-seq analysis comparing male floral development between wild-type and eif4e knock-out mutant plants

We next compared the transcriptomes of WT and mutant male flowers along the four main episodes during floral development defined in the previous section. Of note here is that, according to the data above, no morphological differentiation was observed between WT and mutant male flowers during stages corresponding to the first episode FS. In this section we will refer to the four episodes of male floral development in the mutant as FSmut, GI-Mmut, GM-Mmut, and AN-Mmut, while the corresponding

episodes of the wild type will retain the nomenclature used in the previous chapter. Fifty floral buds were pooled per biological replicate, and three replicates were prepared per each of the four floral episodes. Total RNA was extracted and subjected to next-generation sequencing as was described before. RNA-seq reads were analysed as described in section 4.2.2 (Annex 5, Table 8.5). ~14.500 genes were expressed in each episode (Figure 4.26A). A cluster dendrogram analysis of the mutant gene expression profiles showed that gene expression patterns of biological replicates were highly related (Figure 4.26B). A PCA including all biological replicates (mutant and WT) showed a clear separation in gene expression patterns between the mutant and WT, as well as a separation in gene expression patterns across floral developmental episodes within both the mutant and WT (Figure 4.26C).

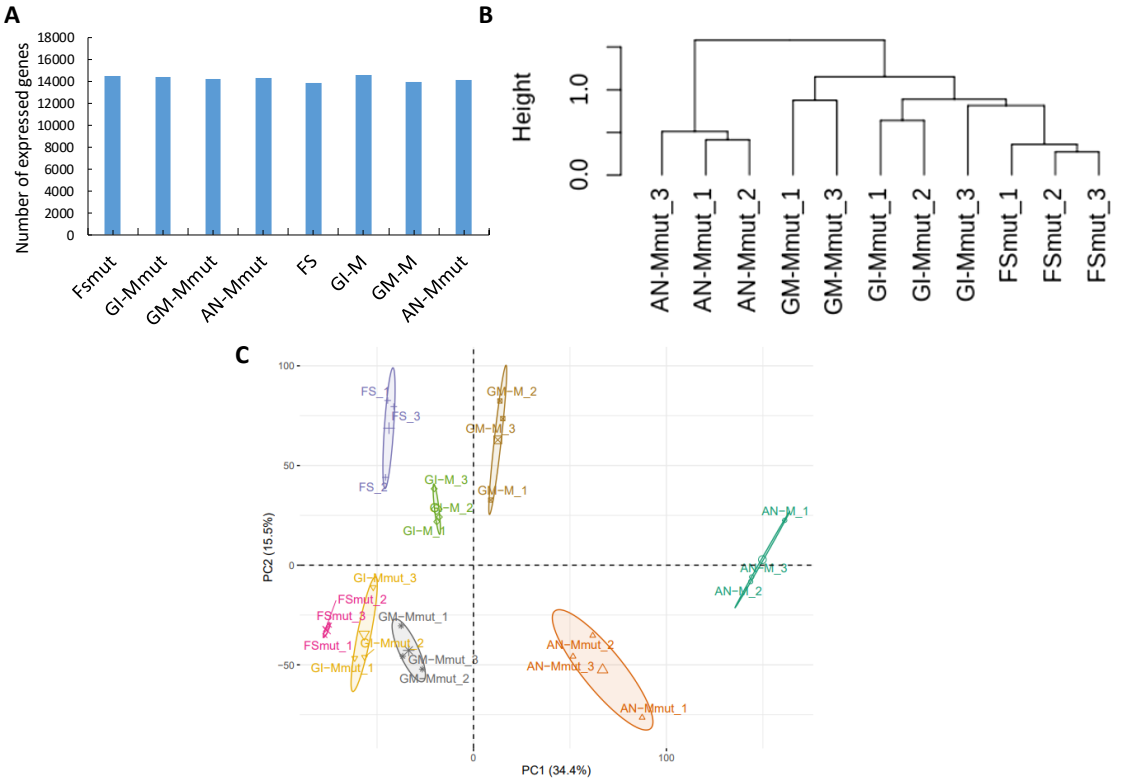

Figure 4.26. RNA-seq along flower developmental episodes for wild-type (WT) and *eif4e* mutant melon plants. Four episodes during floral development were considered: Floral structures formation (FS), gamete initiation (GI), gamete maturation (GM) and anthesis (AN) episodes. (A) Number of expressed genes per floral developmental episode. Expressed genes are considered those with an average value of FPKM (fragments per kilobase per million mapped reads) > 1 in at least one episode. (B) Cluster dendrogram of gene expression profiles between biological replicates and among different developmental episodes. The dendrogram shows the hierarchical clustering of the different replicates according to their gene

expression profiles. (C) Principal Component Analysis (PCA) scores plotted for *eif4e* mutant and WT floral development episodes. PCA was computed using expressed genes. PC1, principal component 1; PC2, principal component 2. The percentage of variance explained by PC1 and PC2 are 34.4 % and 15.5 %, respectively. Confidence ellipses were plotted around group mean points.

4.3.3 Differentially expressed genes during male flower development in male-sterile eif4e mutants

A comparative analysis of DEGs between each of the episodes in the mutant and the corresponding episodes in WT was carried out. Only genes with an adjusted P value < 0.01 and log_2 fold change higher than1 and lower than -1 were considered as DEG. In total, 7,397 DEGs were identified. The comparisons of FSmut *versus* FS, GI-Mmut *versus* GI-M, GM-Mmut *versus* GM-M, and AN-Mmut *versus* AN-M provided 1,649, 1,162, 2,490 and 2,096 DEGs, respectively, with GM-Mmut *versus* GM-M being the episode in which the largest number of DEGs was found (Figure 4.27A). Among these DEGs, only 142 were shared among the four episodes (Figure 4.27B), and included cyclophilin, minichromosome maintenance, pentatricopeptide repeat, Protein kinase superfamily protein, eukaryotic translation initiation factor 3A and GRAS family transcription factor family protein, among others.

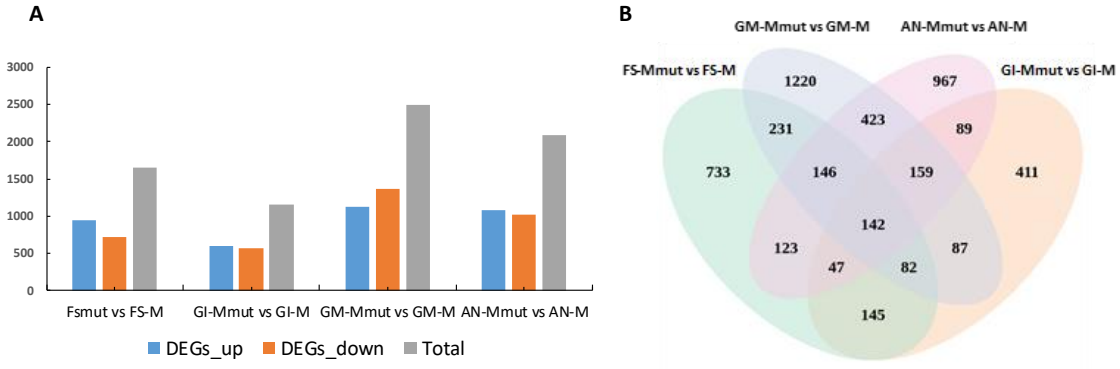

Figure 4.27. Differentially expressed genes (DEGs) along flower developmental episodes for wild-type (WT) and *eif4e* mutant melon plants. (A) Mutant *versus* WT DEGs at different episodes of flower development (adjusted P value < 0.01 and Log_2 fold change >1 and <-1). (B) Venn diagram showing mutant *versus* WT specific or shared DEGs at different episodes of flower development.

4.3.4 Gene ontology terms enriched in DEGs along floral developmental episodes

All DEGs resulting from the mutant-WT comparisons in the four episodes were analysed using GO enrichment functional category analysis. This analysis revealed that DEGs in the FS episode were enriched for “plastid”, “photosynthesis”, “ribosome”, “translation” and “chloroplast”, among others (Figure 4.28). Within the enriched GO categories, several members of chloroplastic ribosomal proteins 30S, 40S, 50S and 60S as well as Peter Pan-like protein and Chloroplastic Translation initiation factor IF-1, were found to be down-regulated. Most chloroplastic proteins related to chlorophyll a and b binding were also found to be down-regulated in this first episode. DEGs in the GI episode were enriched in the categories “MCM complex”, “enzyme inhibitor activity” and “photosystem” (Figure 4.28). Among the enriched GO categories, DNA helicase genes and genes and several Photosystem II protein D1 appeared to be up-regulated. Notably, all genes related to enzyme inhibition activity (Pectinesterase, pectinesterase-like, pectinesterase-inhibitor and pectinesterase inhibitor-like) resulted down-regulated at GI episode. The most representative GO terms enriched categories for the GM episode were “membrane”, “metabolic process”, “rRNA binding”, “cell wall”, “catalytic activity”, “pectin catabolic process”, “transporter activity”, “extracellular region”, “transmembrane transporter activity” and “cellular amino acid biosynthetic process” (Figure 4.28). Within these categories, genes related to enzyme inhibition activity and cell wall (Pectinesterase, pectinesterase-like, pectinesterase-inhibitor and pectinesterase inhibitor-like, Expansin), carbohydrate metabolic process/catalytic activity (Beta-galactosidase, Beta-amylase, Beta-glucosidase, glucan endo-1,3-beta-glucosidase, Endoglucanase), sugar transferase related-genes and proteins (Bidirectional sugar transporter SWEET, sugar transport protein 10-like), cellular amino acid biosynthetic process (Acetolactate synthase, Tryptophan synthase), integral component of membrane (ABC transporter B family protein, ABC transporter G family member, Cytochrome P450, NO EXINE FORMATION 1 family protein) and proteolysis involved in cellular protein catabolic process related-genes (Proteasome subunit alpha type) appeared down-regulated. Finally, AN episode comparison included many GO

terms, being “membrane”, “hydrolase activity”, “carbohydrate metabolic process”, “transporter activity”, “proteasome complex”, “calcium ion transport” and “enzyme inhibitor activity” the most relevant (Figure 4.28). Among them, calcium ion transport related-genes (Calcium-transporting ATPase, vacuolar cation/proton exchanger 3), endopeptidase activity related-genes (Proteasome subunit alpha and beta type), integral component of membrane (ABC transporter B family protein, Bidirectional sugar transporter SWEET, Cellulose synthase, *Cytochrome P450*, F-box protein family, Late embryogenesis abundant protein, Transmembrane protein) showed a down regulation pattern in episode AN whit respect to the WT. Notably, carbohydrate metabolic process/catalytic activity genes (Beta-galactosidase, Beta-amylase, Beta-glucosidase, glucan endo-1,3-beta-glucosidase, Endoglucanase), enzyme inhibition activity and cell wall (Pectinesterase, pectinesterase-like, pectinesterase-inhibitor and pectinesterase inhibitor-like, Expansin) were still down-regulated as in episode GM.

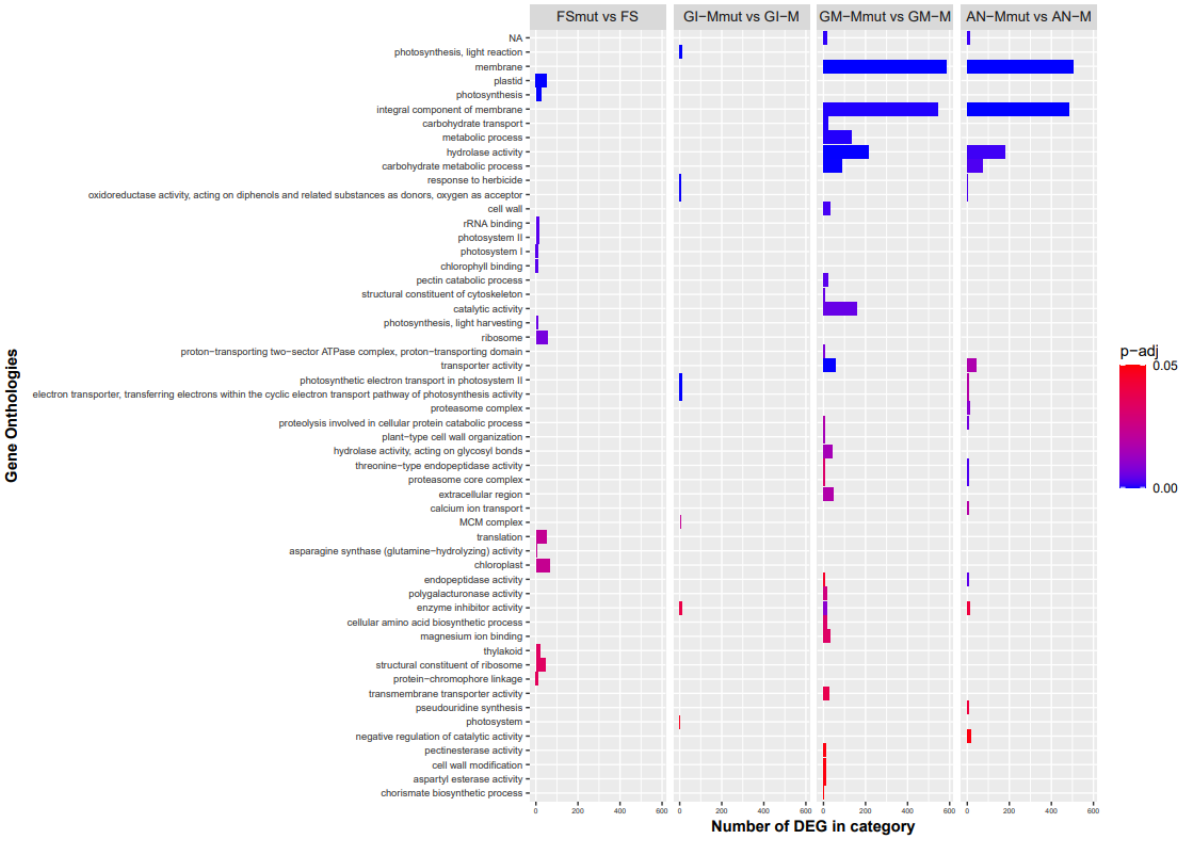

Figure 4.28. Mutant *versus* WT enriched GO terms among different episodes of flower development. The X-axis indicated the enriched categories, and the Y-axis indicated the differentially expressed gene

number in each category. Enriched categories were considered those with a P-adjust lower than 0.05 which is represented here in a coloured scale from 0 (blues) to 0.05 (reds).

4.3.5 Manual inspection of DEGs along floral developmental episodes

4.3.5.1. FSmut *versus* FS

The comparison of FSmut *versus* FS identified 1,649 DEGs, including 938 up-regulated and 711 down-regulated genes (Figure 4.27A). Out of these, 437 up-regulated and 319 down-regulated genes were specific to this first episode (Figure 4.29). The results after manually analysing the data showed that genes implicated in ethylene synthesis (ethylene-responsive transcription factor), stamen filament development (FHA domain-containing protein FHA2), sporopollenin biosynthetic process (tetraketide alpha-pyrone reductase 1), as well as receptor-like kinase related-genes (pollen receptor-like kinase 3), sugar transferase related-genes (bidirectional sugar transporter SWEET) and the genes encoding *EIF4G* and the *EIF3* subunit G-like, were down-regulated in the mutant. By contrast, genes related to gametophyte development and regulation of programmed cell death (apoptosis inhibitor 5-like API5, male gametophyte defective 1, protein XRI1) were up-regulated in the mutant in this episode (Annex 6, Table 8.6).

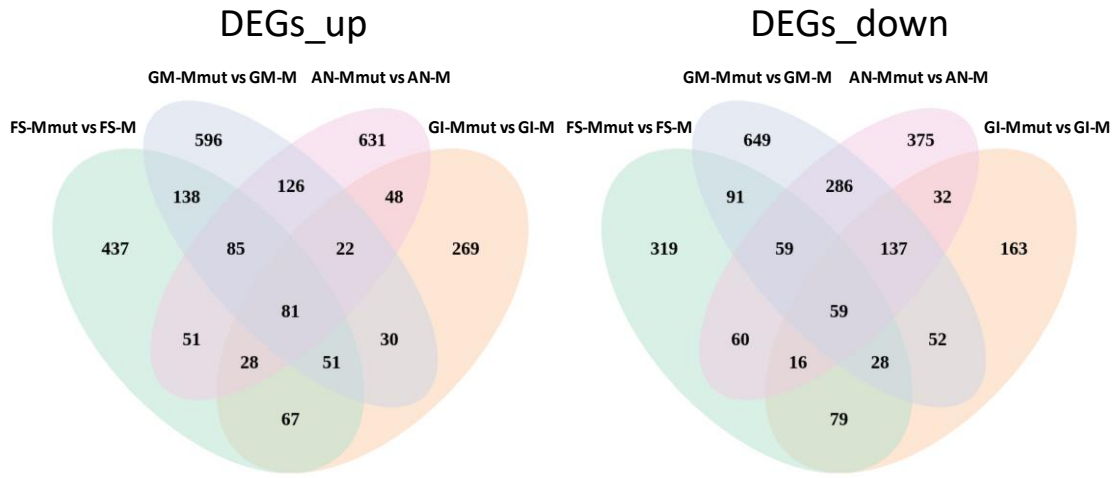

Figure 4.29. Venn diagram showing Mutant *versus* WT differently expressed up (left) and down (right) regulated genes at different episodes of flower development

4.3.5.2. GI-Mmut *versus* GI-M

The comparison of GI-Mmut *versus* GI-M identified 1,162 DEGs, including 596 up-regulated and 566 down-regulated genes (Figure 4.27A). Moreover, we found 269 up-regulated and 163 down-regulated genes that were specific to this episode (Figure 4.29). Manual screening of the DEGs showed that two genes involved in metabolism and ATPase activity such as ABC transporter family genes (ABC transporter G family member 21 and 6, Cytochrome P450), genes encoding two proteins involved in floral development and flowering (MADS-box protein SOC1 and Protein EARLY FLOWERING 3) and pollen wall formation-related proteins (pollen-specific leucine-rich repeat extensin-like protein 3) were down-regulated in GI-Mmut as compared to the GI-M. The gene encoding EIF4G was still down-regulated in this episode, together with that encoding EIF4F subunit p150 isoform 1. On the contrary, the eIF3 subunit G-like encoding gene, that was down-regulated in episode FS, appeared up-regulated in episode GI. Interestingly, apoptosis inhibitor 5-like API5 still showed the same up-regulation pattern as in episode FS, whereas tetraketide alpha-pyrone reductase 1, which is involved in the process of sporopollenin biosynthesis, appeared up-regulated in episode GI, in contrast to what was observed in the previous episode. Another interesting up-regulated protein was MACPF domain-containing protein NSL1, involved in cell death and defence response by callose deposition (Annex 6, Table 8.6).

4.3.5.3. GM-Mmut *versus* GM-M

The comparative analysis of GI-Mmut *versus* GI-M identified 2,490 DEGs, including 1,129 up-regulated and 1,361 down-regulated genes (Figure 4.27A). In addition, we found 596 up-regulated and 649 down-regulated genes that were specific to this episode (Figure 4.29). The results indicated that the DEGs including pollen sperm cell differentiation protein (Alba DNA/RNA-binding protein) encoding genes, (1->3)-Beta-D-glucan biosynthetic process related-genes (callose synthase 5-like), generative cell mitosis/pollen development protein (F-box/LRR-repeat protein 17, Pollen-specific protein, Pollen-specific protein-like), pollen tube development/ polar nucleus fusion related-proteins (O-fucosyltransferase family protein) and pollen exine formation genes (Polygalacturonase QRT3) were down-regulated in episode GM in the mutant with respect to the WT. Furthermore, some genes encoding proteins involved in pollen

recognition (receptor-like serine/threonine-protein kinase SD1-8, Serine/threonine-protein kinase) and pollen exine formation (Transmembrane protein) showed up regulation patterns at GM episode. Notably, at least one gene involved in sporopollenin biosynthetic process, that appeared to be down-regulated at episode FS (tetraketide alpha-pyrone reductase 1), showed an up-regulation profile at episode GM, while the XRI1 protein encoding gene, involved in pollen development, continued to be up-regulated as in episode FS (Annex 6, Table 8.6).

4.3.5.4. AN-Mmut *versus* AN-M

The comparative analysis of AN-Mmut versus AN-M identified 2,096 DEGs, including 1,072 up-regulated and 1,024 down-regulated genes (Figure 4.27A). Moreover, we found 631 up-regulated and 375 down-regulated genes that were specific to this episode (Figure 4.29). Among them, pollen tube growth (Armadillo repeat only protein, DnaJ protein ERDJ3A), (1->3)-Beta-D-glucan biosynthetic process (callose synthase 5-like), structural constituent of cell wall (pollen-specific leucine-rich repeat extensin-like protein 3), flower development (FRIGIDA-like protein), pollen development (Major pollen allergen Ole e 6, Pollen-specific protein, pollen receptor-like kinase 1, tetraketide alpha-pyrone reductase 1) and translation initiation factor activity/cytoplasm related -genes (*EIF4E*, *EIF4G*, *EIF 3* subunit G-like, *EIF1A*, *EIF2D*) were down-regulated in the mutant at episode AN. By contrast genes and proteins related to gametophyte development and regulation of programmed cell death (Apoptosis inhibitor 5-like API5), recognition of pollen (Serine/threonine-protein kinase) and *EIF3* subunit A-like appeared up-regulated (Annex 6, Table 8.6).

5 DISCUSSION

5.1 Editing *CmEIF4E* associates with virus resistance and male sterility

Regeneration and genetic transformation represent the major limitation for gene editing in melon (Chovelon et al., 2011). Therefore, the identification of genotypes with a high regeneration capacity, together with the development of a competent and widely applicable system for *de novo* regeneration, is crucial to achieve successful application of gene editing in this species. In this study, the high levels of regeneration and bud formation in all genotypes evaluated demonstrate that the protocol used for *de novo* regeneration and *in vitro* culture were highly efficient and applicable to a wide range of genotypes. The use of high concentrations of selective agents throughout the culture process after genetic transformation, together with the use of fluorescent markers, has been described as useful to reduce the risk of proliferation of non-transformed tissues and for the early identification of those uniformly transformed, respectively (García-Almodóvar et al., 2017). The application of a high selective pressure during the entire *in vitro* culture process of the transgenic plants (150 mg L^{-1} of kanamycin) allowed us to select only uniformly transformed tissues that were identified by their strong DsRed expression. The fluorescent marker DsRed facilitated the identification and sub cultivation of only uniformly transformed buds which eventually gave rise to rooted transgenic plants. Species like melon in which a large number of escapes are observed need markers to reduce the amount of work associated with the identification of putative transgenic buds. Thus, the use of the DsRed marker contributed to the rapid identification of M2 as the most suitable genotype for genetic transformation. The Agrobacterium-mediated transformation efficiencies obtained in this study with the M2 genotype reached 3 %, being in absolute terms low, but consistent with other studies using the same transformation protocol (García-Almodóvar et al., 2017), and among the highest efficiencies obtained with genotypes belonging to the “Piel de sapo” melon variety. In spite of this, we believe that further efforts could be made to improve efficiency in this species. One of the most immediate strategies to follow would be to further searching for genotypes with higher regeneration efficiencies and good *in-vitro* organogenetic behaviour. Regarding alternative delivery systems to the Agrobacterium-

mediated one, magnetofection and electroporation transformation methods have been proposed, although they were characterised by low transformation efficiencies (Zhao et al., 2017; Bhowmik et al., 2018; Vejlupkova et al., 2020), time consuming technology and unclear applicability to a diverse range of plant species. One of the most promising techniques to overcome the limitations of *in-vitro* culture and transformation of recalcitrant species is *de novo* induction of meristems, which is based on the use of morphogenic regulators (MRs) in plants. This technology possess the potential to produce transgenic plants without the need for a tissue culture procedure (Maher, Nasti, Vollbrecht, Starker, Clark, Voytas, et al., 2020); however, it still needs extensive studies of specific plant MRs before it is applicable to a wide range of species. In conclusion, it looks like we will have to deal with the limitations of classical transformation systems for this species for the near time to come.

Apart from transformation efficiency, other issues of concern when working with the CRISPR/Cas system are the editing efficiency and off-targets events. Many studies have described a great heterogeneity in terms of editing patterns, which can make it difficult to identify the type of mutation obtained and the recovery of transgenic lines that are homozygous for the mutation in the target gene. It is very common, for example, to obtain heterozygous lines, in which the mutation has occurred in only one of the two alleles, or biallelic, in which different types of mutations occur in the two alleles. In the first case, the presence of the non-mutated allele (or WT) could be sufficient to fulfil the functions of the gene to be deleted; in the second case, the presence of different mutations could make it difficult to identify the rupture in the gene's reading frame, and the identification of the type of mutation to be transmitted to the progeny (or its segregation). In our study, two of the three mutated lines obtained presented the same deletion of one nucleotide, in homozygosis already from the T0 generation. This allowed the early identification of the break in the gene sequence that gave rise to a premature stop codon and ensured the knock-out of the target gene. Therefore, and although our numbers are very small, it seems that what limits melon genome editing does not depend that much on the CRISPR/Cas9 tool itself, whose reliability has been shown to be high. The same reasoning can be applied to off targets, as no editing of alternative targets was identified in our work. Another factor not directly

related to CRISPR/Cas technology that greatly limits melon genome editing is the natural tendency to somaclonal variation and polyploidization of melon plants that are grown *in vitro*; in fact, tetrapolid, octapolid, myxploid and aneuploid melon plants have been easily recovered from *in vitro* culture (Kathal et al., 1992; Ezura et al., 1994; Ren et al., 2013). In general, it is important to avoid somaclonal variations in research involving genetic transformation, as genetic stability must be maintained in transgenic plants in order to enable the correct expression of the transgene. Moreover, in genome editing experiments, the presence of polyploid lines can greatly hinder the genotyping of T0 lines due to the presence of multiple alleles characterized by different types of mutations in their sequences. Finally, the polyploid melon lines are affected in their agronomic characteristics and in the viability of their seeds. In our work, the polyploid lines obtained were discarded due to the impossibility of determining the type of mutation they carried, or due to the impossibility of obtaining viable seeds from the self-pollination of acclimatized plants. A crucial point to be considered when working with genome editing is the heritability of the mutations that are generated in the plants obtained *in vitro* and the possibility to segregate the transgene to obtain successive generations of transgene-free plants which retain the desired mutation. Through the crossing of transgenic lines homozygous for the mutation with WT lines of the same genetic background, we were able to obtain an F1 generation including non-transgenic individuals that presented the same single deletion as the T0, but in heterozygosis. These results indicated that transgene insertion was in heterozygosis and very likely single, and demonstrated that induced mutations in melon can be stably transmitted through the germ line.

Our group has previously demonstrated that transgenic RNAi *EIF4E* silenced melon plants show broad virus resistance to CVYV, MNSV, MWMV and ZYMV, as the lack of multiplication of these viruses was associated to reduced *EIF4E* expression levels. (Rodríguez-Hernández et al., 2012). Therefore, we expected our *eif4e* knock-out plants to show the same resistance phenotype. At first, we considered the possibility of using MNSV, which is the model virus of our group in terms of eIF4E-mediated loss of susceptibility, as the virus to be used in the susceptibility assays. The necrotic lesions generated by MNSV in the cotyledons of infected plants from 5 dpi onwards allow easy

and rapid phenotyping. However, we had to reconsider it, as the presence of not fully expanded and flat cotyledons and some naturally occurring necrotic lesions on the mutant plants difficulted the clear identification of the MNSV-induced symptoms. Thus, we decided to use MWMV, whose symptoms are clearly visible on leaves of infected plants, to verify whether the knocking out of *EIF4E* conferred virus resistance in melon. We decided to use as a control plants of the RNAi *EIF4E* silenced melon line. Our results demonstrate that CRISPR/Cas9-mediated *EIF4E* knock-out in homozygous plants of the F2 generation results in resistance to MWMV, as no MWMV-induced symptoms were observed in these plants at 20, 30 and 40 days' post inoculation, and no viral accumulation was detected in any of the plants analysed by RT-qPCR. Furthermore, we demonstrated that a single allelic copy of *EIF4E* was sufficient for virus multiplication, as plants heterozygous for the mutation were susceptible to MWMV. Plants from the RNAi lines, used as controls, also showed neither symptoms nor viral accumulation. Although not tested in this work, it is very likely that the same resistance phenotype would be observed for the other viruses tested by Rodríguez-Hernández et al. (2012).

Four months after inoculation, we observed symptoms compatible with MWMV infection in two of the mutant plants, which we later confirmed to be caused by a resistant breaking isolate that pressented a single nucleotide substitution leading to the single amino-acid change N163Y in the VPg sequence. This was somewhat unexpected, as the absence of eIF4E should have completely prevented viral replication, as the virus accumulation data suggested; viral replication is the essential condition for the occurrence of mutations allowing the virus to overcome the resistance. It has been widely described that mutations in the viral VPg of potyviruses are frequently responsible for the overcoming of resistances associated with eIF4E (Ayme et al., 2007; Moury et al., 2004). Although mutations in the VPg have sometimes been linked to an increased affinity for the resistance version of the eIF4E/(iso)4E protein, in other cases this increased affinity has not been observed. In at least one case, mutation of VPg does not increase its affinity for other eIF4E isoforms either, excluding the possibility that other isoforms of eIF4E are used by the virulent virus (Gallois et al., 2010). It is worth noting that Gallois et al. (2010) described a nucleotide change in TuMV VPg, responsible for the homologous N163Y substitution that we detected in our *eif4e* mutant

plants, as being responsible for conferring virulence towards *A. thaliana* mutants knocked out for eIF(iso)4E and eIF(iso)4G, and they hypothesised that TuMV-N163Y may allow breaking of the resistance phenotype in At-*EIF(iso)4E* knock-out plants by interaction with an alternative, not yet identified partner *in planta*. Bastet et al., (2018) pointed the fact that the redundancy for recessive resistances, associated with mutations in susceptibility factors, could be a double-edged sword affecting resistance durability. In fact, functional redundancy among different paralogs of a given susceptibility factor could either increase or decrease the resistance level or its durability. In the former case, the redundancy would enable the diversification of the susceptibility factors making viruses lose the copy they use for replication without affecting the plant fitness; in the latter case, viruses could evolve to take advantage of multiple copies of a susceptibility factor, which would result in resistance breaking. In addition, the presence of mixed genetic backgrounds could also affect the durability of an eIF4E-based resistance. Mixed genetic backgrounds, in fact, could favour the appearance of a new RB isolate by providing an additional eIF4E factor that the virus can exploit for replication, or by the regulation of eIF4E accumulation level through feedback mechanisms or modulation of the eIF4E level regulation, so that an increased eIF4E accumulation could allow basal virus replication that result in the emergence of RB isolates (Bastet et al., 2018). Although the most immediate solution to achieve durable resistance might seem to mutate all isoforms potentially recruitable by the virus, due to the essential role of eIFs for plant viability, silencing of *EIF4E*, *EIF4G* or *EIF4B* and their corresponding isoforms would for sure lead to imbalances in normal plant development and even to lethal phenotypes (Nicaise et al., 2007; Patrick et al., 2014). An alternative strategy to improve the resistance durability could be the overexpression of resistant variants of *EIF4E* or *EIF(iso)4E* based on amino acids implicated in other potyvirus-eIF4E/iso4E interactions. Overexpression of these variants in transgenic *B. rapa* seemed to provide broad-spectrum and durable resistance to TuMV isolates (Kim et al., 2014). However, overexpression still relies in transgene incorporation into the crop species genome, a condition unacceptable for the general consumer at least in Europe.

Our results showed that acclimatised *eif4e* knock-out plants appeared to have a reduced growth phenotype already at T0, in addition to being androesterile. Segregation

of the mutation in the F2 generation showed a clear mismatch between observed and expected frequencies in the case of homozygous plants, which we attributed to a probable negative effect of *EIF4E* deletion on seed germination capacity. Differences in vegetative growth of the homozygous F2 plants were observed from the flowering stage onwards, when the androsterility phenotype also re-emerged. Edited plants with defects in vegetative growth are not suitable from an agronomic point of view. Therefore, we believe that it is necessary to implement a technology for melon editing that allows the generation of allelic variants of *EIF4E* that are functional for the plant but, at the same time, prevent viral replication. A good strategy in this regard could be to mimic the natural polymorphisms in the *EIF4E* gene through CRISPR/Cas9 base editing. Natural polymorphisms of *EIF4E* alleles are often associated with virus resistance (Robaglia and Caranta, 2006) and several studies have assessed the role of point mutations in resistance or translation initiation function (German-Retana et al. 2008; Moury et al. 2014). In this context, Bastet et al. (2019) have demonstrated the possibility to use CRISPR-nCas9-cytidine deaminase technology to convert Arabidopsis *EIF4E1* susceptibility allele into a resistance allele by introducing single-point mutations through C-to-G base editing to generate resistant plants without affecting the normal development of the plant (Bastet et al., 2019). It is worth mentioning that this technology, which is easily applicable to model species, would require a substantial improvement in the delivery systems of the CRISPR cassettes (see above) before it could be widely applied to recalcitrant species such as melon.

Despite the hopes placed in eIF4E, as we discussed above, it does not seem to be a target free of important limitations for virus resistance breeding. Yeast two-hybrid screens, *in vivo* bimolecular fluorescence complementation assays or *in vitro* co-immunoprecipitation can be useful preliminary steps to identify the specific plant eIF4E isoform-VPg interaction for the virus prior to engineering potyvirus resistance based on manipulation of eIF4E isoforms even if, as mentioned above, functional redundancy between isoforms may weaken these strategies. In spite of the not very encouraging results obtained until now, we should not abandon the idea of editing proviral factors to achieve resistance, but rather continue to look for new good candidate genes and concentrate our efforts on the techniques to predict them. In this sense, the study of

plant-virus interactions and the identification of new susceptibility factors are important activities for the identification of new molecular targets and, therefore, for the breeding of new resistant varieties. In recent decades there has been an increasing use of reverse genetics assays for the identification and characterisation of host genes involved in the viral cycle. However, the most commonly approach used so far to identify sources of resistance to plant viruses is still based on direct genetic studies (Song et al., 2017), in which aggressive isolates or resistance breaking isolates could be used to identify new sources of resistance. We believe that the combined use of these two strategies may be promising in the identification of new candidate proviral genes.

As aforementioned, both the acclimatized T0 mutant plants and the homozygous F2 individuals presented a male sterility phenotype. The appearance of this phenotype was unexpected, since *EIF4E*-silenced RNAi plants, despite having partially impaired vegetative growth, were unaffected in pollen production. A possible explanation for the phenotypic difference between the knock-out and knock-down lines could be that the *EIF4E*-silenced lines do not confer complete silencing, so that residual expression of the gene coding for eIF4E may be sufficient to carry out its function in the pollen development of the RNAi lines. Another possible explanation could be related to the lack of functioning of the RNAi system in germline cells which would determine the presence of pollen in the silenced plants. Given the interest, both in terms of basic research and in terms of biotechnological and breeding applications of the androesterility phenotype, and considering the lack of detailed information on the possible role of eIF4E in determining fertility in plants, we decided to try to characterize this phenotype through a comparative study of the floral development of mutant plants with respect to the wild type of the same genetic background. In order to address this objective, and given the lack of specific studies on floral development in melon, we decided to carry out our own study of floral development to gain knowledge on the mechanisms underlying floral development in this species.

To our knowledge, this is the only work reporting melon genome editing with CRISPR/Cas9 technology to achieve broad-spectrum virus resistance, and the first work describing the association between *EIF4E* editing and the development of male sterility in melon.

5.2 Morphological and transcriptomic analysis of melon flowers at different stages of development

In this work, we analysed the morphogenesis of male and hermaphrodite melon flowers at different developmental stages. In agreement with what has been observed in cucumber (Hao et al., 2003, Bai et al., 2004), we identified 12 stages of floral development, ranging from the appearance of floral meristems to anthesis. Most studies of floral development in the family *Cucurbitaceae* have been carried out on monoecious genotypes, and have shown sex determination to depend on the developmental arrest of sex-specific organs during early stages of flower development caused by the activation or inactivation of specific genes (Boualem et al., 2008, 2015; Rodriguez-Granados et al., 2021). Here, we decided to use an andromonoecious genotype, since we consider that, in addition to sex determination in sex-separated species, it is necessary to address the characterization of andromonoecious varieties, which constitute the majority of the commercial varieties currently cultivated. This genotype is characterized by the presence of both male and hermaphrodite flowers in the same plant. As in sex-separated genotypes, in this variety stages 1 to 5 were shared by male and hermaphrodite flowers, and the first structural differentiations between male and hermaphrodite flowers appeared between stages 6 and 7. Given the large number of flower buds analysed, it can be stated that the length of the flower bud was a good indicator of the stage of development. The developmental patterns corresponding to each length were found to be consistent both within flowers of the same genotype and, in general, conserved between different species such as melon and cucumber. In addition, as different samplings were carried out at different times of the year, these observations do not appear to be strongly affected by environmental conditions.

Since the identified stages involve subtle morphological changes that cannot be identified without a proper microscopy study, for the transcriptome analysis we had to group the flowers according to their size, with pools corresponding to four main episodes along the floral development. The specificity of the morphological analysis, and

the coherence of this with other studies carried out on related species, allowed us to delimit with some clarity each of the episodes, and to group the morphological stages in a way that ensured a good correspondence between stages and episodes based on floral length. By establishing a correlation between developmental stages and episodes, the aim was to try to identify the patterns of gene expression that are specific to a given episode of floral development and to characterise the genes that determine the passage from one stage to the next. The hierarchical clustering analysis of gene expression profiles, together with the PCA, showed that gene expression patterns among biological replicates were highly related except for two replicates, one for GM-H and the other for AN-H, respectively. When these two anomalous replicates were excluded from the analysis, both the PCA and the cluster dendrogram analysis (Figure 4.15B and C) showed that replicates clustered together, providing confidence on the use of floral bud size as indicator of the flower developmental episode. In addition, the PCA showed a clear separation between the clusters of male and hermaphrodite samples. Despite flower bud length being the only discriminating factor, no major overlap between episodes was observed. However, a certain tendency to cluster together could be detected, especially for the consecutive GM and AN episodes in hermaphrodite flowers.

Regarding expressed genes, out of a total of 29,932 total genes annotated in melon, our analysis detected 16,958 expressed genes after filtering for FPKM>1 in the mean of the three replicates. This is within the expected range for a transcriptome like that of melon. Out of these, 13,539 (80 %) were expressed in all four stages in male flowers, whereas 14,581 (86 %) were expressed in hermaphrodite flowers during all episodes. An inspection of the number of genes expressed in only one episode suggested a more complex gene expression landscape during the gamete initiation and anthesis compared to the other episodes for both male and hermaphrodite flowers.

With regard to differentially expressed genes, in general for male flowers, DEGs numbers correlated with the developmental distance among pairs of episodes. By contrast, for hermaphrodite flowers this trend seemed not to emerge with clarity, as the largest number of DEGs was detected between FS vs GI-H whereas FS vs AN-H had a smaller number of DEGs (Figure 4.16). This could appear somehow counter-intuitive, but agrees well with previous results, where episodes FS, AN-H and GM-H appear close in

the PCA and clustering analyses (Figure 4.15B and C). This difference in tendency between male and hermaphrodite flowers could be perhaps explained by the differences in terms of development observed in the analysis carried out by microscopy. While in the male flower the development of the reproductive organs follows a linear progression across the episodes, in the hermaphrodite flower the male reproductive organs start to develop earlier than the female ones. It is only at stage 7, corresponding to a flower length of 0.9 mm, that the carpel primordia begin to differentiate stigma and ovary, while is only at stage 8 that the stigma can be seen growing below an already partially developed anther. So, it is actually in the GI-H episode, that the process of initiation of the gametes of the male and female structures within the same flower really comes together. This mismatch between the development of the reproductive structures within the same flower could be the cause of the highest number of DEGs appearing between two consecutive stages such as FS and GI-H. In the hermaphrodite flower, the developmental processes of male and female gametes within the same flower could depend on the expression of specific and distinct genes between male and female gametes, resulting in a cumulative effect on the number of DEGs coinciding with the GI-H episode, and this cumulative effect would be mitigated by progressing towards a stage where the development of floral structures predominates over gamete development processes. This could explain the higher number of differently expressed genes in the comparisons between GI-H and any other episode, as well as the lower number of DEGs in all the other comparisons.

In total, the pairwise comparisons identified 12,469 and 11,574 DEGs in male and hermaphrodite flowers, respectively. These were the genes considered in the further analyses reported in this thesis. Among the MADS box genes that we believe that may play a role in the floral development in melon, the Arabidopsis homolog MADS-box protein AGL42 (MADS83) encoding gene is a strong candidate; Arabidopsis MADS83 has been reported to play a role in promoting flowering at the shoot apical and axillary meristem. This gene showed elevated expression levels at the FS and GI episodes for both male and hermaphrodite flowers and its expression levels declined, as was to be expected, throughout the flowering process. Homologs of the MADS-box gene encoding protein SOC1 (MADS64 and MADS65), which are transcription activators active in

flowering time control, had an almost male flower-specific expression, which was maintained, with slight fluctuations, throughout the whole process of flower development. The Arabidopsis homologs of AGAMOUS-LIKE proteins MADS25 and MADS27 encoding genes showed an increasing expression pattern throughout male flower development, whereas in the hermaphrodite flower, expression was concentrated in the GI episode. In contrast, *MADS36* and *MADS15*, involved in the determination of floral meristem and sepal identity, were down-regulated throughout floral development for both sexual types. MADS-box gene-expression patterns throughout flower development were quite homogeneous for the genes within the AP3, SEP, SCO1 and SVP families, while they appeared more variable for the remaining families, in general, for both male and hermaphrodite flowers. The analysis of MADS-box gene-expression patterns seemed to coincide with the ABCDE model of floral development in Arabidopsis (Bowman et al., 2012; Guo et al. 2015). It has been indeed described that genes of B-, C-, and E-class complex AGAMOUS (AG)-SEP-AP3-PI specify stamens. In our study, MADS-box genes belonging to these families had elevated expression patterns in the male (and hermaphrodite) flower, especially in the GI-M and GM-M episodes and, in general, after the FS episode. The C- and E-class complex AG-SEP, that specifies carpels, showed elevated expression patterns in correspondence of the GI-H episode. Finally, the D- and E-class complex SEEDSTICK (STK)-SEP, that specifies ovules had a peak of expression in GI-H and maintained a certain basal level throughout development in the hermaphrodite flower. To our knowledge, very little is known about the expression and function of MADS-box genes in melon. Most studies have been carried out in cucumber and all relate the expression of these genes to different reproductive developmental functions and fruit maturation (Cheng et al., 2019; Z. Cheng et al., 2020).

As we have seen for the MADS-box gene-expression patterns, the ABCDE model of flower development involves a complex interaction between different genes from different subfamilies to give rise to the development of the organs that constitute a given flower. To try to bring some order to this complexity and to simplify the characterisation of the different episodes, we manually analysed the expression patterns of DEGs considering as episode-specific genes those DEGs that had a level of

expression 2-fold or more at one episode above those in the remaining episodes, for both flower types. Furthermore, the functional enrichment analysis allowed us to identify functional relationships between the up-regulated genes. The overall number of specifically up-regulated genes appeared to be different between male and hermaphrodite flowers: While the number of DEGs increased in the male flower throughout the episodes, the highest number of DEGs in the hermaphrodite flower was found in the GI-H episode. However, this seemed to be consistent with the trend observed for the number of DEGs between pairs of episodes described above. The genes found to be specifically up-regulated during each episode provided further evidence of the stage-episode correspondence. In the first episode, in fact, many genes related to floral organ growth and development of anther structures were detected, which correspond to the processes characterising the different stages observed by microscopy that were grouped together to identify FS. Consistently, the GI episode was characterised by the presence of genes related to early flower reproductive and pollen development in male flowers and genes related to female gamete development in hermaphrodite flowers. In the FM episode, genes involved in gamete formation, mitotic cycle and pollen tube initiation were observed for male flowers, whereas in the hermaphrodite, post-meiotic pollen development and maturation related genes were detected. Finally, in the AN episode, genes related to photoperiodism and flowering were observed. Among the genes up-regulated across flower development we also found several genes involved in ethylene signalling, many homologs of the cytochrome p450 family, as well as genes of the ABC transporter family (A, B, C, D, F and I). This was consistent with what was described in melon for Dai et al. (2019). In general, the analysis of the enriched terms also gave us a broader view of the set of processes that take place during flower development and seemed to indicate that while metabolic and nuclear processes prevail in the early stages of development, membrane-associated processes predominate in the later stages. This was consistent with what has been observed for other species such as wheat (Feng et al., 2017) or Arabidopsis (Honys & Twell, 2003).

Regarding the expression patterns of sex-determining genes, these were consistent with the model described by Boualem et al. (2015), so that the male flower in our andromonoecious lines was characterised by the lack of *CmACS11* expression and the

consequent expression of *CmWIP1* throughout floral development, which in turn repressed *CmACS7* expression and carpel development (Figure 1.3A and figure 4.22). In contrast, hermaphrodite flowers were characterised by the expression of *CmACS11* and by the expression of a likely non-functional version of the *CmACS7* allele, which is not capable of suppressing stamen development, giving rise to hermaphrodite flowers instead of female (Figure 1.3B and figure 4.22).

To our knowledge, this is the only work coupling a detailed morphological analysis by microscopy to a comprehensive transcriptomic analysis for the characterization of the structural and molecular mechanisms that determine the floral development of an andromonoecious genotype in melon. To deeper investigate the set of changes that characterise the main stages of floral development, the RNA-seq analysis could be coupled to small RNA sequencing, as miRNAs are a class of noncoding RNAs that post- transcriptionally regulate target gene expression levels that have been shown to play pivotal roles in Arabidopsis during the transition from vegetative to reproductive development and the subsequent floral patterning (Chen., 2004; Nag et al., 2009; Luo et al., 2013). In addition, *in situ* hybridisation analysis of genes that are preferentially expressed at key stages of floral development in melon could be performed to further validate gene expression patterns in specific tissues. In any case, taken together, our results provide a first insight into gene regulatory networks in melon floral development that may be critical for floral and pollen development, highlighting potential targets for genetic manipulation to improve melon yield in the future. In this sense, the CRISPR/Cas technology constitutes a valuable tool for the identification of gene functions and the study of the mechanisms underlying floral development in cucurbits for fundamental research (Huimin Zhang et al., 2021), or, once identified, to take advantage of potential biotechnological applications through genome editing, as in the case of the breeding of non-transgenic gynoecious cucumber with CRISPR/Cas9 for hybrid production (B. Hu et al., 2017).

5.3 Comparative analysis of melon male floral development between wild type and *eif4e* knock-out mutant plants

In this study, we performed a comparative analysis of male floral development in mutant *vs* WT plants in order to investigate the possible role of eIF4E in the development of male melon gametes; the aim was dissecting the male sterility phenotype of the *eif4e* mutant plants obtained in objective 1. The knowledge gained from the morphological analysis carried out in the previous section allowed us to identify the stage in which the mutant diverged drastically from the WT in terms of male floral development. In our study, we did not detect significant differences in anther structures in mutant plants compared to WT plants before stage 9, therefore the comparative analysis of anther development was carried out from stage 9 onwards. This was consistent with what has been previously described for male sterile rice lines generated by mutations in the *Oryza sativa No Pollen 1* (*OsNP1*) nuclear male sterility gene (Chang et al., 2016). In melon, structural differences in pollen development became evident at the tetrad stage: In the WT, tetrads were clearly formed and at least three of the four cells of the tetrad could be observed in the flower sections (Figure 4.23C) while in the mutant, microsporocytes seemed to undergo incomplete meiosis and microspore individualization (Figure 4.23D). Furthermore, a remarkable distinction between WT and mutant anthers began to appear between stages 10 and 11: Normal vacuolated round shaped microspores were uniformly distributed along the tapetum side with dark-stained pollen wall corresponding to the exine in the WT (Figure. 4.23G), whereas internal cavities of the mutant anthers became disorganized and collapsed pollen grains in the mutant adhered to unstructured dark stained material that could correspond to incompletely degenerated tapetum inside the locule walls (Figure 4.23H). In this phase, the lumen of the anthers in the mutant was filled by large amounts of stained/dark material (Figure 4.24A, B, C and D) that could originate from droplets of sporopollenin secreted by the tapetum. To obtain better resolution of pollen development in mutant anthers, we also performed a scanning electron microscopy analysis comparing the same structures along the developmental process and the results appeared consistent with sectioning and light microscopy. For other species, such as

Arabidopsis and rice, it has been reported the progressive process of degradation of anther structures caused by the mutation in specific genes, including the apparent imperfect degeneration of the tapetum, the failure in meiotic divisions and individualisation of microspores, and the invasion of the anther lumen by detritus and hypothetical uncontrolled production of exine, leading to complete abortion of pollen grains (Wang et al., 2013; Liang et al., 2020; Li et al., 2020), and these phenomena had a high level of similarity both in terms of processes and timing at which they occur with our observations. Moreover, the observations reported in the present morphological study were also partially consistent with those made by Dai et al. (2019) in melon, although these authors only made a comparative analysis by microscopy of the stages corresponding to a floral length of 1 mm and 2 mm in male fertile versus male sterile melon lines, without reaching the level of detail achieved in the present work (Dai et al., 2019).

We next explored the transcriptomes of WT and mutant male flowers along the four main episodes during floral development defined in the previous section. The stage-episode correspondence tested in the previous study for the WT gave confidence about the possibility of performing a transcriptomic analysis by comparing the same episodes in the mutant and in the WT; the aim was assessing the changes in gene expression patterns specific to a given episode of floral development that associate with the appearance of the male sterility phenotype in the mutant. The cluster dendrogram analysis of the mutant gene expression profiles (Figure 4.26B) showed that gene expression patterns of biological replicates were highly related and the PCA including all biological replicates showed a clear separation in gene expression patterns between the mutant and WT, as well as a separation in gene expression patterns across floral developmental episodes within both the mutant and WT (Figure 4.26C). Regarding expressed genes, out of a total of 29,932 total genes annotated in melon, our analysis detected 15,110 expressed genes (pooling mutant and WT genes) of which 14,132 belonged to the mutant and 14,256 to the WT, after filtering for FPKM>1 in the mean of the three replicates. This is within the expected range for a transcriptome like that of melon. Regarding the differently expressed genes, a total of 7,397 DEGs were identified. The comparisons of FSmut *versus* FS, GI-Mmut *versus* GI-M, GM-Mmut *versus* GM-M,

and AN-Mmut *versus* AN-M provided 1,649, 1,162, 2,490 and 2,096 DEGs, respectively, with GM-Mmut *versus* GM-M being the episode in which the largest number of DEGs was found (Figure 4.27A). Furthermore, the functional enrichment analysis allowed us to identify functional relationships between the DEGs. It is worth mentioning that, as a general trend, the vast majority of the enriched terms in the mutant *versus* WT comparison throughout floral development were characterised by down-regulated genes and that the highest number of enriched terms occurred in the GI_Mmut *versus* GI-M and GM-Mmut *versus* GM-M comparisons.

Pollen development is synergistically controlled by sporophytic and gametophytic factors (McCormick, 2004; Chang et al., 2011). The sporophytic tapetum, adjacent to developing microspores, is crucial for pollen development through its secretions at early stages and programmed cell death (PCD) at late stages (Parish & Li., 2010). Function of the tapetum is controlled by an evolutionarily conserved transcriptional cascade (Wilson & Zhang, 2009; Zhu et al., 2011, 2015) as well as proteins involved in intercellular signalling. Many postmeiotic sporophytic mutants affecting pollen development have been isolated as male-sterile in plants. In the wild-type pollen, the pollen wall is composed by two layers: the exine and the intine. The exine is primarily made up of sporopollenin consisting of simple aliphatic polymers containing aromatic or conjugated side chains and is important, among many other aspects within male gametogenesis, for cell-to-cell recognition during pollination and pollen germination. The surface of the exine exhibits a highly decorated pattern that is species-specific while the intine is structurally simple and is made of cellulose, pectin, and proteins. Several male-sterile mutations that disrupt tapetum function and affect exine and intine formation have been described (Taylor et al., 1998; Ariizumi et al., 2004; Liang et al., 2020; Zhang et al., 2021)

In this study, the comparative analysis of anther development seemed to point to the sterility phenotype being post meiotic and sporophytic, as the unusual secretion of protein material at early stages, and the differences in the timing of tapetum degradation at late stages between the mutant and the WT are characteristic to this type of sterility. Consistent with this, our transcriptomic analysis identified in WT versus *eif4e* mutant male flowers the down-regulation of genes involved in cell growth,

differentiation and cell cycle progression, as well as in photosynthetic processes in the mutant coinciding with the FS episode. Curiously, several genes related to chloroplast and photosynthetic processes are cited in a list of representative chloroplast- and photosynthesis-related genes affected by virus infection (Bhattacharyya & Chakraborty, 2017). Furthermore, the down-regulation of genes implicated in ethylene synthesis, stamen filament development and sporopollenin biosynthetic process, was consistent with what was observed by Dai et al. (2019) for the comparison of DEGs between male fertile (1 mm) *versus* male sterile (1 mm) in melon (Dai et al., 2019). In the GI episode, modifications in the expression patterns of genes related to “MCM complex” and “DNA helicase” may be associated to the meiotic imbalances observed by microscopy in the stages corresponding to this episode, while the down-regulation of genes related to pectin metabolism could be due to impairments in the tapetum development, as both phenomena have been associated with male sterility in Arabidopsis (Ma., 2005). The down-regulation of genes involved in metabolism and ATPase activity was, again, consistent with that described by Dai et al. (2019) in the comparison male fertile (2 mm) *versus* male sterile (2 mm) in melon (Dai et al., 2019) Moreover, misregulation of genes involved in programmed cell death, callose deposition and sporopollenin biosynthesis observed at this episode have often been linked to interferences in the timing of tapetal PCD (Xu et al., 2019; Khan et al., 2021). In the GM episode, the transcriptomic data appeared to closely reflect the observations made by microscopy, so that down-regulation of genes related to membranes, cell wall and transmembrane transporter activity may be associated with the gradual destructuring of the anther walls observed by microscopy between stages 10 and 11 of development. In this context, the gene coding for the NO EXINE FORMATION 1 protein deserves a special mention, since it has been described that the *nef1* mutant of Arabidopsis synthesises sporopollenin, but this is not properly deposited on the pollen membrane, just as it has been observed for the sporocytes of our melon mutant. Moreover, the chloroplasts from *nef1* exhibited significant alterations in chloroplast morphology (Ariizumi et al., 2004). The upregulation of numerous genes involved in sporopollenin production between the GI and GM episodes, on the other hand, could be responsible for the invasion of droplets of potentially sporopollenin-associated material observed by microscopy in the mutant. Regarding the AN episode, defects in the regulation of genes related to endopeptidase

activity have been often associated with failures in protein ubiquitination and subsequent proteolysis and degradation by the proteasome. In fact, a compromised proteasome complex assembly and function lead to reduced proteolytic activities and the accumulation of damaged or misfolded protein species. According to this, the presence of cell detritus in the anther lumen, the failure of anthesis and the irregular degradation of aborted grains observed in stage 11 and 12 could be explained by deregulation of these genes observed at this episode, as they are important mechanisms in the regulation of the cell cycle, cell growth and differentiation, gene transcription, signal transduction and apoptosis. The role of Proteasome subunit alpha and beta type *PSMB1* genes in determining longevity and fertility has been extensively described in animal models and even in humans (Sagi & Kim, 2012; Kapetanou et al., 2022), however, their function does not seem to have been described in plants. Down-regulation of genes related to flowering and pollen development further confirmed what was observed by microscopy in the later stages of flower development. The involvement of Armadillo and FRIGIDA proteins in promoting fertility has been widely described for several plant species as Arabidopsis and rice (Igarashi et al., 2016; Gebert et al., 2008; Deal et al., 2005; Bac-Molenaar et al., 2015), and it is also conserved in animal models (Straschil et al., 2010).

To our knowledge, there are no studies establishing a correlation between *EIF4E* expression and androgenesis in plants. However, animal and plant studies have shown that germ cell and embryonic fates are greatly determined by the eIF4 factor complexes unique to those cells (Dinkova et al., 2005; Friday & Keiper, 2015; Cao & Richter, 2002; Minshall et al., 2007; Hernández et al., 2013; Henderson et al., 2009; Baker & Fuller, 2007; Ruffel et al., 2006). Moreover, the coupled use of genetics and biochemistry identified unique roles for eIF4E and eIF4G isoforms in reproduction, so that eIF4Es in plants, flies and frogs have shown unique roles in sexual development, judging by the reproductive phenotypes resulting from their deficiencies (Ghosh & Lasko, 2015; Rodriguez et al., 1998; Hernández et al., 2005; Patrick et al., 2014).

Our transcriptomic results detected the presence of genes encoding eukaryotic translation initiation factors among the differentially expressed genes in all episodes; in particular, the *EIF4G* has been shown to be down-regulated in the FS, GI and AN

episodes, in the mutant with respect to the WT. The interaction between eIF4E, encoded by the gene that has been knocked out in the mutant, and eIF4G constitutes the core of the eIF4F complex, which plays a key role in the circularisation of mRNAs and their subsequent cap-dependent translation (Marcotrigiano et al., 1999; Merrick, 2015; Ho & Lee, 2017). Multiple studies suggested that eIF4E and eIF4G isoforms are highly selective in translating mRNAs, and there may be a gradation of canonical cap-dependent to non-canonical requirements to the selection. Friday et al. (2015) proposed a model of selective and positive mRNA recruitment in germ cells based on the eIF4E and eIF4G isoforms in *C. elegans* (Friday et al., 2015). Furthermore, in animal and plant studies, polysome and reporter analyses showed that each isoform preferentially recruits a unique subset of mRNAs for CD translation (Henderson et al., 2009; Rodriguez et al., 1998; Dinkova et al., 2005). Based on these observations and in our results, and adapting the Friday et al. (2015) model to the initiation of translation in plants, we could hypothesize a specific role of the eIF4E-eIF4G complex in mRNA translation in male germ cells, being the interaction between these two factors an essential prerequisite to carry out different functions within germ cells, such as gamete maturation, meiotic recombination, sperm and oocyte fate determination and homeostasis (Figure 5.1). In this context, the suppression of *EIF4E* in the mutant plant, and the consequent lack of interaction with eIF4G, would lead to a mismatch in mRNA translation in male germ cells leading to the structural defects that characterize the male sterility phenotype. Of note here is that melon eIF4E has been shown to be required for non-canonical cap-independent 3´-CITE-dependent translation initiation (Truniger et al., 2008; Miras et al., 2017), and also that down-regulating *EIF(iso)4E* gene expression by RNAi in melon has proven impossible in our hands (unpublished results), suggesting that eIF(iso)4E may be playing a housekeeping role in cap-dependent translation initiation in melon, while eIF4E might be fulfilling more specialised roles, including non-canonical translation initiation during stress. In this context, the production of viable female gametes in the mutant plants could have two main possible explanations: One is that the production of female gametes might depend solely on the formation of the (iso)4E-(iso)4G complex; the other is that the translation of mRNAs responsible for the formation of female gametes could be carried out by eIF4G alone (perhaps via internal ribosome entry sites), bypassing eIF4E. This second option, although totally theoretical, could imply an

adaptive mechanism of survival, maintaining a basal process that allows the formation of eggs and cross-fertilization even when self-fertilization is not available, and thus ensuring the perpetuation of the species. But there is still a third option: Three eIF4E isoforms have been described in the *C. elegans* model, one of which seems to be exclusively responsible for cell fate determination. In melon, it is frequently assumed that there are only two eIF4E isoforms, but there is a third one, annotated previously as novel cap-binding protein (nCBP); interestingly, in our transcriptomic analyses, the gene encoding this third isoform appeared to be up-regulated only at the GM-M stage.

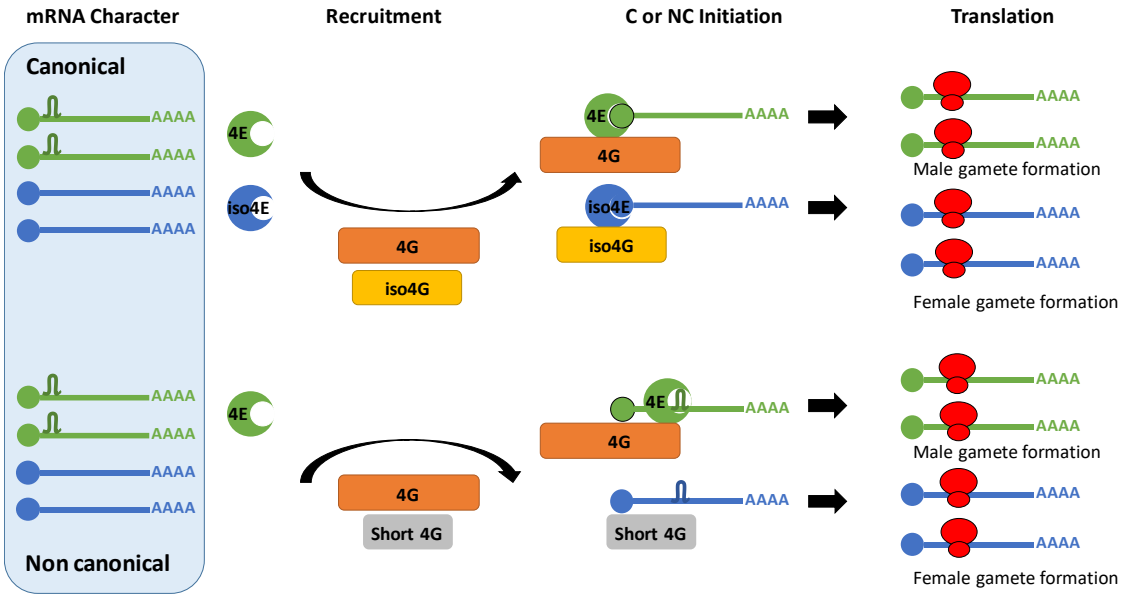

Figure 5.1. Model of selective translational mRNA recruitment in melon germ cells involving eIF4E and eIF4G isoforms. Multiple studies suggest that eIF4E and eIF4G isoforms are selective in translating mRNAs (see text), and there may be a gradation of canonical cap-dependent (CD) to non-canonical (NC) requirements to the selection. Hypothetical CD sex-specific mRNAs recruited to ribosomes by eIF4E (green), eIF(iso)4E (blue) via association with eIF4G (orange) or eIF(iso)4G (yellow) in germ cells are shown. An hypothetical RNA element controlling NC translation (RENT) is shown as an stem in sex-specific mRNAs recruited to ribosomes by eIF4E. Hypothetical short eIF4G isoform (short 4G) recruits identified CI mRNAs without eIF4Es as described for *C. elegans* by Morrison et al. (2014). Figure modified from Friday & Keiper. (2015) and Friday et al. (2015).

To our knowledge, this is the only work coupling a detailed comparative morphological analysis by microscopy to a comprehensive transcriptomic analysis in order to characterize the association between the mutation in *EIF4E* and the generation of a male-sterility phenotype. To deeper investigate the set of changes that characterise

the main stages of anther development in the mutant, the microscopy analysis could be complemented by a TUNEL assay, which would allow to detect DNA fragmentation due to apoptotic signalling cascades in the tapetum. On the other hand, the generation of mutants in the eIF4E and eIF4G isoform encoding genes would allow to genetically dissect the role of translation initiation factors in germ cell regulation and to complete a model of positive translational mRNA recruitment in germ cells in plants that, at the moment, is almost purely speculative. In any case, taken together, our results provide a first insight into gene regulatory networks in melon male gamete development that may be critical for proper pollen formation and maturation. Furthermore, they suggest for the first time a specific role of eIF4E in the regulation of fertility-determining processes in melon.

6 CONCLUSIONS

The results obtained in this thesis allow the following conclusions to be drawn:

1. *Agrobacterium tumefaciens*-mediated melon genetic transformation still represents a limiting factor for genome editing in this species. Further efforts should be made to overcome the limitations of genetic transformation in recalcitrant species like melon.

2. The CRISPR/Cas9 system is a powerful and broadly applicable tool for the generation of melon plants knocked out in a specific gene, including for instance genes encoding proviral factors. Using this technology, I have produced homozygous edited plants in the gene encoding the eukaryotic translation initiation factor (eIF) 4E in melon. The mutation in *eif4e* melon plants likely results in the production of a truncated eIF4E protein.

3. Homozygous *eif4e* mutant plants are resistant to Moroccan watermelon mosaic virus (MWMV) and also show a male sterility phenotype. Both phenotypes are tightly associated with the *EIF4E* mutation.

4. After four months post inoculation of *eif4e* plants, a MWMV-resistance breaking isolate emerged; sequencing of its *VPg* cistron identified a single nucleotide substitution resulting in the N163Y amino acid change in the VPg protein sequence.

5. *EIF4E* is not a target free of limitations for virus resistance breeding. Resistance breaking appeared soon after inoculation of the mutants with MWMV, and male sterility could only be overcome by producing hybrids between mutant and wild type (WT) plants; however, the idea of editing proviral factors for attaining virus resistance should not be abandoned, as the study of plant-virus interactions can provide new candidates for resistance, and adding specificity to the editing events may help overcoming limitations.

6. Melon flower development is consistent with that of other cucurbits, and can be divided into 12 developmental stages. Further efforts should be made for the characterisation of andromonoecious varieties, which constitute the majority of the commercial varieties currently cultivated.

7. The 12 developmental stages were grouped into four major episodes of flower development, showing that a detailed morphological research by microscopy can be coupled to a comprehensive transcriptomic analysis in order to characterise the structural and molecular mechanisms that determine the floral development in melon.

8. A transcriptomic analysis has shown that the MADS-box gene-expression patterns during melon floral development agreed with the ABCDE model of floral development in Arabidopsis. Specific de-regulation of transcript accumulation can be used for the identification of genes that determine the passage from one episode of development to the next.

9. The morphological and transcriptomic observations of floral development allowed the identification of the key stages to be considered in the comparative analysis between *eif4e* mutant and WT plants. Comparative analysis between *eif4e* mutant and WT plants resulted in the identification of common and divergent episodes throughout floral development.

10. The comparative analysis of anther development in WT *versus* mutant plants seemed to point to the sterility phenotype being post meiotic and sporophytic, as the unusual secretion of protein material at early stages, and the differences in the timing of tapetum degradation at late stages between the mutant and the WT are characteristic to this type of sterility. The transcriptomic data were consistent with the observations made by microscopy.

11. Taking into account the phenotype of the mutant plants and the transcriptomic data, a model is proposed in which eIF4E-dependent translation limits male gametogenesis, at least in melon.

7 BIBLIOGRAPHY

Abdul-Razzak, A., Guiraud, T., Peypelut, M., Walter, J., Houvenaghel, M. C., Candresse, T., Le Gall, O., & German-Retana, S. (2009). Involvement of the cylindrical inclusion (CI) protein in the overcoming of an eIF4E-mediated resistance against Lettuce mosaic potyvirus. *Molecular Plant Pathology*, *10*(1), 109–113. https://doi.org/10.1111/j.1364-3703.2008.00513.x

Abiri, R., Valdiani, A., Maziah, M., Shaharuddin, N. A., Sahebi, M., Yusof, Z. N. B., Atabaki, N., & Talei, D. (2016). A critical review of the concept of transgenic plants: Insights into pharmaceutical biotechnology and molecular farming. *Current Issues in Molecular Biology*, *18*(1), 21–42. https://doi.org/10.21775/cimb.018.021

Adelberg, J. W., Rhodes, B. B., Skorupska, H. T., & Bridges, W. C. (1994). Explant origin affects the frequency of tetraploid plants from tissue cultures of melon. *HortScience*, *29*(6), 689–692. https://doi.org/10.21273/hortsci.29.6.689

Akasaka-Kennedy, Y., Tomita, K. O., & Ezura, H. (2004). Efficient plant regeneration and Agrobacterium-mediated transformation via somatic embryogenesis in melon (Cucumis melo L.). *Plant Science*, *166*(3), 763–769. https://doi.org/10.1016/j.plantsci.2003.11.020

Albar, L., Bangratz-Reyser, M., Hébrard, E., Ndjiondjop, M. N., Jones, M., & Ghesquière, A. (2006). Mutations in the eIF(iso)4G translation initiation factor confer high resistance of rice to Rice yellow mottle virus. *Plant Journal*, *47*(3), 417–426. https://doi.org/10.1111/j.1365-313X.2006.02792.x

Anagnostou, K., Jahn, M., & Perl-Treves, R. (2000). Inheritance and linkage analysis of resistance to zucchini yellow mosaic virus, watermelon mosaic virus, papaya ringspot virus and powdery mildew in melon. *Euphytica*, *116*(3), 265-270.

Anders, C., Niewoehner, O., Duerst, A., & Jinek, M. (2014). Structural basis of PAM-dependent target DNA recognition by the Cas9 endonuclease. *Nature*, *513*(7519), 569–573. https://doi.org/10.1038/nature13579

Argyris, J. M., Ruiz-Herrera, A., Madriz-Masis, P., Sanseverino, W., Morata, J., Pujol, M., Ramos-Onsins, S. E., & Garcia-Mas, J. (2015). Use of targeted SNP selection for an improved anchoring of the melon (Cucumis melo L.) scaffold genome assembly. *BMC Genomics*, *16*(1), 1–14. https://doi.org/10.1186/s12864-014-1196-3

Ariizumi, T., Hatakeyama, K., Hinata, K., Inatsugi, R., Nishida, I., Sato, S., Kato, T., Tabata, S., & Toriyama, K. (2004). Disruption of the novel plant protein NEF1 affects lipid accumulation in the plastids of the tapetum and exine formation of pollen, resulting in male sterility in Arabidopsis thaliana. *Plant Journal*, *39*(2), 170–181. https://doi.org/10.1111/j.1365-313X.2004.02118.x

Ashby, J. A., Stevenson, C. E. M., Jarvis, G. E., Lawson, D. M., & Maule, A. J. (2011). Structure-based mutational analysis of eIF4E in relation to sbm1 resistance to Pea seed-borne mosaic virus in Pea. *PLoS ONE*, *6*(1). https://doi.org/10.1371/journal.pone.0015873

Ayme, V., Petit-Pierre, J., Souche, S., Palloix, A., & Moury, B. (2007). Molecular dissection of the potato virus Y VPg virulence factor reveals complex adaptations to the pvr2 resistance allelic series in pepper. *Journal of General Virology*, *88*(5), 1594–1601.

https://doi.org/10.1099/vir.0.82702-0

Ayme, V., Souche, S., Caranta, C., Jacquemond, M., Chadœuf, J., Palloix, A., & Moury, B. (2006). Different mutations in the genome-linked protein VPg of Potato virus Y confer virulence on the pvr23 resistance in pepper. *Molecular Plant-Microbe Interactions*, *19*(5), 557–563. https://doi.org/10.1094/MPMI-19-0557

Bac-Molenaar, J. A., Fradin, E. F., Becker, F. F. M., Rienstra, J. A., van der Schoot, J., Vreugdenhil, D., & Keurentjes, J. J. B. (2015). Genome-wide association mapping of fertility reduction upon heat stress reveals developmental stage-specific QTLs in Arabidopsis Thaliana. *Plant Cell*, *27*(7), 1857–1874. https://doi.org/10.1105/tpc.15.00248

Bai, S. L., Peng, Y. Ben, Cui, J. X., Gu, H. T., Xu, L. Y., Li, Y. Q., Xu, Z. H., & Bai, S. N. (2004). Developmental analyses reveal early arrests of the spore-bearing parts of reproductive organs in unisexual flowers of cucumber (Cucumis sativus L.). *Planta*, *220*(2), 230–240. https://doi.org/10.1007/s00425-004-1342-2

Baker, C. C., & Fuller, M. T. (2007). Translational control of meiotic cell cycle progression and spermatid differentiation in male germ cells by a novel eIF4G homolog. *Development*, *134*(15), 2863–2869. https://doi.org/10.1242/dev.003764

Bastet, A., Lederer, B., Giovinazzo, N., Arnoux, X., German-Retana, S., Reinbold, C., Brault, V., Garcia, D., Djennane, S., Gersch, S., Lemaire, O., Robaglia, C., & Gallois, J. L. (2018). Trans-species synthetic gene design allows resistance pyramiding and broad-spectrum engineering of virus resistance in plants. *Plant Biotechnology Journal*, *16*(9), 1569–1581. https://doi.org/10.1111/pbi.12896

Bastet, A., Zafirov, D., Giovinazzo, N., Guyon-Debast, A., Nogué, F., Robaglia, C., & Gallois, J. L. (2019). Mimicking natural polymorphism in eIF4E by CRISPR-Cas9 base editing is associated with resistance to potyviruses. *Plant Biotechnology Journal*, *17*(9), 1736–1750. https://doi.org/10.1111/pbi.13096

Bennett, A. B., Chi-Ham, C., Barrows, G., Sexton, S., & Zilberman, D. (2013). Agricultural biotechnology: Economics, environment, ethics, and the future. *Annual Review of Environment and Resources*, *38*, 249–279. https://doi.org/10.1146/annurev-environ-050912-124612

Bhattacharyya, D., & Chakraborty, S. (2018). Chloroplast: the Trojan horse in plant–virus interaction. *Molecular Plant Pathology*, *19*(2), 504-518.

Bhowmik, P., Ellison, E., Polley, B., Bollina, V., Kulkarni, M., Ghanbarnia, K., Song, H., Gao, C., Voytas, D. F., & Kagale, S. (2018). Targeted mutagenesis in wheat microspores using CRISPR / Cas9. *Scientific Reports*, *January*, 1–10. https://doi.org/10.1038/s41598-018-24690-8

Birchler, J. A. (2016). Hybrid vigour characterized. *Nature*, *537*(7622), 620-621.

Blanca, J. M., Cañizares, J., Ziarsolo, P., Esteras, C., Mir, G., Nuez, F., Garcia-Mas, J., & Picó, M. B. (2011). Melon Transcriptome Characterization: Simple Sequence Repeats and Single Nucleotide Polymorphisms Discovery for High Throughput Genotyping across the Species. *The Plant Genome*, *4*(2), 118–131.

https://doi.org/10.3835/plantgenome2011.01.0003

Bokros, C. L., Hugdahl, J. D., Kim, H. H., Hanesworth, V. R., Van Heerden, A., Browning, K. S., & Morejohn, L. C. (1995). Function of the p86 subunit of eukaryotic initiation factor (iso)4F as a microtubule-associated protein in plant cells. *Proceedings of the National Academy of Sciences of the United States of America*, *92*(15), 7120–7124. https://doi.org/10.1073/pnas.92.15.7120

Bolger, A. M., Lohse, M., & Usadel, B. (2014). Trimmomatic: A flexible trimmer for Illumina sequence data. *Bioinformatics*, *30*(15), 2114–2120. https://doi.org/10.1093/bioinformatics/btu170

Bolotin, A., Quinquis, B., Sorokin, A., & Dusko Ehrlich, S. (2005). Clustered regularly interspaced short palindrome repeats (CRISPRs) have spacers of extrachromosomal origin. *Microbiology*, *151*(8), 2551–2561. https://doi.org/10.1099/mic.0.28048-0

Bordas, M., González-Candelas, L., Dabauza, M., Ramón, D., & Moreno, V. (1998). Somatic hybridization between an albino Cucumis melo L. mutant and Cucumis myriocarpus Naud. *Plant Science*, *132*(2), 179–190. https://doi.org/10.1016/S0168-9452(97)00265-3

Borgstrøm, B., & Johansen, I. E. (2001). Mutations in pea seedborne mosaic virus genome-linked protein VPg alter pathotype-specific virulence in Pisum sativum. *Molecular Plant-Microbe Interactions*, *14*(6), 707–714. https://doi.org/10.1094/MPMI.2001.14.6.707

Bortesi, L., & Fischer, R. (2015). The CRISPR/Cas9 system for plant genome editing and beyond. *Biotechnology Advances*, *33*(1), 41–52. https://doi.org/10.1016/j.biotechadv.2014.12.006

Boualem, A., Fergany, M., Fernandez, R., Troadec, C., Martin, A., Morin, H., Sari, M. A., Collin, F., Flowers, J. M., Pitrat, M., Purugganan, M. D., Dogimont, C., & Bendahmane, A. (2008). A conserved mutation in an ethylene biosynthesis enzyme leads to andromonoecy in melons. *Science*, *321*(5890), 836–838. https://doi.org/10.1126/science.1159023

Boualem, A., Troadec, C., Camps, C., Lemhemdi, A., Morin, H., Sari, M. A., Fraenkel-Zagouri, R., Kovalski, I., Dogimont, C., Perl-Treves, R., & Bendahmane, A. (2015). A cucurbit androecy gene reveals how unisexual flowers develop and dioecy emerges. *Science*, *350*(6261), 688–691. https://doi.org/10.1126/science.aac8370

Boualem, A., Troadec, C., Kovalski, I., Sari, M. A., Perl-Treves, R., & Bendahmane, A. (2009). A conserved ethylene biosynthesis enzyme leads to andromonoecy in two Cucumis species. *PLoS ONE*, *4*(7). https://doi.org/10.1371/journal.pone.0006144

Bourdenx, B., Bernard, A., Domergue, F., Pascal, S., Léger, A., Roby, D., Pervent, M., Vile, D., Haslam, R. P., Napier, J. A., Lessire, R., & Joubès, J. (2011). Overexpression of Arabidopsis ECERIFERUM1 promotes wax very-long-chain alkane biosynthesis and influences plant response to biotic and abiotic stresses. *Plant Physiology*, *156*(1), 29–45. https://doi.org/10.1104/pp.111.172320

Bowman, J. L., Smyth, D. R., & Meyerowitz, E. M. (2012). The ABC model of flower

development: Then and now. *Development (Cambridge)*, *139*(22), 4095–4098. https://doi.org/10.1242/dev.083972

Browning, K. S. (2004). Plant translation initiation factors: It is not easy to be green. *Biochemical Society Transactions*, *32*(4), 589–591. https://doi.org/10.1042/BST0320589

Bush, M. S., Hutchins, A. P., Jones, A. M. E., Naldrett, M. J., Jarmolowski, A., Lloyd, C. W., & Doonan, J. H. (2009). Selective recruitment of proteins to 5′ cap complexes during the growth cycle in Arabidopsis. *Plant Journal*, *59*(3), 400–412. https://doi.org/10.1111/j.1365-313X.2009.03882.x

Cao, Q., & Richter, J. D. (2002). Dissolution of the maskin-eIF4E complex by cytoplasmic polyadenylation and poly(A)-binding protein controls cyclin B1 mRNA translation and oocyte maturation. *EMBO Journal*, *21*(14), 3852–3862. https://doi.org/10.1093/emboj/cdf353

Castanera, R., Ruggieri, V., Pujol, M., Garcia-Mas, J., & Casacuberta, J. M. (2020). An Improved Melon Reference Genome With Single-Molecule Sequencing Uncovers a Recent Burst of Transposable Elements With Potential Impact on Genes. *Frontiers in Plant Science*, *10*(January), 1–10. https://doi.org/10.3389/fpls.2019.01815

Chandrasekaran, J., Brumin, M., Wolf, D., Leibman, D., Klap, C., Pearlsman, M., Sherman, A., Arazi, T., & Gal-On, A. (2016). Development of broad virus resistance in non-transgenic cucumber using CRISPR/Cas9 technology. *Molecular Plant Pathology*, *17*(7), 1140–1153. https://doi.org/10.1111/mpp.12375

Chang, F., Wang, Y., Wang, S., & Ma, H. (2011). Molecular control of microsporogenesis in Arabidopsis. *Current Opinion in Plant Biology*, *14*(1), 66–73. https://doi.org/10.1016/j.pbi.2010.11.001

Chang, Z., Chen, Z., Wang, N., Xie, G., Lu, J., Yan, W., Zhou, J., Tang, X., & Deng, X. W. (2016). Construction of a male sterility system for hybrid rice breeding and seed production using a nuclear male sterility gene. *Proceedings of the National Academy of Sciences*, *113*(49), 14145–14150. https://doi.org/10.1073/PNAS.1613792113

Charron, C., Nicolaï, M., Gallois, J. L., Robaglia, C., Moury, B., Palloix, A., & Caranta, C. (2008). Natural variation and functional analyses provide evidence for co-evolution between plant eIF4E and potyviral VPg. *Plant Journal*, *54*(1), 56–68. https://doi.org/10.1111/j.1365-313X.2008.03407.x

Chen, H., Sun, J., Li, S., Cui, Q., Zhang, H., Xin, F., Wang, H., Lin, T., Gao, D., Wang, S., Li, X., Wang, D., Zhang, Z., Xu, Z., & Huang, S. (2016). An ACC Oxidase Gene Essential for Cucumber Carpel Development. *Molecular Plant*, *9*(9), 1315–1327. https://doi.org/10.1016/j.molp.2016.06.018

Chen, L., & Liu, Y. G. (2014). Male sterility and fertility restoration in crops. *Annual Review of Plant Biology*, *65*, 579–606. https://doi.org/10.1146/annurev-arplant-050213-040119

Chen, S., Li, Y., Zhao, Y., Li, G., Zhang, W., Wu, Y., & Huang, L. (2021). iTRAQ and RNA-

Seq analyses revealed the effects of grafting on fruit development and ripening of oriental melon (Cucumis melo L. var. makuwa). *Gene*, *766*(September 2020), 145142. https://doi.org/10.1016/j.gene.2020.145142

Chen, X. (2004). A microRNA as a translational repressor of APETALA2 in Arabidopsis flower development. *Science*, *303*(5666), 2022-2025.

Cheng, Y., He, P., Jiang, L., Liu, S., & Zhou, Y. (2019). Identification and characterization of a SEPALLATA-like MADS-box gene from cucumber (Cucumis sativus L.). *Notulae Botanicae Horti Agrobotanici Cluj-Napoca*, *47*(4), 1168–1177. https://doi.org/10.15835/nbha47411610

Cheng, Z., Zhuo, S., Liu, X., Che, G., Wang, Z., Gu, R., Shen, J., Song, W., Zhou, Z., Han, D., & Zhang, X. (2020). The MADS-Box Gene CsSHP Participates in Fruit Maturation and Floral Organ Development in Cucumber. *Frontiers in Plant Science*, *10*(February), 1–13. https://doi.org/10.3389/fpls.2019.01781

Chovelon, V., Restier, V., Giovinazzo, N., Dogimont, C., & Aarrouf, J. (2011). Histological study of organogenesis in Cucumis melo L. after genetic transformation: Why is it difficult to obtain transgenic plants? *Plant Cell Reports*, *30*(11), 2001–2011. https://doi.org/10.1007/s00299-011-1108-9

Collard, B. C. Y., & Mackill, D. J. (2008). Marker-assisted selection: An approach for precision plant breeding in the twenty-first century. *Philosophical Transactions of the Royal Society B: Biological Sciences*, *363*(1491), 557–572. https://doi.org/10.1098/rstb.2007.2170

Combe, J. P., Petracek, M. E., Van Eldik, G., Meulewaeter, F., & Twell, D. (2005). Translation initiation factors eIF4E and eIFiso4E are required for polysome formation and regulate plant growth in tobacco. *Plant Molecular Biology*, *57*(5), 749–760. https://doi.org/10.1007/s11103-005-3098-x

Cooper, I., & Jones, R. A. C. (2006). Wild Plants and Viruses: Under-Investigated Ecosystems. *Advances in Virus Research*, *67*(06), 1–47. https://doi.org/10.1016/S0065-3527(06)67001-2

Culjkovic, B., Topisirovic, I., & Borden, K. L. B. (2007). Controlling gene expression through RNA regulons: The role of the eukaryotic translation initiation factor eIF4E. *Cell Cycle*, *6*(1), 65–69. https://doi.org/10.4161/cc.6.1.3688

Curuk, S., Elman, C., Schlarman, E., Sagee, O., Shomer, I., Cetiner, S., Gray, D. J., & Gaba, V. (2002). A novel pathway for rapid shoot regeneration from the proximal zone of the hypocotyl of melon (Cucumis melo L.). *In vitro Cellular and Developmental Biology - Plant*, *38*(3), 260–267. https://doi.org/10.1079/IVP2001259

Dai, D., Xiong, A., Yuan, L., Sheng, Y., Ji, P., Jin, Y., Li, D., Wang, Y., & Luan, F. (2019). Transcriptome analysis of differentially expressed genes during anther development stages on male sterility and fertility in Cucumis melo L. line. *Gene*, *707*, 65–77. https://doi.org/10.1016/j.gene.2019.04.089

Deal, R. B., Kandasamy, M. K., McKinney, E. C., & Meagher, R. B. (2005). The nuclear actin-related protein ARP6 is a pleiotropic developmental regulator required for

the maintenance of FLOWERING LOCUS C expression and repression of flowering in Arabidopsis. *Plant Cell*, *17*(10), 2633–2646. https://doi.org/10.1105/tpc.105.035196

Decroocq, V., Sicard, O., Alamillo, J. M., Lansac, M., Eyquard, J. P., García, J. A., Candresse, T., Le Gall, O., & Revers, F. (2006). Multiple resistance traits control Plum pox virus infection in Arabidopsis thaliana. *Molecular Plant-Microbe Interactions*, *19*(5), 541–549. https://doi.org/10.1094/MPMI-19-0541

Dehairs, J., Talebi, A., Cherifi, Y., & Swinnen, J. V. (2016). CRISP-ID: Decoding CRISPR mediated indels by Sanger sequencing. *Scientific Reports*, *6*(June), 1–5. https://doi.org/10.1038/srep28973

Demirci, S., Fuentes, R. R., van Dooijeweert, W., Aflitos, S., Schijlen, E., Hesselink, T., de Ridder, D., van Dijk, A. D. J., & Peters, S. (2021). Chasing breeding footprints through structural variations in Cucumis melo and wild relatives. *G3: Genes, Genomes, Genetics*, *11*(1). https://doi.org/10.1093/G3JOURNAL/JKAA038

Dezfulian, M. H., Soulliere, D. M., Dhaliwal, R. K., Sareen, M., & Crosby, W. L. (2012). The SKP1-Like Gene Family of Arabidopsis Exhibits a High Degree of Differential Gene Expression and Gene Product Interaction during Development. *PLoS ONE*, *7*(11), 18–20. https://doi.org/10.1371/journal.pone.0050984

Diaz-Pendon, J. A., Truniger, V., Nieto, C., Garcia-Mas, J., Bendahmane, A., & Aranda, M. A. (2004). Advances in understanding recessive resistance to plant viruses. *Molecular Plant Pathology*, *5*(3), 223–233. https://doi.org/10.1111/j.1364-3703.2004.00223.x

Díaz, J. A., Nieto, C., Moriones, E., Truniger, V., & Aranda, M. A. (2004). Molecular characterization of a Melon necrotic spot virus strain that overcomes the resistance in melon and nonhost plants. *Molecular Plant-Microbe Interactions*, *17*(6), 668–675. https://doi.org/10.1094/MPMI.2004.17.6.668

Dinkova, T. D., Zepeda, H., Martínez-Salas, E., Martínez, L. M., Nieto-Sotelo, J., & Sánchez De Jiménez, E. (2005). Cap-independent translation of maize Hsp101. *Plant Journal*, *41*(5), 722–731. https://doi.org/10.1111/j.1365-313X.2005.02333.x

Doudna, J. A., & Charpentier, E. (2014). The new frontier of genome engineering with CRISPR-Cas9. *Science*, *346*(6213). https://doi.org/10.1126/science.1258096

Duprat, A., Caranta, C., Revers, F., Menand, B., Browning, K. S., & Robaglia, C. (2002). The Arabidopsis eukaryotic initiation factor (iso)4E is dispensable for plant growth but required for susceptibility to potyviruses. *Plant Journal*, *32*(6), 927–934. https://doi.org/10.1046/j.1365-313X.2002.01481.x

Edwards, A. N., Patterson-Fortin, L. M., Vakulskas, C. A., Mercante, J. W., Potrykus, K., Vinella, D., Camacho, M. I., Fields, J. A., Thompson, S. A., Georgellis, D., Cashel, M., Babitzke, P., & Romeo, T. (2011). Circuitry linking the Csr and stringent response global regulatory systems. *Molecular Microbiology*, *80*(6), 1561–1580. https://doi.org/10.1111/j.1365-2958.2011.07663.x

Endl, J., Achigan-Dako, E. G., Pandey, A. K., Monforte, A. J., Pico, B., & Schaefer, H. (2018).

Repeated domestication of melon (Cucumis melo) in Africa and Asia and a new close relative from India. *American Journal of Botany*, *105*(10), 1662–1671. https://doi.org/10.1002/ajb2.1172

Ezura, H., Yuhashi, K. I., Yasuta, T., & Minamisawa, K. (2000). Effect of ethylene on Agrobacterium tumefaciens-mediated gene transfer to melon. *Plant Breeding*, *119*(1), 75–79. https://doi.org/10.1046/j.1439-0523.2000.00438.x

Ezura, Hiroshi, Kikuta, I., & Oosawa, K. (1994). Production of aneuploid melon plants following *in vitro* culture of seeds from a triploid x diploid cross. *Plant Cell, Tissue and Organ Culture*, *38*(1), 61–63. https://doi.org/10.1007/BF00034445

Ezura, H., Amagai, H., Yoshioka, K., & Oosawa, K. (1992). Highly frequent appearance of tetraploidy in regenerated plants, a universal phenomenon, in tissue cultures of melon (Cucumis melo L.). *Plant science*, *85*(2), 209-213.

Fang, G., & Grumet, R. (1990). Agrobacterium tumefaciens mediated transformation and regeneration of muskmelon plants. *Plant Cell Reports*, *9*(3), 160–164. https://doi.org/10.1007/BF00232095

Feng, N., Song, G., Guan, J., Chen, K., Jia, M., Huang, D., Wu, J., Zhang, L., Kong, X., Geng, S., Liu, J., Li, A., & Mao, L. (2017). Transcriptome profiling of wheat inflorescence development from spikelet initiation to floral patterning identified stage-specific regulatory Genes. *Plant Physiology*, *174*(3), 1779–1794. https://doi.org/10.1104/pp.17.00310

Ficcadenti, N., & Rotino, G. L. (1995). Genotype and medium affect shoot regeneration of melon. *Plant Cell, Tissue and Organ Culture*, *40*(3), 293–295. https://doi.org/10.1007/BF00048137

Fraser, R. S. S. (1990). The Genetics of Resistance to Plant Viruses. *Annual Review of Phytopathology*, *28*(1), 179–200. https://doi.org/10.1146/annurev.py.28.090190.001143

Friday, A. J., Henderson, M. A., Morrison, J. K., Hoffman, J. L., & Keiper, B. D. (2015). Spatial and temporal translational control of germ cell mRNAs mediated by the eIF4E isoform IFE-1. *Journal of Cell Science*, *128*(24), 4487–4498. https://doi.org/10.1242/jcs.172684

Friday, A. J., & Keiper, B. D. (2015). Positive mRNA translational control in germ cells by initiation factor selectivity. *BioMed Research International*, *2015*. https://doi.org/10.1155/2015/327963

Fuchs, M., McFerson, J. R., Tricoli, D. M., McMaster, J. R., Deng, R. Z., Boeshore, M. L., Reynolds, J. F., Russell, P. F., Quemada, H. D., & Gonsalves, D. (1997). Cantaloupe line CZW-30 containing coat protein genes of cucumber mosaic virus, zucchini yellow mosaic virus, and watermelon mosaic virus-2 is resistant to these three viruses in the field. *Molecular Breeding*, *3*(4), 279–290. https://doi.org/10.1023/A:1009640229952

Gaj, T., Gersbach, C. A., & Barbas, C. F. (2013). ZFN, TALEN, and CRISPR/Cas-based methods for genome engineering. *Trends in Biotechnology*, *31*(7), 397–405.

https://doi.org/10.1016/j.tibtech.2013.04.004

Galbraith, D. W., Harkins, K. R., & Knapp, S. (1991). *Systemic Endopolyploidy in Arabidopsis thalianal*. *8709697*, 985–989.

Gallois, J. L., Charron, C., Sanchez, F., Pagny, G., Houvenaghel, M. C., Moretti, A., Ponz, F., Revers, F., Caranta, C., & German-Retana, S. (2010). Single amino acid changes in the turnip mosaic virus viral genome-linked protein (VPg) confer virulence towards Arabidopsis thaliana mutants knocked out for eukaryotic initiation factors eIF(iso)4E and eIF(iso)4G. *Journal of General Virology*, *91*(1), 288–293. https://doi.org/10.1099/vir.0.015321-0

Gallois, J. L., Moury, B., & German-Retana, S. (2018). Role of the genetic background in resistance to plant viruses. *International Journal of Molecular Sciences*, *19*(10), 1–20. https://doi.org/10.3390/ijms19102856

Galperin, M., Zelcer, A., & Kenigsbuch, D. (2003). High Competence for Adventitious Regeneration in the BU-21/3 Melon Genotype Is Controlled by a Single Dominant Locus. *HortScience*, *38*(6), 1167–1168. https://doi.org/10.21273/hortsci.38.6.1167

Gamborg, O. L., Miller, R., & Ojima, K. (1968). Nutrient requirements of suspension cultures of soybean root cells. *Experimental cell research*, *50*(1), 151-158.

Gao, Z., Johansen, E., Eyers, S., Thomas, C. L., Ellis, T. H. N., & Maule, A. J. (2004). The potyvirus recessive resistance gene, sbm1, identifies a novel role for translation initiation factor eIF4E in cell-to-cell trafficking. *Plant Journal*, *40*(3), 376–385. https://doi.org/10.1111/j.1365-313X.2004.02215.x

García-Alcalde, F., Okonechnikov, K., Carbonell, J., Cruz, L. M., Götz, S., Tarazona, S., ... & Conesa, A. (2012). Qualimap: evaluating next-generation sequencing alignment data. *Bioinformatics*, *28*(20), 2678-2679.

García-Almodóvar, R. C., Gosalvez, B., Aranda, M. A., & Burgos, L. (2017). Production of transgenic diploid Cucumis melo plants. *Plant Cell, Tissue and Organ Culture*, *130*(2), 323–333. https://doi.org/10.1007/s11240-017-1227-2

Garcia-Mas, J., Benjak, A., Sanseverino, W., Bourgeois, M., Mir, G., Gonźalez, V. M., Heńaff, E., Camĥara, F., Cozzuto, L., Lowy, E., Alioto, T., Capella-Gutieŕrez, S., Blancae, J., Cañizares, J., Ziarsolo, P., Gonzalez-Ibeas, D., Rodriǵuez-Moreno, L., Droege, M., Du, L., … Puigdomeǹech, P. (2012). The genome of melon (Cucumis melo L.). *Proceedings of the National Academy of Sciences of the United States of America*, *109*(29), 11872–11877. https://doi.org/10.1073/pnas.1205415109

Garcia-Ruiz, H. (2018). Susceptibility genes to plant viruses. *Viruses*, *10*(9). https://doi.org/10.3390/v10090484

Garcia-Ruiz, H. (2019). Host factors against plant viruses. *Molecular Plant Pathology*, *20*(11), 1588–1601. https://doi.org/10.1111/mpp.12851

Garciá, J. A., & Pallás, V. (2015). Viral factors involved in plant pathogenesis. *Current Opinion in Virology*, *11*, 21–30. https://doi.org/10.1016/j.coviro.2015.01.001

Gebert, M., Dresselhaus, T., & Sprunck, S. (2008). F-actin organization and pollen tube

tip growth in Arabidopsis are dependent on the gametophyte-specific armadillo repeat protein ARO1. *Plant Cell*, *20*(10), 2798–2814. https://doi.org/10.1105/tpc.108.061028

Gelvin, S. B. (2003). Agrobacterium-Mediated Plant Transformation: the Biology behind the "Gene-Jockeying" Tool. *Microbiology and Molecular Biology Reviews*, *67*(1), 16–37. https://doi.org/10.1128/mmbr.67.1.16-37.2003

German-Retana, S., Walter, J., Doublet, B., Roudet-Tavert, G., Nicaise, V., Lecampion, C., Houvenaghel, M.-C., Robaglia, C., Michon, T., & Le Gall, O. (2008). Mutational Analysis of Plant Cap-Binding Protein eIF4E Reveals Key Amino Acids Involved in Biochemical Functions and Potyvirus Infection. *Journal of Virology*, *82*(15), 7601–7612. https://doi.org/10.1128/jvi.00209-08

Ghosh, S., & Lasko, P. (2015). Loss-of-function analysis reveals distinct requirements of the translation initiation factors eIF4E, eIF4E-3, eIF4G and eIF4G2 in Drosophila spermatogenesis. *PLoS ONE*, *10*(4), 1–22. https://doi.org/10.1371/journal.pone.0122519

Gómez-Aix, C., Pascual, L., Cañizares, J., Sánchez-Pina, M. A., & Aranda, M. A. (2016). Transcriptomic profiling of Melon necrotic spot virus-infected melon plants revealed virus strain and plant cultivar-specific alterations. *BMC Genomics*, *17*(1), 1–17. https://doi.org/10.1186/s12864-016-2772-5

Gomez, M. A., Lin, Z. D., Moll, T., Chauhan, R. D., Hayden, L., Renninger, K., Beyene, G., Taylor, N. J., Carrington, J. C., Staskawicz, B. J., & Bart, R. S. (2019). Simultaneous CRISPR/Cas9-mediated editing of cassava eIF4E isoforms nCBP-1 and nCBP-2 reduces cassava brown streak disease symptom severity and incidence. *Plant Biotechnology Journal*, *17*(2), 421–434. https://doi.org/10.1111/pbi.12987

Gómez, P., Rodríguez-Hernández, A. M., Moury, B., & Aranda, M. (2009). Genetic resistance for the sustainable control of plant virus diseases: Breeding, mechanisms and durability. *European Journal of Plant Pathology*, *125*(1), 1–22. https://doi.org/10.1007/s10658-009-9468-5

Gonsalves, C., Xue Baodi, Yepes, M., Fuchs, M., Ling Kaishu, Namba, S., Chee, P., Slightom, J. L., & Gonsalves, D. (1994). Transferring cucumber mosaic virus-white leaf strain coat protein gene into Cucumis melo L. and evaluating transgenic plants for protection against infections. *Journal of the American Society for Horticultural Science*, *119*(2), 345–355. https://doi.org/10.21273/jashs.119.2.345

Gonzalez-Ibeas, D., Blanca, J., Roig, C., González-To, M., Picó, B., Truniger, V., Gómez, P., Deleu, W., Caño-Delgado, A., Arús, P., Nuez, F., Garcia-Mas, J., Puigdomènech, P., & Aranda, M. A. (2007). MELOGEN: An EST database for melon functional genomics. *BMC Genomics*, *8*, 1–17. https://doi.org/10.1186/1471-2164-8-306

Gonzalez-Ibeas, D., Cañizares, J., & Aranda, M. A. (2012). Microarray analysis shows that recessive resistance to Watermelon mosaic virus in melon is associated with the induction of defense response genes. *Molecular Plant-Microbe Interactions*, *25*(1), 107–118. https://doi.org/10.1094/MPMI-07-11-0193

Goodfellow, I. G., & Roberts, L. O. (2008). Eukaryotic initiation factor 4E. *International*

Journal of Biochemistry and Cell Biology, *40*(12), 2675–2680. https://doi.org/10.1016/j.biocel.2007.10.023

Guis, M., Amor, M. Ben, Latché, A., Pech, J. C., & Roustan, J. P. (2000). A reliable system for the transformation of cantaloupe charentais melon (Cucumis melo L. var. cantalupensis) leading to a majority of diploid regenerants. *Scientia Horticulturae*, *84*(1–2), 91–99. https://doi.org/10.1016/S0304-4238(99)00101-6

Guis, M., Roustan, J. P., Pech, J. C., Dogimont, C., & Pitrat, M. (1998). Melon Biotechnology. *Biotechnology and Genetic Engineering Reviews*, *15*(1), 289–312. https://doi.org/10.1080/02648725.1998.10647959

Guo, S., Sun, B., Looi, L. S., Xu, Y., Gan, E. S., Huang, J., & Ito, T. (2015). Co-ordination of flower development through epigenetic regulation in two model species: Rice and arabidopsis. *Plant and Cell Physiology*, *56*(5), 830–841. https://doi.org/10.1093/pcp/pcv037

Hämäläinen, J. H., Kekarainen, T., Gebhardt, C., Watanabe, K. N., & Valkonen, J. P. T. (2000). Recessive and dominant genes interfere with the vascular transport of Potato virus a in diploid potatoes. *Molecular Plant-Microbe Interactions*, *13*(4), 402–412. https://doi.org/10.1094/MPMI.2000.13.4.402

Hao, X., Fu, Y., Zhao, W., Liu, L., Bade, R., Hasi, A., & Hao, J. (2016). Genome-wide identification and analysis of the MADS-box gene family in melon. *Journal of the American Society for Horticultural Science*, *141*(5), 507–519. https://doi.org/10.21273/JASHS03727-16

Hao, Y. J., Wang, D. H., Peng, Y. Ben, Bai, S. L., Xu, L. Y., Li, Y. Q., Xu, Z. H., & Bai, S. N. (2003). DNA damage in the early primordial anther is closely correlated with stamen arrest in the female flower of cucumber (Cucumis sativus L.). *Planta*, *217*(6), 888–895. https://doi.org/10.1007/s00425-003-1064-x

Harrison, B. D. (2002). Virus variation in relation to resistance-breaking in plants. *Euphytica*, *124*(2), 181–192. https://doi.org/10.1023/A:1015630516425

Hashimoto, M., Neriya, Y., Yamaji, Y., & Namba, S. (2016). Recessive resistance to plant viruses: Potential resistance genes beyond translation initiation factors. *Frontiers in Microbiology*, *7*(OCT), 1–11. https://doi.org/10.3389/fmicb.2016.01695

Henderson, M. A., Croniand, E., Dunkelbarger, S., Contreras, V., Strome, S., & Keiper, B. D. (2009). A germline-specific isoform of eIF4E (IFE-1) is required for efficient translation of stored mRNAs and maturation of both oocytes and sperm. *Journal of Cell Science*, *122*(10), 1529–1539. https://doi.org/10.1242/jcs.046771

Hernández, G., Altmann, M., Sierra, J. M., Urlaub, H., Diez Del Corral, R., Schwartz, P., & Rivera-Pomar, R. (2005). Functional analysis of seven genes encoding eight translation initiation factor 4E (eIF4E) isoforms in Drosophila. *Mechanisms of Development*, *122*(4), 529–543. https://doi.org/10.1016/j.mod.2004.11.011

Hernández, G., Miron, M., Han, H., Liu, N., Magescas, J., Tettweiler, G., Frank, F., Siddiqui, N., Sonenberg, N., & Lasko, P. (2013). Mextli Is a Novel Eukaryotic Translation Initiation Factor 4E-Binding Protein That Promotes Translation in Drosophila

melanogaster. *Molecular and Cellular Biology*, *33*(15), 2854–2864. https://doi.org/10.1128/mcb.01354-12

Herrera-Estrella, L., De Block, M., Messens, E., Hernalsteens, J.-P., Van Montagu, M., & Schell, J. (1983). Chimeric genes as dominant selectable markers in plant cells. *The EMBO Journal*, *2*(6), 987–995. https://doi.org/10.1002/j.1460-2075.1983.tb01532.x

Ho, J. D., & Lee, S. (2016). A cap for every occasion: alternative eIF4F complexes. *Trends in biochemical sciences*, *41*(10), 821-823.

Hofius, D., Maier, A. T., Dietrich, C., Jungkunz, I., Börnke, F., Maiss, E., & Sonnewald, U. (2007). Capsid Protein-Mediated Recruitment of Host DnaJ-Like Proteins Is Required for Potato Virus Y Infection in Tobacco Plants . *Journal of Virology*, *81*(21), 11870–11880. https://doi.org/10.1128/jvi.01525-07

Honys, D., & Twell, D. (2003). Comparative analysis of the Arabidopsis pollen transcriptome. *Plant Physiology*, *132*(2), 640–652. https://doi.org/10.1104/pp.103.020925

Hu, B., Li, D., Liu, X., Qi, J., Gao, D., Zhao, S., ... & Yang, L. (2017). Engineering non-transgenic gynoecious cucumber using an improved transformation protocol and optimized CRISPR/Cas9 system. *Molecular plant*, *10*(12), 1575-1578.

Hu, L., & Liu, S. (2012). Genome-wide analysis of the MADS-box gene family in cucumber. *Genome*, *55*(3), 245–256. https://doi.org/10.1139/g2012-009

Hugdahl, J. D., Bokros, C. L., & Morejohn, L. C. (1995). End-to-end annealing of plant microtubules by the p86 subunit of eukaryotic initiation factor-(iso)4F. *Plant Cell*, *7*(12), 2129–2138. https://doi.org/10.2307/3870156

Hwang, J., Li, J., Liu, W. Y., An, S. J., Cho, H., Her, N. H., Yeam, I., Kim, D., & Kang, B. C. (2009). Double mutations in eIF4E and eIFiso4E confer recessive resistance to Chilli veinal mottle virus in pepper. *Molecules and Cells*, *27*(3), 329–336. https://doi.org/10.1007/s10059-009-0042-y

Igarashi, K., Kazama, T., & Toriyama, K. (2016). A gene encoding pentatricopeptide repeat protein partially restores fertility in RT98-Type cytoplasmic male-sterile rice. *Plant and Cell Physiology*, *57*(10), 2187–2193. https://doi.org/10.1093/pcp/pcw135

Ishibashi, K., & Ishikawa, M. (2013). The Resistance Protein Tm-1 Inhibits Formation of a Tomato Mosaic Virus Replication Protein-Host Membrane Protein Complex. *Journal of Virology*, *87*(14), 7933–7939. https://doi.org/10.1128/jvi.00743-13

Ishibashi, Kazuhiro, Mawatari, N., Miyashita, S., Kishino, H., Meshi, T., & Ishikawa, M. (2012). Coevolution and Hierarchical Interactions of Tomato mosaic virus and the Resistance Gene Tm-1. *PLoS Pathogens*, *8*(10). https://doi.org/10.1371/journal.ppat.1002975

Ishino, Y., Shinagawa, H., Makino, K., Amemura, M., & Nakatura, A. (1987). Nucleotide sequence of the iap gene, responsible for alkaline phosphatase isoenzyme conversion in Escherichia coli, and identification of the gene product. *Journal of*

Bacteriology, *169*(12), 5429–5433. https://doi.org/10.1128/jb.169.12.5429-5433.1987

James, C., & Krattiger, A. F. (1996). Global Review of the Field Testing and Commercialization of Transgenic Plants: 1986 to 1995 The First Decade of Crop Biotechnology. *ISAAA Briefs*, *1*, 1–31.

Jansen, R., Van Embden, J. D. A., Gaastra, W., & Schouls, L. M. (2002). Identification of genes that are associated with DNA repeats in prokaryotes. *Molecular Microbiology*, *43*(6), 1565–1575. https://doi.org/10.1046/j.1365-2958.2002.02839.x

Jenner, C. E., Nellist, C. F., Barker, G. C., & Walsh, J. A. (2010). Turnip mosaic virus (TuMV) is able to use alleles of both eIF4E and eIF(iso)4E from multiple loci of the diploid brassica rapa. *Molecular Plant-Microbe Interactions*, *23*(11), 1498–1505. https://doi.org/10.1094/MPMI-05-10-0104

Liu J, Nannas NJ, Fu FF, Shi J, Aspinwall B, Parrott WA, Dawe RK. Genome-Scale Sequence Disruption Following Biolistic Transformation in Rice and Maize. Plant Cell. 2019 Feb;31(2):368-383. doi: 10.1105/tpc.18.00613. Epub 2019 Jan 16. PMID: 30651345; PMCID: PMC6447018.

Jinek, M., Chylinski, K., Fonfara, I., Hauer, M., Doudna, J. A., & Charpentier, E. (2012). A programmable dual-RNA–guided DNA endonuclease in adaptive bacterial immunity. *science*, *337*(6096), 816-821.

Jones, R. A.C. (2014). Plant virus ecology and epidemiology: Historical perspectives, recent progress and future prospects. *Annals of Applied Biology*, *164*(3), 320–347. https://doi.org/10.1111/aab.12123

Jones, Roger A.C. (2009). Plant virus emergence and evolution: Origins, new encounter scenarios, factors driving emergence, effects of changing world conditions, and prospects for control. *Virus Research*, *141*(2), 113–130. https://doi.org/10.1016/j.virusres.2008.07.028

Jones, Roger A.C. (2018). Plant and Insect Viruses in Managed and Natural Environments: Novel and Neglected Transmission Pathways. In *Advances in Virus Research* (1st ed., Vol. 101). Elsevier Inc. https://doi.org/10.1016/bs.aivir.2018.02.006

Jones, Roger A.C., & Naidu, R. A. (2019). Global Dimensions of Plant Virus Diseases: Current Status and Future Perspectives. *Annual Review of Virology*, *6*, 387–409. https://doi.org/10.1146/annurev-virology-092818-015606

Juarez, M., Legua, P., Mengual, C. M., Kassem, M. A., Sempere, R. N., Gómez, P., Truniger, V., & Aranda, M. A. (2013). Relative incidence, spatial distribution and genetic diversity of cucurbit viruses in eastern Spain. *Annals of Applied Biology*, *162*(3), 362–370. https://doi.org/10.1111/aab.12029

Juárez, M., Rabádan, M. P., Martínez, L. D., Tayahi, M., Grande-Pérez, A., & Gómez, P. (2019). Natural hosts and genetic diversity of the emerging tomato leaf curl New Delhi virus in Spain. *Frontiers in Microbiology*, *10*(FEB).

https://doi.org/10.3389/fmicb.2019.00140

Julio, E., Cotucheau, J., Decorps, C., Volpatti, R., Sentenac, C., Candresse, T., & Dorlhac de Borne, F. (2015). A Eukaryotic Translation Initiation Factor 4E (eIF4E) is Responsible for the "va" Tobacco Recessive Resistance to Potyviruses. *Plant Molecular Biology Reporter*, *33*(3), 609–623. https://doi.org/10.1007/s11105-014-0775-4

Kaboli, S., & Babazada, H. (2018). Crispr-mediated genome engineering and its application in industry. *Current Issues in Molecular Biology*, *26*, 81–92. https://doi.org/10.21775/CIMB.026.081

Kang, B. C., Yeam, I., Frantz, J. D., Murphy, J. F., & Jahn, M. M. (2005). The pvr1 locus in Capsicum encodes a translation initiation factor eIF4E that interacts with Tobacco etch virus VPg. *Plant Journal*, *42*(3), 392–405. https://doi.org/10.1111/j.1365-313X.2005.02381.x

Kang, B. C., Yeam, I., Li, H., Perez, K. W., & Jahn, M. M. (2007). Ectopic expression of a recessive resistance gene generates dominant potyvirus resistance in plants. *Plant Biotechnology Journal*, *5*(4), 526–536. https://doi.org/10.1111/j.1467-7652.2007.00262.x

Kanyuka, K., Druka, A., Caldwell, D. G., Tymon, A., McCallum, N., Waugh, R., & Adams, M. J. (2005). Evidence that the recessive bymovirus resistance locus rym4 in barley corresponds to the eukaryotic translation initiation factor 4E gene. *Molecular Plant Pathology*, *6*(4), 449–458. https://doi.org/10.1111/j.1364-3703.2005.00294.x

Kapetanou, M., Athanasopoulou, S., & Gonos, E. S. (2022). Transcriptional regulatory networks of the proteasome in mammalian systems. *IUBMB Life*, *74*(1), 41–52. https://doi.org/10.1002/iub.2586

Karkute, S. G., Singh, A. K., Gupta, O. P., Singh, P. M., & Singh, B. (2017). CRISPR/Cas9 mediated genome engineering for improvement of horticultural crops. *Frontiers in Plant Science*, *8*(September), 1–6. https://doi.org/10.3389/fpls.2017.01635

Kassem, M. A., Sempere, R. N., Juárez, M., Aranda, M. A., & Truniger, V. (2007). Cucurbit aphid-borne yellows virus is prevalent in field-grown cucurbit crops of southeastern Spain. *Plant Disease*, *91*(3), 232–238. https://doi.org/10.1094/PDIS-91-3-0232

Kassem, Mona A., Juarez, M., Gómez, P., Mengual, C. M., Sempere, R. N., Plaza, M., Elena, S. F., Moreno, A., Fereres, A., & Aranda, M. A. (2013). Genetic diversity and potential vectors and reservoirs of Cucurbit aphid-borne yellows virus in southeastern Spain. *Phytopathology*, *103*(11), 1188–1197. https://doi.org/10.1094/PHYTO-11-12-0280-R

Kathal, R., Bhatnagar, S. P., & Bhojwani, S. S. (1992). Chromosome variations in the plants regenerated from leaf explants of Cucumis melo L.cv. 'Pusa sharbati'. *Caryologia*, *45*(1), 51–56. https://doi.org/10.1080/00087114.1992.10797210

Khan, R. M., Yu, P., Sun, L., Abbas, A., Shah, L., Xiang, X., ... & Cao, L. (2021). DCET1 Controls Male Sterility Through Callose Regulation, Exine Formation, and Tapetal Programmed Cell Death in Rice. *Frontiers in genetics*, *12*.

Kim H, Kim ST, Ryu J, Choi MK, Kweon J, Kang BC, Ahn HM, Bae S, Kim J, Kim JS, Kim SG. A simple, flexible and high-throughput cloning system for plant genome editing via CRISPR-Cas system. *J Integr Plant Biol.* 2016 Aug;58(8):705-12. doi: 10.1111/jipb.12474. Epub 2016 Apr 6. PMID: 26946469.

Kim, J., Kang, W. H., Hwang, J., Yang, H. B., Dosun, K., Oh, C. S., & Kang, B. C. (2014). Transgenic Brassica rapa plants over-expressing eIF(iso)4E variants show broad-spectrum Turnip mosaic virus (TuMV) resistance. *Molecular Plant Pathology*, *15*(6), 615–626. https://doi.org/10.1111/mpp.12120

Kintzios, S. E., & Taravira, N. (1997). Effect of genotype and light intensity on somatic embryogenesis and plant regeneration in melon (Cucumis melo L.). *Plant Breeding*, *116*(4), 359–362. https://doi.org/10.1111/j.1439-0523.1997.tb01012.x

Koncz, C., & Schell, J. (1986). The promoter of TL-DNA gene 5 controls the tissue-specific expression of chimaeric genes carried by a novel type of Agrobacterium binary vector. *Molecular and General Genetics MGG*, *204*(3), 383-396.

Koornneef, M., & Stam, P. (2001). Changing paradigms in plant breeding. *Plant Physiology*, *125*(1), 156–159. https://doi.org/10.1104/pp.125.1.156

Lecoq, H., & Desbiez, C. (2012). Viruses of Cucurbit Crops in the Mediterranean Region. An Ever-Changing Picture. In *Advances in Virus Research* (Vol. 84). https://doi.org/10.1016/B978-0-12-394314-9.00003-8

Lecoq, H., Desbiez, C., Wipf-Scheibel, C., & Girard, M. (2003). Potential involvement of melon fruit in the long distance dissemination of cucurbit potyviruses. *Plant Disease*, *87*(8), 955–959. https://doi.org/10.1094/PDIS.2003.87.8.955

Lee, S. K., Kim, H., Cho, J. Il, Nguyen, C. D., Moon, S., Park, J. E., Park, H. R., Huh, J. H., Jung, K. H., Guiderdoni, E., & Jeon, J. S. (2020). Deficiency of rice hexokinase HXK5 impairs synthesis and utilization of starch in pollen grains and causes male sterility. *Journal of Experimental Botany*, *71*(1), 116–125. https://doi.org/10.1093/jxb/erz436

Lei, Y., Lu, L., Liu, H. Y., Li, S., Xing, F., & Chen, L. L. (2014). CRISPR-P: A web tool for synthetic single-guide RNA design of CRISPR-system in plants. *Molecular Plant*, *7*(9), 1494–1496. https://doi.org/10.1093/mp/ssu044

Lellis, A. D., Kasschau, K. D., Whitham, S. A., & Carrington, J. C. (2002). Loss-of-susceptibility mutants of Arabidopsis thaliana reveal an essential role for eIF(iso)4E during potyvirus infection. *Current Biology*, *12*(12), 1046–1051. https://doi.org/10.1016/S0960-9822(02)00898-9

Léonard, S., Plante, D., Wittmann, S., Daigneault, N., Fortin, M. G., & Laliberté, J.-F. (2000). Complex Formation between Potyvirus VPg and Translation Eukaryotic Initiation Factor 4E Correlates with Virus Infectivity. *Journal of Virology*, *74*(17), 7730–7737. https://doi.org/10.1128/jvi.74.17.7730-7737.2000

Li, H., & Durbin, R. (2009). Fast and accurate short read alignment with Burrows-Wheeler transform. *Bioinformatics*, *25*(14), 1754–1760. https://doi.org/10.1093/bioinformatics/btp324

Li, H. J., Kim, Y. J., Yang, L., Liu, Z., Zhang, J., Shi, H., Huang, G., Persson, S., Zhang, D., & Liang, W. (2020). Grass-specific EPAD1 is essential for pollen exine patterning in rice. *Plant Cell*, *32*(12), 3961–3977. https://doi.org/10.1105/tpc.20.00551

Liang, G., Zhang, H., Lou, D., & Yu, D. (2016). Selection of highly efficient sgRNAs for CRISPR/Cas9-based plant genome editing. *Scientific Reports*, *6*. https://doi.org/10.1038/srep21451

Liang, X., Li, S. W., Gong, L. M., Li, S., & Zhang, Y. (2020). COPII components sar1b and sar1c play distinct yet interchangeable roles in pollen development. *Plant Physiology*, *183*(3), 974–985. https://doi.org/10.1104/pp.20.00159

Liu, H., Ding, Y., Zhou, Y., Jin, W., Xie, K., & Chen, L. L. (2017). CRISPR-P 2.0: An Improved CRISPR-Cas9 Tool for Genome Editing in Plants. *Molecular Plant*, *10*(3), 530–532. https://doi.org/10.1016/j.molp.2017.01.003

Liu, S., Gao, P., Zhu, Q., Zhu, Z., Liu, H., Wang, X., Weng, Y., Gao, M., & Luan, F. (2020). Resequencing of 297 melon accessions reveals the genomic history of improvement and loci related to fruit traits in melon. *Plant Biotechnology Journal*, *18*(12), 2545–2558. https://doi.org/10.1111/pbi.13434

Lobato-Gómez, M., Hewitt, S., Capell, T., Christou, P., Dhingra, A., & Girón-Calva, P. S. (2021). Transgenic and genome-edited fruits: background, constraints, benefits, and commercial opportunities. *Horticulture Research*, *8*(1). https://doi.org/10.1038/s41438-021-00601-3

Luis-Arteaga, M., Alvarez, J. M., Alonso-Prados, J. L., Bernal, J. J., García-Arenal, F., Laviña, A., Batlle, A., & Moriones, E. (1998). Occurrence, distribution, and relative incidence of mosaic viruses infecting field-grown melon in Spain. *Plant Disease*, *82*(9), 979–982. https://doi.org/10.1094/PDIS.1998.82.9.979

Luo, Y., Guo, Z., & Li, L. (2013). Evolutionary conservation of microRNA regulatory programs in plant flower development. *Developmental biology*, *380*(2), 133-144.

Ma, H. (2005). Molecular genetic analyses of microsporogenesis and microgametogenesis in flowering plants. *Annual Review of Plant Biology*, *56*, 393–434. https://doi.org/10.1146/annurev.arplant.55.031903.141717

Maher, M. F., Nasti, R. A., Vollbrecht, M., Starker, C. G., Clark, D., Voytas, D. F., Biology, M., & Biology, C. (2020). *HHS Public Access*. *38*(1), 84–89. https://doi.org/10.1038/s41587-019-0337-2.Plant

Maher, M. F., Nasti, R. A., Vollbrecht, M., Starker, C. G., Clark, M. D., & Voytas, D. F. (2020). of meristems. *Nature Biotechnology*, *38*(January). https://doi.org/10.1038/s41587-019-0337-2

Malmstrom, C. M., Melcher, U., & Bosque-Pérez, N. A. (2011). The expanding field of plant virus ecology: Historical foundations, knowledge gaps, and research directions. *Virus Research*, *159*(2), 84–94. https://doi.org/10.1016/j.virusres.2011.05.010

Marcotrigiano, J., Gingras, A. C., Sonenberg, N., & Burley, S. K. (1999). Cap-dependent translation initiation in eukaryotes is regulated by a molecular mimic of

eIF4G. *Molecular cell*, *3*(6), 707-716.

Martin, A., Troadec, C., Boualem, A., Rajab, M., Fernandez, R., Morin, H., Pitrat, M., Dogimont, C., & Bendahmane, A. (2009). A transposon-induced epigenetic change leads to sex determination in melon. *Nature*, *461*(7267), 1135–1138. https://doi.org/10.1038/nature08498

Martín-Hernández, A. M., & Picó, B. (2021). Natural resistances to viruses in cucurbits. *Agronomy*, *11*(1), 23.

Mascarell-Creus, A., Cañizares, J., Vilarrasa-Blasi, J., Mora-García, S., Blanca, J., Gonzalez-Ibeas, D., Saladié, M., Roig, C., Deleu, W., Picó-Silvent, B., López-Bigas, N., Aranda, M. A., Garcia-Mas, J., Nuez, F., Puigdomènech, P., & Caño-Delgado, A. I. (2009). An oligo-based microarray offers novel transcriptomic approaches for the analysis of pathogen resistance and fruit quality traits in melon (Cucumis melo L.). *BMC Genomics*, *10*, 467. https://doi.org/10.1186/1471-2164-10-467

Mayberry, L. K., Leah Allen, M., Dennis, M. D., & Browning, K. S. (2009). Evidence for variation in the optimal translation initiation complex: Plant eIF4B, eIF4F, and eIF(iso)4F differentially promote translation of mRNAs. *Plant Physiology*, *150*(4), 1844–1854. https://doi.org/10.1104/pp.109.138438

Mazier, M., Flamain, F., Nicolaï, M., Sarnette, V., & Caranta, C. (2011). Knock-down of both eIF4E1 and eIF4E2 genes confers broad-spectrum resistance against potyviruses in tomato. *PLoS ONE*, *6*(12). https://doi.org/10.1371/journal.pone.0029595

McCormick, S. (2004). Control of male gametophyte development. *Plant Cell*, *16*(SUPPL.), 142–153. https://doi.org/10.1105/tpc.016659

Menz, J., Modrzejewski, D., Hartung, F., Wilhelm, R., & Sprink, T. (2020). Genome Edited Crops Touch the Market: A View on the Global Development and Regulatory Environment. *Frontiers in Plant Science*, *11*(October), 1–17. https://doi.org/10.3389/fpls.2020.586027

Merrick, W. C. (2015). eIF4F : A Retrospective *. *Journal of Biological Chemistry*, *290*(40), 24091–24099. https://doi.org/10.1074/jbc.R115.675280

Minkenberg, B., Zhang, J., Xie, K., & Yang, Y. (2019). CRISPR-PLANT v2: an online resource for highly specific guide RNA spacers based on improved off-target analysis. *Plant Biotechnology Journal*, *17*(1), 5–8. https://doi.org/10.1111/pbi.13025

Minshall, N., Reiter, M. H., Weil, D., & Standart, N. (2007). CPEB interacts with an ovary-specific eIF4E and 4E-T in early Xenopus oocytes. *Journal of Biological Chemistry*, *282*(52), 37389–37401. https://doi.org/10.1074/jbc.M704629200

Miras, M., Sempere, R. N., Kraft, J. J., Miller, W. A., Aranda, M. A., & Truniger, V. (2014). Interfamilial recombination between viruses led to acquisition of a novel translation-enhancing RNA element that allows resistance breaking. *New Phytologist*, *202*(1), 233–246. https://doi.org/10.1111/nph.12650

Miras, M., Truniger, V., Silva, C., Verdaguer, N., Aranda, M. A., & Querol-Audí, J. (2017). Structure of eiF4E in complex with an eiF4G peptide supports a universal bipartite

binding mode for protein translation. *Plant Physiology*, *174*(3), 1476–1491. https://doi.org/10.1104/pp.17.00193

Mliki, A., Staub, J. E., Zhangyong, S., & Ghorbel, A. (2001). Genetic diversity in melon (Cucumis melo L.): An evaluation of African germplasm. *Genetic Resources and Crop Evolution*, *48*(6), 587–597. https://doi.org/10.1023/A:1013840517032

Mojica, F. J. M., Díez-Villaseñor, C., García-Martínez, J., & Soria, E. (2005). Intervening sequences of regularly spaced prokaryotic repeats derive from foreign genetic elements. *Journal of Molecular Evolution*, *60*(2), 174–182. https://doi.org/10.1007/s00239-004-0046-3

Morrison, J. K., Friday, A. J., Henderson, M. A., Hao, E., & Keiper, B. D. (2014). Induction of cap-independent BiP (hsp-3) and Bcl-2 (ced-9) translation in response to eIF4G (IFG-1) depletion in C. elegans . *Translation*, *2*(1), e28935. https://doi.org/10.4161/trla.28935

Moury, B., Charron, C., Janzac, B., Simon, V., Gallois, J. L., Palloix, A., & Caranta, C. (2014). Evolution of plant eukaryotic initiation factor 4E (eIF4E) and potyvirus genome-linked protein (VPg): A game of mirrors impacting resistance spectrum and durability. *Infection, Genetics and Evolution*, *27*, 472–480. https://doi.org/10.1016/j.meegid.2013.11.024

Moury, B., Janzac, B., Ruellan, Y., Simon, V., Ben Khalifa, M., Fakhfakh, H., Fabre, F., & Palloix, A. (2014). Interaction Patterns between Potato Virus Y and eIF4E-Mediated Recessive Resistance in the Solanaceae. *Journal of Virology*, *88*(17), 9799–9807. https://doi.org/10.1128/jvi.00930-14

Moury, Benoît, Morel, C., Johansen, E., Guilbaud, L., Souche, S., Ayme, V., Caranta, C., Palloix, A., & Jacquemond, M. (2004). Mutations in Potato virus Y genome-linked protein determine virulence toward recessive resistances in Capsicum annuum and Lycopersicon hirsutum. *Molecular Plant-Microbe Interactions*, *17*(3), 322–329. https://doi.org/10.1094/MPMI.2004.17.3.322

Murashige, T., & Skoog, F. (1962). A revised medium for rapid growth and bio assays with tobacco tissue cultures. *Physiologia plantarum*, *15*(3), 473-497.

Nag, A., King, S., & Jack, T. (2009). miR319a targeting of TCP4 is critical for petal growth and development in Arabidopsis. *Proceedings of the National Academy of Sciences*, *106*(52), 22534-22539.

Naudin, C. V. (1859). Essais d'une monographie des esp`eces et des vari´et´es du genre Cucumis. *Ann. Sci. Nat. Bot., S´er.*, *4*(11), 5–87.

Navas-Castillo, J., Lõpez-Moya, J. J., & Aranda, M. A. (2014). Whitefly-transmitted RNA viruses that affect intensive vegetable production. *Annals of Applied Biology*, *165*(2), 155–171. https://doi.org/10.1111/aab.12147

Nicaise, V. (2014). Crop immunity against viruses: Outcomes and future challenges. In *Frontiers in Plant Science* (Vol. 5, Issue NOV). Frontiers Research Foundation. https://doi.org/10.3389/fpls.2014.00660

Nicaise, V., Gallois, J. L., Chafiai, F., Allen, L. M., Schurdi-Levraud, V., Browning, K. S.,

Candresse, T., Caranta, C., Le Gall, O., & German-Retana, S. (2007). Coordinated and selective recruitment of eIF4E and eIF4G factors for potyvirus infection in Arabidopsis thaliana. *FEBS Letters*, *581*(5), 1041–1046. https://doi.org/10.1016/j.febslet.2007.02.007

Nieto, C., Morales, M., Orjeda, G., Clepet, C., Monfort, A., Sturbois, B., Puigdomènech, P., Pitrat, M., Caboche, M., Dogimont, C., Garcia-Mas, J., Aranda, M. A., & Bendahmane, A. (2006). An eIF4E allele confers resistance to an uncapped and non-polyadenylated RNA virus in melon. *Plant Journal*, *48*(3), 452–462. https://doi.org/10.1111/j.1365-313X.2006.02885.x

Nuñez-Palenius, H. G., Gomez-Lim, M., Ochoa-Alejo, N., Grumet, R., Lester, G., & Cantliffe, D. J. (2008). Melon fruits: Genetic diversity, physiology, and biotechnology features. *Critical Reviews in Biotechnology*, *28*(1), 13–55. https://doi.org/10.1080/07388550801891111

Oh, Y., Lee, B., Kim, H., & Kim, S. G. (2020). A multiplex guide RNA expression system and its efficacy for plant genome engineering. *Plant Methods*, 1–11. https://doi.org/10.1186/s13007-020-00580-x

Oliveros, J. C., Franch, M., Tabas-Madrid, D., San-León, D., Montoliu, L., Cubas, P., & Pazos, F. (2016). Breaking-Cas-interactive design of guide RNAs for CRISPR-Cas experiments for ENSEMBL genomes. *Nucleic Acids Research*, *44*(W1), W267–W271. https://doi.org/10.1093/nar/gkw407

Pagny, G., Paulstephenraj, P. S., Poque, S., Sicard, O., Cosson, P., Eyquard, J. P., Caballero, M., Chague, A., Gourdon, G., Negrel, L., Candresse, T., Mariette, S., & Decroocq, V. (2012). Family-based linkage and association mapping reveals novel genes affecting Plum pox virus infection in Arabidopsis thaliana. *New Phytologist*, *196*(3), 873–886. https://doi.org/10.1111/j.1469-8137.2012.04289.x

Pařenicová, L., De Folter, S., Kieffer, M., Horner, D. S., Favalli, C., Busscher, J., Cook, H. E., Ingram, R. M., Kater, M. M., Davies, B., Angenent, G. C., & Colombo, L. (2003). Molecular and phylogenetic analyses of the complete MADS-Box transcription factor family in Arabidopsis: New openings to the MADS world. *Plant Cell*, *15*(7), 1538–1551. https://doi.org/10.1105/tpc.011544

Parish, R. W., & Li, S. F. (2010). Death of a tapetum: A programme of developmental altruism. *Plant Science*, *178*(2), 73–89. https://doi.org/10.1016/j.plantsci.2009.11.001

Patrick, R. M., & Browning, K. S. (2012). The eIF4F and eIFiso4F complexes of plants: An evolutionary perspective. *Comparative and Functional Genomics*, *2012*. https://doi.org/10.1155/2012/287814

Patrick, R. M., Mayberry, L. K., Choy, G., Woodard, L. E., Liu, J. S., White, A., Mullen, R. A., Tanavin, T. M., Latz, C. A., & Browning, K. S. (2014). Two arabidopsis loci encode novel eukaryotic initiation factor 4E isoforms that are functionally distinct from the conserved plant eukaryotic initiation factor 4E. *Plant Physiology*, *164*(4), 1820–1830. https://doi.org/10.1104/pp.113.227785

Pawełkowicz, M. E., Skarzyńska, A., Pląder, W., & Przybecki, Z. (2019). Genetic and

molecular bases of cucumber (Cucumis sativus L.) sex determination. *Molecular breeding*, *39*(3), 1-27.

Pennisi, E. (2013). The CRISPR craze. *Science*, *341*(6148), 833–836. https://doi.org/10.1126/science.341.6148.833

Pourcel, C., Salvignol, G., & Vergnaud, G. (2005). CRISPR elements in Yersinia pestis acquire new repeats by preferential uptake of bacteriophage DNA, and provide additional tools for evolutionary studies. *Microbiology*, *151*(3), 653–663. https://doi.org/10.1099/mic.0.27437-0

Pozzi, E. A., Bruno, C., Luciani, C. E., Celli, M. G., Conci, V. C., & Perotto, M. C. (2020). Relative incidence of cucurbit viruses and relationship with bio-meteorological variables. *Australasian Plant Pathology*, *49*(2), 167–174. https://doi.org/10.1007/s13313-020-00687-8

Puchta, H. (2017). Applying CRISPR/Cas for genome engineering in plants: the best is yet to come. *Current Opinion in Plant Biology*, *36*, 1–8. https://doi.org/10.1016/j.pbi.2016.11.011

Pyott, D. E., Sheehan, E., & Molnar, A. (2016). Engineering of CRISPR/Cas9-mediated potyvirus resistance in transgene-free Arabidopsis plants. *Molecular Plant Pathology*, *17*(8), 1276–1288. https://doi.org/10.1111/mpp.12417

Radouane, N., Ezrari, S., Belabess, Z., Tahiri, A., Tahzima, R., Massart, S., Jijakli, H., Benjelloun, M., & Lahlali, R. (2021). Viruses of cucurbit crops: current status in the Mediterranean Region. *Phytopathologia Mediterranea*, *60*(3), 493–519. https://doi.org/10.36253/phyto-12340

Ren, Y., Bang, H., Gould, J., Rathore, K. S., Patil, B. S., & Crosby, K. M. (2013). Shoot regeneration and ploidy variation in tissue culture of honeydew melon (Cucumis melo L. inodorus). *In Vitro Cellular and Developmental Biology - Plant*, *49*(2), 223–229. https://doi.org/10.1007/s11627-012-9482-8

Revers, F., Guiraud, T., Houvenaghel, M. C., Mauduit, T., Le Gall, O., & Candresse, T. (2003). Multiple resistance phenotypes to Lettuce mosaic virus among Arabidopsis thaliana accessions. *Molecular Plant-Microbe Interactions*, *16*(7), 608–616. https://doi.org/10.1094/MPMI.2003.16.7.608

Revers, F., & Nicaise, V. (2014). Plant resistance to infection by viruses. *eLS*.

Robaglia, C., & Caranta, C. (2006). Translation initiation factors: A weak link in plant RNA virus infection. *Trends in Plant Science*, *11*(1), 40–45. https://doi.org/10.1016/j.tplants.2005.11.004

Rodriguez-Granados, N. Y., Ramirez-Prado, J. S., Brik-Chaouche, R., An, J., Manza-Mianza, D., Sircar, S., Troadec, C., Hanique, M., Soulard, C., Costa, R., Dogimont, C., Latrasse, D., Raynaud, C., Boualem, A., Benhamed, M., & Bendahmane, A. (2021). CmLHP1 proteins play a key role in plant development and sex determination in melon (Cucumis melo). *Plant Journal*, 1–16. https://doi.org/10.1111/tpj.15627

Rodríguez-Hernández, A. M., Gosalvez, B., Sempere, R. N., Burgos, L., Aranda, M. A., & Truniger, V. (2012). Melon RNA interference (RNAi) lines silenced for Cm-eIF4E

show broad virus resistance. *Molecular Plant Pathology*, *13*(7), 755–763. https://doi.org/10.1111/j.1364-3703.2012.00785.x

Rodriguez, C. M., Freire, M. A., Camilleri, C., & Robaglia, C. (1998). The Arabidopsis thaliana cDNAs coding for eIF4E and eIF(iso)4E are not functionally equivalent for yeast complementation and are differentially expressed during plant development. *Plant Journal*, *13*(4), 465–473. https://doi.org/10.1046/j.1365-313X.1998.00047.x

Roy, B., & Arnim, A. G. von. (2013). Translational Regulation of Cytoplasmic mRNAs. *The Arabidopsis Book*, *11*(1), e0165. https://doi.org/10.1199/tab.0165

Rubio, M., Nicolaï, M., Caranta, C., & Palloix, A. (2009). Allele mining in the pepper gene pool provided new complementation effects between pvr2-eIF4E and pvr6-eIF(iso)4E alleles for resistance to pepper veinal mottle virus. *Journal of General Virology*, *90*(11), 2808–2814. https://doi.org/10.1099/vir.0.013151-0

Ruffel, S., Gallois, J. L., Moury, B., Robaglia, C., Palloix, A., & Caranta, C. (2006). Simultaneous mutations in translation initiation factors eIF4E and eIF(iso)4E are required to prevent pepper veinal mottle virus infection of pepper. *Journal of General Virology*, *87*(7), 2089–2098. https://doi.org/10.1099/vir.0.81817-0

Ruggieri, V., Alexiou, K. G., Morata, J., Argyris, J., Pujol, M., Yano, R., Nonaka, S., Ezura, H., Latrasse, D., Boualem, A., Benhamed, M., Bendahmane, A., Cigliano, R. A., Sanseverino, W., Puigdomènech, P., Casacuberta, J. M., & Garcia-Mas, J. (2018). An improved assembly and annotation of the melon (Cucumis melo L.) reference genome. *Scientific Reports*, *8*(1), 0–9. https://doi.org/10.1038/s41598-018-26416-2

Sáez, C., Flores-León, A., Montero-Pau, J., Sifres, A., Dhillon, N. P. S., López, C., & Picó, B. (2022). RNA-Seq Transcriptome Analysis Provides Candidate Genes for Resistance to Tomato Leaf Curl New Delhi Virus in Melon. *Frontiers in Plant Science*, *12*(January). https://doi.org/10.3389/fpls.2021.798858

Sagi, D., & Kim, S. K. (2012). An engineering approach to extending lifespan in C. elegans. *PLoS Genetics*, *8*(6). https://doi.org/10.1371/journal.pgen.1002780

Sanfaçon, H. (2015). Plant translation factors and virus resistance. *Viruses*, *7*(7), 3392–3419. https://doi.org/10.3390/v7072778

Sato, M., Nakahara, K., Yoshii, M., Ishikawa, M., & Uyeda, I. (2005). Selective involvement of members of the eukaryotic initiation factor 4E family in the infection of Arabidopsis thaliana by potyviruses. *FEBS Letters*, *579*(5), 1167–1171. https://doi.org/10.1016/j.febslet.2004.12.086

Schaad, M. C., Anderberg, R. J., & Carrington, J. C. (2000). Strain-specific interaction of the tobacco etch virus Nla protein with the translation initiation factor eIF4E in the yeast two-hybrid system. *Virology*, *273*(2), 300–306. https://doi.org/10.1006/viro.2000.0416

Serrano, C., González-Cruz, J., Jauregui, F., Medina, C., Mancilla, P., Matus, J. T., & Arce-Johnson, P. (2008). Genetic and histological studies on the delayed systemic movement of Tobacco Mosaic Virus in Arabidopsis thaliana. *BMC Genetics*, *9*, 1–11.

https://doi.org/10.1186/1471-2156-9-59

Song, J., Li, Z., Liu, Z., Guo, Y., & Qiu, L. J. (2017). Next-generation sequencing from bulked-segregant analysis accelerates the simultaneous identification of two qualitative genes in soybean. *Frontiers in Plant Science*, *8*(May), 1–11. https://doi.org/10.3389/fpls.2017.00919

Sorel, M., Garcia, J. A., & German-Retana, S. (2014). The potyviridae cylindrical inclusion helicase: A key multipartner and multifunctional protein. *Molecular Plant-Microbe Interactions*, *27*(3), 215–226. https://doi.org/10.1094/MPMI-11-13-0333-CR

Sorel, M., Svanella-Dumas, L., Candresse, T., Acelin, G., Pitarch, A., Houvenaghel, M. C., & German-Retana, S. (2014). Key mutations in the cylindrical inclusion involved in lettuce mosaic virus adaptation to eIF4E-mediated resistance in lettuce. *Molecular Plant-Microbe Interactions*, *27*(9), 1014–1024. https://doi.org/10.1094/MPMI-04-14-0111-R

Stein, N., Perovic, D., Kumlehn, J., Pellio, B., Stracke, S., Streng, S., Ordon, F., & Graner, A. (2005). The eukaryotic translation initiation factor 4E confers multiallelic recessive Bymovirus resistance in Hordeum vulgare (L.). *Plant Journal*, *42*(6), 912–922. https://doi.org/10.1111/j.1365-313X.2005.02424.x

Strange, R. N., & Scott, P. R. (2005). Plant disease: A threat to global food security. *Annual Review of Phytopathology*, *43*(Figure 1), 83–116. https://doi.org/10.1146/annurev.phyto.43.113004.133839

Straschil, U., Talman, A. M., Ferguson, D. J. P., Bunting, K. A., Xu, Z., Bailes, E., Sinden, R. E., Holder, A. A., Smith, E. F., Coates, J. C., & Tewari, R. (2010). The armadillo repeat protein PF16 is essential for flagellar structure and function in Plasmodium male gametes. *PLoS ONE*, *5*(9). https://doi.org/10.1371/journal.pone.0012901

Sun, L., Xiang, X., Yang, Z., Yu, P., Wen, X., Wang, H., Abbas, A., Khan, R. M., Zhang, Y., Cheng, S., & Cao, L. (2018). OsGPAT3 plays a critical role in anther wall programmed cell death and pollen development in rice. *International Journal of Molecular Sciences*, *19*(12). https://doi.org/10.3390/ijms19124017

Takakura, Y., Udagawa, H., Shinjo, A., & Koga, K. (2018). Mutation of a Nicotiana tabacum L. eukaryotic translation-initiation factor gene reduces susceptibility to a resistance-breaking strain of Potato virus Y. *Molecular Plant Pathology*, *19*(9), 2124–2133. https://doi.org/10.1111/mpp.12686

Tavert-Roudet, G., Abdul-Razzak, A., Doublet, B., Walter, J., Delaunay, T., German-Retana, S., Michon, T., le Gall, O., & Candresse, T. (2012). The C terminus of lettuce mosaic potyvirus cylindrical inclusion helicase interacts with the viral VPg and with lettuce translation eukaryotic initiation factor 4E. *Journal of General Virology*, *93*(1), 184–193. https://doi.org/10.1099/vir.0.035881-0

Taylor, P. E., Glover, J. A., Lavithis, M., Craig, S., Singh, M. B., Knox, R. B., Dennis, E. S., & Chaudhury, A. M. (1998). *Genetic control of male fertility in Arabidopsis thaliana : structural analyses of postmeiotic developmental mutants*. *61*, 492–505.

Thiémélé, D., Boisnard, A., Ndjiondjop, M. N., Chéron, S., Séré, Y., Aké, S., Ghesquière,

A., & Albar, L. (2010). Identification of a second major resistance gene to Rice yellow mottle virus, RYMV2, in the African cultivated rice species, O. glaberrima. *Theoretical and Applied Genetics*, *121*(1), 169–179. https://doi.org/10.1007/s00122-010-1300-2

Truniger, V., & Aranda, M. A. (2009). Recessive resistance to plant viruses. In *Advances in virus research* (Vol. 75, Issue 09). Elsevier. https://doi.org/10.1016/s0065-3527(09)07504-6

Truniger, Verónica, Nieto, C., González-Ibeas, D., & Aranda, M. (2008). Mechanism of plant eIF4E-mediated resistance against a Carmovirus (Tombusviridae): Cap-independent translation of a viral RNA controlled in cis by an (a)virulence determinant. *Plant Journal*, *56*(5), 716–727. https://doi.org/10.1111/j.1365-313X.2008.03630.x

Vallés, M. P., & Lasa, J. M. (1994). Agrobacterium-mediated transformation of commercial melon (Cucumis melo L., cv. Amarillo Oro). *Plant Cell Reports*, *13*(3–4), 145–148. https://doi.org/10.1007/BF00239881

van Eck, J. (2020). Applying gene editing to tailor precise genetic modifications in plants. *Journal of Biological Chemistry*, *295*(38), 13267–13276. https://doi.org/10.1074/jbc.REV120.010850

Vasil, I. K. (2003). The science and politics of plant biotechnology - A personal perspective. *Nature Biotechnology*, *21*(8), 849–851. https://doi.org/10.1038/nbt0803-849

Vejlupkova, Z., Warman, C., Sharma, R., Scheller, H. V., Mortimer, J. C., & Fowler, J. E. (2020). No evidence for transient transformation via pollen magnetofection in several monocot species. *Nature Plants*, *6*(November). https://doi.org/10.1038/s41477-020-00798-6

Villalba-Bermell, P., Marquez-Molins, J., Marques, M. C., Hernandez-Azurdia, A. G., Corell-Sierra, J., Picó, B., ... & Gomez, G. G. (2021). Exploring the miRNA-mediated response to combined stresses in melon plants. *bioRxiv*.

Wang, A., & Krishnaswamy, S. (2012). Eukaryotic translation initiation factor 4E-mediated recessive resistance to plant viruses and its utility in crop improvement. *Molecular Plant Pathology*, *13*(7), 795–803. https://doi.org/10.1111/j.1364-3703.2012.00791.x

Wang, H., Lu, Y., Jiang, T., Berg, H., Li, C., & Xia, Y. (2013). The Arabidopsis U-box/ARM repeat E3 ligase AtPUB4 influences growth and degeneration of tapetal cells, and its mutation leads to conditional male sterility. *Plant Journal*, *74*(3), 511–523. https://doi.org/10.1111/tpj.12146

Wang, R. Y. L., & Nagy, P. D. (2008). Tomato bushy stunt virus Co-Opts the RNA-Binding Function of a Host Metabolic Enzyme for Viral Genomic RNA Synthesis. *Cell Host and Microbe*, *3*(3), 178–187. https://doi.org/10.1016/j.chom.2008.02.005

Wang, T., Zhang, H., & Zhu, H. (2019). CRISPR technology is revolutionizing the improvement of tomato and other fruit crops. *Horticulture Research*, *6*(1).

https://doi.org/10.1038/s41438-019-0159-x

Wang, X., Kohalmi, S. E., Svircev, A., Wang, A., Sanfaçon, H., & Tian, L. (2013). Silencing of the Host Factor eIF(iso)4E Gene Confers Plum Pox Virus Resistance in Plum. *PLoS ONE*, *8*(1). https://doi.org/10.1371/journal.pone.0050627

Wilson, Z. A., & Zhang, D. B. (2009). From arabidopsis to rice: Pathways in pollen development. *Journal of Experimental Botany*, *60*(5), 1479–1492. https://doi.org/10.1093/jxb/erp095

Wu, X., Valli, A., García, J. A., Zhou, X., & Cheng, X. (2019). The Tug-of-War between plants and viruses: Great progress and many remaining questions. *Viruses*, *11*(3), 1–25. https://doi.org/10.3390/v11030203

Xu, D., Qu, S., Tucker, M. R., Zhang, D., Liang, W., & Shi, J. (2019). *Ostkpr1 functions in anther cuticle development and pollen wall formation in rice*. 1–13.

Yadav, R. C., Saleh, M. T., & Grumet, R. (1996). High frequency shoot regeneration from leaf explants of muskmelon. *Plant Cell, Tissue and Organ Culture*, *45*(3), 207–214. https://doi.org/10.1007/BF00043632

Yamasaki, S., Fujii, N., & Takahashi, H. (2003). Characterization of ethylene effects on sex determination in cucumber plants. *Sexual Plant Reproduction*, *16*(3), 103–111. https://doi.org/10.1007/s00497-003-0183-7

Yano, R., Ariizumi, T., Nonaka, S., Kawazu, Y., Zhong, S., Mueller, L., Giovannoni, J. J., Rose, J. K. C., & Ezura, H. (2020). Comparative genomics of muskmelon reveals a potential role for retrotransposons in the modification of gene expression. *Communications Biology*, *3*(1), 1–13. https://doi.org/10.1038/s42003-020-01172-0

Yin, K., Gao, C., & Qiu, J. L. (2017). Progress and prospects in plant genome editing. *Nature Plants*, *3*(July). https://doi.org/10.1038/nplants.2017.107

Yoshii, M., Nishikiori, M., Tomita, K., Yoshioka, N., Kozuka, R., Naito, S., & Ishikawa, M. (2004). The Arabidopsis Cucumovirus Multiplication 1 and 2 Loci Encode Translation Initiation Factors 4E and 4G . *Journal of Virology*, *78*(12), 6102–6111. https://doi.org/10.1128/jvi.78.12.6102-6111.2004

Zhang, D., Zhang, Z., Unver, T., & Zhang, B. (2021). CRISPR/Cas: A powerful tool for gene function study and crop improvement. *Journal of Advanced Research*, *29*, 207–221. https://doi.org/10.1016/j.jare.2020.10.003

Zhang, Hong, Li, X., Yu, H., Zhang, Y., Li, M., Wang, H., Wang, D., Wang, H., Fu, Q., Liu, M., Ji, C., Ma, L., Tang, J., Li, S., Miao, J., Zheng, H., & Yi, H. (2019). A High-Quality Melon Genome Assembly Provides Insights into Genetic Basis of Fruit Trait Improvement. *IScience*, *22*, 16–27. https://doi.org/10.1016/j.isci.2019.10.049

Zhang, Huimin, Li, S., Yang, L., Cai, G., Chen, H., Gao, D., Lin, T., Cui, Q., Wang, D., Li, Z., Cai, R., Bai, S., Lucas, W. J., Huang, S., Zhang, Z., & Sun, J. (2021). Gain-of-function of the 1-aminocyclopropane-1-carboxylate synthase gene ACS1G induces female flower development in cucumber gynoecy. *Plant Cell*, *33*(2), 306–321. https://doi.org/10.1093/PLCELL/KOAA018

Zhang, R., Chang, J., Li, J., Lan, G., Xuan, C., Li, H., ... & Wei, C. (2021). Disruption of the bHLH transcription factor Abnormal Tapetum 1 causes male sterility in watermelon. *Horticulture research*, *8*.

Zhao, X., Meng, Z., Wang, Y., Chen, W., Sun, C., Cui, B., Cui, J., Yu, M., Zeng, Z., Guo, S., Luo, D., Cheng, J. Q., Zhang, R., & Cui, H. (2017). with magnetic nanoparticles as gene carriers. *Nature Plants*, *3*(December). https://doi.org/10.1038/s41477-017-0063-z

Zhu, E., You, C., Wang, S., Cui, J., Niu, B., Wang, Y., Qi, J., Ma, H., & Chang, F. (2015). The DYT1-interacting proteins bHLH010, bHLH089 and bHLH091 are redundantly required for Arabidopsis anther development and transcriptome. *Plant Journal*, *83*(6), 976–990. https://doi.org/10.1111/tpj.12942

Zhu, J., Lou, Y., Xu, X., & Yang, Z. N. (2011). A genetic pathway for tapetum development and function in Arabidopsis. *Journal of Integrative Plant Biology*, *53*(11), 892–900. https://doi.org/10.1111/j.1744-7909.2011.01078.x

Zuker, M. (2003). Mfold web server for nucleic acid folding and hybridization prediction. *Nucleic Acids Research*, *31*(13), 3406–3415. https://doi.org/10.1093/nar/gkg595

8 Annexes

8.1 Annex 1

Table 8.1. Summary of sequencing and mapping results along flower developmental episodes

		Raw data	Filtering by quality*		Mapping aginst melon genome (v3.6.1)				Mappging aginst mRNAs (v4.0)	
		Total	Total	%	Coverage mean	Mapping QC mean	Mapping reads	%	Assigned mapped	%
FS	Replicate 1	72.034.596	72.034.486	100,00	21,49	54,00	43.879.532	60,91	25.628.131	58,41
	Replicate 2	69.030.098	69.022.776	99,99	20,69	54,19	41.015.274	59,42	22.608.913	55,12
	Replicate 3	75.518.218	75.515.464	100,00	23,00	54,13	45.391.008	60,11	25.800.002	56,84
GI-M	Replicate 1	81.157.866	81.149.016	99,99	25,10	54,39	48.687.914	60,00	28.476.342	58,49
	Replicate 2	80.585.452	80.580.908	99,99	24,60	54,47	49.482.342	61,41	31.262.697	63,18
	Replicate 3	75.345.722	75.342.116	100,00	22,95	54,27	46.324.318	61,49	28.587.197	61,71
GM-M	Replicate 1	69.141.598	69.136.900	99,99	21,36	54,35	42.701.006	61,76	27.384.603	64,13
	Replicate 2	75.119.432	75.115.866	100,00	23,01	53,96	44.635.742	59,42	24.983.712	55,97
	Replicate 3	67.903.570	67.896.826	99,99	20,66	54,04	41.280.099	60,80	24.301.381	58,87
AN-M	Replicate 1	85.883.350	85.879.198	100,00	26,19	54,49	53.306.401	62,07	33.408.796	62,67
	Replicate 2	75.730.306	75.728.038	100,00	23,31	54,69	47.448.789	62,66	31.337.531	66,04
	Replicate 3	74.368.674	74.364.146	99,99	22,97	54,71	46.922.279	63,10	31.712.915	67,59
GI-H	Replicate 1	77.548.692	77.546.080	100,00	24,01	55,63	53.393.857	68,85	41.817.895	78,32
	Replicate 2	76.690.030	76.688.520	100,00	23,77	55,29	52.676.472	68,69	39.553.689	75,09
	Replicate 3	73.276.224	73.274.582	100,00	22,54	55,38	49.467.419	67,51	37.243.176	75,29
GM-H	Replicate 1	80.046.740	80.041.736	99,99	24,03	54,48	50.648.897	63,28	31.570.421	62,33
	Replicate 2	66.200.246	66.200.154	100,00	20,23	54,32	40.508.989	61,19	24.596.618	60,72
	Replicate 3	85.830.840	85.824.628	99,99	26,31	54,25	51.968.427	60,55	30.411.626	58,52
AN-H	Replicate 1	70.388.654	70.386.450	100,00	21,57	54,35	43.093.847	61,22	25.578.442	59,36
	Replicate 2	72.570.416	72.568.248	100,00	21,95	54,43	46.421.245	63,97	29.988.336	64,60
	Replicate 3	79.342.038	79.340.110	100,00	23,80	54,40	49.650.855	62,58	30.075.696	60,57

* Reads were filtered out by quality (>30) and by length (>70).

8.2 Annex 2

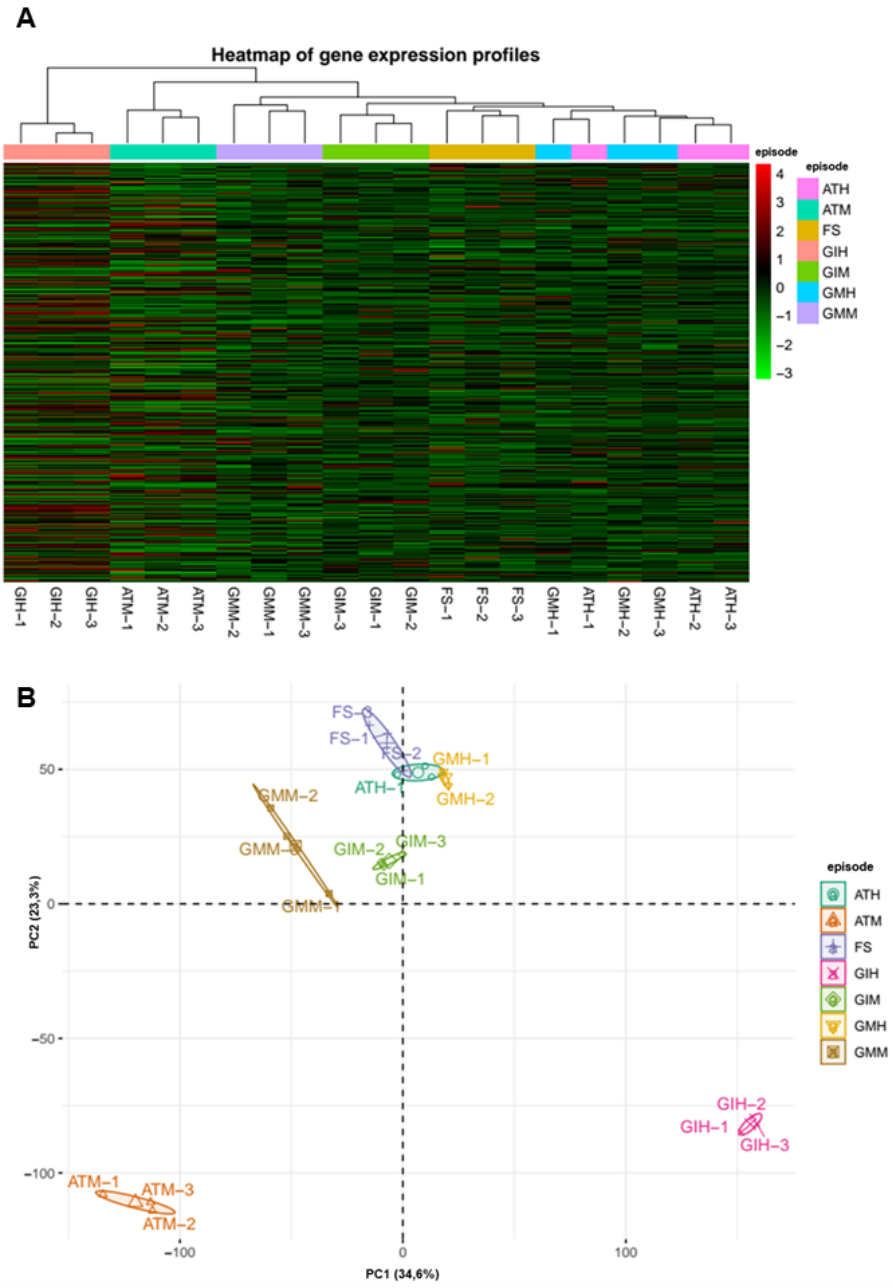

Figure 8.1. Clustered heatmap of gene expression profiles between biological replicates and among different developmental episodes (A) and Principal Component Analysis (PCA) scores plotted for male and hermaphrodite floral development episodes (B).

8.3 Annex 3

Table 8.2. FPKM values of MADS-box genes expressed* in male and hermaphrodite episodes

Gene ID	Gene	Subfamily	FS	GI-M	GM-M	AN-M	GI-H	GM-H	AN-H
MELO3C002691.2	CmMADS01	AG	NA	NA	NA	NA	4,040380969	-0,216573792	-0,711068003
MELO3C007181.2	CmMADS03	AG	-0,240103278	1,618414752	1,175757225	0,433118607	3,754269003	1,485346964	1,071419127
MELO3C033521.2	CmMADS05	AG	NA	NA	NA	NA	3,665409586	-0,057317884	-0,2424438
MELO3C022516.2	CmMADS07	AGL6	1,032947024	1,774418026	1,614031094	0,890992664	3,428061287	0,867788663	-0,235222837
MELO3C002050.2	CmMADS14	AP1/FUL	0,817508911	1,44627719	NA	1,242036485	4,070157304	0,392892228	0,132113213
MELO3C011409.2	CmMADS15	AP1/FUL	-1,860174309	-3,553892604	-1,804423501	-3,516382898	0,127513552	NA	-4,686645572
MELO3C003778.2	CmMADS16	AP3/PI	0,895202431	1,096993706	2,298018674	1,695981243	2,850584767	0,231704167	-0,256562674
MELO3C010515.2	CmMADS17	AP3/PI	-0,183994648	-0,478359885	1,443616689	0,819803485	3,414014835	-1,368695324	-1,211989183
MELO3C005393.2	CmMADS21	SCO1	-2,625966141	-3,665986935	NA	NA	2,236442817	NA	-2,796517052
MELO3C006159.2	CmMADS22	SCO1	-1,023385523	-1,717056028	-1,943497668	NA	0,547333457	-1,930568852	-1,629147027
MELO3C002049.2	CmMADS24	SEP	-1,518314479	-0,309471388	-1,149025112	0,773550605	0,695533945	-3,078954407	-3,203490215
MELO3C022316.2	CmMADS25	SEP	-0,276577698	1,896976011	2,306816441	3,146754869	3,585669202	1,14178739	1,542616971
MELO3C026300.2	CmMADS27	SEP	0,49114734	0,895000079	1,045522934	1,892772846	3,693664816	0,988532226	0,464997249
MELO3C007716.2	CmMADS29	SVP	1,026960754	-0,384024475	-2,26367411	-2,230495395	1,37053246	-1,052971121	-1,774660164
MELO3C011093.2	CmMADS31	SVP	-0,403185531	-2,106052179	NA	NA	0,664532073	-1,317992759	-0,379430839
MELO3C018601.2	CmMADS36	SVP	-2,475385074	-3,493886422	-4,33678278	-5,959899598	1,090977851	-3,022485269	-4,344490611
MELO3C003801.2	CmMADS38	Malpha	NA	-0,401433032	0,269468699	NA	-1,084409832	-0,669309925	0,452564824
MELO3C018030.2	CmMADS40	Malpha	NA	NA	NA	4,91490159	-3,264532327	NA	NA
MELO3C000260.2	CmMADS47	Mdelta	NA	1,570767355	2,326227808	1,870252817	4,98664017	NA	0,779308153
MELO3C001111.2	CmMADS48	Mdelta	1,08371579	1,825164043	0,944051427	0,452786482	2,570468098	NA	0,477986558
MELO3C001991.2	CmMADS49	Mdelta	0,996177367	-0,172790667	0,855592121	1,045630423	1,048117536	1,154265616	0,751468485
MELO3C007017.2	CmMADS53	Mdelta	NA	NA	NA	0,364778161	-4,385065031	NA	NA
MELO3C011410.2	CmMADS55	Mdelta	NA	-2,544020937	-0,482870532	NA	0,641017944	-3,701991922	NA
MELO3C022515.2	CmMADS59	Mdelta	-3,253789957	-2,843660826	NA	-2,045610427	0,100669682	NA	-3,375035616
MELO3C026299.2	CmMADS60	Mdelta	-0,906824134	-1,149204618	-1,573751598	NA	0,905839783	-2,509588835	-2,404841191
MELO3C002369.2	CmMADS63	Unclassified	-1,510571536	-0,724872935	-0,377964544	-2,806338868	1,553579653	NA	-3,392572263
MELO3C006940.2	CmMADS64	Unclassified	2,243296985	3,166450712	2,643333719	3,75515759	3,652199433	2,412697058	2,038874536
MELO3C011103.2	CmMADS65	Unclassified	1,346949651	1,987410176	1,422183259	1,864445466	2,689589227	2,223308005	1,437058974
MELO3C019694.2	CmMADS66	Unclassified	NA	-0,980920003	0,890043342	-0,359206903	3,79472488	1,100465595	-1,215579904
MELO3C022991.2	CmMADS83	Unclassified	4,849218267	5,125579425	1,645488389	NA	8,437782246	2,018259775	3,533355655

* Expressed genes were considered those among the DEGs obtained in all comparisons with FPKM>1 in the mean of the three replicates in at least one episode.

8.4 Annex 4

Table 8.3. FPKM values of selected episode-specific genes during male flower development

Gene ID	FS	GI-M	GM-M	AN-M	Gene Description
MELO3C011413.2	13,7766978	3,453838928	4,655056045	0,401448326	cytochrome P450 78A5
MELO3C019506.2	104,5681854	51,63797006	44,74173594	11,28385976	ethylene-responsive transcription factor ERF109
MELO3C026157.2	10,78621846	1,203795134	0,804380021	0,45416766	floricaula/leafy homolog
MELO3C024739.2	10,72957907	3,924773955	3,590233907	0,744360454	growth-regulating factor 4-like
MELO3C015838.2	7,101000128	2,536847681	0,943682748	2,082937247	Protein FANTASTIC FOUR 2
MELO3C019777.2	1,80300477	0,845923314	0,183921252	0,40734833	U4/U6 small nuclear ribonucleoprotein PRP4-like protein
MELO3C006252.2	6,179877168	27,90471908	8,186365273	1,003025237	protein ECERIFERUM 1-like
MELO3C012407.2	2,088554643	8,243175364	2,359490024	2,388657938	SKP1-like protein 12
MELO3C009739.2	0,503099456	5,334507008	1,547928484	1,967681753	WAT1-related protein
MELO3C012108.2	90,91088087	76,77143215	257,3770268	113,2918676	Expansin
MELO3C018743.2	5,742955518	8,158909848	30,75505643	2,944726628	expansin-B3-like
MELO3C015098.2	31,83244947	20,51358246	124,682665	20,06309394	Tubulin beta chain
MELO3C003616.2	8,564933865	7,385042736	22,14377408	7,532655953	xyloglucan glycosyltransferase 4
MELO3C017159.2	1,305450797	2,982086082	2,59812623	6,63969535	ABC transporter A family member 2
MELO3C008741.2	0,306293392	1,145402247	0,600962776	5,923972502	ABC transporter B family protein
MELO3C006969.2	6,438822909	8,961514265	4,672992716	69,58690831	ABC transporter C family member 10
MELO3C018990.2	1,502130746	2,436078463	2,846530477	9,92423296	ABC transporter D family member 1
MELO3C022421.2	4,237185024	5,996160558	8,19066748	17,262661	ABC transporter F family-like protein
MELO3C024080.2	1,663501502	2,172338769	1,862629777	11,56635396	ABC transporter family protein
MELO3C009480.2	1,256153051	0,790095678	1,282433902	3,320633251	ABC transporter family protein
MELO3C004931.2	0,030987201	0,009227461	0,146369087	3,750036285	ABC transporter G family member 28
MELO3C011435.2	0,874664531	0,839792447	2,204440546	16,11702504	ABC transporter G family member 29-like
MELO3C024523.2	0,210039845	0,181816133	0,147964499	1,787180163	ABC transporter G family member 39-like
MELO3C014214.2	0,78579797	0,526929175	0,618133709	2,589690067	ABC transporter G family-like protein
MELO3C021130.2	5,703206911	6,580869356	29,76769678	59,60770099	ABC transporter I family member 19-like
MELO3C025524.2	4,055961863	5,490993424	12,69708376	72,43939012	ABC transporter I family protein
MELO3C012236.2	0,952407214	1,042262092	1,18313397	7,889448088	accelerated cell death 11
MELO3C023484.2	0,802168665	2,632429872	3,124717895	7,345504452	AP2-like ethylene-responsive transcription factor At1g16060
MELO3C022528.2	0,579682853	0,506350491	0,507637335	3,158036466	AP2-like ethylene-responsive transcription factor SNZ
MELO3C007572.2	3,01657188	2,764939461	4,708988749	12,14032899	AP2-like ethylene-responsive transcription factor TOE3
MELO3C026666.2	0,993123235	2,806314429	5,194056407	10,73348982	Cytochrome b5
MELO3C006316.2	27,75756135	51,32342165	43,17875986	139,3234203	cytochrome b5
MELO3C016512.2	1,875122105	3,056712384	2,478010576	6,581452209	Cytochrome c oxidase copper chaperone
MELO3C005130.2	0,297166143	0,752559508	0,874939204	2,708128424	Cytochrome C oxidase subunit
MELO3C015922.2	3,976878727	6,173755261	5,482104097	12,57523124	cytochrome c oxidase subunit 5C-like
MELO3C005473.2	2,52803784	4,397260327	4,185619486	17,30457417	Cytochrome P450
MELO3C006168.2	0,893941578	0,943471055	1,619193043	4,838577189	Cytochrome P450
MELO3C019884.2	19,83932779	8,079927688	20,96973525	47,10228784	cytochrome P450 77A3-like
MELO3C017559.2	3,519504575	3,951630403	8,730830693	21,30544115	cytochrome P450 90B1
MELO3C005570.2	3,329711149	6,689684669	27,86804486	238,5791911	Cytochrome P450 family protein
MELO3C007480.2	0,646234546	0,799528422	2,132589889	5,414885998	Cytochrome P450 family protein
MELO3C005571.2	1,558437487	2,10938885	13,25939831	96,06839049	Cytochrome P450 family protein
MELO3C005686.2	7,457863213	5,446144301	20,84148346	44,29668644	Cytochrome P450 family protein
MELO3C014879.2	0,379842242	0,507220361	0,20324619	3,128242742	Cytochrome P450 family protein
MELO3C007482.2	1,147262586	2,009950282	1,617252493	109,1485027	Cytochrome P450 family protein
MELO3C005607.2	0,672476396	1,146875725	3,528057218	11,99873271	Cytochrome P450, putative
MELO3C014230.2	18,4762713	18,7256659	16,58366719	176,3574189	Ethylene insensitive 2
MELO3C014181.2	0,985106765	1,498018761	2,684362442	10,81727839	ethylene-responsive transcription factor 3
MELO3C005466.2	6,652140673	23,78897108	4,418375788	55,57654749	ethylene-responsive transcription factor ERF106-like
MELO3C008331.2	0,328265528	0,913301157	5,028539516	83,49951008	ethylene-responsive transcription factor ERF113-like
MELO3C022358.2	1,628657285	3,054475304	3,54677771	27,51320283	ethylene-responsive transcription factor ERF113-like
MELO3C007242.2	1,774707882	1,594558131	0,956200694	9,339684747	Ethylene-responsive transcription factor, putative
MELO3C026759.2	1,885599	3,490351725	3,307951413	10,98659019	Eukaryotic initiation factor 4F subunit p150 isoform 1
MELO3C017385.2	0,192598098	0,202309769	0,319293614	1,888517455	pollen receptor-like kinase 1
MELO3C004667.2	3,701372878	3,354159334	5,498198237	29,03575746	pollen receptor-like kinase 3
MELO3C010412.2	0,12795977	0,119884093	0,511822188	7,709840927	pollen receptor-like kinase 4
MELO3C024410.2	1,768420295	1,387138213	0,499200368	8,160525048	Protein EARLY FLOWERING 3
MELO3C010174.2	7,494924574	15,19409212	15,03480456	54,32364479	protein ECERIFERUM 3
MELO3C015633.2	65,1660279	78,4557466	96,15852946	224,6571852	protein ETHYLENE INSENSITIVE 3
MELO3C030034.2	25,57827065	37,42791365	49,18050706	103,2010899	protein GIGANTEA-like
MELO3C022345.2	6,186058108	8,635791363	24,36111198	53,22334276	somatic embryogenesis receptor kinase 2-like
MELO3C018930.2	0,232686082	0,172057948	0,290760155	1,79225625	zinc finger protein CONSTANS-LIKE 2

Table 8.4. FPKM values of selected episode-specific genes during hermaphrodite flower development

Gene ID	FS	GI-H	GM-H	AN-H	Gene Description
MELO3C011413.2	13,7766978	4,795012048	0,144349295	1,430838117	cytochrome P450 78A5
MELO3C019506.2	104,5681854	42,52668491	5,29823862	10,88135014	ethylene-responsive transcription factor ERF109
MELO3C026157.2	10,78621846	0,738754839	0,431798201	0,714719215	floricaula/leafy homolog
MELO3C024739.2	10,72957907	5,282130547	0,183766412	5,182085167	growth-regulating factor 4-like
MELO3C015838.2	7,101000128	1,260071183	2,268921328	0,374870163	Protein FANTASTIC FOUR 2
MELO3C019777.2	1,80300477	0,697979135	0,328645132	0,717073736	U4/U6 small nuclear ribonucleoprotein PRP4-like protein
MELO3C005924.2	0,201389826	1,852075119	0,448383766	0,337257249	ABC transporter A family member 1
MELO3C008741.2	0,306293392	1,789466046	0,497494145	0,422865366	ABC transporter B family protein
MELO3C011894.2	1,064838935	3,945154741	1,225892912	1,363284365	ABC transporter C family member 3
MELO3C024398.2	0,843026992	2,364616748	0,941054943	0,880711559	ABC transporter C family member 8
MELO3C005244.2	1,640061525	4,880943727	2,378924253	1,381786271	ABC transporter F family member 3
MELO3C006247.2	0,726929694	1,537129608	0,377071387	0,448061781	ABC transporter family protein
MELO3C012998.2	2,921703007	6,454011392	2,021161772	2,901152166	ABC transporter G family member 29-like
MELO3C004967.2	1,149025792	4,532237127	1,825229459	1,962278953	ABC transporter G family member 3
MELO3C010074.2	0,277415574	1,17862318	0,475631044	0,256398232	Abc transporter, putative
MELO3C002960.2	1,146711422	2,390307145	1,053493142	0,884075339	anaphase-promoting complex subunit 2
MELO3C016840.2	0,704907021	7,624096052	0,508155557	0,636972546	AP2-like ethylene-responsive transcription factor
MELO3C007572.2	3,01657188	13,70395032	5,66071893	6,549238281	AP2-like ethylene-responsive transcription factor TOE3
MELO3C007237.2	2,219125275	7,168445489	2,74736501	3,407554398	Apoptosis inhibitor 5-like protein API5
MELO3C028792.2	0,034420325	1,603224327	0,189729692	0,121523446	callose synthase 7
MELO3C016973.2	2,171389554	10,39803081	3,157754929	2,585531707	CHD3-type chromatin-remodeling factor PICKLE
MELO3C006601.2	7,921911519	17,91880361	8,03768533	7,958832136	chromatin structure-remodeling complex protein SYD isoform X1
MELO3C006168.2	0,893941578	4,719816499	2,069283479	1,292322755	Cytochrome P450
MELO3C022045.2	0,434325343	5,160668027	0,902959762	0,786590179	Cytochrome P450
MELO3C000655.2	1,306582608	7,755819401	1,352678696	0,395208199	cytochrome P450 76C4
MELO3C021851.2	0,265078704	4,022563093	1,35278864	0,853049059	cytochrome P450 89A2-like
MELO3C030701.2	0,938449523	5,971978841	1,898846306	2,771174319	cytochrome P450 CYP72A219-like
MELO3C026489.2	2,391275516	6,236443548	2,802613805	2,718520832	cytochrome P450 CYP82D47-like
MELO3C013867.2	0,426382346	3,755750665	0,94696465	0,396193582	Cytochrome P450 family ent-kaurenoic acid oxidase
MELO3C007480.2	0,646234546	5,83714695	1,959687829	1,106913489	Cytochrome P450 family protein
MELO3C007482.2	1,147262586	4,998439108	2,268429318	1,090463665	Cytochrome P450 family protein
MELO3C005602.2	1,777750928	14,07908689	2,520764598	3,064093175	Cytochrome P450, putative
MELO3C003287.2	0,603223044	4,152479803	0,391488058	0,378567721	DYAD protein
MELO3C016085.2	1,968762941	4,817733007	2,062422041	2,381111961	E3 ubiquitin-protein ligase Arkadia
MELO3C017645.2	1,900276874	7,92565201	1,094704715	1,374511883	ethylene-responsive transcription factor ERF106
MELO3C008331.2	0,328265528	1,885472338	0,267837263	0,51324278	ethylene-responsive transcription factor ERF113-like
MELO3C012242.2	0,854838377	5,921418462	2,055057144	1,632598284	ethylene-responsive transcription factor ERF118
MELO3C028860.2	0,457553197	2,724896032	0,342786341	0,067958203	ethylene-responsive transcription factor-like protein At4g13040
MELO3C025602.2	0,4253719	3,688573579	0,367474393	0,348546313	germinal center kinase 1 isoform X1
MELO3C016045.2	0,648940178	3,572808441	0,625436223	0,804256115	homeobox protein LUMINIDEPENDENS
MELO3C005461.2	0,175885937	2,57498848	0,152401605	0,226947965	Kokopelli
MELO3C018601.2	0,179818695	2,130183702	0,123066903	0,049224126	MADS box protein
MELO3C002050.2	1,762360312	16,79729833	1,313023036	1,095897762	MADS box transcription factor
MELO3C007181.2	0,846684698	13,49421364	2,799845005	2,101499521	MADS box transcription factor AGAMOUS
MELO3C006159.2	0,49196053	1,461382116	0,262325716	0,323279285	MADS-box protein
MELO3C022991.2	28,8243919	346,7572522	4,050948586	11,57833304	MADS-box protein AGL42-like isoform X1
MELO3C006940.2	4,734778662	12,57249813	5,324688241	4,10924838	MADS-box protein SOC1
MELO3C003778.2	1,859870834	7,212926722	1,174221166	0,837079949	MADS-box transcription factor
MELO3C010515.2	0,880262279	10,6591082	0,387241285	0,431673016	MADS-box transcription factor
MELO3C026300.2	1,405562241	12,93909506	1,984165307	1,380314721	MADS-box transcription factor
MELO3C026299.2	0,533357903	1,873634808	0,17560565	0,188829858	MADS-box transcription factor
MELO3C022316.2	0,825547025	12,00587961	2,206542279	2,913224676	MADS-box transcription factor
MELO3C022516.2	2,046199801	10,7633949	1,824863638	0,849553768	MADS-box transcription factor
MELO3C033745.2	1,462613613	5,103190451	1,932957462	1,585262855	Maternal effect embryo arrest 22
MELO3C030739.2	8,121651948	17,12108593	8,013746923	5,896772706	Myb family transcription factor
MELO3C031382.2	1,601455332	7,128636028	1,78520748	0,901198078	myb family transcription factor APL
MELO3C009874.2	1,056599555	6,128026022	2,62853412	2,76106401	Myb family transcription factor family protein
MELO3C007988.2	1,108588442	7,870058833	2,214383139	2,421550628	Myb family transcription factor family protein
MELO3C012077.2	0,549369373	3,726043396	1,195470332	0,697244364	Myb family transcription factor family protein
MELO3C009708.2	0,334481109	6,001234309	1,051376055	1,676043221	MYB transcription factor
MELO3C012105.2	0,587421581	2,394271811	0,368099508	0,143321608	Myb transcription factor
MELO3C009633.2	2,661839681	7,128222365	2,454972822	2,448039812	PHOTOPERIOD-INDEPENDENT EARLY FLOWERING 1 family protein
MELO3C023383.2	0,171387396	1,538287702	0,29830333	0,29572203	Pleiotropic drug resistance ABC transporter
MELO3C012945.2	1,002322962	3,24594983	0,856597107	1,586642601	Pleiotropic drug resistance ABC transporter
MELO3C021823.2	1,24403436	3,548333091	0,473905826	0,765487112	Pleiotropic drug resistance ABC transporter
MELO3C014907.2	3,554462648	28,15849237	4,896021755	3,063596062	Pollen Ole e 1 allergen and extensin family protein
MELO3C007159.2	3,397500551	19,04086166	2,791118484	3,917813922	Programmed cell death protein 5
MELO3C007268.2	0,59743336	2,323449421	0,638379361	0,629966882	protein FRIGIDA-ESSENTIAL 1 isoform X1
MELO3C032275.2	1,485033152	8,440199671	2,457127166	2,34287012	protein YABBY 4-like
MELO3C025486.2	3,580859656	2,518270531	8,949786244	2,946776039	ABC transporter G family member 6
MELO3C031734.2	3,52688243	1,666825592	9,706450333	4,46960653	Bidirectional sugar transporter SWEET
MELO3C020044.2	0,712410456	0,693901076	1,759683026	0,714696109	PHD finger protein MALE STERILITY 1
MELO3C031014.2	0,215271364	0,212300325	0,280237509	2,016328217	Protein nuclear fusion defective 4
MELO3C010979.2	1,20904434	1,064326979	2,026804393	4,462987449	WAT1-related protein

8.5 Annex 5

Table 8.5. Summary of sequencing and mapping results in *eif4e* knock-out mutant flowers

		Raw data	Filtering by quality*		Mapping aginst melon genome (v3.6.1)				Mappging aginst mRNAs (v4.0)	
		Total	Total	%	Coverage mean	Mapping QC mean	Mapping reads	%	Assigned mapped	%
FSmut	Replicate 1	138.457.306	138.455.770	100,00	42,52	54,08	86.133.332	62,21	51.860.362	60,21
	Replicate 2	161.131.030	161.129.476	100,00	49,58	54,15	99.639.065	61,84	59.642.235	59,86
	Replicate 3	106.781.878	106.781.038	100,00	32,63	53,96	65.444.364	61,29	37.392.289	57,14
Glmut-M	Replicate 1	108.124.002	108.123.000	100,00	33,46	53,63	62.947.057	58,22	34.643.767	55,04
	Replicate 2	107.683.712	107.683.094	100,00	33,24	53,61	61.747.888	57,34	32.243.171	52,22
	Replicate 3	104.990.294	104.989.198	100,00	32,33	54,04	63.091.940	60,09	36.341.425	57,60
GMmut-M	Replicate 1	109.157.116	109.156.010	100,00	33,08	53,85	66.329.575	60,77	38.486.391	58,02
	Replicate 2	113.404.832	113.403.958	100,00	35,52	53,91	64.799.146	57,14	34.813.797	53,73
	Replicate 3	161.502.534	161.500.244	100,00	50,11	53,96	96.467.506	59,73	58.311.130	60,45
ANmut-M	Replicate 1	156.411.244	156.409.114	100,00	49,03	54,25	93.421.436	59,73	56.784.183	60,78
	Replicate 2	152.092.768	152.091.814	100,00	46,33	54,48	94.301.567	62,00	61.107.086	64,80
	Replicate 3	166.142.280	166.141.108	100,00	51,82	54,00	99.145.377	59,68	60.619.388	61,14

* Reads were filtered out by quality (>30) and by length (>70)

8.6 Annex 6

Table 8.6. Selected differentially expressed genes during male flower development in male-sterile *eif4e* mutants

FSmut versus FS							
GeneID	baseMean	log2FoldChange	lfcSE	stat	pvalue	padj	Gene_description
MELO3C007237.2	704,2133864	1,326477173	0,364315073	3,641016443	0,000271564	0,003163174	Apoptosis inhibitor 5-like protein API5
MELO3C008417.2	3528,391737	-1,308020453	0,209546706	-6,242142772	4,32E-10	6,12E-08	Bidirectional sugar transporter SWEET
MELO3C005758.2	1467,982643	-2,469692894	0,351893805	-7,018290336	2,25E-12	7,34E-10	Bidirectional sugar transporter SWEET
MELO3C022341.2	3669,317871	-3,462272444	0,875679526	-3,953812257	7,69E-05	0,001149903	Bidirectional sugar transporter SWEET
MELO3C015961.2	1799,56506	-1,240362818	0,259830798	-4,773732853	1,81E-06	5,71E-05	Ethylene receptor
MELO3C017940.2	153,7744199	-2,760256574	0,477872466	-5,776136465	7,64E-09	6,39E-07	Ethylene-responsive transcription factor
MELO3C014441.2	411,7120135	-1,38312477	0,31047831	-4,454819312	8,40E-06	0,000199281	ethylene-responsive transcription factor 3-like
MELO3C005465.2	165,6686375	-1,969711237	0,608431462	-3,237359277	0,001206414	0,009781202	ethylene-responsive transcription factor ERF105
MELO3C021306.2	3536,602112	-1,294296722	0,308487021	-4,195627797	2,72E-05	0,000498944	ethylene-responsive transcription factor RAP2-3-like
MELO3C001947.2	902,2931563	-1,253393143	0,319039738	-3,928642713	8,54E-05	0,001254592	eukaryotic translation initiation factor 3 subunit G-like
MELO3C020380.2	7060,019315	-1,070385774	0,204173668	-5,242526053	1,58E-07	7,96E-06	Eukaryotic translation initiation factor 4G
MELO3C022717.2	849,0112378	-1,284613703	0,252873703	-5,080060468	3,77E-07	1,57E-05	FHA domain-containing protein FHA2
MELO3C007468.2	1020,437469	1,394280965	0,380864029	3,660836565	0,000251393	0,002964074	Male gametophyte defective 1
MELO3C004667.2	681,5668714	-1,628869386	0,371559249	-4,383875218	1,17E-05	0,000257038	pollen receptor-like kinase 3
MELO3C024046.2	749,3084162	1,568180352	0,335879069	4,668883825	3,03E-06	8,81E-05	Protein XRI1
MELO3C013473.2	5485,980468	-2,878672747	0,292447476	-9,8433838	7,32E-23	1,34E-18	tetraketide alpha-pyrone reductase 1
GImut-M versus GI-M							
GeneID	baseMean	log2FoldChange	lfcSE	stat	pvalue	padj	Gene_description
MELO3C020400.2	663,0962885	-1,662640113	0,446845441	-3,720839375	1,99E-04	2,90E-03	ABC transporter G family member 21
MELO3C025486.2	2230,038087	-1,476335508	0,398812406	-3,701829451	2,14E-04	3,08E-03	ABC transporter G family member 6
MELO3C007237.2	704,2133864	1,337663016	0,365220854	3,662614011	2,50E-04	0,00346385	Apoptosis inhibitor 5-like protein API5
MELO3C005473.2	500,8277454	-1,353354402	0,262270095	-5,160155224	2,47E-07	1,32E-05	Cytochrome P450
MELO3C011413.2	323,167111	1,34207876	0,391642049	3,426799452	6,11E-04	6,81E-03	cytochrome P450 78A5
MELO3C019206.2	797,587466	-2,33213805	0,328663954	-7,095813291	1,28593E-12	4,26709E-10	cytochrome P450 81E8-like
MELO3C018259.2	1198,48083	1,133243706	0,263316062	4,303739385	1,68E-05	4,13E-04	cytochrome P450 CYP82D47-like
MELO3C026491.2	77,03835804	-3,745944237	1,025740994	-3,651939679	2,60E-04	0,003570512	cytochrome P450 CYP82D47-like
MELO3C007480.2	214,3263893	2,258246851	0,523926913	4,31023258	1,63E-05	4,02E-04	Cytochrome P450 family protein
MELO3C007481.2	89,66505357	2,956621002	0,870395236	3,396871766	6,82E-04	7,44E-03	Cytochrome P450, putative
MELO3C026759.2	1218,575927	-1,015658183	0,276107553	-3,678487505	2,35E-04	3,30E-03	Eukaryotic initiation factor 4F subunit p150 isoform 1
MELO3C035644.2	488,3204186	1,573628969	0,441137942	3,567203855	0,000360811	0,004560616	eukaryotic translation initiation factor 3 subunit A-like
MELO3C020380.2	7060,019315	-1,231358465	0,204444974	-6,022933427	1,71284E-09	2,11163E-07	Eukaryotic translation initiation factor 4G
MELO3C021195.2	280,0171795	-8,231725733	1,291353302	-6,374495436	1,84E-10	3,26E-08	LOW QUALITY PROTEIN: pollen-specific leucine-rich repeat extensin-like protein 3
MELO3C000439.2	32,60402736	2,458449412	0,625765802	3,928705284	8,54044E-05	0,001502485	MACPF domain-containing protein NSL1
MELO3C006940.2	593,67716	-1,288716306	0,290021555	-4,443519047	8,85E-06	0,000247278	MADS-box protein SOC1
MELO3C010769.2	814,6897542	-1,109187375	0,310945668	-3,567142077	3,61E-04	0,004560616	Protein EARLY FLOWERING 3
MELO3C013473.2	5485,980468	2,114765252	0,293208272	7,212502023	5,49E-13	2,11231E-10	tetraketide alpha-pyrone reductase 1
GMmut-M versus GM-M							
GeneID	baseMean	log2FoldChange	lfcSE	stat	pvalue	padj	Gene_description
MELO3C004397.2	15,19993202	-8,174364274	2,399082222	-3,407288087	0,000656118	0,004703573	Alba DNA/RNA-binding protein
MELO3C023241.2	782,5566464	-5,802492331	0,849023883	-6,8343099	8,24E-12	6,00E-10	callose synthase 5-like
MELO3C015764.2	1698,234989	-1,072825018	0,255405293	-4,200480757	2,66E-05	0,000326627	F-box/LRR-repeat protein 17
MELO3C018902.2	859,8885756	-1,589810503	0,250776049	-6,339562763	2,30E-10	1,21E-08	O-fucosyltransferase family protein
MELO3C007031.2	314,47568	-2,336574137	0,457919495	-5,102587163	3,35E-07	7,46E-06	Polygalacturonase QRT3
MELO3C024046.2	749,3084162	1,442623507	0,338040752	4,267602349	1,98E-05	0,00025333	Protein XRI1
MELO3C002541.2	12,00075028	5,835825858	1,724513773	3,384041316	0,000714273	0,005033808	receptor-like serine/threonine-protein kinase SD1-8
MELO3C018777.2	317,270956	2,465954696	0,436118043	5,654328533	1,56E-08	5,12E-07	Serine/threonine-protein kinase
MELO3C018168.2	291,8477294	1,085532829	0,313230762	3,465600958	0,000529048	0,003961654	Serine/threonine-protein kinase
MELO3C016574.2	296,0353632	3,833411025	0,447799428	8,560553637	1,12E-17	2,72E-15	Serine/threonine-protein kinase
MELO3C031872.2	452,8391878	1,635217583	0,348188187	4,696361464	2,65E-06	4,49E-05	Serine/threonine-protein kinase
MELO3C016135.2	1917,036016	3,413824872	0,572641941	5,961534817	2,50E-09	1,03E-07	Serine/threonine-protein kinase
MELO3C007338.2	616,4394961	2,442796574	0,358111479	6,821329996	9,02E-12	6,47E-10	Serine/threonine-protein kinase
MELO3C002524.2	417,9389393	1,028557179	0,254874426	4,035544862	5,45E-05	0,000593225	Serine/threonine-protein kinase
MELO3C013473.2	5485,980468	1,524656182	0,29763661	5,122542492	3,01E-07	6,83E-06	tetraketide alpha-pyrone reductase 1
MELO3C010012.2	1158,509672	1,06708994	0,272805935	3,911534911	9,17E-05	0,000917833	Transmembrane protein
ANmut-M versus AN-M							
GeneID	baseMean	log2FoldChange	lfcSE	stat	pvalue	padj	Gene_description
MELO3C020400.2	663,0962885	-1,365818728	0,446022444	-3,06221973	0,002197021	0,01427542	ABC transporter G family member 21
MELO3C007237.2	704,2133864	1,300945783	0,369715104	3,518779107	0,000433538	0,003778167	Apoptosis inhibitor 5-like protein API5
MELO3C005473.2	500,8277454	-1,189004515	0,252718281	-4,704861512	2,54E-06	5,04E-05	Cytochrome P450
MELO3C019206.2	797,587466	-1,413344816	0,330031895	-4,282449178	1,85E-05	0,000276837	cytochrome P450 81E8-like
MELO3C035644.2	488,3204186	1,57617869	0,444924833	3,542572974	0,000396244	0,003492468	eukaryotic translation initiation factor 3 subunit A-like
MELO3C020380.2	7060,019315	-1,086158722	0,20399723	-5,324379766	1,01E-07	3,22E-06	Eukaryotic translation initiation factor 4G
MELO3C021195.2	280,0171795	-10,92536171	0,896055537	-12,19272831	3,40E-34	4,65E-31	LOW QUALITY PROTEIN: pollen-specific leucine-rich repeat extensin-like protein 3
MELO3C013473.2	5485,980468	-1,175491161	0,295897684	-3,972627115	7,11E-05	0,000854312	tetraketide alpha-pyrone reductase 1